

Studies in Systems, Decision and Control 49

Andrey E. Gorodetskiy *Editor*

Smart Electromechanical Systems

 Springer

Studies in Systems, Decision and Control

Volume 49

Series editor

Janusz Kacprzyk, Polish Academy of Sciences, Warsaw, Poland
e-mail: kacprzyk@ibspan.waw.pl

About this Series

The series “Studies in Systems, Decision and Control” (SSDC) covers both new developments and advances, as well as the state of the art, in the various areas of broadly perceived systems, decision making and control- quickly, up to date and with a high quality. The intent is to cover the theory, applications, and perspectives on the state of the art and future developments relevant to systems, decision making, control, complex processes and related areas, as embedded in the fields of engineering, computer science, physics, economics, social and life sciences, as well as the paradigms and methodologies behind them. The series contains monographs, textbooks, lecture notes and edited volumes in systems, decision making and control spanning the areas of Cyber-Physical Systems, Autonomous Systems, Sensor Networks, Control Systems, Energy Systems, Automotive Systems, Biological Systems, Vehicular Networking and Connected Vehicles, Aerospace Systems, Automation, Manufacturing, Smart Grids, Nonlinear Systems, Power Systems, Robotics, Social Systems, Economic Systems and other. Of particular value to both the contributors and the readership are the short publication timeframe and the world-wide distribution and exposure which enable both a wide and rapid dissemination of research output.

More information about this series at <http://www.springer.com/series/13304>

Andrey E. Gorodetskiy
Editor

Smart Electromechanical Systems

 Springer

Editor

Andrey E. Gorodetskiy
Institute of Problems of Mechanical
Engineering
Russian Academy of Sciences
Saint Petersburg
Russia

ISSN 2198-4182

ISSN 2198-4190 (electronic)

Studies in Systems, Decision and Control

ISBN 978-3-319-27545-1

ISBN 978-3-319-27547-5 (eBook)

DOI 10.1007/978-3-319-27547-5

Library of Congress Control Number: 2015957234

© Springer International Publishing Switzerland 2016

This work is subject to copyright. All rights are reserved by the Publisher, whether the whole or part of the material is concerned, specifically the rights of translation, reprinting, reuse of illustrations, recitation, broadcasting, reproduction on microfilms or in any other physical way, and transmission or information storage and retrieval, electronic adaptation, computer software, or by similar or dissimilar methodology now known or hereafter developed.

The use of general descriptive names, registered names, trademarks, service marks, etc. in this publication does not imply, even in the absence of a specific statement, that such names are exempt from the relevant protective laws and regulations and therefore free for general use.

The publisher, the authors and the editors are safe to assume that the advice and information in this book are believed to be true and accurate at the date of publication. Neither the publisher nor the authors or the editors give a warranty, express or implied, with respect to the material contained herein or for any errors or omissions that may have been made.

Printed on acid-free paper

This Springer imprint is published by SpringerNature

The registered company is Springer International Publishing AG Switzerland

*Physics is moving forward on the shoulders
of the skeptics, and not believers.*

—Edwin T. Jaynes

Preface

Smart electromechanical systems (SEMS) are used in cyber physical systems (CPS). The term “cyber physical systems” was proposed in 2006 by Helen Gill in order to emphasize the distinctive feature of the seminar NSF CPS Workshop she organized. At that time, she was a director of Integrated and Hybrid Systems at the National Science Foundation. Organizers of the seminar were trying to redefine the role of embedded systems, and they succeeded; they caught the general trend, and after a couple of years, the rapid development of CPS began. Progress in this class of systems has been recognized as one of the most important technological developments in the USA and later in Europe. CPS show the ability to integrate computing, communication and storage of information, and monitoring and control over the objects of the physical world. The main tasks in the field of theory and practice of CPS are to ensure the efficiency, reliability, and safety of functioning in real time.

CPS relate to a new scientific field, i.e., cybernetic physics, which is identified by the author of this trend Alexandr Fradkov, the head of the laboratory. IPME RAS of the Academy of Sciences (St. Petersburg, Russia) in his book “Cybernetic Physics” is aimed at the study of physical systems through cybernetic methods. Although some selected publications, using the idea of control theory, started to appear in physics journals a long time ago, an independent branch of science at the intersection of physics and control theory began to take shape only in the 1990s due to the rapid growth in areas such as control of chaos and control over quantum systems, and a number of publications are now estimated at several thousands.

SEMS have been widely employed since 2000 in parallel robots, or so-called parallel kinematic machines. They provide good opportunities in terms of accuracy, rigidity, and ability to manipulate heavy loads. Currently, SEMs are widely used not only in intelligent robots, but also in astronomy, machine tools, medicine, and other fields.

The objective of the publication of this collection of articles is to introduce the latest achievements of the scientists of the Russian Academy of Sciences in the field

of theory and practice of SEMS. At the same time, a lot of attention here is given to methods of designing and modeling of SEMS based on the principles of adaptability, intelligence, biomorphism of parallel kinematics, and parallelism in information processing and control computation. The most complete are the following points of interest:

- methods of design of SEMS modules and intelligent robots based on them;
- synthesis of neural systems of automatic control over SEMS modules;
- mathematical and computer modeling of SEMS modules and CPS based on them;
- vitality control and reliability analysis based on logic and probabilistic and logic and linguistic forecasting;
- methods of optimization of SEMS control systems based on mathematical programming methods in ordinal scale and generalized mathematical programming;
- information-measuring software of SEMS modules and CPS based on them.

This book is intended for students, scientists, and engineers specializing in the field of SEMS and robotics, and includes many scientific domains such as kinematics, dynamics, and control theory.

I am grateful to many people for the support I received while writing this book. Their names cannot be given here, but their assistance is deeply appreciated.

Saint Petersburg
2015

Andrey E. Gorodetskiy

Contents

Part I Methods of Designing

Technical Systems Control: From Mechatronics to Cyber-Physical Systems	3
V.P. Shkodyrev	
Smart Electromechanical Systems Modules	7
A.E. Gorodetskiy	
Smart Electromechanical Systems Architectures	17
A.E. Gorodetskiy	
Methods of Synthesis of Optimal Intelligent Control Systems SEMS . . .	25
A.E. Gorodetskiy, V.G. Kurbanov and I.L. Tarasova	
Logical Analysis of Data and Knowledge with Uncertainties in SEMS	45
B.A. Kulik and A.Ya. Fridman	
Active Data in Digital Software Defined Systems Based on SEMS Structures	61
V.V. Alexandrov, S.V. Kuleshov and A.A. Zaytseva	
Part II Synthesis of Automatic Control Systems	
Automatic Control Systems of SEMS	73
V.G. Kurbanov, A.E. Gorodetskiy and I.L. Tarasova	
Neuroprocessor Automatic Control System of the Module SEMS	81
I.L. Tarasova, A.E. Gorodetskiy and V.G. Kurbanov	
Development of Algorithms and Software for Neurocomputer Systems of SEMS Automatic Control Modules	93
V.N. Ruchkin and V.A. Romanchuk	

Intelligence System for Active Vibration Isolation and Pointing of Ultrahigh-Precision Large Space Structures in Real Time	103
S.N. Sayapin and Y.N. Artemenko	
Semi-automatic Mechatronic Drive Control System Using Bioelectric Potentials	117
V.G. Gradetsky, I.L. Ermolov, M.M. Knyazkov, A.N. Sukhanov and A.A. Kryukova	
Part III Mathematical and Computer Modeling	
The Direct Problem of Kinematics SM8 SEMS.	129
A.E. Gorodetskiy, V.G. Kurbanov and I.L. Tarasova	
The Inverse Problem of Kinematics SM8 SEMS.	143
V.G. Kurbanov, A.E. Gorodetskiy and I.L. Tarasova	
Mathematical Models of the Automatic Control Systems SEMS Modules	149
I.L. Tarasova, A.E. Gorodetskiy and V.G. Kurbanov	
Definition of a Rigidity of a Hexapod.	159
A.Yu. Kuchmin and V.V. Dubarenko	
Computer Modeling ACS of SEMS Actuator of Space Radio Telescope Subdish.	165
I.L. Tarasova, A.E. Gorodetskiy and V.G. Kurbanov	
Features of Manipulator Dynamics Modeling into Account a Movable Platform	177
Yu.N. Artemenko, A.P. Karpenko and P.P. Belonozhko	
Part IV Vitality Control and Reliability Analysis	
Control of Vitality and Reliability Analysis	193
V.Y. Ziniakov, A.E. Gorodetskiy and I.L. Tarasova	
System Failure Probability Modelling.	205
V.Y. Ziniakov, A.E. Gorodetskiy and I.L. Tarasova	
Methods of Dealing with Jamming in Automatic Control Systems of the Modules SEMS	217
A.E. Gorodetskiy, I.L. Tarasova and V.G. Kurbanov	
Expert System for Condition Estimation of a Faulty SEMS Module . . .	225
V.Y. Ziniakov	

Part V Information-Measuring Soft and Hardware

SEMS-Use Platform with a Matrix Receiver for Obtaining the Radio Images of Astronomy	235
A.E. Gorodetskiy, V.G. Kurbanov and I.L. Tarasova	
Analysis of Errors at Optic-Electronic Autocollimation Control System with Active Compensation	251
A.E. Gorodetskiy, I.A. Konyakhin, I.L. Tarasova and Li Renpu	
Optic-Electronic Autocollimation Sensor for Measuring Angular Shifts of the Radiotelescope Subdish	259
I.A. Konyakhin, A.E. Gorodetskiy, Hoang Van Phong and A.I. Konyakhin	
Electrooptic Converter for Measuring Linear Shifts of the Section Boards at the Main Dish of the Radiotelescope	269
I.A. Konyakhin, A.S. Vasilev and A.V. Petrochenko	

Part I
Methods of Designing

Technical Systems Control: From Mechatronics to Cyber-Physical Systems

V.P. Shkodyrev

Abstract In this paper discussed the evolution development processes of modern control theory for technical systems. Perspective trends are analyzed via fundamental principle of analogy searching for evolution behavior of complex biological and information processing cybernetic systems. A new class of cyber-physical systems with adaptive behavior has been reviewed as a prototype of new paradigms for technical system control. Evolutionary cognitive systems with a special emphasis on synergistic mechanisms of self-organization and knowledge-based activity are proposed for providing an appropriate level of adaptation for goal directed behavior.

Keywords Technical systems control · Evolutionary cybernetics · Cyber-physical systems

1 Introduction

The development of modern control theory is currently one of the most urgent and rapidly developing areas of fundamental research, which largely determines the future trends for a wide range of applications and practical usage. Special attention in this process is attracted by the relationship between the general laws of technical systems development and the fundamental laws of nature development that characterize world evolution.

One of the basic principles, which opens the possibility of understanding promising directions in creating the concept of a new generation of control systems, is the search for similarities in the behavior and the evolution of complex biological and cybernetic systems applying various methods of processing and usage of information for learning and adaptation to constantly changing environmental

V.P. Shkodyrev (✉)

Peter the Great St.Petersburg Polytechnic University, St.Petersburg, Russia
e-mail: shkodyrev@mail.ru

influences. In fact, the question is to find analogues for the evolution of well-functioning and developing living organisms to construct cybernetic systems using artificial intelligence mechanisms in goals formation and achievement by supporting targeted behaviors. The principle of evolution elaborated for this by nature clearly reflects the general laws of evolutionary improvement in the organization—or rather, in the self-organizing of complex systems. Analysis of these laws allows formulating the general mechanisms of information cybernetic systems construction and functioning in terms of principles of information processing and exchange with other systems and the environment, including the mechanisms of control and development. Such approach, based on fundamental evolution laws and development mechanisms, has formed the basis for the formation and later development of new promising directions in interdisciplinary research of information control systems, known as “cybernetics evolutionary” [1, 2].

2 Evolution of Cybernetic Systems

Development of the cybernetic evolutionary principles to the study of complex developing control systems and the use of intelligence as a regulator in developing of self-organizing structures opens new perspectives in the creation of artificial objects control models in hierarchy of interacting systems [3]. The new class of complex cyber-physical systems has become the closest prototype that implements these trends [4]. Their distinguishing feature is the unification of cybernetic beginning of cognitive information control systems built into their environment and the ability to perceive its changes by diverse sensors and react to possible changes, learn and adapt for quality performance goals [5, 6].

A **model of complex hybrid evolving cognitive system** is offered to describe and study the general mechanisms of evolutionary systems development implementing the basic principles of synergetic methodology of intelligent systems development that integrate the beginning of cybernetic information control environment with the physical elements of perception and affect the environment. This class of systems is the most promising for the development of the basic paradigm of adaptive self-learning systems based on the principles of integration of control information systems with elements of accumulation and application of knowledge to achieve complex objective functions. At the same time, control remains the key question in such models, because the effectiveness of system operation depends on how the chosen behavior corresponds with reality.

System approach to the analysis of the evolutionary development of such information cybernetic systems can be divided into three strategic directions. At this moment, the first and most actively developing one is the *intellectualization* of control systems and complexes [7]. The key point in the definition of “intelligence” is the ability of the system to extract, accumulate and use knowledge as one of the basic entities of artificial intelligence. It allows the system to operate under autonomous control, perceive the environment and stay in it for a long time,

adapting to changes and achieving the stated goal. The ability to produce new knowledge and reason on its basis allows intelligent system to generate strategies that are more effective itself in continuous changes of external influences, lack of or incomplete information, influence of disturbing factors. This corresponds to the basic principle of the *unity of intelligence and performance in complex systems* using intelligence as a regulator of effective performance in the behavior of complex systems.

The second strategic direction is associated with the development of the *principles of network organization* and *group control of individual intelligent systems* that make up a distributed environment of artificial intelligence. The determining factor in this case is the priority of coordination—horizontal interactive links above the vertical “purely competitive” strategies in complex integrated systems. Cybernetic solutions in this direction over all suggest the creation of a full-related multi-agent system, which includes the relationship between control agents (Vehicle-to-Vehicle, V2V) and between each agent and the outer surrounding infrastructure (Vehicle-to-Infrastructure, V2I).

The emergence of horizontal relationships of cooperation and coordination between the individual cognitive units plays a key role in the formation process of multi-level integrated structures with elements of group control strategies [8]. This is caused by inefficiency (and in some cases impossibility) of solving complex problems by individual isolated subsystems. Such integration serves as prerequisite for hybridization and multidimensionality of intelligent systems, characteristic attribute of which is the ability to assess, predict and control collective behavior and group dynamics of cognitive systems on the meta-level.

The third strategic direction involves the use the principles of self-organization and development. This is determined by the key principles of complex (after G. Haken and I. Prigogine) hybrid system functioning, whose evolutionary development is based on fundamental processes of interaction between its components, the cooperation and coordination in particular [9, 10].

Models of recurrent self-organizing and training in ANN give researchers and engineers’ one of the effective tools to implement the adaptive behavior of complex information systems, operating under the need to analyze large flows of heterogeneous information or a priori uncertainty. Implementation of the principles of adaptive self-organization opens up possibilities for solving tasks such as extracting the maximum amount of information from the experimental data in physical measurements, the creation of intelligent control of distributed objects, computer and telecommunication networks, groups of robots, effective search and cognitive systems, in a row of other applications.

The extraction of maximum amount of information from the experimental data has always been one of the key tasks of physical experiment. A significant number of works was devoted to this problem, including adaptive filtering techniques, experimental design, and other approaches. However, despite the abundance of such works, most of the proposed approaches since the classical work by Wiener adaptive filtering was based on the error minimizing criteria by the method of least squares. This approach greatly limits the ability to adapt systems, without allowing

to extract additional information from the data or to build more flexible optimization algorithms.

To eliminate some restrictions an algebraic approach to the construction of models of recurrent training is proposed, interpreting it as an optimization problem of maximizing the information extracted from the data in the process of network training. The developed approach offers a number of recurrent models of self-organizing ANNs from the position of maximizing entropy characteristics of the amount of information extracted from the data in the analysis of statistically significant features, modeling complex dependencies, separating weakly connected components in a priori uncertainty of their characteristics. The basis of such approach is the creation of algebraic criteria for neural network training, which maximizes mutual information on the outputs of the neural processor.

3 Conclusion

Described mechanisms in this paper can be used in the construction of different classes of robotic systems that allows refer them into a new class of information cybernetic systems—cyber-physical systems, whose feature is to associate disparate components into single integrated environment, actively interacting with external factors for purposeful behavior in achieving objective functions of control.

References

1. Turchin, V.F.: *The Phenomenon of Science. Cybernetic Approach to Evolution.* Science, Moscow (1993)
2. Redko, V.G.: *Evolutionary Cybernetics.* Science, Moscow (2001)
3. Russell, S., Norvig, P.: *Artificial Intelligence: A Modern Approach*, vol. 25. Prentice-Hall, Englewood Cliffs (1995)
4. White, J., et al.: R&D challenges and solutions for mobile cyber-physical applications and supporting Internet services. *J. Internet Serv. Appl.* **1**(1), 45–56 (2010)
5. Lee, E.: *Cyber Physical Systems: Design Challenges.* University of California, Berkeley. Technical Report No. UCB/ECS-2008-8, 23 Jan 2008
6. Lee, J., Bagheri, B., Kao, H.A.: Recent advances and trends of cyber-physical systems and big data analytics in industrial informatics. *International Conference on Industrial Informatics (INDIN)*, 2014
7. Castillo, O., Xu, L., Ao, S.-I.: *Trends in Intelligent Systems and Computer Engineering.* Lecture Notes in Electrical Engineering. Springer, Berlin (2008)
8. Baldassarre, G., Nolfi, S., Parisi, D.: Evolving mobile robots able to display collective behaviors. *Artif. Life* **9**(3), 255–267 (2003)
9. Haken, G.: *Synergetics. Hierarchy Instabilities in Self-Organizing Systems and Devices.* Springer, Berlin (1985)
10. Nicolis, G., Prigogine, I.: *Self-Organization in Nonequilibrium Systems: From Dissipative Structures to Order Through Fluctuations*, p. 512p. Wiley, New York (1979)

Smart Electromechanical Systems Modules

A.E. Gorodetskiy

Abstract The article considers design features of standard modules of smart electromechanical systems (SM SEMS). Also, shows that a variety of structures SM SEMS allow a variety of system design with broad technological capabilities. Further analyzed the applicability of various types of SM SEMS in different areas, taking into account their strengths and weaknesses. In conclusion, noted the expediency of building and exploring mathematical models, above all, the module SM8 SEMS, since it has the most complete functionality, and other modules are in some of the simplification.

Keywords Smart electromechanical systems · Standard module · Structure · Mathematical models

1 Introduction

The main elements of the SEMS is standard modules (standard modules—SM), having a structure such as hexapods. They allow you to maximize the accuracy of the actuators with the minimum travel time by introducing parallelism in measuring, calculating, moving and using precision motors. But however, such mechanisms have a more complex kinematics, which requires more advanced control algorithms and solving new, complex optimization problems, ensuring the implementation of the optimum path without jamming.

A.E. Gorodetskiy (✉)
Institute of Problems of Mechanical Engineering, Russian Academy of Sciences,
Saint-Petersburg, Russia
e-mail: g27764@yandex.ru

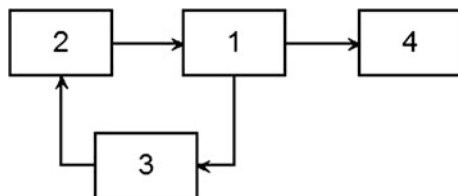


Fig. 1 The block diagram of SM SEMS

When building SEMS for various purposes can be used a wide variety of different standard modules. All they usually contain (see Fig. 1) electromechanical system (EMS) (1), a parallel type, an automatic control system (ACS) (2), the measuring system (MS) (3) and docking system (DS) (4).

EMS comprises a movable and a stationary platform and usually six legs. The difference of certain SM SEMS from each other mainly lies in the design platforms. The core of ACS is neuroprocessor automatic control system (NACS). The main function of NACS is the automatic control of the movement of the upper platform, which has, as a rule, 6-axis positioning system with a control unit. Also part of the function of NACS is the automatic configuration management upper and lower platforms by extending the control rod. MS generally contains, opto-electronic sensors elongation and displacement, tactile sensors and force sensors. DS, as a rule, contains a vision system with intelligent recognition unit.

Next, consider the design of the main modules SM SEMS.

2 Tripod—Module SM1 SEMS

Tripods comprise (see Fig. 2) the lower 1 and an upper platform 2 interconnected three legs 3–5 with the motors 6–8 through 9–14 two-stage hinges providing a change in their length, thus, it is possible to conduct positioning 3-linear m (X, Y, Z) and three angular coordinates (rotation around respective axes Qx, Qy, Qz) [1]. Tripods normally used as a platform to support the weight and maintain the stability of the fortified her another object, such as a camera or camcorder. They provide resistance against downward forces and horizontal forces and movements about horizontal axes. Positioning of three feet from the vertical center of gravity makes it easier to provide arms to resist lateral forces.

The main advantages of tripod are: small size, great rigidity, high positioning accuracy, freely configurable in terms of support, high repeatability of structural elements, the possibility of excluding backlash and no need for fine adjustment during assembly.

The disadvantages are the tripod: the complexity of manufacturing the linear actuator legs, complexity of the joints and complex control algorithms.

Fig. 2 The circuit design tripod and an example of its execution



3 Hexapod—Module SM2 SEMS

Hexapod or Hugh Stewart platform is a type of parallel manipulator, which uses the octahedral arrangement of pillars [1]. Hexapod has six degrees of freedom (three translational and three rotational, as an absolutely solid). The unit has (see Fig. 3) lower platform (LP) (1), the upper platform (AP) (2) and six legs—actuators (LA) (3–8). The lower and upper platform (5 and 6) each comprise a supporting platform (SP) (9 and 10), at least three rods (attached at one end to SP, and the other—to the mounting pads (MP) (17–19 and 20–22), to which may be attached, for example screwed, at least three telescopic spring-loaded rods (TSLR) (23–25 and 26–28).

LA contain electric drives (ED) with gearboxes (G), displacement sensors (DS), such as opto-electronic, and force sensors (FS), such as piezoelectric, and lower hinges (LH), attached to the mounting pads lower platform and top hinges (TH), attached to the mounting pads of the upper platform. By varying the length of the legs with the help of controlled drives, you can change the orientation of a single platform while fixing another.

Hexapod mechanisms used in those areas where it is necessary to control with great precision the object on three axes such as high-precision automatic machines, in medicine for complex operations. Just hexapod machines with high payloads are used in aircraft simulators and radio telescopes.

The main advantages compared with hexapod tripod are: good dynamic characteristics, and lack of accumulation of positional errors.

Hexapod disadvantages are the complexity of manufacturing the linear actuator leg joints complexity, complex control algorithms and possible seizure in violation of the synchronization of linear actuators.

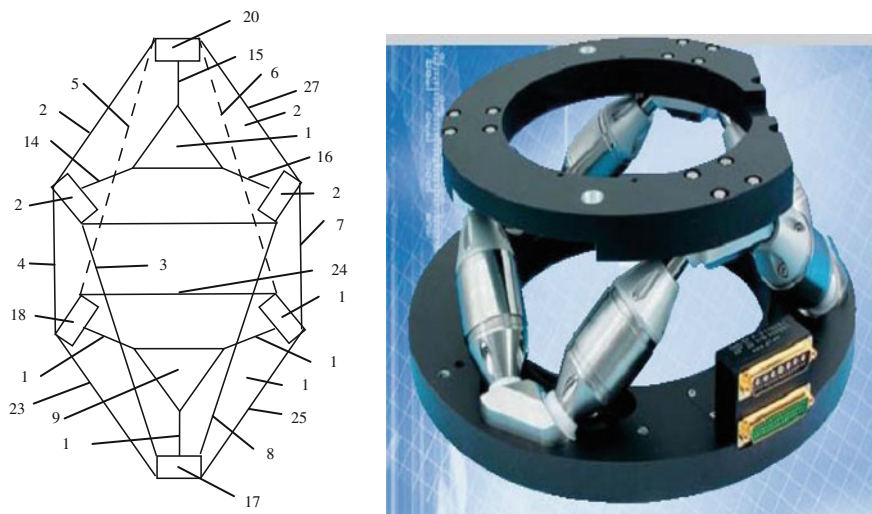


Fig. 3 Driving hexapod design and its general appearance

4 The Module SM3 SEMS

Unlike hexapod the module (see Fig 4) has rods 29–31 and 32–34, which are mounted on the MP 17–19 and/or 20–22 platforms 1 and/or 2 to rotate in planes passing through the points of attachment rods and center of the platform 1 and/or 2 perpendicular to the latter by means of a controlled drive 35–37 and 38–40. The rods 29–31 and 32–34 can change their length by means of linear control actuators 41–43 and 44–46. These rods make the module SM3 SEMS moved by their simultaneous turning and changing lengths. The latter can be used in the design of robots able to move, such as pipes or vessels [2]. Sometimes rods 29–31 and 32–34 can be elastic, which can be useful in medical robots.

SM3 SEMS module has the same advantages and disadvantages as the hexapod, but additionally has the ability to move in space.

5 The Module SM4 SEMS

Unlike module SM2 SEMS that module (see Fig. 5) has rods 47–49 and 50–52, inwardly directed platforms and which are mounted on the SP 9 and/or 10 the platforms 1 and/or 2. They can be rotated in planes reference platforms 9 and/or 10, using of controlled drives 53–55 and 56–58. The rods 47–49 and 50–52 can change their length by means of linear control actuators 59–61 and 62–64. The latter can be used in constructions gripper robots to capture different objects rods 47–49 and 50–52. Just as in the previous case, rods 47–49 and 50–52 can be flexible, which

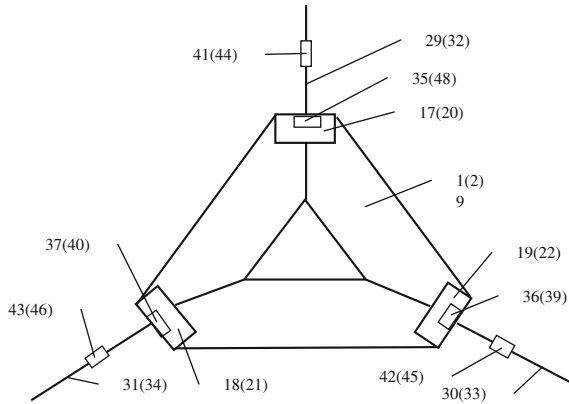


Fig. 4 Design platform of module SM3 SEMS

may be useful in medical robots, such as the Elizarova devices used for bone fixation at fractures [3].

6 The Module SM5 SEMS

The module SM5 SEMS unlike hexapod in rods 11–13 and/or 14–16) have (see Fig. 6) actuators 65–67 and/or 68–70, which allow you to change their length, i.e., making them the control rods (CR).

Usually CR actuators contain gearboxes (G), displacement sensors (DS), for example, optoelectronic, force sensors (FS), such as piezoelectric and controllers (C).

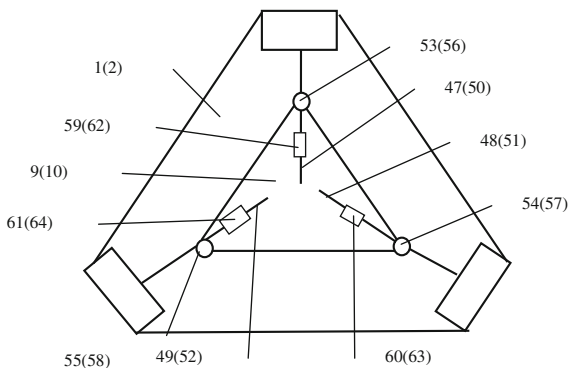
MP 17–19 and 20–22 comprise two grooves for securing TSLR 23–25 and 26–28, and two slots for threaded joint with other similar universal modules. In addition MP 17–19 and 20–22 may contain CCD and LED arrays docking system.

SP 9 lower platform includes grooves with thread for articulation with other similar modules and CCD docking system.

SP 10 upper platform includes grooves with thread and an array of LEDs docking system.

SM5 SEMS module has the same advantages and disadvantages as the hexapod, but unlike hexapod provides not only the shifts and turns of the upper platform, but also the compression and expansion of the upper and lower platforms. This, together with control systems, measurement and docking increases its versatility [4, 5].

Fig. 5 The design platform of module SM4 SEMS

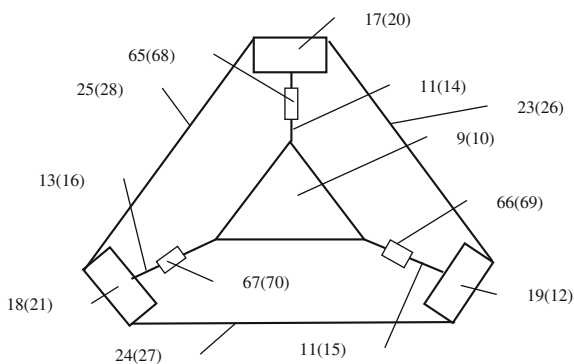


7 The Module SM6 SEMS

This module (see Fig. 7), in contrast to the module SM5 SEMS, has rods 29–31 and 32–34, which are mounted on the MP 17–19 and 20–22. They can be rotated in a plane passing through the points of attachment rods and center of the platform 1 and/or 2 perpendicularly to the latter, using of controlled drives 35–37 and 38–40. The rods 29–31 and 32–34 can change their length by means of linear control actuators 41–43 and 44–46. These rods make the module SM6 SEMS moved by their simultaneous turning and changing lengths. Sometimes the rods 29–31 and 32–34 can be elastic, which can be useful in medical robots.

SM6 SEMS module has the same advantages and disadvantages as the SM5 SEMS, but has a greater flexibility due to the ability to move in space with a simultaneous change of its size and turns.

Fig. 6 The circuit design of the module SM5 SEMS



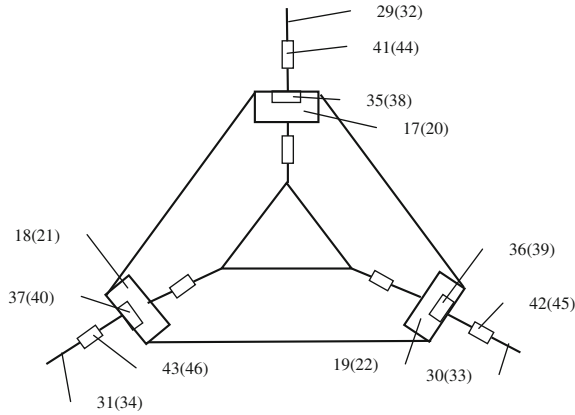


Fig. 7 The design platform of the module SM6 SEMS

8 The Module SM7 SEMS

Module SMS SM7 (see Fig. 8), unlike SMS module SM5, has the rods 47–49 and 50–52, which are mounted on the support plate 9 and/or 10 the platforms 1 and/or 2. They are directed inwards and can be rotated in the plane of the support areas 9 and/or 10 by means of controlled actuators 53–55 and 56–58. The rods 47–49 and 50–52 can change their length by means of linear control actuators 59–61 and 62–64. The latter can be used in the construction of the robot gripper as different objects. As in SM4 SEMS rods 47–49 and 50–52 may be elastic.

SM7 SEMS module has the same advantages and disadvantages as the SM5 SEMS, but has a greater flexibility by providing capture different subjects.

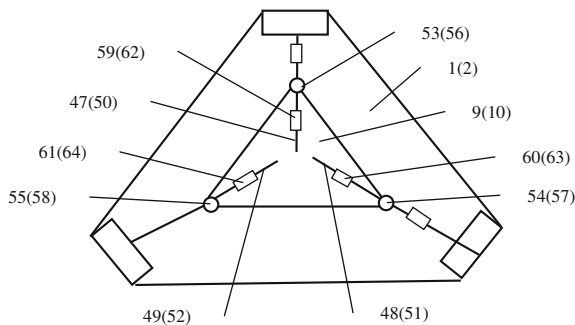


Fig. 8 Design platform of the module SM7 SEMS

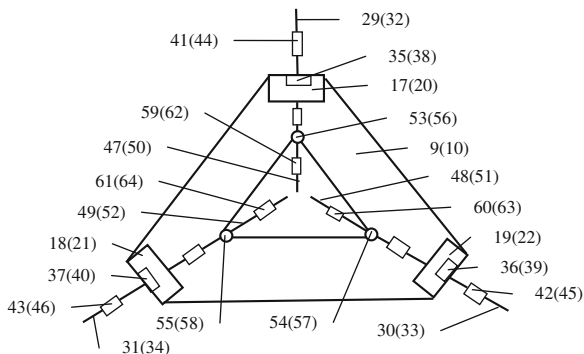


Fig. 9 The design platform of the module SM8 SEMS

9 The Module SM8 SEMS

This module (see Fig. 9), unlike the module SM5 SEMS, has rods 29–31 and 32–34, which are mounted on the MP 17–19 and/or 20–22 platform 1 and/or 2. They can be rotated in a plane passing through the points of attachment rods and center of the platform 1 and/or 2 perpendicular to the latter by means of a controlled drive 35–37 and 38–40. The rods 29–31 and 32–34 can change their length by means of linear control actuators 41–43 and 44–46.

Additionally, this module further has rods 47–49 and 50–52, which are mounted on the support plate 9 and/or 10 the platforms 1 and/or 2. They can be rotated in the plane of the support areas 9 and/or 10 by means of controlled actuators 53–55 and 56–58. The rods 47–49 and 50–52 inwardly directed platform (Fig. 9), and can change their length by means of linear control actuators 59–61 and 62–64.

SM8 SEMS module has the same advantages and disadvantages as the SM5 SEMS, but has a greater flexibility due to a combination of additional features and modules SM6 SEMS SM7 SEMS.

10 Conclusion

There is quite a large variety of standard models of SEMS, on the basis of which it is possible to design a variety of intelligent robots with parallel architecture type of SEMS. Modules such as a tripod have now limited the use of simple designs for a number of inherent weaknesses. Most have full functionality module SM8 SEMS and it can be called a universal module. The other modules are in some of the simplification. It is therefore advisable to study and construction of mathematical models, especially the module in order to study the characteristics and properties discussed SEMS standard modules.

References

1. Merlet, J.P: Parallel robots, 2nd edn., p 383. Springer Publ., Inria, Sophia-Antipolis, France (2006)
2. Agapov, V.A. (RU), Gorodetskiy, A.E. (RU), Kuchmin, A.J. (RU), Selivanova, E.N. (RU): Medical microrobot. Patent RU, no. 2469752 (2011)
3. Ilizarov, G.A.: Transosseous compression and distraction osteosynthesis in traumatology and orthopedics/collection of scientific papers. Issue 1, p 344, Soviet Urals, Kurgan (1972) (In Russian)
4. Gorodetsky, A.E., Tarasova, I.L., Kurbanov, V.G., Agapov, V.A.: Mathematical model of automatic control system for SEMS module. *Informatsionno-upravliaiushchie sistemy* **3** (59):40–45 (2015) (In Russian)
5. Gorodetsky, A.E., Tarasova, I.L., Kurbanov, V.G.: Universal module of smart electromechanical sestems (UM SEMS). *Int. J. Intell. Syst. Appl. Eng. (IJISAE)*

Smart Electromechanical Systems Architectures

A.E. Gorodetskiy

Abstract The article considers various types smart electromechanical systems architectures. It is shown that various associations (serial, parallel, tree, etc.). SEMS structures make it easy to design a variety of intelligent robots with broad technological capabilities (relief structures, combination in a single mechanism of transportation and processing operations, design flexibility, etc.). Analyzed the applicability of various structures in different areas, taking into account their strengths and weaknesses.

Keywords Architecture · Smart electromechanical systems · Intelligent robots

1 Introduction

The use of intelligent robots (IR) hexapod structures of electromechanical intelligent systems (SEMS—smart electromechanical systems) makes it possible to obtain maximum precision actuators with minimal travel time. This is achieved by the introduction of parallelism in the process of measuring, calculating and movement and the use of high-precision piezomotor able to work in extreme conditions, including in outer space [1]. Various associations (serial, parallel, tree, etc.). SEMS structures make it easy to design a variety of intelligent robots with broad technological capabilities (relief structures, combination in a single mechanism of transportation and processing operations, design flexibility, etc.). However, such mechanisms have a more complex kinematics. The latter requires more advanced control algorithms and solving new, complex optimization problems,

A.E. Gorodetskiy (✉)

Institute of Problems of Mechanical Engineering, Russian Academy of Sciences,
Saint-Petersburg, Russia
e-mail: g27764@yandex.ru

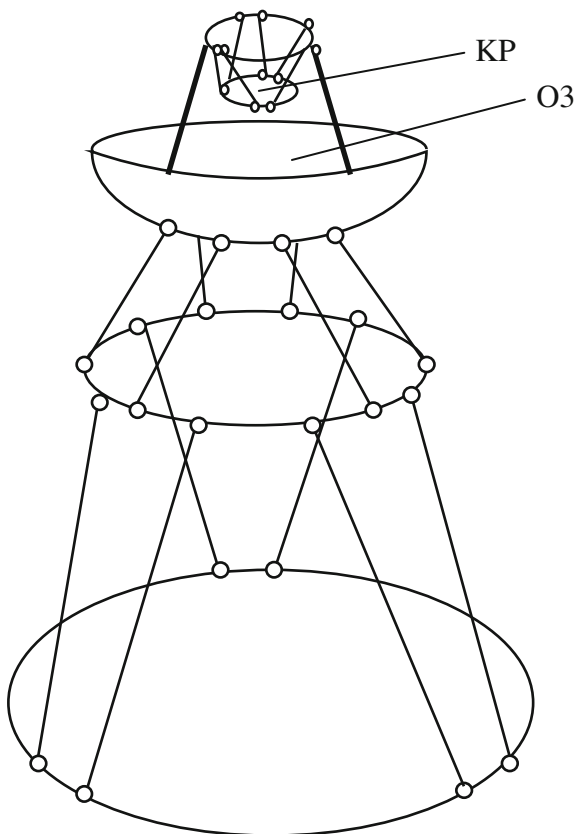
ensuring the implementation of the optimum path without jamming. In addition to the inclusion of SEMS wireless network interface such as Wi-Fi and intellectual system of strategic planning of cooperative behavior of several SEMS will further expand the scope of R&D [2].

Consider the kinds of architectures SEMS with examples of their application.

2 Serial Architecture

Typical SEMS modules in serial architecture are connected in series with each other, i.e. lower platform subsequent module is attached to the top—the previous (see Fig. 1). A typical example of such an architecture can be support-rotating device antenna space radio telescope [3]. As illustrated in [4] in the space radio telescope (SRT) antenna device, it is advisable to use a design consisting of a series connection of hexapods (see Fig. 2). It is necessary for issuing a predetermined shape and

Fig. 1 Serial architecture



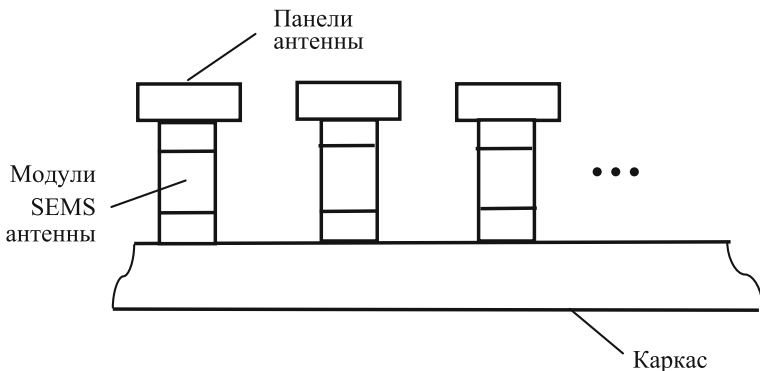


Fig. 2 Parallel architecture

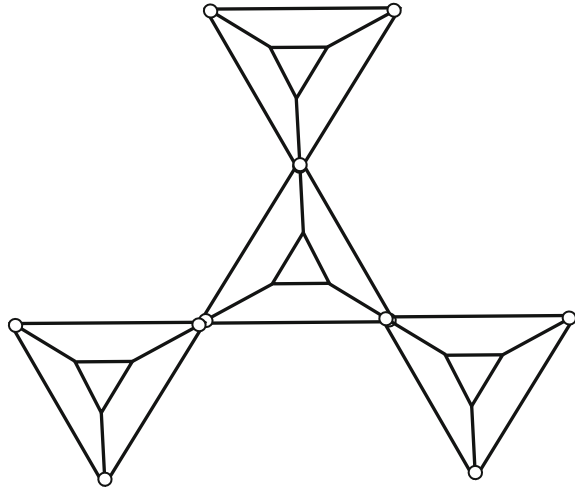
position of their mirror surfaces after the disclosure of the antenna and a possible correction of the periodic as well as to restore the telescope to a given light source. At the same time the main dish (MD) attached to the top platform of the compounds 2–3 hexapods and subdish to the lower platform of another hexapod upper platform which is attached to the respective uprights MD. For automatic control of the spatial position of the mirror elements of such a structure commonly used neuroprocessor systems. Features of operation of such SEMS in space is the need to ensure the efficiency of electric system in a high vacuum, and that is particularly difficult to implement, at temperatures up to 4°K. Therefore, conventional principles of construction of control systems based on DC motors or asynchronous motors with digital controllers based on microcontrollers and industrial general purpose computing stations in this case can not be used. In [5] it is shown that one of the most promising solutions to this problem is to build neuroprocessor automatic control system (NUAU) using a piezoelectric actuator motors SEMS legs.

Thus, the use in the design of support-rotating device antenna space radio telescopes serial communications modules SEMS provides a compact antenna placement in the delivery of its orbit, fast and reliable disclosure, as well as the precise positioning and tracking with the help of neuroprocessor automatic control system.

3 Parallel Architecture

The parallel architecture SEMS typical modules are connected in parallel with each other, i.e. lower the platform of all the modules are attached to a support surface (see Fig. 2). A typical example of such an architecture can be adaptive surface of the main dish and subdish radio telescope [6], using modules such as “hexapod”.

Fig. 3 Architecture of the “star”



In [5] it is shown that one of the most promising solutions to the problem of control such surfaces is also building a NUAU using piezoelectric actuator motors in legs, which is especially promising for space telescopes. The latter provides a rapid and accurate surface shape changes depending on the change in the wavelength of the radiation and their adaptation to different perturbations, thermal, weight, wind and others.

4 Architecture of the “Star”

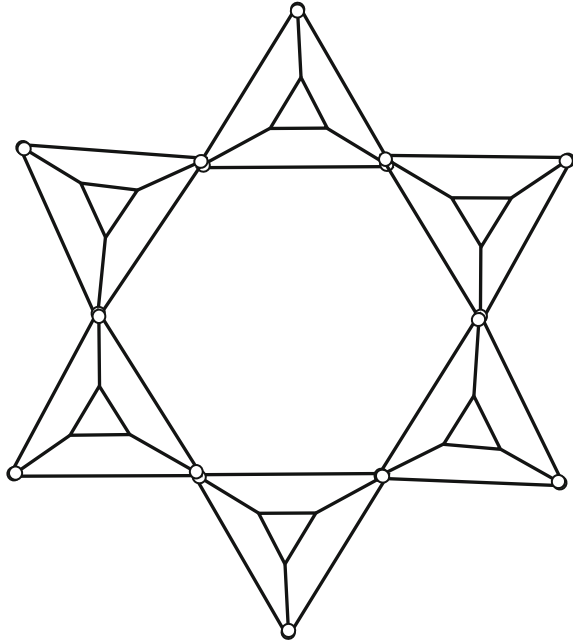
In the “star” architecture of the SEMS series-connected of standard modules are connected at the top and/or lower platform of the basic module is usually larger (see Fig. 3). A typical example of such an architecture can capture the adaptive industrial robot [7], which uses a module type UM5 SEMS.

Use these grips NUAU quickly and accurately adapt the surface of the palm and fingers grip. Furthermore gripping force can be adapted for gripping an object, thereby improving reliability of industrial robot performing various processing operations.

5 Architecture of the “Ring”

The architecture of the SEMS type “Ring” series-connected types of modules form a ring by connecting the upper platform of the last module of the first lower platform (see Fig. 4). A typical example of such an architecture can capture the

Fig. 4 Architecture of the “ring”



adaptive industrial robot [7], using modules of type UM4 SEMS, or UM7 SEMS. In such grips NUAU use as quickly and accurately adapt the surface and grip force for gripping an object, thereby increasing the reliability of the industrial robot perform various processing operations.

6 Architecture of the “Tree”

Architectures such as “tree” may in one SEMS any combination of the above architectures. At the same time it is also possible to use any type of universal modules SEMS. A typical example of such an architecture can be a medical micro-robots [8] (see Fig. 5). The design of the robot comprises a body 1 consisting of a series connection of the modules, such as the type UM5 SEMS, propeller 2, which is attached to the bottom platform of the first module housing and consists of a series connection of the modules, such as the type UM5 SEMS, adaptive grippers 3, which are attached to the upper platform of the last the module housing and consist of a series connection of the modules, such as the type UM5 SEMS, and paddle-4 stops, which are attached to the upper and/or lower platforms intermediate housing units and consist of serial communication modules, such as the type UM5 SEMS.

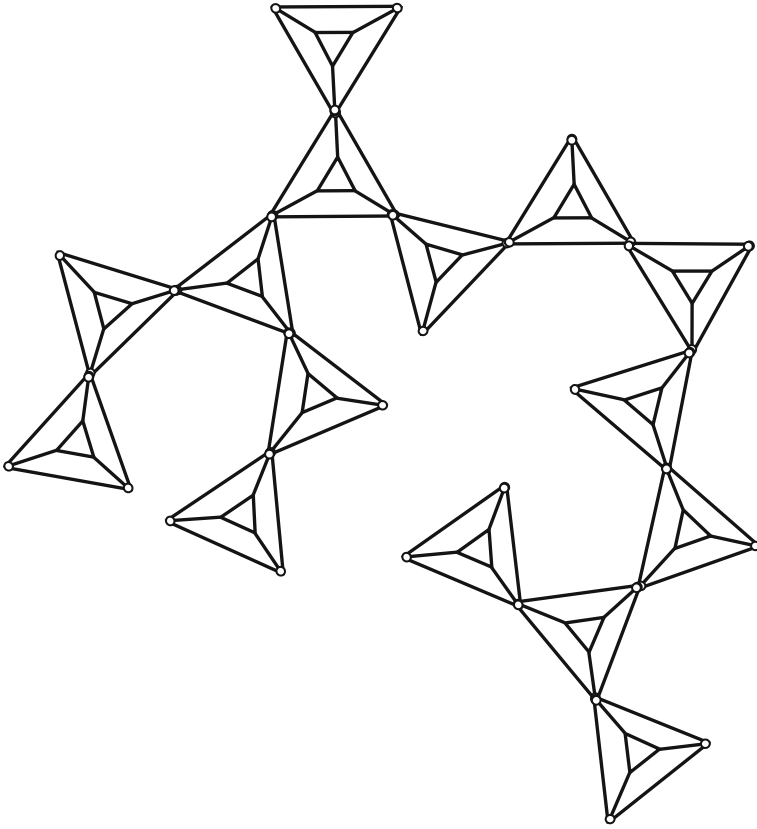


Fig. 5 Architecture of the “tree”

7 Conclusion

Using different association SEMS units by type of building different architectures of computer networks (serial, parallel, star, ring, tree) allows the construction of intelligent robotic systems for various purposes with the parallel structures that provide high accuracy and speed.

References

1. Merlet, J.P.: Parallel robots, 2nd edn., p. 383, Springer Publ., Inria, Sophia-Antipolis, France (2006)
2. Gorodetskiy, A.E.: Osnovy teorii intellektual'nyh sistem upravleniia [Fundamentals of the Theory of Intelligent Control Systems], p. 314. LAP LAMBERT Academic Publ., Berlin (2011)

3. Artemenko, N.Y., Gorodetsky, A.E., Doroshenko, M.S., Konovalov, A.S., Kuchmin, A.Y., Tarasova, I.L.: Problems of the choice of electric drives of space radio-telescope system dish system. *Mehatronica, Avtomatizacia, Upravlenie* **1**, 26–31 (2012) (In Russian)
4. Artemenko, N.Y., Gorodetsky, A.E., Dubarenko, V.V., Kuchmin, A.J., Agapov, V.A.: Analysis of the dynamics of actuators automatic control systems of space radio telescope subdish. *Informatsionno-upravliaiushchie sistemy* **6**, 2–5 (2011) (In Russian)
5. Gorodetsky, A.E., Tarasova, I.L.: *Upravlenie i neironiy seti [Control and neural networks]*, p. 312. Politekhnikeskii universitet Publ., Saint-Petersburg (2005) (In Russian)
6. A method of adapting the reflective surfaces of the antenna. Patent RU, no. 2518398 (2014)
7. Vacilenko, N.V., Nikitin, K.D., Ponomarev, V.P., Smolin, A.J.: *Fundamentals of robotics*. Tomsk MGP « RASKO » 1993
8. Agapov, V.A., Gorodetskiy, A.E., Kuchmin, A.J., Selivanova, E.N.: *Medical microrobot*. Patent RU, no. 2469752 (2011)

Methods of Synthesis of Optimal Intelligent Control Systems SEMS

A.E. Gorodetskiy, V.G. Kurbanov and I.L. Tarasova

Abstract The article considers methods of optimization of control systems SEMS: mathematical programming, mathematical programming in the ordinal scale, generalized mathematical programming and multi-step generalized mathematical programming. We analyze the complexity and applicability of each method in the synthesis of SEMS. The algorithms to solve these optimization problems.

Keywords Intelligent control systems · Smart electromechanical systems · Optimization · Mathematical programming

1 Introduction

In the synthesis of control systems, first of all, there is a question of finding the best in one sense or another, or optimal control object or process. This could be, for example, of optimality in the sense of speed, t. E. Towards the goal in the shortest time, or, for example, the achievement of goals with minimum error, and etc.

The largest number of optimal control methods considering such management processes, each of which smears be described a system of ordinary differential equations:

$$dx_i/dt = f_i(x_1, x_2, \dots, x_n, u_1, u_2, \dots, u_m), \quad i = 1, 2, \dots, n, \quad (1)$$

A.E. Gorodetskiy (✉) · V.G. Kurbanov · I.L. Tarasova
Institute of Problems of Mechanical Engineering, Russian Academy of Sciences,
Saint-Petersburg, Russia
e-mail: g27764@yandex.ru

V.G. Kurbanov
e-mail: vugar_borchali@yahoo.com

I.L. Tarasova
e-mail: g17265@yandex.ru

where x_1, x_2, \dots, x_n —a process value, i.e. the phase coordinates of the control object, determine its state at any given time t , and u_1, u_2, \dots, u_m —control parameters (including configurable controller parameters) that determine the course of the process.

To move a managed process has been determined at some point in time $t_0 \leq t \leq t_1$, enough to make at this point in time have been set in the time control settings

$$u_j = u_j(t), \quad j = 1, 2, \dots, m. \quad (2)$$

Then, for given initial conditions

$$x_i(t_0) = x_{i0}, \quad i = 1, 2, \dots, n, \quad (3)$$

the solution of (1) is uniquely determined. Be solved variational problem associated with the controlled process (1) is as follows.

An integral functionals:

$$J = \int_{t_0}^{t_1} f^0(x_1, \dots, x_n, u_1, \dots, u_m) dt, \quad (4)$$

where $f^0(\cdot)$ —a given function.

For each unit (2), given at a time interval $t_0 \leq t \leq t_1$ is uniquely determined by the course of the controlled process, and the integral (4) takes a certain value.

Let us assume that there exists a control (2) transferring the control object from a given initial state (3) in the prescribed terminal phase state:

$$x_i(t_1) = x_{i1}, \quad i = 1, 2, \dots, n. \quad (5)$$

Required to find a control

$$u_j(t), \quad j = 1, 2, \dots, m, \quad (6)$$

which will transfer the control object from the state (3) to state (5) in such a manner that a functional (4) has a minimum value. At this time instants t_0, t_1 are not fixed, but is only required that at the initial time the object was in the state (3), and in the end—in the state (5) and to the functional (4) reaches a minimum (it may be the case when t_0, t_1 are not fixed).

The technical problems of the control parameters cannot take any arbitrary value. Therefore, for every point that characterizes the current value of the control must be satisfied $(u_1, \dots, u_m) \in U$. The choice of U should reflect the specifics of the object of control. In many technical problems this set is closed. The introduction of these restrictions leads to nonclassical problems of the calculus of variations that are best solved computational methods.

Often there are problems on the optimal transition of the control object from an initial variety M_0 points in phase space for a finite set of the M_1 , and the dimensions of these varieties can be arbitrary. In particular, when the two varieties are zero, then we come to the initial problem.

It is obvious that in technical systems not only control parameters, but also the phase coordinates of the control object should be subject to some physical limitations. For example, the height of the airplane cannot be negative. Therefore, in general, must fulfill the conditions: $(x_1, \dots, x_n) \in X$, where X is the set reflects the specificity of the object of control and protection of its functioning.

Another object of the optimal control may be the problem of optimal contact with the moving point of the phase space.

Suppose that in the phase space has a moving point:

$$z_i = Q_i(t), \quad i = 1, 2, \dots, n. \quad (7)$$

Then there is the problem of optimal reduction of the object (1) in agreement with the moving point (7). This problem is easily reduced to the first, if we introduce new variables, putting:

$$y_i = x_i - Q_i(t), \quad i = 1, 2, \dots, n. \quad (8)$$

As a result of this conversion system (1) is transformed into a new, though not autonomous, and to manage the reduction of the object becomes объекта y_1, y_2, \dots, y_n at fixed point $(0, 0, \dots, 0)$ of the phase space.

It is very important to the case where the object pursued is manageable and its motion is described by a system of differential equations:

$$dz_i/dt = g_i(z_1, z_2, \dots, z_n, u_1, u_2, \dots, u_m). \quad (9)$$

The control problem is that, knowing the technical possibilities of the object pursued, i.e. the system of Eq. (9) and its position at any given time, to determine the control of pursuing the object in the same moment in time so that the persecution was carried out optimally. In this formulation, the problem is considered in the differential game theory [1, 2]. It is assumed that in the initial moment of time the position of the object pursued is known, and its further behavior is described probabilistically and the process of its motion is considered Markov. Under these assumptions, management sought a haunting object (1), in which the meeting of a small neighborhood of the object (1) with the object pursued (9), or a small neighborhood is the most likely.

This problem can be reversed, i.e. control is sought for the persecuted of the object (9), is to meet a small neighborhood of the object (9) with a haunting object (1) or a small neighborhood is the least likely. Moreover it can be a challenge when pursuing several objects. All these tasks are related to the theory of differential games, and the optimal solution is sought in the conditions of incomplete certainty.

Finally, the complex intellectual systems having appropriate behavior, which include intelligent control systems SEMS, control may be to select the best solution from a variety of alternatives when unclear and do not necessarily probabilistic or statistical, describing the dynamics of the control object and the environment, as well as in quality Score is not scalar control. These problems belong to the theory of decision-making [3], i.e., tasks decision (CRA) about the optimal system. In cases when it is possible to specify the scale—the objective function, which determines the value of a solution are known and well-developed theory and methods of mathematical programming [4], allowing to carry out a qualitative and numerical analysis arising in this clear objectives optimization solutions. Uncertainty that may arise in solving the problems of decision-making in the fuzzy modeling of complex systems operating in poorly formalized environment allows the use of these methods of mathematical programming with more or less success in these cases [5].

In the simplest case, a decision the decision-maker (DM)—a developer has one goal and this goal can be formally defined as a scalar function, i.e., quality criterion of choice. The values of quality criteria can be obtained for any valid set of values for the arguments. It is assumed also that the region is known for determining the parameters of choice, i.e., component selected vector or, anyway, for any given point can be determined whether it is a valid option, i.e. whether it belongs to the domain of the criterion of quality solutions. In this situation, the task of choosing the solution can be formalized and described a model of mathematical programming (MP). In other cases, you should use mathematical programming in an ordinal scale (MPOS), generalized mathematical programming (GMP) or multi-step tasks generalized mathematical programming (MSGMP) [6].

2 Mathematical Programming

The problem MP is required to calculate the n -dimensional vector X , optimizing (drawn in maximum or minimum, depending on the content formulation of the problem) criterion of quality solutions $f_0(x)$ subject to the restrictions $f_j(x) \leq u_j$, $j \in 1, 2, \dots, r$, $x \in G$, where f_j —known scalar functional, u_j —given numbers, G —predetermined set of n -dimensional space R^n .

Thus, the task MP is:

$$f_0(x) \rightarrow \text{ext}/f_j(x) \leq u_j, \quad j \in 1, 2, \dots, r, \quad x \in G \subseteq R^n \quad (10)$$

Depending on the properties of the function $f = \langle f_0, f_1, f_j, \dots, f_n \rangle$ and set G is a particular class of optimization problems. If all the functions f_j —linear, and G —polyhedral set, it is the problem of linear mathematical programming (LMP). If, among the functions f_j are found non-linear, it is a problem of nonlinear mathematical programming (NMP). Among the extreme nonlinear problems isolated convex problem that maximize the subject concave functions $f_0(x)$ at the concave functionals restrictions $f_j(x)$ and a convex domain G . Problems in which G has a

finite or countable number of points highlighted in a special section mathematical programming—integer or discrete mathematical programming (DMP). If the quadratic functional $f_0(x)$, and all other linear functions f_j and G polyhedral set, it is the task of the quadratic mathematical programming (QMP), which can lead to problems (LMP) using the Kuhn-Tucker theorem [5].

In the process of solving the majority of optimization problems, including finding optimal control systems SEMS, you can come to the problems of MP in selecting the optimal solution when there is a possibility of constructing a scalar quality criterion, including the attributes of logical variables.

When the logic-probabilistic description of uncertainties [7] in order to optimize may find the identity of the rows of the system logic equations describing the closeness of the synthesized optimal logic-probability model (LPM) control systems to the ideal, giving the true values of logic functions y_i with the maximum value of the probability $P\{y_i = 1\}$. Then the quality criterion can be expressed as follows:

$$f_0(Y) = \sum_{i=1}^n P\{y_i = 1\} \rightarrow \max \quad (11)$$

the values of the probabilities $P\{y_i = 1\}$ can be calculated approximately by the method described in [7] algorithm. If the analysis LPM a complex system of SEMS will be revealed that the influence of one or another component y_i its behavior is different, the quality criteria (11) it is advisable to the form:

$$f_0(Y) = \sum_{i=1}^n \beta_i P\{y_i = 1\} \rightarrow \max, \quad (12)$$

where β_i —assigns weights.

In the above approach, the quality of the optimization will be mainly determined by the proper construction of a binary relation, describing the measure of closeness designed to SEMS perfect. This can be time-consuming and difficult task, often associated with the solution of a number of logical problems. The quality of formulation and solution of these problems depends on the experience and skills of the developer, as the decision makers. To increase objectivity in the evaluation of the optimal model it is advisable to make a collective decision-maker with the involvement of the customer to work on the construction of a binary relationship.

When the logic-linguistic description of uncertainties to optimize can be as search for identity matrix rows of logic equations describing the closeness of the synthesized optimal logical-linguistic model (LLM) to the ideal, giving the true values of logic functions y_i with maximum values of membership functions $\mu(y_i)$. Then the quality criterion can be expressed as follows:

$$f_0(\mathbf{Y}) = \sum_{i=1}^n \mu(y_i) \rightarrow \max \quad (13)$$

The values of the membership functions $\mu(y_i)$ can be calculated from those described in [7] algorithms.

If the analysis LLM any complex system SEMS will be revealed that the influence of one or another component y_i its behavior is different, the quality criteria (13) it is advisable to the form:

$$f_0(\mathbf{Y}) = \sum_{i=1}^n \beta_i \mu(y_i) \rightarrow \max, \quad (14)$$

where β_i —assigns weights.

To increase objectivity in the evaluation of the optimal model it is advisable to make a collective decision-maker with the involvement of the customer to work on the construction of a binary relationship.

When the logic-interval uncertainty control is a set of logical variables that have the attribute part of the intervals $[a_{ji}, b_{ji}]$. The task of finding the optimal control, specified as a logical-interval model (LIM) can be reduced to problems of mathematical programming with the following scalar functionals:

$$J_1 = \sum_j^m \sum_i^n k_{ji}(b_{ji} - a_{ji}) \rightarrow \min \quad (15)$$

$$J_2 = \sum_j^n \sum_i^n [k_{ji}(b_{ji} - a_{ji}) - c_{ji}]^2 \rightarrow \min \quad (16)$$

$$J_3 = \sum_j^m \sum_i^n k_{ji}[(b_{ji} - a_{ji}) - (b_{ji}^0 - a_{ji}^0)]^2 \rightarrow \min \quad (17)$$

$$J_4 = \sum_j^m \sum_i^n [k_{ji}^b (b_{ji} - b_{ji}^0)^2 + k_{ji}^a (a_{ji} - a_{ji}^0)^2] \rightarrow \min, \quad (18)$$

where: k_{ji} , k_{ji}^b , k_{ji}^a —coefficients of the preferences of the person receiving the decision maker (DM) of optimality, c_{ji} —DM desired width of the interval, b_{ji}^0 , a_{ji}^0 —DM desired border intervals.

3 Mathematical Programming in the Ordinal Scale

Since the decision on the optimality of the synthesized system often take the people for them is often the concept of consistent preference for one of the options being compared to another—a more natural way to select a rational alternative than the formulation of the objectives and the approach to it. In this case, the feasible set of alternatives it is advisable not to ask inequalities and certain conditions preference chooses. Such situations occur, in particular in the synthesis of SEMS, when the selection should provide a number of purposes, and it is permissible to determine different people in charge of different resources, limiting the choice. To solve such problems can be generalized scheme of mathematical programming, shifting from quantity to ordinal scales, i.e. moving from models require functional task, defining the objectives and constraints of the problem, a model taking into account the preferences of persons involved in the selection decision. This extends the range of applications of the theory of extreme problems and may prove useful in a number of situations of choice. In particular to the problems of mathematical programming in an ordinal scale (MPOS) can be obtained in the process of solving the problems of optimal synthesis of SEMS, which describes the optimal control of the LPM, LLM or LIM. Then, when you select the optimal solution of logical equations of the attributes of logical variables is linguistic expressions describing the preferences in the form of, for example, estimates ball formed on the basis of the analysis of the views of decision-makers. In this case, there is a fundamental possibility of ordering preferences.

Consider the simplest transition from extreme problems in a quantitative scale of the problem in terms of an ordinal scale.

Let G be a fixed compact set in R^n , $g_j, j = 0, 1, 2, \dots, r$ —reflexive, transitive and complete binary relations in G , describing the preferences of individuals, limiting the possible solutions, g_0 —the preference of the decision maker. $g_j, j = 1, 2, \dots, r$ —can be interpreted as individual preferences, restrict, each in its own way, the set of feasible control plans. Some of the relationships g_j can be determined by conventional functional inequalities that limit the ranges of the various components of the model.

We denote by $u_j, j = 1, 2, \dots, r$ —a priori defined path in G , and assume that the plan $x_i \in G$ is admissible on the j th constraint when $x_i g_j u_j$ i.e. if the pair $(x_i, u_j) \in g_j$. Accordingly, the plan is called $x_i \in G$ feasible solution if $x_i g_j u_j, j = 1, 2, \dots, r$. MPOS task is the task of choosing the “best” (in the sense of a binary relation g_0) among feasible solutions, i.e. as close as possible to the reference solution x_0 . It is necessary to find one solution x_0 —such that:

$$x_0 g_0 x_0 \text{ at: } x_0 g_j u_j, \quad x_0 g_j u_j, \quad j = 1, 2, \dots, r, (y_0, y_0) \in G \quad (19)$$

When determining the optimum SEMS, LPM described, and, accordingly, g_0, g_j can be expressed as a logical equation:

$$C_0Q = Y, \quad (20)$$

$$C_jQ = Z, \quad (21)$$

where: vector Y logical variables y_j , characterizing the optimized model parameters that have to attribute part of the probability $P\{y_i = 1\} = P_i^y$ and established by the decision maker, ballroom estimate the closeness of the model parameters to the standard $b_i \in B$ and the coefficients of their significance v_i , vector Z is logical variables z_j , characterized by a limited model parameters that have to attribute part of the probability $P\{z_j = 1\} = P_j^z$ and established parties, restrictive solutions, ballroom estimate the closeness to the standard $a_j \in A$, Q vector has components $\langle q_1, q_2, \dots, q_n, q_1q_2, \dots, q_1q_n, q_2q_3, \dots, q_{n-1}q_n, q_1q_2q_3, \dots, q_{n-2}q_{n-1}q_n, \dots, q_1q_2, \dots, q_{n-1}q_n \rangle$, identification line C_0 and C_j contain elements 0 and 1 in a predetermined order (e.g. $C_0 = |1\ 0\ 0\ 1\ 0\ \dots\ 1|$ and $C_j = |0\ 1\ 1\ 0\ \dots\ 0|$) dimensional vector Q and lines C_0 , C_j coincide, q_i —logical variables characterizing x_3 and x_0 [7].

Then, if $\forall q_i$ probability $P(q_i) = 1$, the process of determining the optimal x_0 can be easily automated by calculating

$$J(x_i) = \sum_{i=1}^m v_i b_i \quad (22)$$

and finding x_i , the maximum value $J(x_i)$ subject to the limitations:

$$a_i \geq a_{imin}, \quad i = 1, \dots, m, \quad (23)$$

where a_{imin} —the minimum allowable assessment of the i th parameter.

If:

$$\exists q_i, P(q_i) < 1, \quad (24)$$

MPOS the problem is complicated, because now you must first calculate the probabilities P_i^y and P_i^z , then search for the maximum value x_i

$$J(x_i) = \sum_{i=1}^m v_i b_i P_i^y, \quad (25)$$

subject to the restrictions (23), and additional constraints of the form:

$$P_i^z \geq P_{imin}, \quad i = 1, \dots, m, \quad (26)$$

where P_{imin} —minimum allowable probability of logical variable z_i .

MPOS task becomes even more complicated if the condition (24) and, in addition, one or another point scoring a_i and b_{ij} are set makers and restrictive solutions, with some associated probabilities P_{ij}^b and P_{ij}^a (see Tables 1 and 2).

Table 1 Probability scores b_{ij}

Parameter model	Probability scores b_{ij}					Probability	Coefficients significant
y_1	$b_{11};P_{11}^b$	$b_{12};P_{12}^b$	$b_{13};P_{13}^b$...	$b_{1n};P_{1n}^b$	P_1^y	v_1
y_2	$b_{21};P_{21}^b$	$b_{22};P_{22}^b$	$b_{23};P_{23}^b$...	$b_{2n};P_{2n}^b$	P_2^y	v_2
...
y_m	$b_{m1};P_{m1}^b$	$b_{m2};P_{m2}^b$	$b_{m3};P_{m3}^b$...	$b_{mn};P_{mn}^b$	P_m^y	v_m

Table 2 Probability scores a_{ij}

Parameter model	Probability scores a_{ij}					Probability
y_1	$a_{11};P_{11}^b$	$a_{12};P_{12}^b$	$a_{13};P_{13}^b$...	$a_{1n};P_{1n}^b$	P_1^z
y_2	$a_{21};P_{21}^b$	$a_{22};P_{22}^b$	$a_{23};P_{23}^b$...	$a_{2n};P_{2n}^b$	P_2^z
...
y_m	$a_{m1};P_{m1}^b$	$a_{m2};P_{m2}^b$	$a_{m3};P_{m3}^b$...	$a_{mn};P_{mn}^b$	P_m^z

$$J(x_i) = \sum_{i=1}^m v_i P_i^y \sum_{j=1}^n b_{ij} P_{ij}^b \tag{27}$$

subject to the restrictions (26),

$$\sum_{j=1}^n a_{ij} P_{ij}^a \geq A_i \min, \quad i = 1, \dots, m; \quad j = 1, \dots, n, \tag{28}$$

where $A_i \min$ —minimum allowable probability estimate for the i th parameter.

The exact calculation of probabilities P_i^y and P_i^z even with a small number of logical variables q_i is a very time-consuming task which, as was shown in [7], it is advisable to be solved approximately.

In determining the optimal SEMS, described LPM instead of probabilistic estimates of the solutions of Eqs. (20) and (21) use minimax estimation of the membership function solutions $\mu(y_i)$ and $\mu(z_i)$, which has been shown in [7], is calculated using the rules:

$$\mu(q_i \vee q_j) = \max\{\mu(q_i), \mu(q_j)\} \quad \text{and} \quad \mu(q_i \wedge q_j) = \min\{\mu(q_i), \mu(q_j)\}.$$

When solving a simple problem of synthesis of optimal SEMS, in which the control is set LIM, the choice of optimal solutions of systems (20) and (21) reduces to finding the maximum value of the functional form (22). This points compared b_i for management options are given in the form of an expert system of inequalities or logical rules. If the decision maker is a team of several experts, ballroom assessment may be given in some bands $[b_{i1}, b_{i2}]$. Then the functional index of the same quality

will be obtained in a certain interval $J(x_i) = [J_{51}, J_{52}]$, computed according to the rule of interval algebra

$$J_{51} = \sum_{i=1}^m v_i b_{1i}, \quad (29)$$

$$J_{52} = \sum_{i=1}^m v_i b_{2i}. \quad (30)$$

Therefore, choosing the best option in this case it is necessary to introduce the rules of their ranking based on interval assignment functional quality.

The problem of finding the best solution even more complicated if the decision-maker, which is a team of several experts, sets the interval, not only ballroom assessment, but the preference coefficients $v_i = [v_{i1}, v_{i2}]$. This functionality is the same quality index will be obtained in a range of $J_5(x_i) = [J_{51}, J_{52}]$, calculated in accordance with the rules of interval algebra by the following formulas:

$$J_{51} = \sum_{i=1}^m \min_{g_j} (v_{qi} b_{ji}), \quad (31)$$

$$J_{52} = \sum_{i=1}^m \max_{q_j} (v_{qi} b_{ji}). \quad (32)$$

To select the best alternative in this case also need to enter their ranking rules.

Most nonlinear problems MPOS has no solution acceptable complexity of the procedure. However, for problems of convex MPOS, i.e. for problems in which the set G is convex and preferences g_j , $j = 0, 1, 2, \dots, r$ —concave, developed an interactive method of solution. This procedure allows for consistent requirements and alternatives to obtain a local preference information g_j on respective pairs of options to get ε approximate solution. When expanding the concept of “optimization of binary relation” and expanding the concept of “ ε in g_0 optimal solution”, it is possible to generalize the method of solution of the convex problem MPOS to arbitrary (non-reflexive, incomplete and not transitive) binary relations [3]. It is expected that significant progress in addressing the challenges MPOS be able to achieve through the use of neural networks.

4 The Generalized Mathematical Programming (GMP)

A generalized mathematical programming (GMP)—a methodology that applies the principles and methods of traditional mathematical programming in the case of vector and vector criteria limits. Unlike traditional optimization theory GMP

schemes do not assess the admissibility and quality of each alternative, and approach to the solution in the process of comparing pairs of alternatives. Optimization and restrictions on weapons of mass destruction are interpreted in terms of preference relations.

As used GMP approach to choice-making takes into account the preferences of decision-makers. It is assumed that each participant decision-making process induces a set of alternatives, some binary relations and stores them in the process of solving the problem. In contrast to the problem MPOS optimization method generalized mathematical programming (GMP) corresponds to the selection system, based on a comparison of its characteristics with the characteristics of an ideal system, not their parameters.

When solving a simple problem of synthesis of optimal SEMS, in which the control is given LPM, formally record the model GMP is:

Model 1 $\forall q_i, P(q_i) = 1$, then:

$$f_0(x_0)g_0.f_0(x_s) \text{ at } f_j(x_0)g_ju_j, f_j(x_s)g_ju_j, j = 1, \dots, r, (x_0, x_s) \in G \subseteq R^n, \tag{33}$$

where $f_i(x_0)$ and $f_i(x_s)$ —asked some functions R_j^m preferences of decision-makers; $i = 0, 1, \dots, r$; u_j - fixed vector in R_j^m restrictions set by decision-makers; $g_j, j = 0, 1, 2, \dots, r$ —binary relations on $G \subseteq R^n$.

In this case, the model will be optimal x_0 , for which the condition (33).

Model 2 $\forall q_i, P(q_i) < 1$, then:

$$f_0(x_0)g_0.f_0(x_s) \rightarrow opt \text{ at } f_j(x_0)g_ju_j, f_j(x_s)g_ju_j, j = 1, \dots, r, (x_0, x_s) \in G \subseteq R^n, \tag{34}$$

In Model 1, GMP reduces to the construction of optimal binary relations g_j .

In Model 2 GMP finding optimal SEMS after building binary relations g_j and selection of candidates for optimality based on their defined boundary probabilities or membership functions for type Eqs. (19) and (20) requires further analyze complex linguistic expressions, which are attributes (w_i) or formed from attributes (w_i) logical variables q_i , which are components of the vector Q in the logical expressions (20) and (21), characterized by an optimal LPM (g_0) and the appropriate limits (g_j) objects. At the same time, if these linguistic expressions can be reduced to a logical expression of the form:

$$F_i = C_0^i W, \tag{35}$$

$$S_i = C_j^i W \tag{36}$$

where: F_i —vector logical variables y_j , characterizing the optimized characteristics of the model, S_i —vector logical variables z_j , characterized by a limited characteristics of the model, W —a vector of logical variables, components of which are

logical variables w_i , attributes which can be only their probability P_i^v , or their membership functions $\mu(w_i)$, C_0^i and C_j^i —identification strings containing elements 0 and 1 in a predetermined order, (for example $C_0^i = |1\ 0\ 0\ 1\ 0\ \dots\ 1|$ and $C_j^i = |0\ 1\ 1\ 0\ \dots\ 0|$) the dimension of the vector W and rows C_0^i , C_j^i match, then the solution can be automated in software artificial intelligence [7].

Algorithm optimization Model 2 GMP comprises the following steps:

1. Construction of the binary relationship $f_0(x_0)g_0 f_0(x_0)$, $f_j(x_0)g_j u_j$, $f_j(x_0)g_j u_j$.
2. The construction of logical expressions $C_0 Q = Y$, $C_j Q = Z$.
3. The calculation of probabilities P_i^y, P_i^z and a membership function $\mu(y_i)$, $\mu(z_i)$.
4. If evaluation of the characteristics of the model close to the standard b_i and a_i assessment limiting characteristics defined faces decision-makers precisely the selection of models for which the following conditions:

$$a_i \geq a_{imin} \ (i = 1, \dots, m); P_i^z \geq P_{imin}, \quad \text{or} \quad \mu(z_i) \geq \mu_{imin} \ (i = 1, \dots, m);$$

$$J(x_i) = \sum_{i=1}^m v_i b_i P_i^y \geq J_{imin}, \quad \text{or} \quad J(x_i) = \sum_{i=1}^m v_i b_i \mu_i(y) \geq J_{imin}$$

5. If the characteristics of the model valuation close to the standard b_i and assessment limiting characteristics of persons are given a_i decides not exactly corresponding with some probability P_{ij}^b and P_{ij}^a (see Tables 1 and 2), or membership functions $\mu_{ij}(b)$ and $\mu_{ij}(a)$, the selection of models for which the following conditions:

$$\sum_{j=1}^n a_{ij} P_{ij}^a \geq A_{imin}, \quad \text{or} \quad \sum_{j=1}^n a_{ij} \mu_{ij}(a) \geq A_{imin} \ (i = 1, \dots, m; j = 1, \dots, n);$$

$$P_i^z \geq P_{imin}, \quad \text{or} \quad \mu(z_i) \geq \mu_{imin} \ (i = 1, \dots, m);$$

$$J(x_i) = \sum_{i=1}^m v_i P_i^y \sum_{j=1}^n b_{ij} P_{ij}^b \geq J_{imin}$$

or

$$J(x_i) = \sum_{i=1}^m v_i \mu_i(y) \sum_{j=1}^n b_{ij} \mu_{ij}(b) \geq J_{imin}$$

6. For the selected models to build logical expressions:

$$F_i = C_0^i W, \quad S_i = C_j^i W$$

7. The calculation of probabilities P_i^f and P_i^s , or a membership function $\mu(f_i)$ and $\mu(s_i)$.
8. If the assessment proximity b_i and a_i are set limiting the assessment individuals decision-makers exactly the model search, for which

$$J(x_i) = \sum_{i=1}^m v_i b_i P_i^f \rightarrow \max \quad \text{or} \quad J(x_i) = \sum_{i=1}^m v_i b_i \mu_i(f) \rightarrow \max$$

under the following conditions:

$$a_i \geq a_{imin} (i = 1, \dots, m); \quad P_i^s \geq P_{imin}, \quad \text{or} \quad \mu(s_i) \geq \mu_{imin} (i = 1, \dots, m)$$

9. If the assessment proximity b_i and a_i are set limiting the assessment individuals decides not exactly corresponding with some probability, P_{ij}^b and P_{ij}^a (see Tables 1 and 2) or membership functions $\mu_{ij}(b)$ and $\mu_{ij}(a)$, the search for a model for wherein:

$$J(x_i) = \sum_{i=1}^m v_i P_i^f \sum_{j=1}^n b_{ij} P_{ij}^b \rightarrow \max, \quad \text{or}$$

$$J(x_i) = \sum_{i=1}^m v_i \mu_i(f) \sum_{j=1}^n b_{ij} \mu_{ij}(b) \rightarrow \max$$

under the following conditions:

$$\sum_{j=1}^n a_{ij} P_{ij}^a \geq A_{imin}, \quad \text{or} \quad \sum_{j=1}^n a_{ij} \mu_{ij}(a) \geq A_{imin} \quad (i = 1, \dots, m; j = 1, \dots, n);$$

$$P_i^s \geq P_{imin}, \quad \text{or} \quad \mu(s_i) \geq \mu_{imin} \quad (i = 1, \dots, m)$$

When solving a simple problem of synthesis of optimal SEMS, in which the control is set LLM, formally record the problem of GMP is:

Problem 1 If $\forall q_i, \mu(q_i) = 1$, then:

$$f_0(x_0) g_0 f_0(x_3) \text{ at } f_j(x_0) g_j \mu_j, f_j(x_3) g_j \mu_j, \quad j = 1, \dots, r, \quad (x_0, x_3) \in G \subseteq R^n, \quad (37)$$

where $f_i(x_0)$ and $f_i(x_3)$ —asked some functions R_j^n preferences of decision-makers; $i = 0, 1, \dots, r$; u_j —fixed vector in R_j^m restrictions set by decision-makers; $g_j, j = 0, 1, 2, \dots, r$ —binary relations on $G \subseteq R^n$.

In this case, the model will be optimal x_0 , for which the condition (37).

Problem 2 If $\forall q_i, \mu(q_i) < 1$, then:

$$f_0(x_0) g_0 f_0(x_3) \rightarrow \text{opt at } f_j(x_0) g_j \mu_j, f_j(x_3) g_j \mu_j, \quad j = 1, r, \quad (x_0, x_3) \in G \subseteq R^n, \quad (38)$$

In this case, there will be several models, satisfying (37) with a different membership function, and to select the optimal model is required to analyze other linguistic attributes of the logical variables q_i .

In Problem 1 GMP optimization reduces to the construction of optimal binary relations g_j .

In task 2 GMP finding optimal logical-linguistic ISC after building binary relations g_j and selection of candidates for optimality based on their defined boundary membership functions require further analyze complex linguistic expressions, which are attributes (w_i) or generated attribute (w_i) logical variables q_i , which are components of the vector \mathbf{Q} in the logical expressions of the form (20) and (21), characterized by an optimal logical-linguistic ISC(g_0) and the appropriate limits (g_j).

Thus, if the said linguistic expressions can be reduced to the form of logical expressions (35) and (36), then a solution as in the case of LPM can be automated by software AI [7].

The optimization algorithm in the Problem 2 GMP comprises the following steps:

10. Construction of the binary relationship $f_0(x_0)g_0, f_0(x_0), f_j(x_0)g_j\mu_j, f_j(x_0)g_j\mu_j$
11. The construction of logical expressions $\mathbf{C}_0\mathbf{Q} = \mathbf{Y}, \mathbf{C}_j\mathbf{Q} = \mathbf{Z}$
12. Calculation of the membership functions $\mu(y_i)$ and $\mu(z_i)$
13. If the characteristics of the model valuation close to the standard b_i and a_i assessment limiting characteristics defined faces decision-makers precisely the selection of models for which the following conditions:

$$a_i \geq a_{imin} \quad (i = 1, \dots, m); \quad \mu(z_i) \geq \mu_{imin}, \quad J(x_i) = \sum_{i=1}^m v_i b_i \mu(y_i) \geq J_{imin},$$

14. If the characteristics of the model valuation close to the standard b_i and assessment limiting characteristics of persons are given a_i decides not exactly with some relevant membership functions $\mu(b_{ij})$ and $\mu(a_{ij})$, the selection of models for which the following conditions:

$$\sum_{j=1}^n a_{ij} \mu(a_{ij}) \geq A_{imin}, \quad \mu(z_i) \geq \mu_{imin}, \quad (i = 1, \dots, m);$$

$$J(x_i) = \sum_{i=1}^m v_i \mu(y_i) \sum_{j=1}^n b_{ij} \mu(z_j) \geq J_{imin} \quad (i = 1, \dots, m; j = 1, \dots, n);$$

15. For selected models build logical expressions:

$$\mathbf{F}_i = \mathbf{C}_0^i \mathbf{W}, \quad \mathbf{S}_i = \mathbf{C}_j^i \mathbf{W}$$

16. If the evaluation of proximity b_i and a_i are set limiting the assessment individuals decision-makers exactly the model search, for which

$$J(x_i) = \sum_{i=1}^m v_i b_i \mu(f_i) \rightarrow \max$$

under the following conditions:

$$a_i \geq a_{imin} \quad (i = 1, \dots, m); \quad \mu(s_i) \geq \mu_{imin}, \quad (i = 1, \dots, m)$$

- Static error

$$\delta = |x_y - x_3|/x_3, \quad (39)$$

where: x_y and x_3 —steady and predetermined values;

- Time of transition

$$t_p = t_{min}/\delta \leq \delta_\delta, \quad (40)$$

where δ_δ —permissible value of static error;

- deregulation

$$\sigma = |x_{max} - x_y|/x_y \quad (41)$$

Then, as previously MPOS, introduced scores of these parameters and their preference coefficients for comparable variants. Then made their ranking and selection of the best options.

When compared trajectory change output parameters of various embodiments SEMS with ideal path (2), they are close to ideal can be estimated by the following values [5]:

- Mean square error (MSE)

$$E_1 = \frac{1}{n} \sum_{i=1}^n (y_i^u - y_i^j)^2, \quad (42)$$

where y_i^u and y_i^j — i th coordinates ideal trajectory and j th the comparable ISU, n —the number of points carried trajectories compared (usually split evenly trajectory of the X -axis);

- Modified MSE

$$E_2 = \frac{1}{n} \sum_{i=1}^n ((y_i^u - y_i^j)/\varepsilon)^2, \quad (43)$$

where $0 < \varepsilon < 2$ reliability factor assessment, depending on the method of interpreting the results of the comparison (the sign, ordinal, and others.);

- Generalized MSE

$$E_3 = \frac{1}{n} \sum_{i=1}^n k_i (y_i^u - y_i^j)^2, \quad (44)$$

where k_i —weight of i th coordinate trajectory;

– The absolute cumulative error

$$E_4 = \sum_{i=1}^n |y_i^u - y_i^j|; \tag{45}$$

– Maximum error

$$E_5 = \max |y_i^u - y_i^j|; \tag{46}$$

– is the average of the relative variation

$$E_6 = \sum_{i=1}^n (y_i^u - y_i^j)^2 / \sum_{i=1}^n (y_i^u - \langle y_i^j \rangle)^2, \tag{47}$$

where $\langle y_i^j \rangle$ evaluation of the average value of the coordinates y_i^j . The value E_6 provides a good score close to the case when the ideal trajectory parallel to the axis X (Fig. 2).

In the case where the compared characteristics of various embodiments are multidimensional SEMS figures last step can be divided into some number of two-dimensional shapes (curves) for each of the obtained pieces to use estimates of the proximity type (42)–(47).

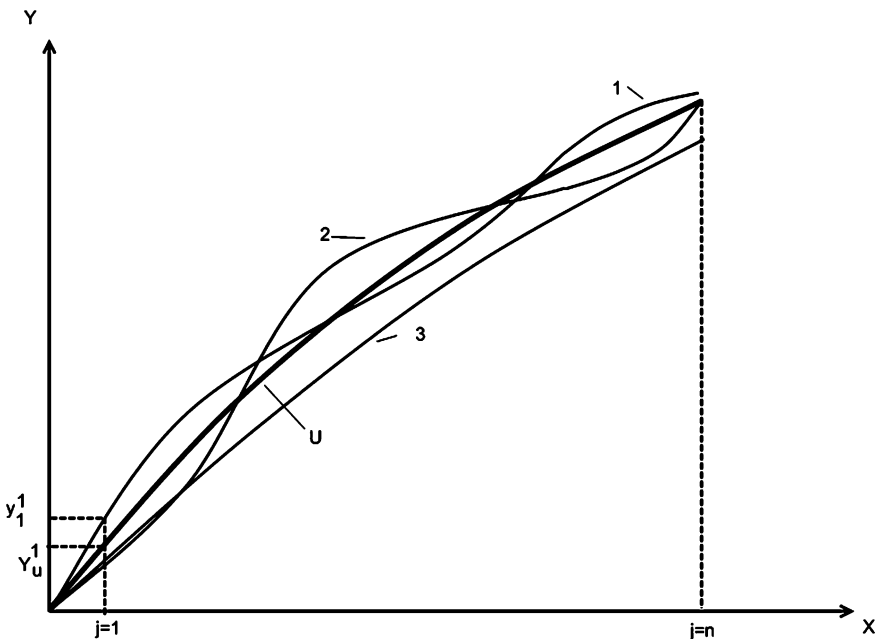


Fig. 2 The trajectories of change of output parameters. U ideal SEMS, 1 option 1 SEMS, 2 option 2 SEMS, 3 Option 3 SEMS

Obviously, the task of GMP can go to MPOS tasks and task management in a LPM and LLM. This approach is the most preferred as to obtain an acceptable complexity of solving the problems of GMP is usually necessary that the characteristics of the vector function $f_j(x)$, the domain of the solution G and used binary relations g_j satisfy some special requirements. Thus, the design methods of analysis problems GMP can be built for cases where the components of the vector function $f_j(x)$ —straight or concave function, G —convex set, and the binary relations g_j —continuous, concave, monotonous and regular preferences [3]. Such models are called GMP models generalized convex programming (GCP). Meeting the challenges GMP is currently associated with the use of neural networks and media such as A-life [6].

5 Multistep Generalized Mathematical Programming

In the case where the function selection (FS) determined preferences of decision-makers, changes in the operation of SEMS, you must use a multi-step in the optimization of a multistep generalized mathematical programming (MGMP)

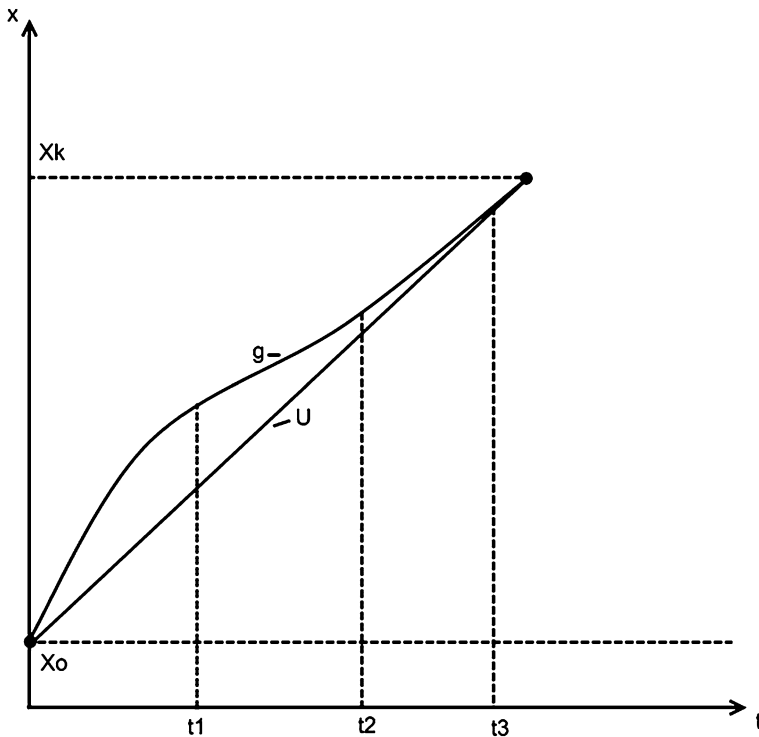


Fig. 3 Simplest task of optimizing the SEMS. U the ideal trajectory, g admissible trajectory

allows you to implement an arbitrary FS on a finite set of options. Therefore MGMP scheme is a set of consecutive tasks GMP, each of which corresponds to a fixed presentation of the set of ideal characteristics of X . Of course, the computational complexity of solving MGMP rapidly increases with the number of steps.

The simplest task of optimizing the SEMS is a problem of transition from one point of the phase space X_0 to another X_k quite remote (Fig. 3), at least when it approaches the requirements to such parameters of the transition process, as the deregulation σ and the error δ and are subject to change and at the same time their coefficients and significance ν_σ and ν_δ . In this case, the control can be divided into a number of stages (steps), and at each step to change the requirements to the parameters or mean perfect transition. At each step, you will select its function and, therefore, an option will change the optimal control.

6 Conclusion

If the developer of a SEMS, has one goal and this goal can be formally defined as a scalar function, i.e., quality criterion of choice, the task of choosing the optimal solution can be formalized and described a model of mathematical programming (MP). In other cases, you should use mathematical programming in an ordinal scale (MPOS), generalized mathematical programming (GMP) or multi-step tasks generalized mathematical programming (MGMP).

If you have a developed SEMS uncertainties logical-probabilistic, logical-linguistic and logical-interval type search for the optimal SEMS can be carried out by means of mathematical programming, when there is a fundamental possibility of constructing a scalar quality criterion, including of the attributes (probability, of membership functions or intervals) logical variables. The quality of the optimization will be mainly determined by the proper construction of a binary relation, describing the measure of closeness designed to SEMS perfect. This can be time-consuming and difficult task, often associated with the solution of a number of logical problems. The quality of formulation and solution of these problems depends on the experience and skills of the developer, as the decision makers (decision maker). To increase objectivity in the evaluation of the optimal model it is advisable to make a collective decision-maker with the involvement of the customer to work on the construction of a binary relationship.

If you are using when searching for the optimum SEMS methods of mathematical programming in an ordinal scale (MPOS), generalized mathematical programming (GMP) and multistep generalized mathematical programming (MGMP) pass from the quantitative to the ordinal scales, i.e. moving away from models that require functional task, defining the objectives and constraints of the problem, a model taking into account the preferences of persons involved in the selection decision. In this case, the parameters are estimated MPOS options SEMS, and

MGMP or GMP and their characteristics. The practical solution of such problems are currently associated with the use of neural networks and media types A-life.

References

1. Vaisbord, E.M., Zhukovsky, V.I.: Introduction to the Differential Game of Several Persons and Their Application, 304 p. Sovetskoe Radio, Moscow (1980)
2. Isaacs, R.: Differential Games, 479p. Mir, Moscow (1967)
3. Yudin, D.B.: Computational Methods of Decision Theory, 320p. Nauka, Moscow (1989)
4. Tobacco, D., Kuo, B.: Optimal Control and Mathematical Programming, 280p. Nauka, Moscow (1975)
5. Gorodetskiy, A.E., Tarasova, I.L.: Control and Neural Networks, 312p. Publishing House of the Polytechnic. University Press, SPb (2005)
6. Gorodetskiy, A.: Foundations of the Theory of Intelligent Control Systems, 313c. LAP LAMBERT Academic Publishing GmbH @ Co. KG, (2011)
7. Gorodetskiy, A.E., Tarasova, I.L.: Fuzzy Mathematical Modeling Badly Formalized Processes and Systems, 336p. Publishing House of the Polytechnic. University Press, SPb (2010)

Logical Analysis of Data and Knowledge with Uncertainties in SEMS

B.A. Kulik and A. Ya. Fridman

Abstract Developers of intelligence systems to control SEMS often face situations when incompleteness of their knowledge results in uncertain definitions of initial data (for instance, as some hypotheses to be proved or refuted, possible incompatible variants or special cases to be generalized, or probabilistic models). To investigate and consider such uncertainties, many researchers in artificial intelligence use non-classical logics, which violate some laws of algebra of sets. Conversely, in the given paper we propose techniques to analyze data and knowledge with uncertainties within the classical approach by using our earlier developed n -tuple algebra.

Keywords Smart electromechanical systems · Uncertainties · Hypotheses · Modal logic · Classical logics · Abductive conclusions · N-Tuple algebra · Logical-Probabilistic analysis

1 Introduction

To represent uncertainties during logical analysis of data and knowledge in automatic control systems for SEMS, two kinds of models are often used; they are quantitative models estimating the degree of uncertainties for some events or statements as numbers and nonquantitative (logic-semantical) methods where such uncertainties are expressed as hypotheses to be proved or refuted, possible incompatible variants or

B.A. Kulik (✉)

Institute of Problems in Mechanical Engineering, Russian Academy of Sciences,
61 Bol'shoi pr, St. Petersburg, Russia 199178
e-mail: ba-kulik@yandex.ru

A.Ya.Fridman

Institute for Informatics and Mathematical Modelling,
Kola Science Centre of Russian Academy of Sciences, Murmansk, Russia
e-mail: fridman@iimm.ru

special cases to be generalized. Quantitative methods exploit fuzzy and logic-probabilistic modelling techniques [1, 2]. Their application domains and capabilities are fairly described in the monograph [3].

To model logic-semantical uncertainties in artificial intelligence, many authors propose usage of non-classical logics, nonmonotonic and modal logics in particular [4–6]. The classical logic (CL) is considered poorly suitable for analysis of such uncertainties. In the authors' opinion, this statement is not grounded enough. In the given chapter, we describe some CL-based techniques to analyze logic-semantical uncertainties and substantiate appropriateness of the classical approach to logical analysis in some kinds of reasoning where some researchers advise applying of non-classical logics (NCLs). For example, the following tasks belong to such cases:

- (1) analysis of hypotheses and abductive conclusions;
- (2) modeling of some kinds of reasoning where nonmonotonic logics are often used;
- (3) modeling of some kinds of reasoning where modal logics are often used;
- (4) modeling of the situations where uncertainty of variables (attributes) results from their interval estimates or definitions as lists of possible values.

As a methodological basis for CL's usage in modelling of "non-classical" kinds of reasoning, we propose our earlier developed n -tuple algebra (NTA) [7]. One of the proved NTA features is the possibility to use logic-probabilistic modelling not only for systems with two admissible states [2] (we can model such systems by formulas of the propositional calculus), but for systems with any number of admissible states as well. Besides, this paper introduces the results obtained within the above-mentioned research domain.

2 Features of the Classical Approach to Logical Analysis

One of the main arguments to substantiate applicability of non-classical approach and even level it with the classical one arises from the axiomatic (formal) method that became generally acknowledged in the 20th century and was applied to the theoretical construction of logic. According to this method, all conventional variants of logics are built on the basis of some allegedly unprovable statements (axioms). As the axioms are accepted by agreement, if certain rules (independence, completeness, etc.) are observed, it is not easy to prefer this or that choice of a logical system. Moreover, NCLs usage often induces difficulties in interpretation and ambiguities in choosing among numerous kinds of logics developed to model uncertainties and defeasible reasoning. That is why a question appears whether CL is applicable for such cases. Below we answer this question positively.

Within the modern conceptions, CL differs from NCLs in contents of the axioms and inference rules. We can treat these differences in another way, if we analyze characteristic violations of laws of algebra of sets and Boolean algebra, which are typical for NCLs. For instance, fuzzy logic breaks laws of non-contradiction and excluded

middle, nonmonotonic logics violate the monotony law, some kinds of multivalued logics do not provide uniqueness of negation, and so on. Many of those “violations” have a rigorous mathematical justification for a certain interpretation. For instance, laws of fuzzy logic completely correspond to algebra of multisets, to the set of integers partially ordered by divisibility, to minimax models, etc. We can suppose that correctness of the choice among certain logics depends on the degree of adjacency between the mathematical interpretation of a logic and the given model of reasoning. In particular, the logic completely complying with the laws of algebra of sets (that is CL) seems to be preferable for modelling sets and relations. Below, we propose a substantiation for the laws of algebra of sets that corresponds to the laws of Boolean algebra and to the CL’s laws therefore. Let us call this substantiation a *direct-search* one.

Suppose, an algebra of sets is determined by definitions of some basic operations (intersection, union and complement) and relations (equality, inclusion). Semantics of these operations and relations is clear, it is adequate to many cases when the logic-semantical analysis is used. For example, a set of objects featured with a combination of attributes P and Q can be defined as the intersection of the sets of objects having every value from this combination. To ground laws containing two sets X and Y , let us describe all possible relations between them. For simplification and visualization, we can draw an Euler diagram (see Fig. 1) representing these sets and the universe (U) enclosing them:

In the diagram, we separate partitions a, b, c and d , which have no inner borders. This way we construct *decomposition* of the universe into non-overlapping (elementary) sets. Such decomposition allows for representing any set in Fig. 1 as a union of the elementary sets. Then we have $U = \{a, b, c, d\}$; $X = \{a, b\}$; $Y = \{b, c\}$. Let us suppose also that some (or all) sets can be absent. Thus, we consider all possible variants of relations between two arbitrary sets. It is provable for the universe of 4 elements that there only exist 16 such variants including Gergonne relations. The diagram in Fig. 1 visualizes all relations between two sets, and, on the other hand, it is possible to prove that four elements are enough to represent these relations.

Evidently, *the mentioned relations do not depend on the real composition and number of elements in the sets X, Y and U* . We will accept these relations as the given data and prove one of De Morgan’s laws, namely the law $\overline{X \cap Y} = \overline{X} \cup \overline{Y}$.

By operations of algebra of sets, we can get:

- (1) $X \cap Y = \{b\}$;
- (2) $\overline{X \cap Y} = \{a, c, d\}$;
- (3) $\overline{X} = \{c, d\}$;
- (4) $\overline{Y} = \{a, d\}$;

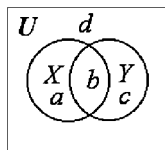


Fig. 1 Euler diagram for two sets with the universe

$$(5) \quad \overline{X \cup Y} = \{a, c, d\};$$

(6) comparing (2) and (5), we conclude that $\overline{X \cap Y} = \overline{X \cup Y}$, Q.E.D.

Let us prove the contraposition law: if $X \subseteq Y$, then $\overline{Y} \subseteq \overline{X}$. The diagram in Fig. 1 does not work immediately since the set X is not included into the set Y as this law requires. However, if we delete the area a , we provide the necessary inclusion $X \subseteq Y$. After this deletion, the composition of sets becomes as follows: $U = \{b, c, d\}$; $X = \{b\}$; $Y = \{b, c\}$. To prove the contraposition law, we need:

$$(1) \quad \text{calculate } \overline{X} = \{c, d\};$$

$$(2) \quad \text{calculate } \overline{Y} = \{d\};$$

(3) comparing \overline{X} and \overline{Y} , we can see that $\overline{Y} \subseteq \overline{X}$, Q.E.D.

The presented proofs are not exhaustive. For instance, to prove De Morgan's law comprehensively, we need to consider some more cases as well (when the sets X and Y do not overlap, when one of them is included into the other, etc.). The total number of cases is 16, and we can prove this law for all of these cases, if we can spare some time for this.

To prove the laws containing three sets (the distributive property gives an example of such laws), we can build a similar system for these sets. We will not need more complicated systems as the axiomatic construction of algebra of sets and the propositional calculus does not require for greater number of objects.

Now we can conclude that **laws of algebra of sets can be proved without any axioms**, just by definitions for operations of this algebra and by evident equality or inclusion checks for two sets where we compare their elements. To our minds, the main advantage of the introduced direct-search technique compared to the axiomatic one is in absence any space for posers like "Why have we chosen these axioms?" or "How can we be sure in their total trueness?". Just such questions give an indirect substantiation for applying non-classical logics with breaking some laws of algebra of sets.

3 N-Tuple Algebra

N -tuple algebra (NTA) is an algebra of arbitrary n -ary relations. In NTA, such relations can be expressed as four types of structures called *NTA objects*. Every NTA object is immersed into a certain space of *attributes*. Names of NTA objects contain an identifier followed by a sequence of attributes names in square brackets; these attributes determine the *relation diagram* in which the NTA object is defined. For example, $R[XYZ]$ denotes an NTA object defined within the space of attributes X , Y and Z .

NTA objects contain n -tuples of sets and provide a condensed representation of n -ary relations. When necessary, by means of specific algorithms these objects can be transformed into ordinary n -ary relations containing sets of n -tuples called *elementary n -tuples* in NTA. NTA objects defined on the same relation diagram are called *homotopic* ones. NTA objects look like matrices having subsets of

corresponding attributes (**components**) rather than elements as their cells. Let us introduce main NTA structures, namely *C*-systems and *D*-systems.

A *C*-system is denoted as a matrix in square brackets. It contains set components. For example, $R[XYZ] = \begin{bmatrix} A_1 & * & A_3 \\ B_1 & B_2 & * \end{bmatrix}$ is a *C*-system consisting of subsets of corresponding attributes that is $A_1 \subseteq X$, $A_3 \subseteq Z$, etc. The component “*” is called the *complete component*; it equals to the whole domain of the corresponding attribute in the relation diagram. For instance, the value of * in the first row of $R[XYZ]$ is the domain of the attribute *Y*. $R[XYZ]$ can be transformed into an ordinary relation (i.e. a set of elementary *n*-tuples) as follows: $R[XYZ] = (A_1 \times Y \times A_3) \cup (B_1 \times B_2 \times Z)$.

C-systems are convenient for representing disjunctive normal forms (DNFs) of unary predicates. A one-line *C*-system is called a *C*-*n*-tuple. In logic, a *C*-*n*-tuple corresponds to a separate conjunct in a DNF.

D-systems model conjunctive normal forms (CNFs) of unary predicates. We denote a *D*-system as a matrix of component sets framed with reversed square brackets. *D*-systems provide easy calculating of *C*-systems’ complements. To do so, it is enough to replace components of a *C*-system with their complements. The component \emptyset is called the **empty component** since it equals to the empty set and models the complement of the component *. The components \emptyset and * are called **dummy components**.

For instance, the *D*-system $\bar{T}[XYZ] = \begin{bmatrix} \bar{A} & \emptyset & \bar{C} \\ \bar{D} & \bar{E} & \emptyset \end{bmatrix}$ is the complement of the *C*-system $T[XYZ] = \begin{bmatrix} A & * & C \\ D & E & * \end{bmatrix}$. It can be transformed into an ordinary relation by the formula:

Alike a *C*-system, a one-line *D*-system is called a *D*-*n*-tuple. In logic, a *D*-*n*-tuple models a separate disjunct of a CNF.

$$\bar{T}[XYZ] = ((\bar{A} \times Y \times Z) \cup (X \times Y \times \bar{C})) \cap ((\bar{D} \times Y \times Z) \cup (X \times \bar{E} \times Z)).$$

Alike a *C*-system, a one-line *D*-system is called a *D*-*n*-tuple. In logic, a *D*-*n*-tuple models a separate disjunct of a CNF.

Calculations of unions and intersections for *C*- and *D*-structures are specific; you can find their description in [7]. To process NTA objects defined on different diagrams, we have developed some **operations on attributes**, addition of a dummy attribute (+Attr) and elimination of an attribute (-Attr) in particular. The operation +Attr corresponds to the **rule of generalization** in predicate calculus. This rule states that formula $\forall x(A)$ is deducible from formula *A*, if the latter does not contain the variable *x*. Thus, the operation +Attr does not change the semantics of any relations because any value of a variable absent in a relation cannot change the sense of a statement. For example, if a relation contains data on names, positions and ages of personnel, any color of eyes is admissible since the relation has no information about it. This operation upon any NTA object simultaneously adds the name of a new attribute into the relation diagram and adds a new column with dummy components into the corresponding place of a matrix representation.

For example, if the C -system $R_k[XZ] = \begin{bmatrix} A_1 & A_3 \\ B_1 & B_3 \end{bmatrix}$ models the predicate $R_k(x, z)$, adding the dummy attribute Y into $R_k[XZ]$ models the formula $\forall y(R_k(x, z))$. In NTA, adding the attribute gives the C -system $+Y(R_k[XZ]) = \begin{bmatrix} A_1 & * & A_3 \\ B_1 & * & B_3 \end{bmatrix}$. Consider that dummy components $*$ are used in C -structures, and dummy components \emptyset are used in D -structures.

Elimination of an attribute ($-Attr$) is done in the following way: a column is removed from an NTA object, and the corresponding attribute is removed from the relation diagram. The sense of this operation depends on the type of an NTA object. Let the NTA object $R[XYZ]$ models the logical formula $F(x, y, z)$. If $R[XYZ]$ is C -system, then $-Y(R[XYZ])$ equals to the formula $\exists y(F(x, y, z))$, and if $R[XYZ]$ is a D -system, then $-Y(R[XYZ])$ models the formula $\forall y(F(x, y, z))$. **Projections of NTA objects** are calculated by eliminating certain attributes from C -systems. All mentioned statements have exhaustive proofs.

The operation $+Attr$ is often used to reduce some different-type NTA objects to the same relation diagram by adding the missed attributes. Then we can perform all necessary operations and checks by means of standard NTA algorithms. Considering this, we have introduced *generalized operations* (\cap_G , \cup_G and complement). They differ from similar operations of algebra of sets by the only feature: NTA objects are reduced to the same relation diagram before execution of these operations, which are semantically equal to logical connectives: disjunction, conjunction and negation correspondingly. *Generalized relations* (\subseteq_G \neq_G) are defined as well. Algebra of n -ary relations with the mentioned generalized operations and relations is proved to be isomorphic to the ordinary algebra of sets. This way we have eliminated the restriction in the theory of relations stating that algebra-of-sets laws are only applicable to the relations defined upon the same Cartesian product.

Below, we describe capabilities of the classical approach to logical analysis of such kinds of reasoning where many authors ([4–6] and others) propose usage of NCLs.

4 Hypotheses and Abductive Conclusions

For some reason, it is believed that any mention of hypotheses in logical analysis of systems and reasoning stipulates usage of NCLs. Arguments for this seem to arise from the conviction that the classical approach is only applicable to the systems containing just indisputably true statements. However, such systems are rather exceptions than rules in subject domains for artificial intelligence. Moreover, hypotheses as statements are formally indistinguishable from the statements expressed by means of classical logic. We see a solution of this problem in development of formal methods to prove or deny correctness of hypotheses.

In [7, 8], collisions analysis is proposed with this purpose. Collisions are generally defined as formally recognizable situations resulting in violations of certain constraints accepted for the given system. The impossibility of “extinction” for certain values of a given attribute after incorporation the analyzed hypothesis into the set of axioms gives an example of such a constraint.

NTA techniques to analyze hypotheses and search for abductive conclusions are thoroughly described in [8]. Here we will present just a summary of the obtained results. To receive them better, it is reasonable to start from basics of deductive analysis in NTA. Theoretical principles of NTA provide solving the following problems of deductive analysis [7].

- (1) *Problem of correctness check for an alleged consequence B from the given premises A_i .*
- (2) *Problem of derivation of possible consequences from the given premises A_i considering certain semantical constraints, for instance, presence of given variables or their combinations in a consequence, deriving a consequence with the minimal number of significant variables, etc.*

Unlike other logical systems that solve such problems by using inference rules with hardly optimized order of their implementation, NTA solves these problems by means of certain standard algorithms. To do so, we transform classical logic’ formulas expressing premises and consequences into NTA objects and subject these objects to generalized operations and checks of equality ($=_G$) or inclusion (\subseteq_G). The transition to the algebraic representation becomes clearer, if we consider that NTA objects model scope of truth for logical formulas. Then the correctness proof for an alleged consequence B from the premises A_i (the consequence and the premises can be different-type NTA objects) requires for calculation of generalized intersections and check the following generalized inclusion:

$$(A_1 \cap_G \dots \cap_G A_n) \subseteq_G B \tag{1}$$

Considering (1), the problem of derivation of possible consequences $\{B_j\}$ from the given premises A_i can be solved in NTA with using the relation that must be true for every B_j : $A \subseteq B_j$, where $A = A_1 \cap_G \dots \cap_G A_n$. Thus, any correct consequence from premises A_i can be modeled by an NTA object representing a superset of A . Techniques to find such objects satisfying certain limitations are expounded in [7].

Let us analyze processing of hypotheses. Suppose, we have the above-introduced system of logical inference and some statements H_k considered as hypotheses. Features of hypotheses are as follows. First, they must differ from both axioms and consequences. So, the relationship $(A_1 \cap_G \dots \cap_G A_n) \subseteq_G H_k$ must be false for any hypothesis H_k . Second, the hypotheses can be accepted or refuted basing on some criteria. If a hypothesis is supposed to be an axiom, the whole system of logical inference can change significantly. This can result in violations of some limitations, which have semantical sense mostly. For instance, if a system contains two statements like “all birds can fly” and “all birds cannot fly”, it does not

lead to inconsistency of the system since the formal contradiction appears from another pair of statements, namely “all birds can fly” and “some birds cannot fly”. Thus, the first pair of statements leads to the conclusion that the set of birds equals to the empty set. Since we discuss birds on our planet, this result can be estimated as a semantical inconsistency or a discrepancy with facts. We have proposed to denote and treat violations of such (semantical or structural) limitations after adding some hypotheses into the set of axioms as *collisions*, more details are in [7, 8].

Now we proceed with techniques to formalize abductive conclusions in NTA.

Abduction is forming of an explanatory hypothesis when we know some of the premises and an estimated consequence that is confirmed with facts or reasonable arguments, but a formal check does not infer it from the given premises. For example, abduction is used during diagnostics.

Let us now define abduction formally. If B is an estimated consequence of the premises A_1, \dots, A_n expressed as NTA objects and the statement $A \subseteq_G B$ is known to be false (once again, $A = A_1 \cap_G \dots \cap_G A_n$), then a formula H is an admissible abductive conclusion when the two following conditions are met:

- (i) H is a hypothesis (i.e. $A \subseteq_G H$ is false) and $H \cap_G A$ is not empty;
- (ii) $(H \cap_G A) \subseteq_G B$, that is, adding H into the system of premises results in deducibility of the estimated consequence B .

Algorithms to search for abductive conclusions are described in [8].

5 Defaults and Nonmonotonicity of Inference

In the classical variant of the mathematical logic, monotonicity is an inseparable property of logical inference. The essence of monotonicity is as follows. If a set of premises Γ allows to infer a statement B , the same statement can be inferred after adding any premise (for example, A) to Γ .

In algebra of sets, the property of monotonicity is expressed by the following law: if the correlation $G \subseteq B$ is true for the given sets G and B , then $(G \cap A) \subseteq B$ is true for any A .

The proof of this law is simple. According to definition of intersection of sets, $(G \cap A) \subseteq G$. Using the law of transitivity for $(G \cap A) \subseteq G$ and $G \subseteq B$, we infer $(G \cap A) \subseteq B$, Q.E.D.

This law is true for logical inference in NTA as well. As NTA is isomorphic to algebra of sets, it is clear that after adding any premise (for example, C) to the left part of (1) the correlation $(A_1 \cap_G \dots \cap_G A_n \cap_G C) \subseteq_G B$ is true too. By means of NTA, we examined many examples from [4–6], which had to illustrate non-monotonicity of logical inference. This examination discovered collisions in all such cases rather than violations of classical logic’ laws [8].

For instance, an example of nonmonotonicity in [6] is given as a pair of premises: (i) “all birds can fly” and (ii) “Titi is a bird, but it cannot fly”. It is easy to show that implementation of non-classical logic is not necessary to settle this issue.

It is enough to detect a collision in this reasoning and correct premises without breaking the laws of classical logic. One of the premises is evidently wrong in the given example. Semantical analysis allows to suppose that the first premise is wrong because there exist birds, which cannot fly.

In many cases, examples with usage nonmonotonic logics do not contain any structures breaking the laws of classical logic and Boolean one. Such breaking is supposed to arise from bringing some revised inference rules, which become applicable under certain preconditions. So, default logic exploits rules like:

$$P : J_1, \dots, J_n / C,$$

where P is a premise, C is a conclusion, and J_1, \dots, J_n are preconditions (justifications). If any of justifications are proved to be false, we cannot infer the conclusion. In other words, prior to using this rule we have to make sure that all preconditions J_1, \dots, J_n are true for the given conditions and facts. Many researchers prefer this kind of rules as they do not require for explicit enumeration of exceptions intrinsic to the given system. However, we cannot see how and why laws of classical logic are violated in such cases.

6 Modalities

We have also investigated reasoning models where *modal logics* are advised to apply. They are usually used in cases when some statements are assigned with modal operators \Box (necessarily, always true, etc.) and \Diamond (possibly, sometimes true, etc.). Formal connections between these operators completely correspond to the connections between quantifiers \forall and \exists . In some cases, when we analyzed real problems intended for solving by modal logics, formalization of such problems happened to become simpler after using our techniques for hypotheses check or for analysis of possible variants of answers instead of modal operators. As an example, we solve the Three wise-men problem [6] that served McCarthy a standard sample for testing different logics of belief and knowledge. This problem is as follows. A king wanted to check insights of his three advisors (wise-men). Then he painted a spot on the forehead of every wise-man. The spots could be either white or black, and at least one of them is white. Every wise-man can see the spots on foreheads of the others, but cannot see his own spot. For each wise-man, the goal is to determine the colour of his spot. Traditionally, this problem is solved with using a multimodal logic with modal operators $[i]$: « i th wise-man knows that ...». In [6] you can find schemes of axioms for this logic that provides a formal solution of the Three wise-men problem. Below, we propose another solution that is based on analysis of hypotheses and does not require for usage of non-classical logic.

The statement of this problem shows that there exist both univocal and uncertain situations. For instance, the situation is univocal when two wise-men have black spots and one wise-man has a white spot. Then the man who sees two black

spots knows he has the white spot and announces the correct answer. Other univocal situations are searched by checking hypotheses.

For other variants, univocal situations can be treated as inadmissible ones since they stipulate that the right answer is already known while it is not so because no one of wise-men has reported his answer. Suppose two wise-men have white spots and one has a black spot. Then the man who sees one white and one black spot can advance a hypothesis that he has a black spot, but this leads to the inadmissible univocal situation. So, the correct answer can only be “I have a white spot”. Consequently, this variant belongs to a univocal situation as well.

Let us now analyze the variant with three white spots. Every man who sees two white spots can advance a hypothesis that he has a black spot, but this leads to the inadmissible univocal situation again. So, the correct answer can only be “I have a white spot”.

More detailed analysis can be done, if its algorithm contains time periods (steps). Then the first of above-described univocal situations can be settled on the first step, the second situation will take two steps, and the third one will need three steps for settling. Wise-men are supposed to be wise enough to sequentially estimate every situation for one step. If the wise-man who sees two white spots concludes he also has a white spot at the second rather than at third step, he will take the risk of a wrong answer.

Sure, the formal method to solve the Three wise-men problem by means of a multimodal logic [6] looks preferably since the solution can be found by a clear algorithm. We describe our way to solve this problem (by advancing and checking hypotheses) here in order to show that applicability modal logics to solving some problems does not contradict with possibility to solve such problems within classical logic.

Modal logic is intended to formalization of reasoning where hypotheses and assumption can occur. Conversely, processing of hypotheses works better by means of collisions analysis rather than by using modal operators. Appropriateness of collisions analysis to defeasible reasoning is dictated by the following reasons:

- (1) the content of collisions is wider and more specific compared to the situations modeled by nonmonotonic and modal logics, so collisions usage enlarges capacity for semantical analysis of information;
- (2) integration of different logics into a single system of logical analysis is fairly complicated. In particular, it is difficult to find an acceptable number of defaults rules for systems with big quantity of such rules [5], this leads to loss of modularity;
- (3) hardship in using nonmonotonic logics for analysis of defeasible reasoning has driven many researchers to conclude necessity of “thinking over integration means to form defaults reasoning into probability theory” [5]. In NTA, this problem is generally solved since there are methods to immerse logical models into the probabilistic space [7].

7 Uncertainties in Forms of Alternative Values or Probabilities

Suppose, we are going to model a system where values of some variables are vaguely expressed by listing of possible (admissible) variants of these values. For the first glance, the classical predicate calculus will not do for presentation of this model since it admits only two variants to represent variables in formulas, namely complete ambiguity when the variable name is used (x , for instance) and total clarity when the variable is substituted with a constant or a function of a constant. Substitution a set of constants instead of one constant is not really practicable for analysis of formulas in the predicate calculus.

At the same time, it is possible to show that formulas of classical propositional and predicate calculi often contain several variants of variables values or their combinations. For instance, the propositional calculus' formula $F = A \vee (B \wedge \neg C) \vee (\neg B \wedge C)$ contains a set of satisfying substitutions, which can be seen after representing this formula in NTA structures:

$$F[ABC] = \begin{bmatrix} \{1\} & * & * \\ * & \{1\} & \{0\} \\ * & \{0\} & \{1\} \end{bmatrix}$$

To find all satisfying substitutions for this formula, it is enough to calculate Cartesian products in every row and their union. In the first row, we have the Cartesian product $\{1\} \times \{0,1\} \times \{0,1\}$ containing 4 different n -tuples. For example, the n -tuple (1, 0, 1) corresponds to the satisfying substitution $A = true, B = false, C = true$. The total number of satisfying substitutions in this formula equals 6, which indicate its degree of uncertainty. Thus, we can see that uncertainty exists in formulas of propositional and predicate calculi actually always. This is why additional means to simulate uncertainty are redundant in many cases; they just sophisticate the model and its interpretation.

If we have a logical system as a set of premises A_i , then their conjunction represent a formula containing a set of satisfying substitutions; the number of these substitutions is bigger than 2 generally. Thus, the reasoning system can contain several alternative variants specified more exactly when new data come to the system. However, this "alterability" is not evident in logical formulas. For example, you may substitute variables in a formula with their single values only. Conversely, NTA always admits the possibility to define a value of a variable (attribute) as a set of variants.

NTA structures consist of sets n -tuples being Cartesian products in essence. A measure (a probabilistic measure as well) can be easily calculated for a Cartesian product, that is why NTA structures can be readily immersed into a probabilistic space. We have developed algorithms to transform any NTA structure to an orthogonal C -system that is a C -system with non-overlapping pairs of C - n -tuples.

For such a C -system, its measure equals to the sum of measures for the C - n -tuples comprising it.

Logic-Probabilistic Analysis (LPA) for systems modeled by logical functions has been developed by Ryabinin and his colleagues [2]. To analyze safety and reliability of such systems, LPA exploits mathematical models of the propositional calculus mostly. So, these methods means are good for systems with two possible states (for example, normal function and failure). Systems with many (more then 2) possible states are present in LPA for separate specific cases only. We have found that NTA provides techniques suitable for LPA, and these techniques have wider modeling capabilities. In particular, they support logic-probabilistic modeling of multistate systems.

Let us introduce NTA-based methods of probabilistic simulation in greater detail. The basic cross-linking concept of NTA is the concept of C - n -tuple. If we know the probabilistic measures of components of a C - n -tuple, then the measure of the C - n -tuple can be calculated as the product of the measures of its components. For example, when the C - n -tuple $R = [ABC]$ is given in measurable attributes and the measures of its components equal to $\mu(A)$, $\mu(B)$, and $\mu(C)$, respectively, then $\mu(R) = \mu(A) \cdot \mu(B) \cdot \mu(C)$.

If we want to embed logical formulas in the probabilistic space, then all attributes of the space, in which the totality of NTA objects is given, have measure 1, and all NTA objects have measures that do not exceed 1. This corresponds to the probabilistic measure not in numerical relations only, but also due to the fact that the system of events simulated by NTA is isomorphic to the algebra of sets.

To compute the measures of NTA objects different from C - n -tuples, it is necessary to *orthogonalize* them.

Definition 1 A C -system is called *orthogonal*, if the intersection of any pair of its C - n -tuples is an empty set.

Orthogonalization techniques are based on the following correlation proved by P.S. Poretsky for formulas of propositional calculus. Let H_1, H_2, \dots, H_k be logical formulas. Then:

$$H_1 \vee H_2 \vee \dots \vee H_k = (H_1) \vee (\overline{H_1} \wedge H_2) \vee \dots \vee (\overline{H_1} \wedge \overline{H_2} \wedge \dots \wedge \overline{H_{k-1}} \wedge H_k). \quad (2)$$

Using (2) for NTA, we have proved a number of theorems, which result in development of orthogonalization algorithms for any NTA objects. Now we will formulate a theorem helping to transform any D - n -tuple into an orthogonal C -system. Let $Q_1, Q_2, \dots, Q_{m-1}, Q_m$ be components of the D - n -tuple.

Theorem 1 D - n -tuple $]Q_1 Q_2 \dots Q_{m-1} Q_m[$ is equal to the orthogonal

$$C - system \begin{bmatrix} \underline{Q_1} & * & \dots & * & * \\ \underline{Q_1} & Q_2 & \dots & * & * \\ \dots & \dots & \dots & \dots & \dots \\ \underline{Q_1} & \underline{Q_2} & \dots & \underline{Q_{m-1}} & * \\ \underline{Q_1} & \underline{Q_2} & \dots & \underline{Q_{m-1}} & Q_m \end{bmatrix}.$$

To transform a *D*-system into a *C*-system, we firstly use Theorem 1 to calculate equivalent orthogonal *C*-systems for all *D*-*n*-tuples comprising the *D*-system, and then intersect the obtained *C*-systems. After the intersection, we get an orthogonal *C*-system too, according to the following theorem.

Theorem 2 If *P* and *Q* are orthogonal *C*-systems, their intersection is either empty, either contains a single *C*-*n*-tuple, either equals to an orthogonal *C*-system.

Please note that the measure of an orthogonal *C*-system is equal exactly to the sum of the measures of *C*-*n*-tuples that belong to it. In addition, the following regularity has been established: the orthogonalization not only allows to prepare an NTA object for calculating its probability, but also, in many cases, substantially reduces the computational complexity in solving other problems (e.g., in solving the satisfiability problem).

If an NTA object is a representation of formulas of propositional calculus, then it is given in the universe $\{0, 1\}^n$, where *n* is the number of logical variables in the formula. Each column of a *C*-*n*-tuple or a *C*-system is related to a certain logical variable. The variable x_k corresponds to the *k*th column, the state 1 in the NTA object corresponds to the literal x_k , and the state 0 corresponds to the literal $\neg x_k$. Any row (*C*-*n*-tuple) in a *C*-system corresponds to the conjunction of the formula expressed as a disjunctive normal form (DNF). If some conjunct misses the variables that are involved in the composition of formula, then the corresponding dummy variable “*” is inserted in the *C*-*n*-tuple instead of these variables.

Example 1 Assume that the formula of propositional calculus

$$F_Q = (x_1 \wedge \neg x_3) \vee (\neg x_2 \wedge x_3) \vee (\neg x_1 \wedge x_2). \tag{3}$$

is given. Since there are three logical variables here, this formula can be represented as an NTA object *Q* in the universe $\{0, 1\}^3$

$$Q = \begin{bmatrix} \{1\} & * & \{0\} \\ * & \{0\} & \{1\} \\ \{0\} & \{1\} & * \end{bmatrix}.$$

This formula and the NTA object that corresponds to it are orthogonal; therefore *Q* can be expressed directly in terms of the probabilistic measure. Assume that in the NTA object *Q*, the probabilities of events are given as follows: p_i is the probability of the event 1 in the *i*th attribute, and $1-p_i$ is the probability of the event 0 in the *i*th attribute. Taking into account that the measure of a *C*-*n*-tuple is equal to

the product of the measures of its components, and the measure of an orthogonal C -system is the sum of the measures of C - n -tuples belonging to it, we obtain the formula

$$p(Q) = p_1(1-p_3) + (1-p_2)p_3 + (1-p_1)p_2. \quad (4)$$

In the LPA, formula (4) is called the probabilistic function (PF) of formula (3). This function can also be derived from the orthogonal C -system by replacing its components with the corresponding probabilities and the following transformation of the system into a polynomial. At the first glance, it seems that NTA structures provide only a different way for expressing logical formulas. However, when the models get complicated (in particular, when we investigate many-state systems), using NTA provides for essential simplification of the algorithms for solving a number of problems considered in LPA. In addition, embedding NTA objects into the probabilistic space exploits the concept of “regression equation” that allows for posing and solving the problem of probabilistic logic in accordance with the N. Nilsson statement. *If in the probabilistic functions of type (4), we suppose that p_i are variables rather than fixed numbers, then these formulas are an exact regression equation of the corresponding logical formula.* The proof of this proposition can be found in [9]. Let us consider an example of many-state system.

Example 2 Let $R = \left[\begin{array}{cc} \{a_1, a_2\} & \{b_1, b_3\} \\ \{a_3\} & \{b_1, b_2\} \end{array} \right]$ be an orthogonal C -system with three states given in the space $\{a_1, a_2, a_3\} \times \{b_1, b_2, b_3\}$ with probabilities $p(a_i)$ and $p(b_i)$; besides, $p(a_3) = 1 - p(a_1) - p(a_2)$ and $p(b_3) = 1 - p(b_1) - p(b_2)$. Then, the probability of the event expressed by the NTA object R , if the required probabilities are substituted, is

$$p(R) = (p(a_1) + p(a_2))(1 - p(b_2)) + (1 - p(a_1) - p(a_2))(p(b_1) + p(b_2)).$$

The presented approach corresponds to the *direct problem* of logical-probabilistic analysis when, for given probabilities of elementary events, the probability of a complex event is calculated. In the *inverse problem*, the statement is different. It is necessary to calculate probabilities of elementary events based on the data about probabilities of certain complex events. After this, we can calculate the probabilities of other complex events. Problems solved in probabilistic logic are of this type [9].

8 Conclusion

Results of our research show that the classical approach to NTA-based modeling uncertainties in data and knowledge allows for integrating various methods of solving this problem.

Acknowledgements The authors would like to thank the Russian Foundation for Basic Researches (grants 13-07-00318, 14-07-00256, 14-07-00257, 14-07-00205, 15-07-04760, and 15-07-02757) for partial funding of this research.

References

1. Zadeh, L.A.: A computational approach to fuzzy quantifiers in natural languages. *Comput. Math. Appl.*: Spec. Issue *Comput. Linguist.* **9**(1), 149–184 (1983)
2. Ryabinin, I.A.: *Reliability and Safety of Structural Complex Systems*. Polytechnic, St. Petersburg (2000) (in Russian)
3. Gorodetskiy, A.E., Tarasova, I.L.: *Fuzzy Mathematical Modelling of Poorly Formalized Processes and Systems*. SPbSTU Publishing, St.Petersburg (2010) (in Russian)
4. Vagin, V.N., Golovina, E.Y., Zagoryanskaya, A.A., Fomina, M.V.: Exact and plausible reasoning in intelligent systems. In: Vagin, V.N., Pospelov, D.A.(eds.). *Fizmatlit, Moscow* (2004) (in Russian)
5. Russell, S.J., Norvig, P.: *Artificial Intelligence: A Modern Approach*, 2nd edn. Prentice Hall, Upper Saddle River (2003)
6. Thaysse, A., et al.: *Approche Logique de L'intelligence Artificielle Tome 2: De la Logique Modale à la Logique des Bases de Données*. Dunod, Paris (1989)
7. Kulik, B., Zuenko, A., Fridman, A.: *An Algebraic Approach to Intelligent Processing of Data and Knowledge*. Polytechnic University, Saint Petersburg (2010)
8. Kulik, B., Fridman, A., Zuenko, A.: Logical inference and defeasible reasoning in N-tuple algebra. In: *Diagnostic Test Approaches to Machine Learning and Commonsense Reasoning Systems*, pp. 102–128. IGI Global (2013)
9. Kulik, B.A.: N-Tuple algebra-based probabilistic logic. *Syst. Anal. Oper. Res.* **46**(1), 111–120 (2007)

Active Data in Digital Software Defined Systems Based on SEMS Structures

V.V. Alexandrov, S.V. Kuleshov and A.A. Zaytseva

Abstract The article proposes the further development of terminal programs approach (the programs which being transmitted instead of data and executed on receiver side are restoring the data to be transmitted) to the concept of active data providing automatic reconfiguration of software defined equipment needed for self propagation control through communication environment. Active data being terminal programs are configuring the software defined equipment and controlling self propagation through communication environment.

Keywords Terminal program · Active data · Infocommunication · Software defined · Homoiconicity

1 Introduction

Modern tendencies of software defined and software configurable systems development [1] are intensifying the growth of new data representation and processing methods. The paper considers the organization and control of the adaptive communication environment if a workframe of digital programmed infocommunication [2].

For this purpose the paper proposes the further development of terminal programs approach (the programs which being transmitted instead of data and executed on receiver side are restoring the data to be transmitted) [3, 4] to the concept of

V.V. Alexandrov (✉) · S.V. Kuleshov · A.A. Zaytseva
St. Petersburg Institute for Informatics and Automation of RAS,
Russian Academy of Sciences, Saint Petersburg, Russia
e-mail: alexandr@iias.spb.su

S.V. Kuleshov
e-mail: kuleshov@iias.spb.su

A.A. Zaytseva
e-mail: cher@iias.spb.su

active data. Active data (AD) being the terminal programs are configuring the software defined equipment and controlling self propagation through communication environment.

Providing the terminal programs with ability to take active actions not only on receiver side but also on intermediate nodes taking part in communication process will expand the abilities of data transmission networks converting them into software defined systems (the development of SDR—Soft Defined Radio principles).

This allows the real time change of data transmission formats, frequency ranges, modulation types, radio network topologies which in turn provides the ability to dynamically form the special data transmission networks from a general purpose devices temporarily reconfiguring them for data transmission task between transmitter and receiver beyond radio visibility range.

2 Terminal Programs

The example of such terminal program is a self extracting archive (executive SFX archive) despite the fact that such archive file is not a strictly terminal program it demonstrates its external behavior. In SFX archives the decompressing program is the same for any input data which in turn are input for decompressing program but are stored in the same file.

In programming the notion of homoiconicity exist—the feature of some languages to similarly represent executable code and data. This allows to treat data as executable and vice versa [5].

Unfortunately, this possibility of languages traditionally used only to facilitate metaprogramming, super-compilation [6] or the runtime virtualization techniques (virtual machines).

Homoiconicity in infocommunication tasks increases the flexibility of programmed channels by the ability to transmit decoding programs via same channels as the compressed data including the possibility to transmit individual decoding program for each transmitted data block.

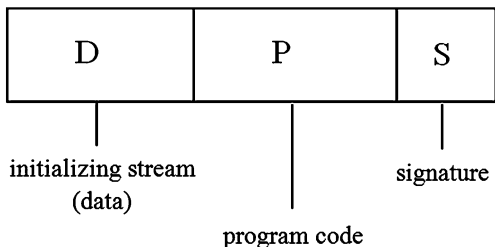
In addition to mentioned above, the papers [7] are known to propose dynamically reconfigurable nodes based on automation theory.

3 From Terminal Programs to Active Data

The principle of digital content separation to the transport (initializing) stream and the generating program [8, 9] enables flexible adaptation of the content to the existing features and limitations of the physical transmission channels.

Within the active data conception the decoding program can be generated on transmitter side for every data type to be sent and be transmitted before initializing stream. If predetermined standard data types are to be used (in this case, on the

Fig. 1 The format of active data packet (container)



receiving side, there is a set of standard data recovery programs needed) it is possible to transfer only the index of the program required for recovery of digital information object.

The approach of software defined systems being configured in accordance to demands and specifics of the transmitted active data enables to create flexible virtual communication environment.

The single packet of active data can be described as a bit structure containing three components (Fig. 1): signature S, program P and initializing stream D. The only mandatory component is the signature which is needed for the active data packet (ADP) identification and the program to be executed on receiver side. Initializing stream (based on terminology in [8]) is an input data for the program P and is being transmitted to ADP only if it is needed.

In graphic description of active data behavior the designations are as shown on Fig. 2. The term of runtime environment is referring to software and hardware resources of the network node.

The basic operations for the active data processors are register operations, logical and arithmetical operations and conditional jumps. Besides, AD need access to input and output buffer memory (for the network devices). Code self modification needs also to be allowed.

The basic recommended libraries are: compression and noise immunity codecs, encryption/decryption functions.

Every device should be able to return the list of available functions and libraries to the program.

For the correct sequencing of functions to be executed from the arriving AD packets any program is advised to make all necessary checks and actions in advance

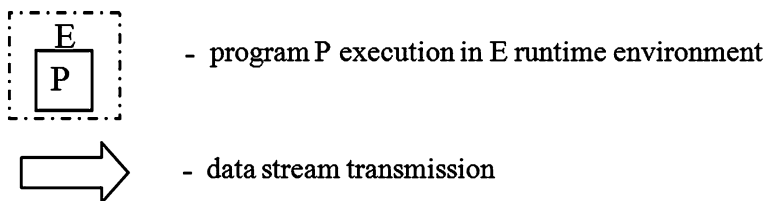


Fig. 2 Employed designations

to provide execution of its main function. This means inability for some programs to redefine available software and hardware in advance for the next arriving packets.

4 The Basic Scenarios for Active Data Usage

Hereby we consider the basic usage scenarios for active data without specification of ADP representation formats.

1. *Terminal program transmission.* The most simple usage scenario is sending the terminal program P to receiver and executing to obtain the data D^* (Fig. 3). Due to insufficient theoretical research of such program generation for arbitrary bit streams, this scenario represents rather theoretical interest than practical data coding method.
2. *The decoder program usage.* The program P is being transmitted with initializing stream D (usually compressed bit stream) as a one AD packet where P is a decoder program for D . The execution of decoding program on receiver side forms D^* (Fig. 4).
3. *Identification and preparation of the environment E for the receiving node* (Fig. 5). The program P being transmitted to the receiving node detects the presence of decoding program P_d to restore the data D . In the presence of suitable decoder it is being executed on D to obtain the resulting D^* . If the suitable decoder is absent the program P requests the decoding program from the sending node or the other nodes of communication environment.
4. *Using AD fragmentation.* In case of big data volume transmission it is possible to fragment it into the sequence of ADP each of which contains own copy of the program P and can be transmitted separately. After execution of program P on the receiving node it waits for the rest packets D_1, \dots, D_5 to be received and then executes on the merged sequence to obtain D^* (Fig. 6).



Fig. 3 Terminal program transmission

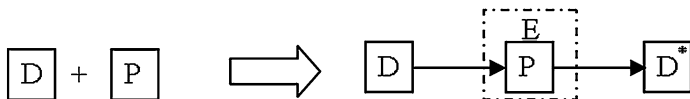


Fig. 4 The decoder program usage

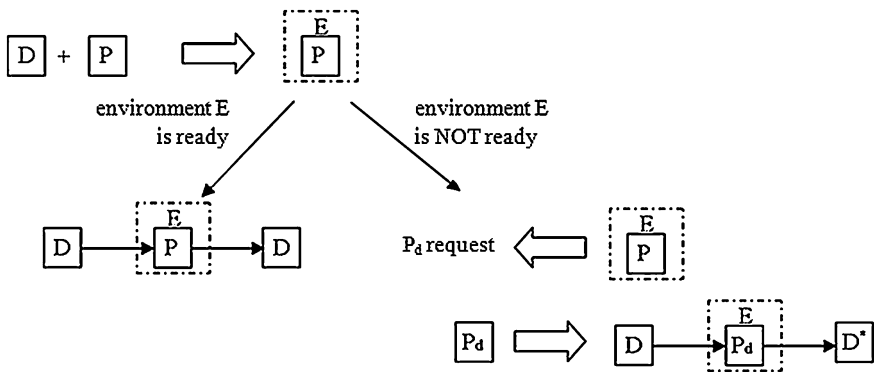


Fig. 5 Identification and preparation of the environment E for the receiving node

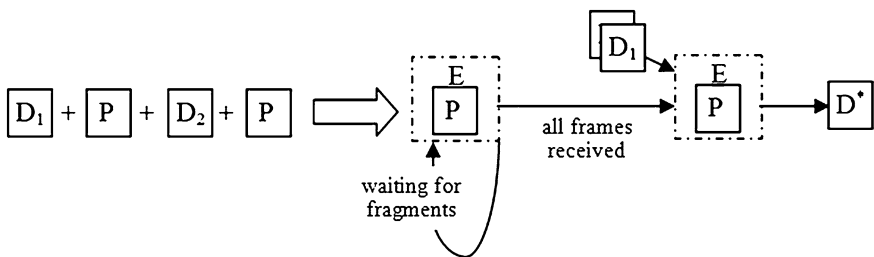


Fig. 6 Fragmentation of the AD

5. *Providing the reliability and accuracy.* When needed, the program P being executed on receiving node is able to request resending of the AD packet using the majority principle (Fig. 7).
6. *Search for the node with suitable environment for program P execution* (Fig. 8). This and the subsequent scenarios of AD usage are to be considered on the example of network represented as a graph where the nodes N_1, \dots, N_5 are the devices and the links represent physical channels. The node N_1 needs to transmit the AD to the receiving node N_5 given that the receiving node does not dispose the suitable environment. In this case the search for the nearest (in sense of minimizing communication expenses) node with suitable environment for execution of P (the node N_3 in this example) is

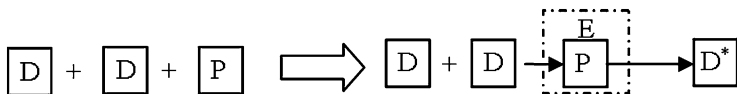


Fig. 7 Providing the reliability and accuracy

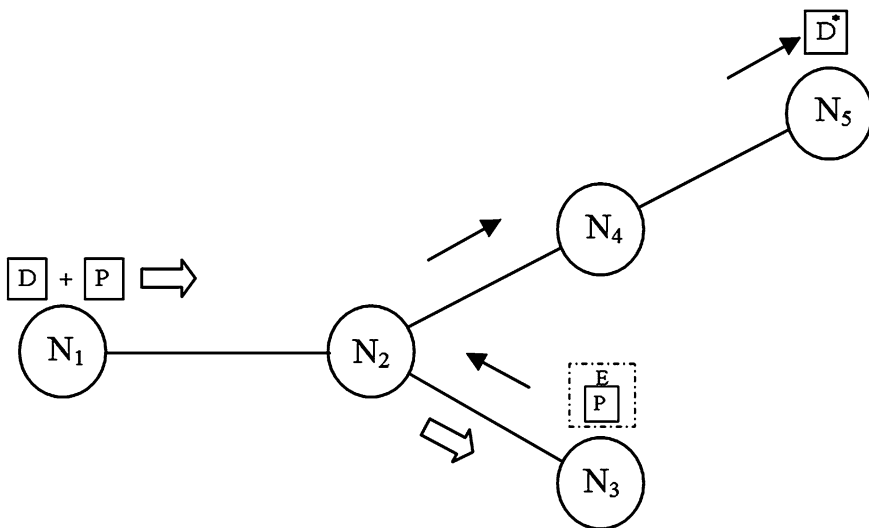


Fig. 8 Finding the node with suitable environment

performed followed by execution of P and transmission of the results D* to the receiving node N5.

7. *Transmission of the AD using navigation functions.* When transmitting the AD via complex networks with the dynamically changing architecture (i.e. mobile systems of objects control) the function of navigation can be used by executing the program P on every node which it is passed through (Fig. 9). In this case special marks or tokens can be saved on the node containing results of delivery

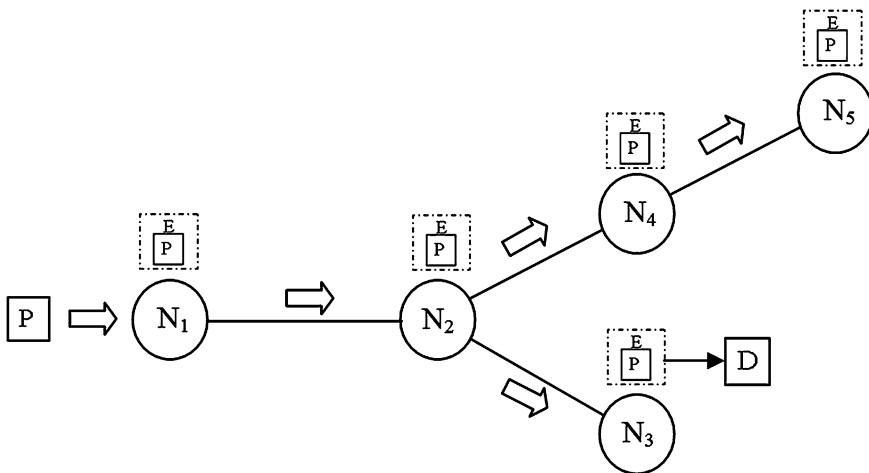


Fig. 9 The transmission of ADP to all nodes of the network

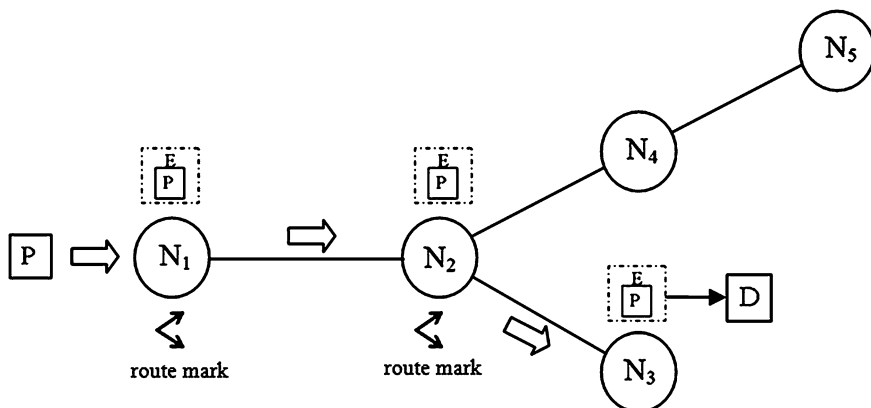


Fig. 10 The transmission of ADP using the navigation functions

of ADP to other nodes via different routes. These marks can be used by P to optimize the further delivery cost or time (Fig. 10).

8. Dynamic reconfiguration of the nodes. The AD are being transmitted from source node N_1 to node receiver N_3 . The program P being executed on the node N_4 (Fig. 11) is detecting the possibility to create new communication channel to the node N_3 by reconfiguring hardware or software of this node. If the results of reconfiguration are optimal in sense of transmission time or cost then the transmission of ADP through new channel is taking place.

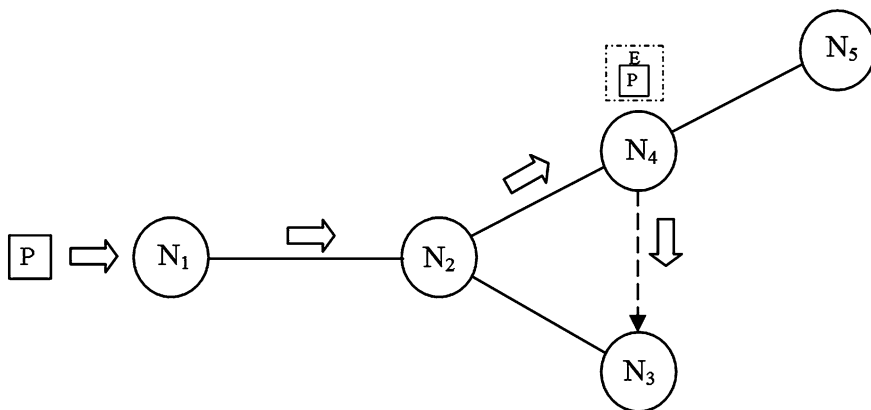


Fig. 11 Dynamic reconfiguration of the nodes

5 Infocommunication Environment and Reconfigurable Systems

Some of the considered above usage scenarios have analogies in the technologies of packet data transmission and global communication networks.

The example of the most similar approach for developing self organizing reconfigurable infocommunication networks are the mesh grids.

In contrast to mesh grids the proposed approach of active data not only operate on the level of content independent network reconfiguration but is capable of configuring networks for optimal and reliable delivery of specified content, providing network monitoring activity, unauthorized access detection etc.

6 Conclusion

The paper considers the concept of the active data transmission systems development. Being terminal programs the active data are able to configure the software defined equipment on the nodes of the network in order to control self propagation through communication environment.

The main advantage of proposed approach is an ability of fast deployment of specific communication systems on the basis of available shared facilities within the radio availability range with active data conception support.

The additional result is an increase in radio resources usage efficiency and providing electromagnetic compatibility by utilization of unused at the moment bandwidth of digital communication channels without introducing new transmitters. Also this conception increases the reliability of communication systems in general.

Further research will refine the formalization of active data description language including the demands for the set of operators necessary for active data functioning, the formats of active data representation, and standards for converting active data into executable code.

Also the equipment architecture and requirements will be proposed which includes the processor (or virtual machine) extension capable of active data code execution.

References

1. Alexandrov, V.V., Kuleshov, S.V., Tsvetkov, O.V., Zaitseva, A.A.: The conception of infotelecommunication building (the SDR prototype). Tr. SPIIRAN **6**, 51–57 (2008)
2. Alexandrov, V.V., Kuleshov, S.V., Tsvetkov, O.V.: Tsifrovaya tekhnologiya infokommunikatsii. Peredacha, khraneniye i semanticheskiy analiz teksta, zvuka, video, p. 244. SPb, Nauka (2008)

3. Alexandrov, V.V., Kuleshov, S.V.: Narrative representation of information processes. *Inf. Processes* **4**(2), 160–169 (2004). www.jip.ru
4. Kuleshov, S.V.: The Terminal programs of «digital» transmission and processing of data, energy and information equivalence. *Inf. Measuring Control Syst.* **9** (2007)
5. Homoiconic—<http://en.wikipedia.org/wiki/Homoiconic>
6. Nemytykh, A.P.: about supercompilation. http://conf.nsc.ru/files/conferences/Lyap-100/fulltext/69293/69928/nemytykh_supercompilation_Lyapunov100.pdf
7. Attie, P.C., Lynch, N.A.: Dynamic input/output automata: a formal and compositional model for dynamic systems. In: Computer Science Artificial Intelligence Laboratory Technical Report, July 2013
8. Kuleshov, S.V.: *Metody i tekhnologiya postroyeniya tsifrovyykh programmiruyemykh infokommunikatsionnykh sistem*. Diss. na soiskaniye stepeni d-ra tekhnicheskikh nauk, p. 240. SPb (2011). (Uchrezhdeniye Rossiyskoy akademii nauk Sankt-Peterburgskiy institut informatiki i avtomatizatsii RAN)
9. Kuleshov, S.V.: Hybrid codecs and application in digital programmed data transmission channels. *Inf. Measuring Control Syst.* **10**(5), 41–45 (2012)

Part II
Synthesis of Automatic Control Systems

Automatic Control Systems of SEMS

V.G. Kurbanov, A.E. Gorodetskiy and I.L. Tarasova

Abstract The structure of the automatic control systems of SEMS and construction principles of basic subsystems are considered in the paper. The emphasis is put on the usefulness of neuroprocessor modules in subsystems in order to improve the accuracy and speed of their work, as well as calculators of extensions and turns (optimum without jamming) of moving parts of SEMS modules. The expediency of the use of adaptive CCDs in machine vision systems of SEMS.

Keywords Module SEMS · Automatic control · Adaptive CCDs · Machine vision · Neuroprocessor

1 Introduction

The research into the development of the intelligent robots (IR) intended for functioning in the conditions of aprioristic uncertainty of dynamically changing environment is actively conducted in all industrialized countries of the world. Implementation of such robots is extensive and various: automated production, transport, household, medicine, space, defense, underwater researches, rescue and repair work in extreme conditions, etc. In many of them, the presence of a person is undesirable or basically impossible. Therefore for successful performance of

V.G. Kurbanov (✉) · A.E. Gorodetskiy · I.L. Tarasova
Institute of Problems of Mechanical Engineering, Russian Academy of Sciences,
199178 Saint Petersburg, Russia
e-mail: vugar_borchali@yahoo.com

A.E. Gorodetskiy
e-mail: g27764@yandex.ru

I.L. Tarasova
e-mail: g17265@yandex.ru

working operations, IR, just like the advanced living beings, have to possess such important quality as adaptability to unformalized changing working environment [1]. The latter assumes that the control system of IR will be able to solve a number of complex problems.

First of all, there are problems of adequate perception and recognition of the environment, purposeful planning of behavior, and effective execution of the planned actions. The last problem is rather successfully solved by the methods of the automatic control theory with the use of the computer of traditional architecture with the consecutive principle of data processing. The solution of the first two problems using the same computing means is connected with considerable difficulties. The reason is not only the need of processing of large amounts of data from the parallel-functioning sensors distributed in space and working in real time, but also application of new intellectual ways of data processing which cannot be carried out by these computers [2].

Therefore, to ensure high performance control systems IR, built on the basis of SEMS, it is expedient in the Automatic Control Systems (ACS) SEMS use the neuroprocessors providing parallelization of process control computation [3].

2 Architecture of Control Systems of Modules SEMS

ACS SEMS considered structures are usually the architecture of the “tree” (see Fig. 1), comprising a Central Control Computer (CCC) and following Neuroprocessor Modules:

- Simulation (S);
- Optimization (O);

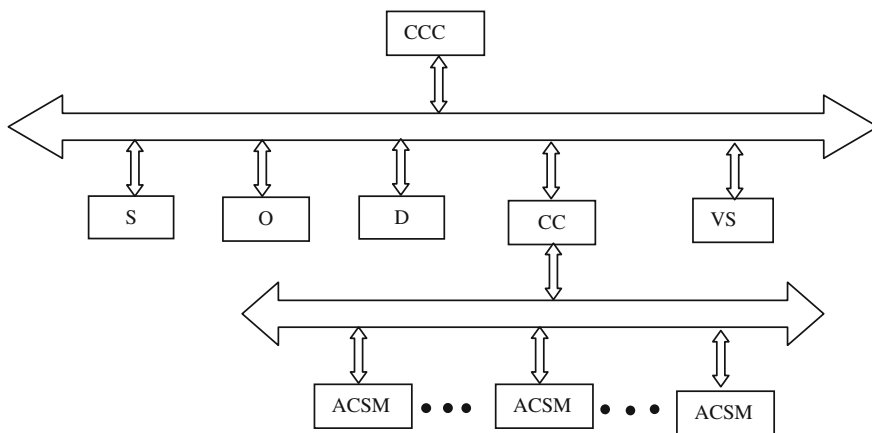
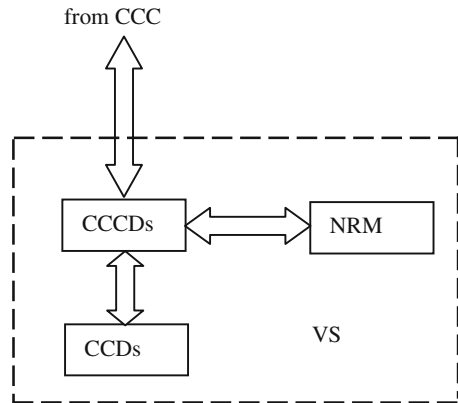


Fig. 1 Architecture of ACS SEMS

Fig. 2 The structure of VS

- Decision (D);
- Control Computation (CC);
- Vision System (VS).

CCC provides a solution to problems of selection implementation strategies required by the operator and/or the higher level system tasks and generating a sequence of actions (algorithms) are necessary for its realization. In addition, it should ensure a prompt correction of behavior depending on the information about the change of the environment, coming from VS and coordination of the subsystems. Operation CCC requires advanced skills to acquire knowledge about the laws of the environment, to the interpretation, classification and identification of emerging situations, to analyze and memorize the consequences of their actions on the basis of experience (property of the self).

Neuroprocessor Modules S, O, D, CC, VS together provide a solution to the problem of tactical level control. It is primarily concerned with finding a solution to one of the key tasks associated with the planning of routes and tracks progress towards the objectives are not fully certain conditions, including various obstacles, taking into account the dynamics of the executive subsystems and current changes in the operational environment. This should be provided not only to progress towards the goal of a priori given by routes and paths, but also arbitrary changes needed to promote a given target.

Module VS (see Fig. 2) through the Controller CCDs (CCCDs) on the signals of the CCC controls the parameters CCDs of the modules SEMS. Same VS collects information from the modules SEMS and transfers it to Neuroprocessor Recognition Module (NRM). NRM produces identification of surrounding objects and the operation state of the environment and transmits the information through CCCDs in CCC. CCDs may be provided with switches pixels. Pixels can change the configuration and size of the matrix by commands from CCCDs, ensuring their adaptation to the parameters identified objects [4, 5].

Module O performs scheduling optimal trajectories platform modules SEMS and reconfigurations. To do this, it uses the information received from module VS about the environment and the requirements of algorithms behavior formed in CCC. Module O also has to ensure the operational restructuring of the trajectories within the constraints and dynamics of executive subsystems.

Module S provides a prediction of the dynamics of the executive subsystems for issuing corrections planned Module O optimal trajectories and adaptation parameters computed control actions. This Module D determines the conditions under which in Modules O and CC adjustments will be made.

The information receives from Module S, O and D in the Module CC. Then, in accordance with algorithms coming from CCC generated control actions for Automatic Control Systems modules (ACSM) SEMS. These effects make the necessary movement of SEMS for the surrounding area, turns, compression and extension modules, as well as the capture and relocation of various objects.

3 Automatic Control Subsystems of Mobile Elements of Modules SEMS

The structure and operation ACSM consider the example module SM8 SEMS, which was shown in [6] is the most versatile. Others ACSM can be prepared from this by simplification.

ACSM SM8 SEMS has an architecture such as “tree” (see Fig. 3) and contains Neuroprocessor Calculation Module Optimal Movement (NCMOM). This module receives information from the CC and calculates the optimum without jamming leg lengthening of Legs L1–L6, extension reconfiguration of Control Rods CR1–CR6 of module platform, turns and extension of the Control Rods Movement CRM1–CRM6, as well as twists and extension of the Control Rods Gripping CRG1–CRG6. Calculated NCMOM linear and angular movements act on the corresponding Group Controls Legs (GCL), Group Control Rods Reconfiguration (GCRR), Group Control Rods Movement (GCRM) and Group Control Rod Gripping (GCRG).

GCL (see Fig. 3) generates and outputs the control actions in Automatic Control System of the Legs (ACSL). In ACSL Controllers Legs (CL1)–(CL6) (see Fig. 4) using sensor signals of feedback, [Linear Displacement Sensors (LDS), Angular Displacement Sensors(ADS), Force Sensors (FS) and the Tactile Sensor (TS)] calculated error signals and produce for given control law (for example PID laws) control actions on the appropriate Motors Legs (ML1–ML6), and which carry out the required lengthening of Legs (L1)–(L2).

GCRR (see Fig. 3) generates and outputs the control actions in Automatic Control System of Rods a Reconfiguration (ACSRR). Structure ACSRR analogous to the structure ACSL (see Fig. 4), But it has Controllers Control Rods Reconfiguration (CCRR) which, using sensor signals of feedback, [Linear Displacement Sensors (LDS), Angular Displacement Sensors(ADS), Force Sensors (FS) and the Tactile

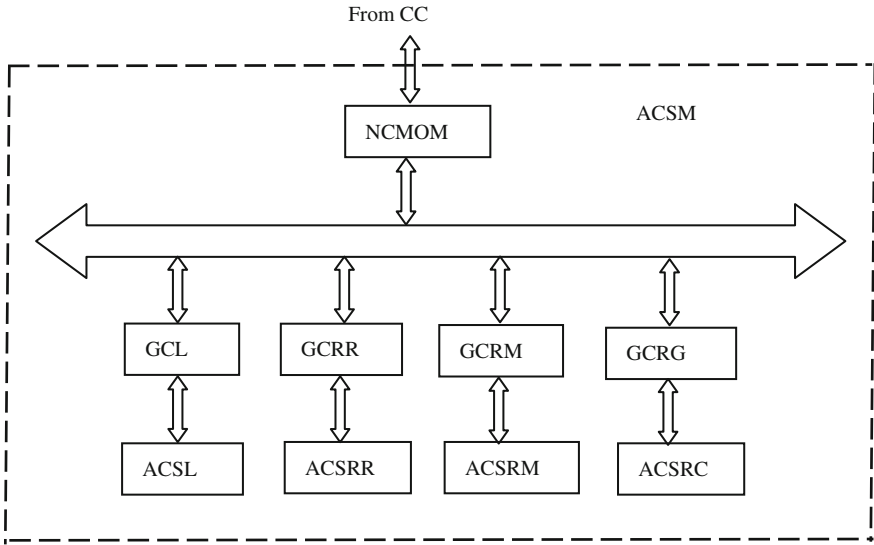


Fig. 3 The structure of ACSM

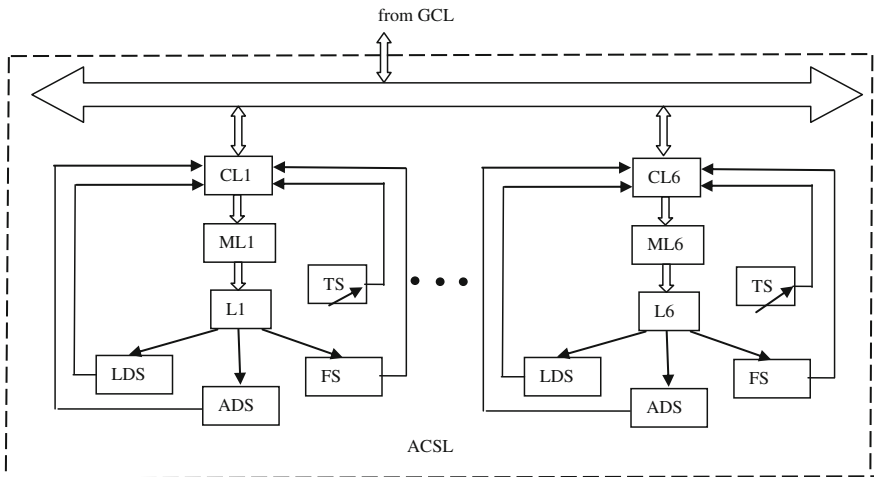


Fig. 4 Structure ACSL

Sensor (TS)], calculated error signals and produce for given control law (for example PID laws) control actions on the appropriate Motors Rods Reconfiguration (MRR1–MRR6), and which carry out the required lengthening of the Rods Reconfiguration (RR1)–(RR6).

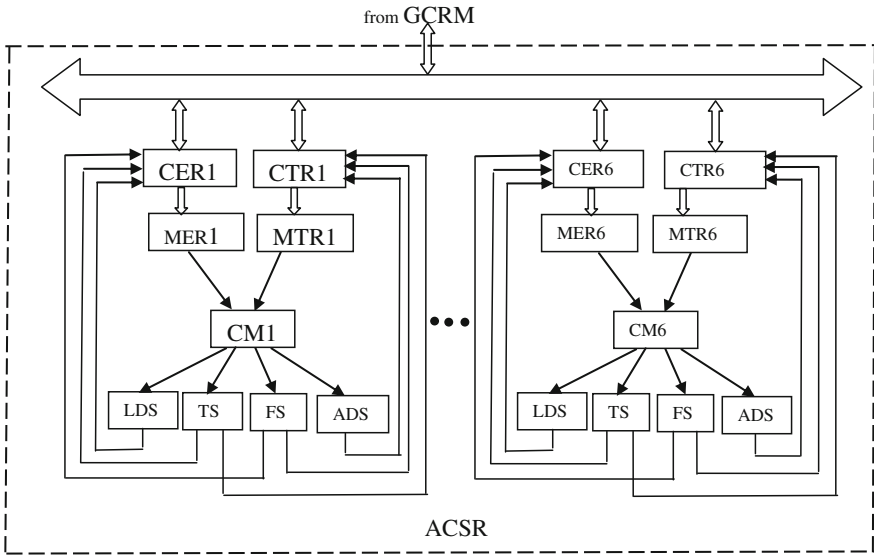


Fig. 5 Structure ACSR

GCRM (see Fig. 3) generates and outputs the control actions in Automatic Control System of Rod Movement (ACSRM). In contrast to the ACSL and ACSRR the system operates as an extension of the rods and their rotation. Therefore, it contains not only the Controllers of Elongation Rods (CER1)–(CER6) and Motors of Elongation Rods (MER1)–(MER6) but and the Controllers of Turning Rods (CTR1)–(CTR6) and Motors of Turning Rods (MTR1)–(MTR6) (see Fig. 5).

GCRG (see Fig. 3) generates and outputs the control actions in Automatic Control System of Rods Capture (ACSRC). This system is similar to ACSR (see Fig. 5) once it control elongation and turning Rods Capture (RC1)–(RC6).

Tactile sensors and force sensors normally used for the adaptation of automatic control systems. Sensors of linear and angular displacements provide circuit of automatic control loop during transients.

4 Conclusion

Automatic control systems SEMS are constructed as multi-level system architecture of the “tree”. This central control computer performs like a top-level function of coordinating the work of all subsystems, and problem solving strategies to meet the required selection of the operator and/or systems of higher level tasks and generating a sequence of actions (algorithms), required for its implementation.

Problem solving tactical level control subsystem perform the next level. This is usually used neuroprocessor modules to easily parallelize the calculation process to improve the speed and accuracy of calculations. At the same time they need to ensure not only progress towards the goal of a priori given by routes and paths, but also necessary to promote arbitrary changes sets the target.

The vision systems appropriate to use adaptive CCD. These CCD provide adaptation to the parameters identified objects by controlling the pixels. This is achieved by changing the configuration and size of the matrix on commands from the controller. It also allows you to increase the accuracy and speed of recognition due to the transfer of the recognition algorithm into hardware.

Subsystems automatic control of the movable elements of modules SEMS also have the architecture of the “tree” (see Fig. 3). Subsystems generally contain neuroprocessor optimal displacement calculation block that calculates optimum elongation without jamming and turns. At the same time they are the group controls of the same elements, tactile sensors and force sensors that are essential for the adaptation of automatic control systems, and linear and angular displacements sensors that provide circuit automatic feedback control to improve transient.

References

1. Popov, E.P., Pismennov, G.V.M. (eds.): *Fundamentals of Robotics* (1990)
2. Chernukhin, Y.V., Pisarenko, S.N.: Extrapolation structures in neural network-based control systems for intelligent mobile robots. *Opt. Mem. Neural Networks* **11**(2), 105–115 (2002)
3. Gorodetskiy, A.E., Tarasova, I.L., Kurbanov, V.G., Agapov, V.A.: Mathematical model of automatic control system for SEMS module. *Informatsionno-upravliaiushchie sistemy [Inf. Control Syst.]* **3**, 40–45 (2015) (In Russian)
4. Gorodetskiy, A.E., Kurbanov, V.G., Tarasova, I.L., Agapov, V.A.: Problems of increase of efficiency of use of matrix receivers for radio images in astronomy. *Radio Eng.* **1**, 88–96 (2015)
5. Gorodetskiy, A.E., Tarasova, I.L.: Detection and identification of dangerous space objects using adaptive matrix receivers radio. *Informatsionno-upravliaiushchie sistemy [Inf. Control Syst.]* **5**, 18–23 (2014) (In Russian)
6. Gorodetskiy, A.E., Kurbanov, V.G., Tarasov, I.L.: Smart electromechanical systems modules (in this volume)

Neuroprocessor Automatic Control System of the Module SEMS

I.L. Tarasova, A.E. Gorodetskiy and V.G. Kurbanov

Abstract The article covers the neuroprocessor automatic control system of the SEMS module. The system must operate in real time with the use of new ways of parallel data processing and control computation to achieve maximum precision of actuators with minimal travel time through using hexapod structures of SEMS. The use of force sensors in feedback simplifies the algorithms of operation and improves the accuracy of calculation of the control actions.

Keywords Module SEMS · Automatic control · Intelligent robot · Parallel data processing · Neuroprocessor

1 Introduction

The main element of the control system modules SEMS is a Neuroprocessor Automatic Control System (NACS) module SEMS. The main function of NACS is the automatic movement of the upper platform of control module having a 6-axis positioning system with controllers. The platform is driven by a 6-independent precision motors actuators of module legs. Therefore it is possible to carry out positioning platform on 3rd linear (X , Y , Z) and three angular coordinates (rotation around respective axes Q_x , Q_y , Q_z) [1]. In addition, it is possible to automatically control the radii of the upper and lower module platforms from three precision motors of the three control rods in each platform.

I.L. Tarasova (✉) · A.E. Gorodetskiy · V.G. Kurbanov
Institute of Problems of Mechanical Engineering, Russian Academy of Sciences,
Saint Petersburg, Russia
e-mail: g17265@yandex.ru

A.E. Gorodetskiy
e-mail: g27764@yandex.ru

V.G. Kurbanov
e-mail: vugar_borchali@yahoo.com

Fig. 1 Sketch module SEMS

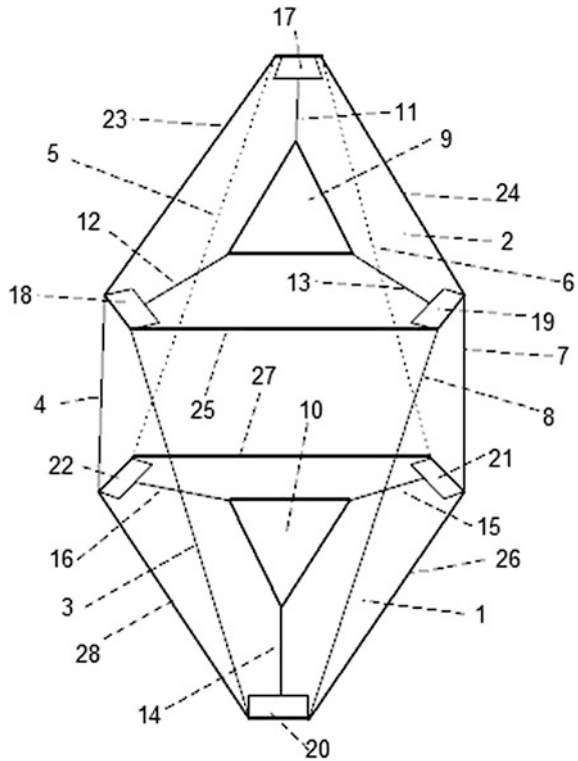


Figure 1 shows a standard module SEMS. It contains: a Lower Platform (LP) (1), upper platform (UP) (2) six Legs—Actuators (LA) (3–8) and the Supporting Pad (SP) (9 and 10), having at least three Control Rods (CR) (11–13 and 14–16), attached at one end to the SP, and the other—to the Mounting Pad (MP) (17–19 and 20–22), in which are mounted, for example screwed, at least three Spring-Loaded Telescopic Rods (SLTR) (23–25 and 26–28).

Interaction NACS SEMS models at various levels to successfully carry out the necessary Intelligent Robot (IR) working operations is carried out, as a rule, a system of planning and management of purposeful behavior [2].

2 Neuroprocessor Automatic Control System

The block diagram of NACS is shown in Fig. 2. The system includes a Control Computer (CC), for example, based on neuro-processor NM 6406 with 12 analogue and 8 digital inputs and outputs for connection of sensors and controllers, Controllers Leg-Actuators (CLA), Motors Legs (ML), Controllers Rods Upper Platform (CRUP), Motors Rods of the Upper Platform (MRUP), Controllers Rods

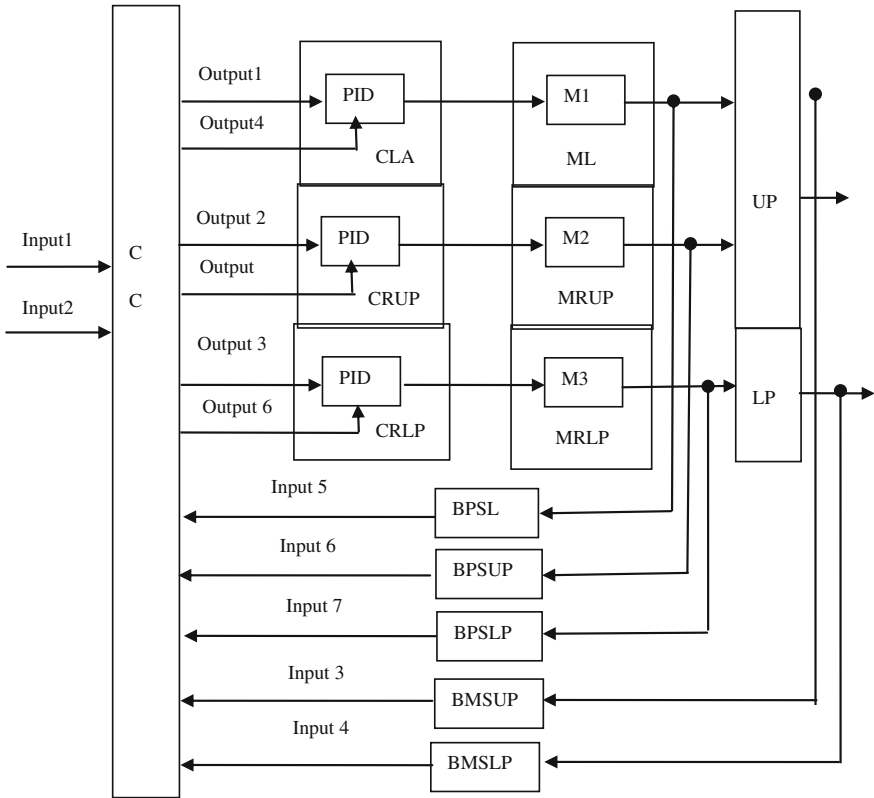


Fig. 2 The block diagram of NACS

Lower Platform (CRLP), Motors Rods Lower Platform (MRLP), Block of Pressure Sensors in the Legs (BPSL), Block of Pressure Sensors in the rods of the Upper Platform (BPSUP), Block of Pressure Sensors in the rods Lower Platform (BPSLP), Block of Moving Sensors of the Upper Platform (BMSUP), Block of Moving Sensors of the Lower Platform (BMSLP), as well as an Upper Platform (UP) and Lower Platform (LP).

Six PID regulators block CLA, three PID block CRUP and three PID block CRLP admission control actions U with a yield 1–3 CC generates a control voltage V in accordance with the law of the equation:

$$V = k_1U + k_2U/p + k_3pU, \text{ где } p = d/dt$$

Regulators CLA, CRUP and CRLP are adaptive and can change the values of the coefficients k1, k2, k3 on adaptation signals Ua, outputted from a yield 4–6 UVM.

Six motor legs (), three motor rods of the upper platform (MRUP) and three motor rods lower platform (MRLP) described by the following system of equations:

$$\begin{aligned} e &= V - kv\omega \\ Md &= Ke/(Tp + 1) \\ \omega &= (Md - Mc)/Jp \\ l &= kpe/p \\ Mc &= f(l) \end{aligned}$$

Settings kv , K , T , kpe , J determined by the design and parameters of the electric motors. Function $Mc = f(l)$ is usually determined by the results of experiments in the pre-commissioning. As a rule, it has a non-linear form of a dead zone and saturation.

In blocks BPSL, BPSUP and BPSLP commonly used piezoelectric pressure sensor with digital output, consistent with the inputs 5–7 of the CC, and in blocks BMSUP and BMSLP—optoelectronic moving sensors with digital output, consistent with the inputs 2 and 4 of the CC. Setting the operator is supplied to the input 1 CC through the man-machine interface. CC contains neuroprocessor and software package.

The structure of the neuroprocessor NM 6403 is shown in Fig. 3. It is a high performance microprocessor with elements of VLIW SIMD architectures.

NM 6403 includes the control unit, calculating the address and scalar processing and assembly to support operations on vectors with elements of variable bit length. Furthermore, it has two identical programmable interface for use with various types of external memory, and two communication ports are compatible with the ports TMS320C4x, for the possibility of constructing a multiprocessor system. Neuroprocessor designed to handle 32-bit scalar data and a programmable bit packed in 64-bit words.

CC software package contains a parallel operating Control SubSystem of the Upper Platform (CSSUP) and control subsystem of the lower platform (CSSLP) (Fig. 4).

NACS operates as follows.

On input 1 of CSSUP (Fig. 4) from the operator or from the higher-level control system in CSSUP enter given the linear coordinates of the upper platform x_{bz} , y_{bz} , z_{bz} , given the angular coordinates of the upper platform u_{bz} , v_{bz} , w_{bz} , as well as given the radius of the upper platform R_{bz} . At the same time the input 2 of the CSSUP from BMSUP enter the current linear coordinates of the upper platform x_{br} , y_{br} , z_{br} , the current angular coordinates of the upper platform u_{br} , v_{br} , w_{br} , as well as the current radius of the upper platform R_{br} .

According to these signals in the Model of the Upper Platform (MUP) are calculated the required changes Δl_i leg length and lengths of the control rod ΔR_{bi} of upper platform. The received signals are supplied to the Optimizer of the Trajectory of the Upper Platform (OTUP) that calculates a control action $U_i(t)$. These actions come in the Multiplier Block of Upper Platform (MBUP) and then on output 1 in

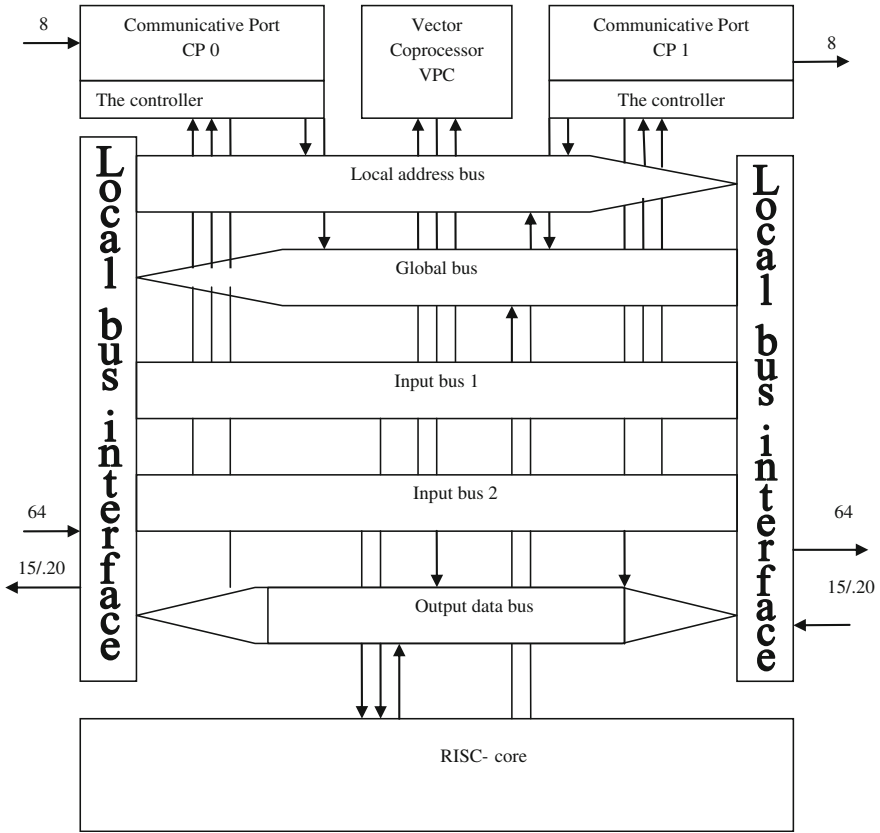


Fig. 3 Processor NM 6403 architecture

the form of analog signals U_1-U_6 for CLA and on output 3 as analog signals U_7-U_9 for CRUP. Control signals from the CLA arrive at the motors of the legs ML, which changes the length of the legs, providing linear and angular displacement of the upper platform. Control signals from the CRUP arrive at the motors of the rods of the upper platform (MRUP), which change the length of the rods, providing change in the radius of the upper platform.

MBUP provides ban passing signals $U_i(t)$, when there is not synchronization of motors by entering its second input signals $Q_i = 0$. These signals creates a Logical Block of the Upper Platform (LBUP) whose input is via the input 5 receives signals F_1-F_6 from BPSL and through the input 6 signals F_7-F_9 from BPSUP. LBUP checks the following types of rules:

If for any i th actuator $F_i > F_{di}$ (allowable excess), then $Q_i = 0$, otherwise $Q_i = 1$.

In CSSLP work is organized similarly. However, it is not required to develop control signals for motors of the legs.

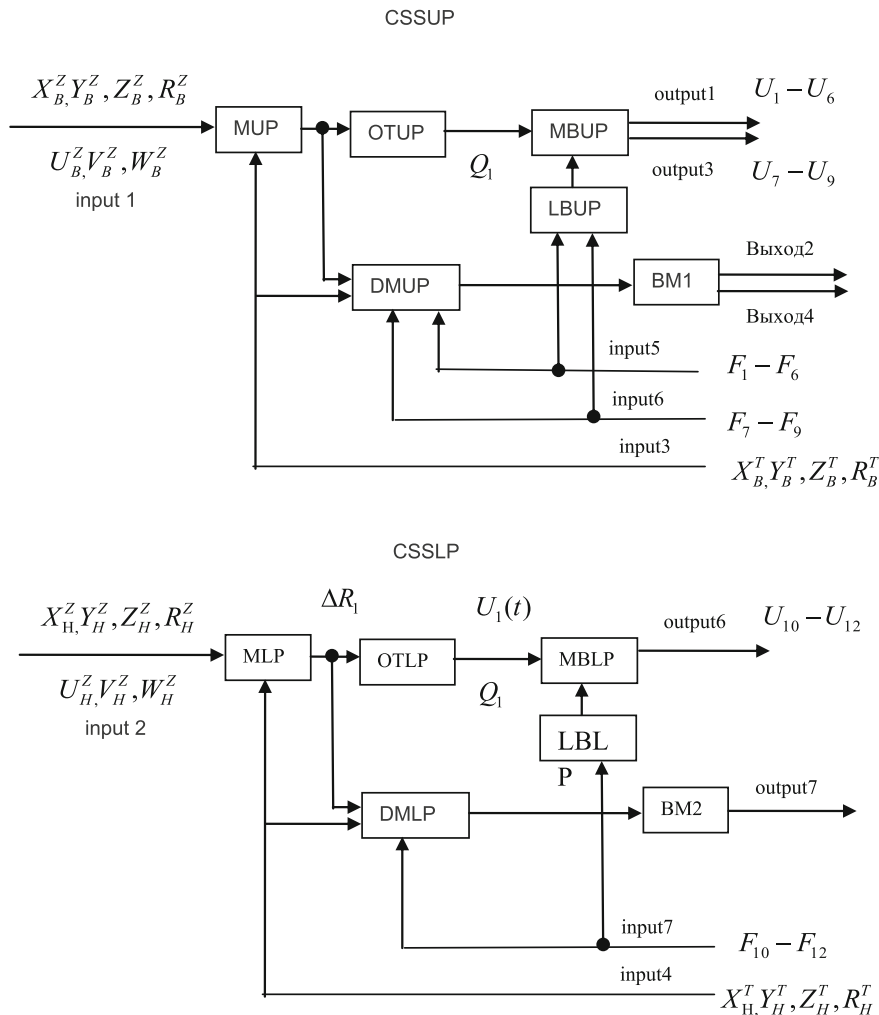


Fig. 4 A block diagram of the interaction of software modules

To improve the dynamics in NACS provided adaptation PID controllers due to a change of the coefficients κ_1 , κ_2 and κ_3 . The required values of these coefficients are selected from the Memory Blocks MB1 and MB2 of the measured values x_{br} , y_{br} , z_{br} , u_{br} , v_{br} , w_{br} , R_{br} or или x_{ht} , y_{ht} , z_{ht} , u_{ht} , v_{ht} , w_{ht} , R_{ht} . These coefficients are served in the CLA though the exit 4 CC, in the CRUP through the exit 5 and in the CRLP through the exit 6.

In BM1 these coefficients are recorded in a table. They are calculated in a dynamic model of the upper platform (DMUP) using measured and calculated parameters of UP, entering the input 2 from BMSUP, the input 5 from BPSL, the

input 6 of BPSUP, as well as from the MUP. Similarly, in the BM2 these factors are recorded in a table which is calculated in a dynamic model of the lower platform (DMPL) using measured and calculated parameters of LP, coming from BMSLP, BPSLP and model of the lower platform (MLP).

Features of the software blocks of the control subsystems.

MUP module calculates the required changes Δli length legs and lengths of the control rods ΔR_{Bi} upper platform using the following equation (see Fig. 5):

$$\Delta li(x, y, z, u, v, w, \Delta R_B, \Delta R_H) = li(x, y, z, u, v, w, \Delta R_B, \Delta R_H) - li(0) \quad (1)$$

$$\Delta R_B = R_{BT} - R_{BZ} \quad (2)$$

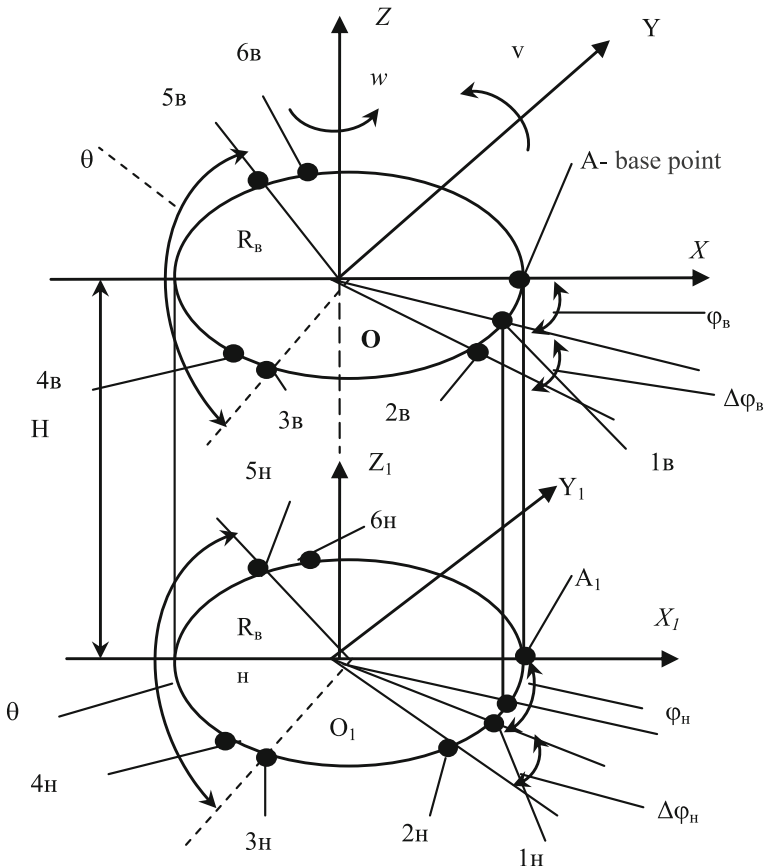


Fig. 5 The scheme of module SEMS

where:

$$\begin{aligned} \text{li}(x, y, z, u, v, w, \Delta R_B, \Delta R_H) = & \left((\text{ri}_{BX}(x, y, z, u, v, w, \Delta R_B) - \text{ri}_{HX}(\Delta R_H))^2 \right. \\ & + (\text{ri}_{BY}(x, y, z, u, v, w, \Delta R_B) - \text{ri}_{HY}(\Delta R_H))^2 \\ & \left. + (\text{ri}_{BZ}(x, y, z, u, v, w, \Delta R_B) - \text{ri}_{HZ}(\Delta R_H))^2 \right)^{1/2} \end{aligned} \quad (3)$$

$$\begin{aligned} \mathbf{r}_{iB}(x, y, z, u, v, w, \Delta R_B(t)) = & \mathbf{C}_u \mathbf{C}_v \mathbf{C}_w (\mathbf{r}_{iB}(\mathbf{0}) + \mathbf{A} + \mathbf{B}_{iB}(t)) \\ = & |\text{ri}_{BX}(x, y, z, u, v, w, \Delta R_B); \text{ri}_{BY}(x, y, z, u, v, w, \Delta R_B); \\ & \text{ri}_{BZ}(x, y, z, u, v, w, \Delta R_B)|^T \end{aligned} \quad (4)$$

$$\mathbf{r}_{iH}(\Delta R_H(t)) = (\mathbf{r}_{iH}(\mathbf{0}) + \mathbf{B}_{iH}(t)) = |\text{ri}_{HX}(\Delta R_H); \text{ri}_{HY}(\Delta R_H); \text{ri}_{HZ}(\Delta R_H)|^T \quad (5)$$

$$C_u = \begin{vmatrix} 1 & 0 & 0 \\ 0 & \cos(u(t)) & -\sin(u(t)) \\ 0 & \sin(u(t)) & \cos(u(t)) \end{vmatrix} \quad (6)$$

$$C_v = \begin{vmatrix} \cos(v(t)) & 0 & \sin(v(t)) \\ 0 & 1 & 0 \\ -\sin(v(t)) & 0 & \cos(v(t)) \end{vmatrix} \quad (7)$$

$$C_w = \begin{vmatrix} \cos(w(t)) & -\sin(w(t)) & 0 \\ \sin(w(t)) & \cos(w(t)) & 0 \\ 0 & 0 & 1 \end{vmatrix} \quad (8)$$

$$\mathbf{A} = |x(t); y(t); z(t)|^T \quad (9)$$

$$\mathbf{B}_{iB}(t) = |\mathbf{B}_{1B}(t); \mathbf{B}_{2B}(t); \mathbf{B}_{3B}(t); \mathbf{B}_{4B}(t); \mathbf{B}_{5B}(t); \mathbf{B}_{6B}(t)|^T \quad (10)$$

$$\mathbf{B}_{iH}(t) = |\mathbf{B}_{1H}(t); \mathbf{B}_{2H}(t); \mathbf{B}_{3H}(t); \mathbf{B}_{4H}(t); \mathbf{B}_{5H}(t); \mathbf{B}_{6H}(t)|^T \quad (11)$$

$$\mathbf{B}_{1B}(t) = |\Delta R_B(t) \sin \varphi_B; \Delta R_B(t) \cos \varphi_B; 0|^T \quad (12)$$

$$\mathbf{B}_{2B}(\mathbf{t}) = |\Delta R_B(t) \sin(\varphi_B + \Delta\varphi_B); \Delta R_B(t) \cos(\varphi_B + \Delta\varphi_B); 0|^T \quad (13)$$

$$\mathbf{B}_{3B}(\mathbf{t}) = |\Delta R_B(t) \sin(\varphi_B + 30^\circ); \Delta R_B(t) \cos(\varphi_B + 30^\circ); 0|^T \quad (14)$$

$$\mathbf{B}_{4B}(\mathbf{t}) = |\Delta R_B(t) \sin(\varphi_B + \Delta\varphi_B + 30^\circ); \Delta R_B(t) \cos(\varphi_B + \Delta\varphi_B + 30^\circ); 0|^T \quad (15)$$

$$\mathbf{B}_{5B}(\mathbf{t}) = |\Delta R_B(t) \sin(\varphi_B + 60^\circ); \Delta R_B(t) \cos(\varphi_B + 60^\circ); 0|^T \quad (16)$$

$$\mathbf{B}_{6B}(\mathbf{t}) = |\Delta R_B(t) \sin(\varphi_B + \Delta\varphi_B + 30^\circ); \Delta R_B(t) \cos(\varphi_B + \Delta\varphi_B + 30^\circ); 0|^T \quad (17)$$

$$\mathbf{B}_{1H}(\mathbf{t}) = |\Delta R_H(t) \sin \varphi_H; \Delta R_H(t) \cos \varphi_H; 0|^T \quad (18)$$

$$\mathbf{B}_{2H}(\mathbf{t}) = |\Delta R_H(t) \sin(\varphi_H + \Delta\varphi_H); \Delta R_H(t) \cos(\varphi_H + \Delta\varphi_H); 0|^T \quad (19)$$

$$\mathbf{B}_{3H}(\mathbf{t}) = |\Delta R_H(t) \sin(\varphi_H + 30^\circ); \Delta R_H(t) \cos(\varphi_H + 30^\circ); 0|^T \quad (20)$$

$$\mathbf{B}_{4H}(\mathbf{t}) = |\Delta R_H(t) \sin(\varphi_H + \Delta\varphi_H + 30^\circ); \Delta R_H(t) \cos(\varphi_H + \Delta\varphi_H + 30^\circ); 0|^T \quad (21)$$

$$\mathbf{B}_{5H}(\mathbf{t}) = |\Delta R_H(t) \sin(\varphi_H + 60^\circ); \Delta R_H(t) \cos(\varphi_H + 60^\circ); 0|^T \quad (22)$$

$$\mathbf{B}_{6H}(\mathbf{t}) = |\Delta R_H(t) \sin(\varphi_H + \Delta\varphi_H + 30^\circ); \Delta R_H(t) \cos(\varphi_H + \Delta\varphi_H + 30^\circ); 0|^T \quad (23)$$

$$\mathbf{r}_{iB}(\mathbf{0}) = |r_{1B}; r_{2B}; r_{3B}; r_{4B}; r_{5B}; r_{6B}|^T \quad (24)$$

$$\mathbf{r}_{iH}(\mathbf{0}) = |r_{1H}; r_{2H}; r_{3H}; r_{4H}; r_{5H}; r_{6H}|^T \quad (25)$$

$$\mathbf{r}_{1B} = |r_{1Bx}; r_{1By}; r_{1Bz}|^T = |R_B \sin \varphi_B; R_B \cos \varphi_B; 0|^T \quad (26)$$

$$\mathbf{r}_{2B} = |r_{2Bx}; r_{2By}; r_{2Bz}|^T = |R_B \sin(\varphi_B + \Delta\varphi_B); R_B \cos(\varphi_B + \Delta\varphi_B); 0|^T \quad (27)$$

$$\mathbf{r}_{3B} = |r_{3Bx}; r_{3By}; r_{3Bz}|^T = |R_B \sin(\varphi_B + 30^\circ); R_B \cos(\varphi_B + 30^\circ); 0|^T \quad (28)$$

$$\mathbf{r}_{4B} = |r_{4Bx}; r_{4By}; r_{4Bz}|^T = |R_B \sin(\varphi_B + \Delta\varphi_B + 30^\circ); R_B \cos(\varphi_B + \Delta\varphi_B + 30^\circ); 0|^T \quad (29)$$

$$\mathbf{r}_{5B} = |r_{5Bx}; r_{5By}; r_{5Bz}|^T = |R_B \sin(\varphi_B + 60^\circ); R_B \cos(\varphi_B + 60^\circ); 0|^T \quad (30)$$

$$\mathbf{r}_{6B} = |r_{6Bx}; r_{6By}; r_{6Bz}|^T = |R_B \sin(\varphi_B + \Delta\varphi_B + 60^\circ); R_B \cos(\varphi_B + \Delta\varphi_B + 60^\circ); 0|^T \quad (31)$$

$$\mathbf{r}_{1H} = |r_{1Hx}; r_{1Hy}; r_{1Hz}|^T = |R_H \sin \varphi_H; R_H \cos \varphi_H; -H|^T \quad (32)$$

$$\mathbf{r}_{2H} = |r_{2HX}; r_{2HY}; r_{2HZ}|^T = |R_H \sin(\varphi_H + \Delta\varphi_H); R_H \cos(\varphi_H + \Delta\varphi_H); -H|^T \quad (33)$$

$$\mathbf{r}_{3H} = |r_{3HX}; r_{3HY}; r_{3HZ}|^T = |R_B \sin(\varphi_H + 30^\circ); R_B \cos(\varphi_H + 30^\circ); -H|^T \quad (34)$$

$$\mathbf{r}_{4H} = |r_{4HX}; r_{4HY}; r_{4HZ}|^T = |R_B \sin(\varphi_H + \Delta\varphi_H + 30^\circ); R_B \cos(\varphi_H + \Delta\varphi_H + 30^\circ); -H|^T \quad (35)$$

$$\mathbf{r}_{5H} = |r_{5HX}; r_{5HY}; r_{5HZ}|^T = |R_B \sin(\varphi_H + 60^\circ); R_B \cos(\varphi_H + 60^\circ); -H|^T \quad (36)$$

$$\mathbf{r}_{6H} = |r_{6HX}; r_{6HY}; r_{6HZ}|^T = |R_B \sin(\varphi_H + \Delta\varphi_H + 60^\circ); R_B \cos(\varphi_H + \Delta\varphi_H + 60^\circ); -H|^T \quad (37)$$

Equations (1)–(37) can be considered as a system, which is a hexapod kinematic model for the calculation of defined and measured movements.

To solve the problem will require about 3000 pairs of multiplication-addition operations. At the same time the frequency of calculation and issuing job calculation extensions Δli leg actuators and elongation ΔR_B control rods should be at least $f_{\text{рмин}} = 100$ Hz.

The module MLP in principle to solve the same problem that the module MUP. Therefore, it should have the same performance. However, when the module SEMS is off-line, module MLP solves a simple problem of computing $\Delta R_H = R_{HT} - R_{HZ}$ (37).

Module OTUP must choose control actions $U_i(t)$, to ensure the transition from the initial position to a predetermined, so that would not be in the area of jamming, which is described by a system of linear constraints on Δli and ΔR_{bi} . Such restrictions may be of the order of 200 to 18 variables: $x_{bT}, y_{bT}, z_{bT}, u_{bT}, v_{bT}, w_{bT}, R_{bT}, t, \Delta l_1, \Delta l_2, \Delta l_3, \Delta l_4, \Delta l_5, \Delta l_6, \Delta R_{b1}, \Delta R_{b2}, \Delta R_{b3}, f_p$. The values for calculating and outputting frequency effects should be less than $f_{\text{рмин}} = 100$ Hz.

Module OTLP in principle to solve the same problem that the module OTUP. Therefore, it should have the same performance. However, when the module SEMS is off-line, the module OTLP solves a simple problem with 5 variables $\Delta R_{H1}, \Delta R_{H2}, \Delta R_{H3}, t, f_p$.

Module MBUP should develop the controlling actions $U1-U9$ by calculating the 9 simple products $U_i(t) \times Q_i$ with at least $f_{\text{рмин}} = 100$ Hz. Obviously, it is desirable that the module MBLP had similar performance, although in this case the number calculated in it works less.

Modules LBUP and LBLP should determine the value of logical variables Q_i and Q_j by inspection type rules:

If $F_i > F_{di}$, then $Q_i = 0$, or $Q_i = 1$.

1) If $F_j > F_{dj}$, then $Q_j = 0$, or $Q_j = 1$.

The number of such rules is not more than 9. The frequency of issuance Q_i and Q_j values must be at least $f_{\text{рмин}} = 100$ Hz.

DMUP and DMLP modules is used to calculate the optimal values of K1, K2 and K3 PID controllers, excluding jamming and ensures smooth movement hexapod platform. The main computational procedure in these modules is the procedure of matrix-vector multiplication [3]. As is known, to calculate the product matrix-vector must be performed mn multiplications and $m(n - 1)$ additions, where m —the number of rows of the matrix; n —the number of columns. Estimated turns out about 3000 pairs of multiply-add operations. The values of the frequencies for calculating and outputting the control object on the control actions must be at least $f_{\text{рмин}} = 100$ Hz. Bit computing program blocks determined by the type of the module SEMS and requirements for accuracy and reliability of the control system. Bit ADC on the input CC and DAC—on outputs in these systems is typically at least 12, and the frequency conversion of at least 200 Hz.

3 Conclusion

Neuroprocessor automatic control system allows you to parallelize the process of calculating of control actions and signaling adaptation modules SEMS. This improves the speed and accuracy of control. The main computational element of the system is neuroprocessor for processing 32-bit scalar data and programmable bit packed into 64-bit words. In neuroprocessor software implements the functions of the main units NACS. Use NACS force sensor simplifies algorithms blocks LBUP, LBLP, DMUP and DMLP and improve the accuracy of the calculation. The accuracy of the sensors in BMSUP and BDPNP determines the maximum attainable accuracy of positioning of mobile platform modules SEMS.

References

1. Merlet, J.P.: *Parallel Robots*, 2nd edn, p. 383. Springer, INRIA; The Netherlands, Sophia-Antipolis (2006)
2. Gorodetsky, A.E., Tarasova, I.L.: *Upravlenie i neironiy seti (Control and neural networks)*, p. 312. Politekhnikeskii universitet Publ., Saint-Petersburg (2005) (In Russian)
3. Artemenko, J.N., Agapov, V.A., Dubarenko, V.V., Kuchmin, A.J.: Group control of radiotelescope subdish actuators. *Informatsionno-upravliaiushchie sistemy* **4**(59), 2–9 (In Russian)

Development of Algorithms and Software for Neurocomputer Systems of SEMS Automatic Control Modules

V.N. Ruchkin and V.A. Romanchuk

Abstract The article discusses the issues of developing of algorithms and software for specialized computing devices based on neuroprocessors to be used in automatic control of electric-mechanical system modules (in this case study, a hexapod) in a mode that is close to real time. The practical implementation employs the NM6406 neuroprocessor based on the MC 51.03 tool module and MB 77.07 microcomputer being developed by the R&D centre “Module”.

Keywords Neuroprocessor-based computing system · Hexapod · Control · Matrix computation

1 Introduction

Controlling dynamic objects type SEMS involves two modes: operation and standby, due to the rigid necessity of high-speed processing of great amounts of data. In fact, no computing control system today can ensure such processing of data at a set tempo, when such input is fed from multiple sensors; therefore, computing operations have to be parallelized into additionally connected specialized computational devices (SCDs). Such task sharing supports the unsteady condition, without slowing down the basic computing process. Two primary tasks require real-time problem-solving: the computation of control action and integration of a differential equation system. Transforming the differential system into a system of algebraic equations (vector-matrix) is convenient, as far as it enables its implementation in digital computing, namely in SCDs: their processor modules will simultaneously perform accumulative multiplication actions with multiple operands [1].

V.N. Ruchkin · V.A. Romanchuk (✉)
Ryazan State University Named for S.Yesenin, Ryazan, Russia
e-mail: v.romanchuk@rsu.edu.ru

V.N. Ruchkin
e-mail: v.ruchkin@rsu.edu.ru

To develop and implement the corresponding mathematical content, algorithms and software, we propose to activate a selected set of hardware tools: neuroprocessor devices based on special-class processors (Generation 6), widely used in data processing. The choice of neuroprocessors considered such parameters as the speed of parallel processing, availability of accumulative addition, and high energy efficiency [2]. In our case, we chose the NeuroMatrix 640X processor family, manufactured by the Module Research and Development Centre (Moscow, Russia) [3].

The input data parameters for development of algorithms and software are as follows:

- definition of digital signals from sensors;
- description of algorithms for generation of management signals;
- a mathematical model implemented in a SIMULINK module model of the MATLAB software package.

The source data of algorithms developed include the following:

- definition of sensor signals received after conversion of analog signals from the hexapod into digital form (via an analog-digital converter).

The output data of algorithms developed include the following:

- control signals, converted into analog (via a digital-analog converter);
- auxiliary and maintenance signals.

2 Mathematical Formalization of SCD Operational Tasks

The flowchart of an SCD is shown in Fig. 1. The device's functional purpose is to calculate optimal parameter values for a shared controller and to calculate quotients (k_1 , k_2 , k_3) of PID controllers of the hexapod's movement engine, to ensure seizure-free and smooth motion of the hexapod's platform.

The chart uses the following symbols:

$\tilde{\Phi}, \tilde{\Phi}, \tilde{S}, \tilde{S}, \tilde{G}, \tilde{\Phi}$	operational matrixes received from the parameter matrixes of the hexapod and from those of the correction filters;
P', P	parameter matrixes of correction associations (6×100);
$\alpha * (t)$	program vector function (18×1);
$Y(t)$	vector function of observation (signals received from the measuring system) (30×1);
$X(t), X * (t)$	vector function of the system's current state and of its programmed state at Step i of its control (100×1);
$X(t+h), X * (t+h)$	the same at Step $(i + 1)$ (100×1);
$U(t)$ and $U(t+h)$	vector of control influences at Steps i and $(i + 1)$ of control (30×1);

where $MK = \{MK_1, MK_2, \dots, MK_i, \dots, MK_I\}$ —is a set of microcommands written in the internal language of the processor; K_i —is the minimal number of microcommands that is necessary for implementation of the O_m operation.

Depending on the solution of task (3), at the next stage each j -numbered processing algorithm should be associated with a certain $PR^{(j)}$ program, i.e., a φ view should be defined:

$$\varphi : A^{(j)} \rightarrow PR^{(j)}, j = \overline{1, N}. \tag{4}$$

The $PR^{(j)}$ program is a tuple of microcommands:

$$PR^{(j)} = \langle MK_1, MK_2, \dots, MK_i, \dots, MK_I \rangle .. \tag{5}$$

Thus, proceeding from formula (3) we can say that the basis of a neuroprocessor unit is an emulation of a formal neuron, which is mathematically a total of operations of addition and multiplication, i.e., “accumulative multiplication”.

From the hexapod control algorithm, it becomes clear that the main procedure in the SCD is the multiplication of the matrixes by the vector:

$$\begin{aligned} \Phi \times X &= \begin{bmatrix} \Phi_{11} & \Phi_{12} & \dots & \Phi_{1n} \\ \Phi_{21} & \Phi_{22} & \dots & \Phi_{2n} \\ - & - & - & - \\ \Phi_{m1} & \Phi_{m2} & \dots & \Phi_{mn} \end{bmatrix} \times \begin{bmatrix} x_1 \\ x_2 \\ \vdots \\ x_n \end{bmatrix} \\ &= \begin{bmatrix} \Phi_{11}x_1 + \Phi_{12}x_2 + \dots + \Phi_{1n}x_n \\ \Phi_{21}x_1 + \Phi_{22}x_2 + \dots + \Phi_{2n}x_n \\ - & - & - & - \\ \Phi_{m1}x_1 + \Phi_{m2}x_2 + \dots + \Phi_{mn}x_n \end{bmatrix} \end{aligned} \tag{6}$$

One of the vector result components is the sum of the item products of matrix lines by the corresponding items of the vector-column. This sequence of operations should be repeated as many times there are lines in a matrix. To calculate the product of matrixes by the vector, it is necessary to perform multiplication of operations $T_{YBM} = m \times n$, where m is the number of line in the matrixes; n is the number of columns, and N_{CMB} is the number of addition operations, defined by the formula: $N_{CMB} = m \times (n - 1)$ addition operations, or approximately 3000 pairs of “multiplication—addition” operations. Thus, the neuron model (2) can be used in implementation of control tasks, including the operations of multiplication of matrixes by columns (6).

3 Development of Algorithm Support of the SCD

As the conducted experimental research employed an NM6406 neuroprocessor based on an MC 51.03 toolkit and an MB 77.07 microcomputer, we have to say that parallelizing is made effective due to hardware support of the vector-matrix multiplication operation in the NeuroMatrix NM6406 neuroprocessor. All arithmetic computing directly related to computation of control influences is performed on a vector coprocessor. As the vector node allows handling data with variable width, it is convenient to allocate 32 bits to the integral part and 32 bits to the real part.

For development of algorithms and of program code, subprograms of the following functional items (of the mathematical model of a hexapod-controlling SCD) were implemented [3].

1. A matrix multiplier and a matrix multiply-accumulator.

Differential equations describing the hexapod motion can be shown as differences in vector-matrix form, which is convenient for computer hardware implementation. So, the chief operation of the SCD consists in multiplication of matrixes which can be split into a couple of elementary operations «multiplication–addition» (accumulative multiplication). For this operation, a vector coprocessor is used, i.e., a shared matrix node, to perform operations of accumulative multiplication with arithmetic and logical operations, masking, and enabling vectors and matrixes.

Figure 2 shows the layout of a vector coprocessor.

This is the basic functional item with a register file of general purpose. It is a 64×64 matrix structure, randomly divided into columns and rows.

The accumulative multiplication is performed in the operational matrix of the neuroprocessor:

$$Z_i = Y_i + \sum (X_i W_{ij}); i = \overline{1, m}; j = \overline{1, n},$$

where

X_i is a data item sent to the vector coprocessor input;

Y_j is the subsum accumulated at the previous stage of weighted addition, or the remainder from the previous operation;

Y_0 an item of data vector input;

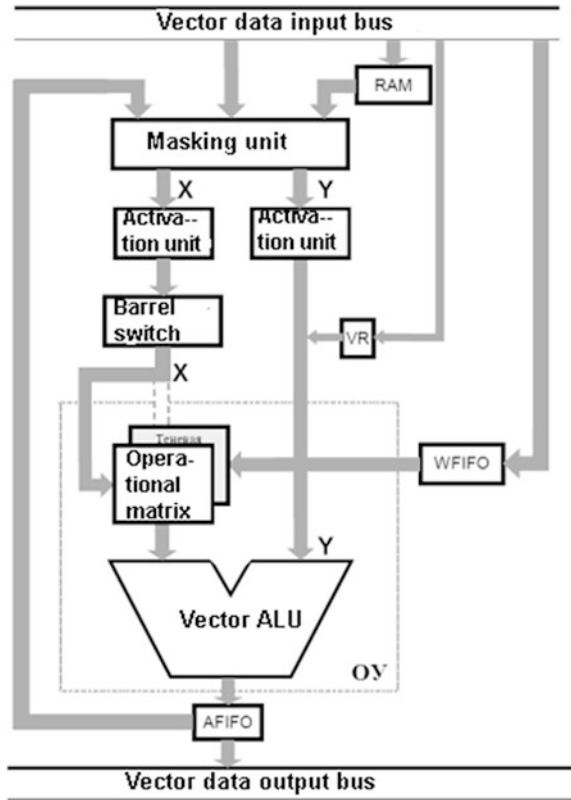
W_{ij} the weight quotient, stored in a dedicated cell of the operating matrix of the processor;

m the number of columns in the operative matrix of the processor;

n the number of lines in the operative matrix of the processor

The operating matrix allows 2 inputs:

Fig. 2 Layout of a vector coprocessor



$$X = \{x_1, x_2, \dots, x_n\} - 64 - \text{bit};$$

$$Y = \{y_1, y_2, \dots, y_m\}.$$

Data input at X should be multiplied by the number of the matrix cells, they are further added column-wise, which means that in case of overflow there occurs a loss of sign bits. Data from the Y input are added item-wise with the multiplication product, resulting from operations with the data of the X input.

To perform weighted addition, we must first export W_{ij} weighted quotients into the matrix. For this, two options are possible: direct export into the operational matrix, or through a shadow matrix. Uploading weight quotients via a shadow matrix is more effective, as it occurs within one processor stroke. The shadow matrix exists in the neuroprocessor vector node for acceleration, because weight quotients are loaded within 32 strokes in the background mode. Overflow of weight quotients from the shadow matrix to the operational matrix happens within one stroke.

Partitioning of matrixes into lines is defined in the *sb2* operational registry. It provides preliminary partitions of 64-bit input data words that are sent to the

Y input. Operational matrix partitioning into column is set in **nb2** operational registry. The same registry defines partitioning of 64-bit data at the Y input and is also preliminarily entered as a word in the registry. The same registry defines the computing bit rate that will move to the AFIFO buffer registry in the end. Thus, input data (operands) and output values are packed into 64-bit words during partitioning. All operations in the matrix are performed as parallel within one stroke.

2. Accumulator of two or more operands.

The accumulator of two or more operands is implemented via a vector unit of the processor and operations of weighted addition (Fig. 1) with void multiplication, i.e., a “single” shadow and operational matrix (where each 64×32 bit is filled with single bits). The effectiveness of this operation depends on the bit rate of input data, as the computing speed is increased via matrix partitioning into rows and columns, because work is performed simultaneously on several operands. One important property of a vector processor is its ability to work with operands of various length.

3. Activation (overflowing) function.

Activation functions are implemented with the help of the processor’s vector unit and operations of weighted addition (Fig. 1). Subprograms of two activation function types are implemented: the threshold function and the overflow function. In activation units computation is performed on packed data words. Activation units allow using activation functions on all items of a packed word simultaneously. The main role in controlling the activation functions is that of the **f1cr** and **f2cr** registries. The activation units are located between the masking device and the operational matrix or the vector calculator. The activation function may be performed on input X or Y data, or on both inputs.

All elemental basic operators are implemented in macros form in the neu-rassembler language.

4 Development of Software for SCD Operation

For work convenience with various source data a task model was implemented, to automatically control electric and mechanical systems in the developed Visual Programming subsystem of the NP Studio software platform (Fig. 3).

The chief item in the subsystem is the notion of a functional unit, connectable to other functional units to perform certain functions.

During the first stage, the user describes the functional units (FU) and connections between them, using their software graphic representation.

The workspace of the software application is divided into functional parts:

1. The area of functional units, instance of which may be transferred to the modeling workspace with the drag-and-drop function. The same area contains control items for visualization and deletion of connections between items. When

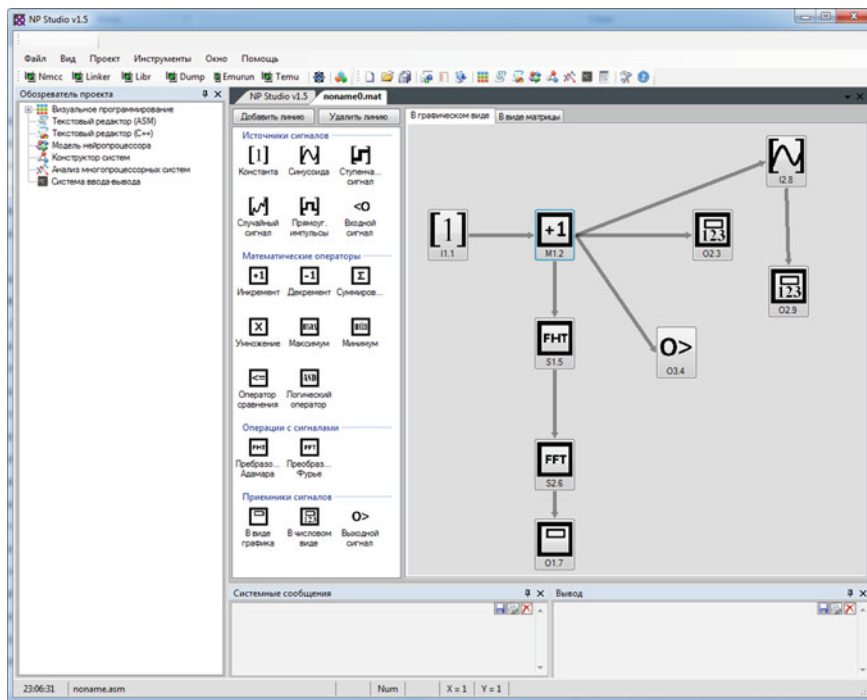


Fig. 3 Task model of automatic control of electric and mechanical system modules in the developed visual programming subsystem of the NP studio software platform [4-6]

added to the workspace, each item gets a unique ID, which is a concatenation of the item category, the item number within the category and the index number of the item, e.g., “O2.9” defines an item from category Output Signals, Number, with “9” as its unique ID.

2. The workspace (which, in its turn, can be represented as visual items and connections between them, or as a matrix of connections between items (Fig. 4).

5 Conclusion

The article proposes algorithms and software for a specialized computational device based on neuroprocessors, to be used in automatic control of electric-mechanical systems (in this case study, a hexapod) in a mode that is close to real-time, employing a novel computing device, an NM6406 neuroprocessor based on an MC 51.03 tool module and an MB 77.07 microcomputer, developed by the Module Research and Development Centre. The research proves effectiveness of the

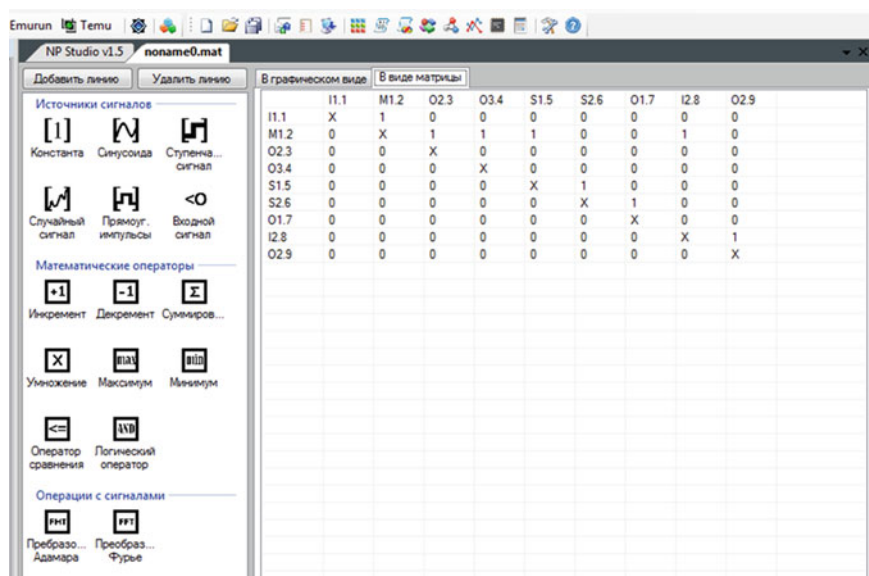


Fig. 4 Task model of automatic control of electric and mechanical system modules in the developed Visual Programming subsystem as matrix connections

neuroprocessor in performing tasks of automatic control of electromechanical system modules, through parallel processing and consequent speed gain, use of the accumulative addition operation, and low power consumption.

References

1. Ruchkin, V., Romanchuk, V., Sulitsa, R.: Clustering, restorability and designing of embedded computer system based on neuroprocessors. In: Proceedings of the 2nd Mediterranean Conference on Embedded Computing (MECO), pp. 58–62. Budva, Montenegro (2013)
2. Galushkin, A.I.: Neurocomputers, p. 528. Bk.3. M, IPRZhR (2000)
3. Viksne, P.E., Fomin, D.V., Chernikov, V.M.: The single-crystal digital neuroprocessor with variable digit capacity of operands. In: News of Higher education institutions, Instrument making, vol. 39, no. 7 (1996)
4. Romanchuk, V.A., Ruchkin, V.N.: Development of software of the analysis of neuroprocessor systems. RSREU Bull. **2**(32), 61–67 (2010)
5. Romanchuk, V.A., Ruchkin, V.N., Fulin, V.A.: Development of a complex neuroprocessor system model. Digital Proc. Signals Ryazan Inf. Technol. **4**, 70–74 (2012)
6. Ruchkin, V.N., Romanchuk, V.A., Fulin, V.A.: Cognitology and artificial intellect. p.260. Ryazan: Uzorochye (2012)

Intelligence System for Active Vibration Isolation and Pointing of Ultrahigh-Precision Large Space Structures in Real Time

S.N. Sayapin and Y.N. Artemenko

Abstract In this article, we examine the problem of ensuring of ultrahigh precision for the cryogenic large space telescope (10 μm), its ultrahigh-precision pointing (one second of arc), and stabilization (0.2 of second of arc) in real time that must be dealt with. We suggest the novel concept design of the intelligence system of the active vibration protection and ultrahigh-precision pointing the cryogenic large space telescope of the observatory *Millimetron* aimed at addressing abovementioned problems.

Keywords Cryogenic large space telescopes · Space observatory millimetron · Ultrahigh-Precision pointing · Intelligence active structures · Parallel mechanisms

1 Introduction

There are many unsolved problems and fundamental challenges for various high-precision and ultrahigh-precision large deployable space structures, for example, the orbital telescopes, the satellite microwave antennas and so on [3, 5]. In particular, one of the problems is ensuring of ultrahigh precision for the cryogenic large space telescopes (CLST) of the space observatories (SO). The precision of space telescope and sizes its main mirror depend on wavelength range. Table 1 gives comparison of main features of advanced space observatories: JWST, Millimetron and SPICA [4].

S.N. Sayapin

The Bauman Moscow State Technical University, The Blagonravov Institute for Machine Science of the Russian Academy of Sciences, Moscow, Russia
e-mail: S.Sayapin@rambler.ru

Y.N. Artemenko (✉)

The Astrospace Center of P.N. Lebedev Physical Institute of the Russian Academy of Sciences, Moscow, Russia
e-mail: Artemenko.AKC@yandex.ru

Table 1 Comparison of main features of latest generation large cryogenic space telescopes

	Project		
	JWST (USA, Europe, Canada)	Millimetron (Russia, Europe)	SPICA (Japan, Europe)
Launch date	2018	2019	2022
Orbit	L2 point vicinity	L2 point vicinity	L2 point vicinity
Wavelength	0.6–28.3 (μm)	0.02–3; 0.3–17 (mm)	5–210 (μm)
Telescope operating mode	Single-dish	Single-dish, interferometer	Single-dish
Diameter (m) and type main mirror	6.5, folding	10, folding	3.5, solid
Temperature modes and cooling system	Reflector 45 K, active and passive	Reflector 4.5 K, active and passive	Reflector < 6 K, active and passive

We begin this chapter with a general description of the problem of ensuring of precision for the large space telescope by the example of largest ultrahigh-precision CLST of SO Millimetron. Next, we examine the method of decision this problem by the intelligence system for active vibration isolation and pointing of ultrahigh-precision CLST, and finally, a conclusion and a list basic reference and journal articles are supplied at the end of this chapter.

2 The Description of the Problem Ensuring of Ultrahigh Precision for the CLST of SO Millimetron

Millimetron is a Russian-led 10 m diameter submillimeter and far-infrared SO which is included in the Space Plan of the Russian Federation for launch around 2019. Head scientific organization: the Astrospace Center of P.N. Lebedev Physical Institute of the Russian Academy of Sciences. Parent enterprise: the Federal State Unitary Enterprise “Lavochkin Research and Production Association” [4, 12, 14, 15, 18]. A general view and a disclosure cyclogram of the SO Millimetron are given in the Fig. 1. It’s intended for operation in conditions of high vacuum and ultralow temperature (4.5 K). This SO includes CLST with the main parabolic mirror diameter of 10 m which will be unfolded on the specified orbit. CLST is the ultrahigh-sensitivity system and temperature modes its reflector is 4.5 K. Therefore, it is need of the cryo shield with a cooling system and the system of heat shields. All space telescope large elements (mirror, heat shields, cryo shield and radiators) are performed transformable.

There are following the basic ultrahigh-precision characteristics of CLST: surface accuracy of main mirror $\leq 10 \mu\text{m}$ (RMS); orientation (pointing) accuracy ≤ 1 s of arc; stabilization accuracy ≤ 0.2 of second of. These ultrahigh-precision characteristics and the main parabolic mirror diameter (10 m) follow from the wavelength ranges CLST (0.02–3 mm and 0.3–16 mm) and its ultrahigh sensitivity.

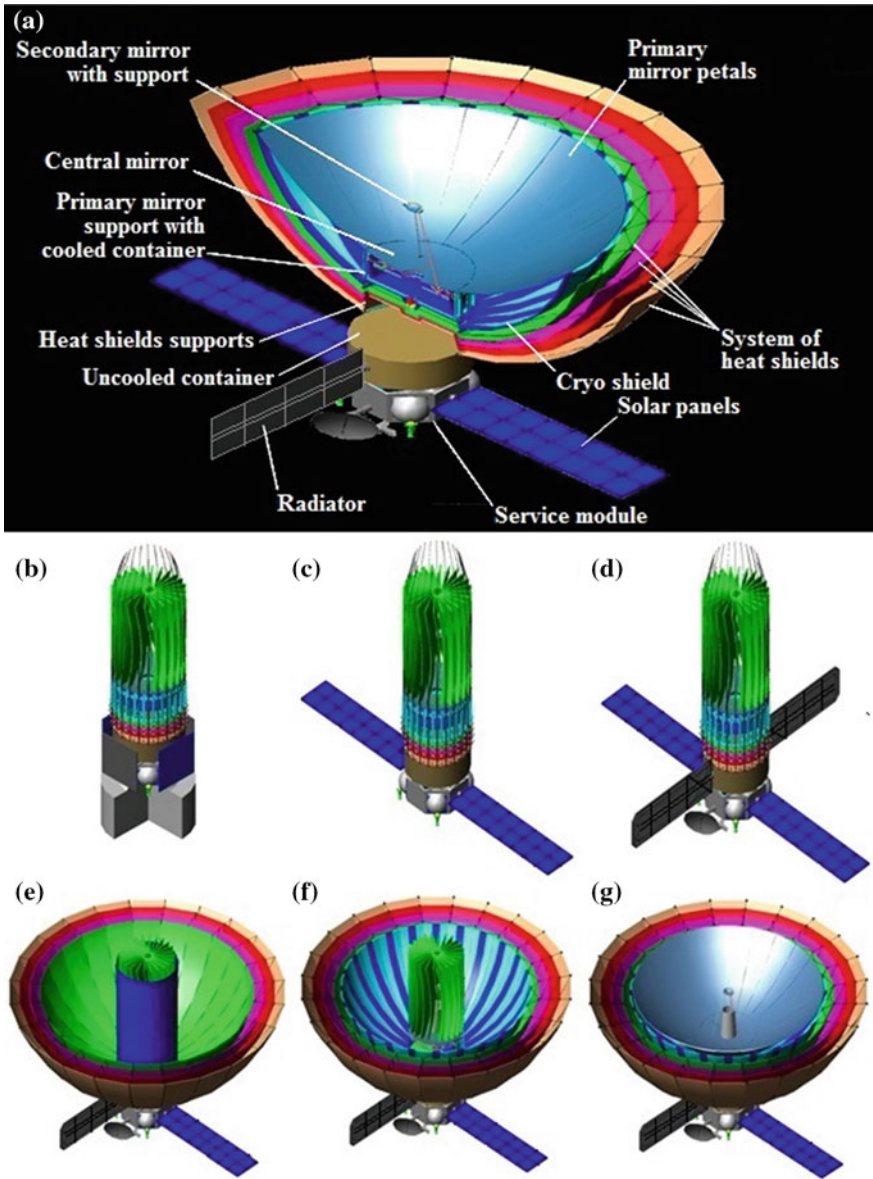


Fig. 1 General view (a) and a disclosure cyclogram of the SO Millimetron: Spacecraft in the transportation configuration (b); Solar-panels disclosure (c); Radiators and service systems disclosure (d); Disclosure of 4 heat shields (e); Cryo shield disclosure (f); Mirror disclosure (g)

CLST is mounted on a service module (SM). However, the accuracy of the orientation and stabilization CLST by SM is less than it is [14]. The very large elements of CLST and SM are lengthy structures of low stiffness that are

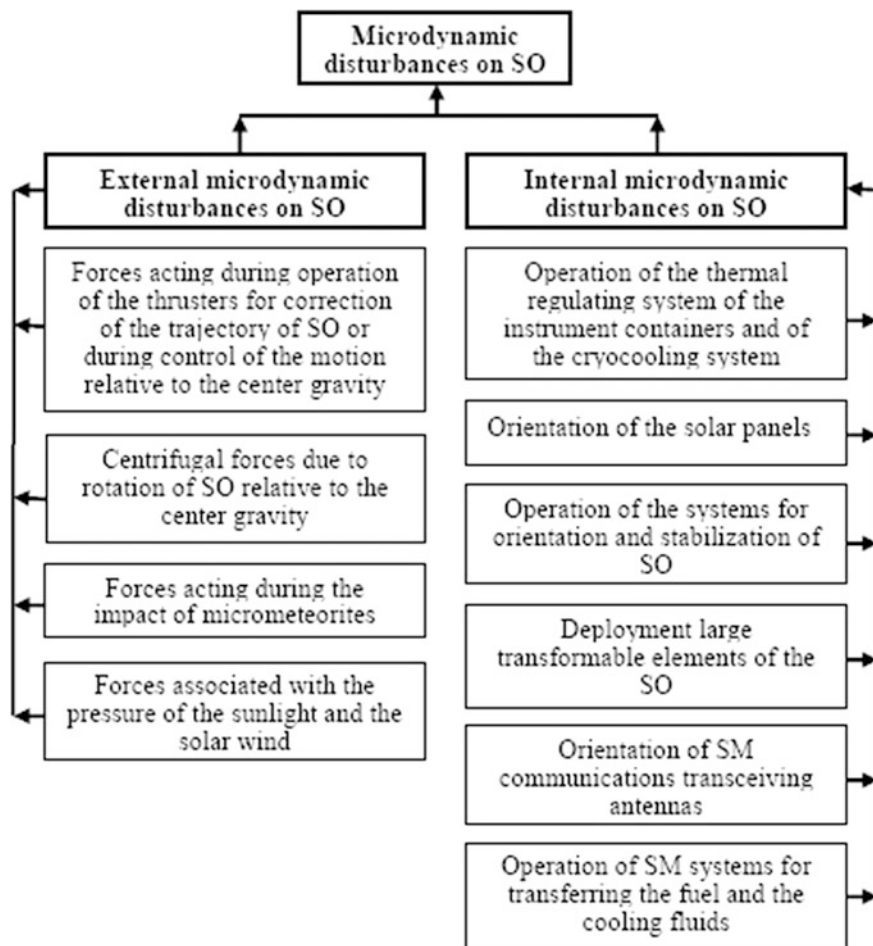


Fig. 2 Classification the microdynamic disturbances on SO in the orbital flight

deployable in orbit. Therefore the low frequency oscillations of the lengthy elastic elements of the service module structures and CLST that arise from the external and internal microdynamic disturbances (Fig. 2) in the course of orbital flight lead to deflection working surface and deviation of the actual axis of CLST beyond the acceptable limits, and consequently, degradation of the basic ultrahigh-precision characteristics of CLST. Therefore, to solve this problem, while reducing vibration activity sources microdynamics disturbances to apply effective systems of vibration isolation and pointing of ultrahigh-precision pointing CLST on the studied objects in real-time. Thus, the solution of the problem of low-frequency vibration isolation and ultrahigh-precision of CLST is urgent and challenging [1, 12, 14, 15, 17].

The orbit of SO Millimetron will be located in the vicinity of the Lagrangian point L2 in the Sun-Earth system at an average distance of 1.5 million km from the Earth. Operating time of SO Millimetron will be about 10 years. Therefore, it is in need of an intelligence system for real-time control.

3 Validation of the Intelligence System for Active Vibration Isolation and Pointing of Ultrahigh-Precision CLST of SO Millimetron

High demands on the precision of CLST and their enormous distances from Earth pose to developers a number of problems whose solution requires the development of new effective concept design solutions. One such problem is the problem of gravitational-inertial sensitivity of CLST to the external and internal microdynamic disturbances (Fig. 2). Here, in accordance with the terminology in [7], the gravitational-inertial sensitivity is the degradation of the basic ultrahigh-precision characteristics of CLST from the external and internal microdynamic disturbances in the orbital flight [7, 12, 14, 15, 17].

Another problem is ensuring of the ultrahigh-precision pointing (accuracy ≤ 1 s of arc) and stabilization (accuracy ≤ 0.2 of second of) of CLST in real-time and periodic control of the geometry of the main mirror.

The main direction of solving the first problem now is to find ways of reducing the external and internal microdynamic disturbances from SM on the ultrahigh-precision CLST. This can be achieved by reducing the level of disturbance operating systems SM or SM interchange payload by applying a soft connection in the form of a flexible interface, or gimbals, as well as through the use of effective intelligent systems active spatial vibration isolation in the form of parallel mechanisms established between the SM and CLST. It should be noted that, despite the efficiency, the organization of the junction SM with large payloads weighing several tons, is currently and in the near future hardly feasible task. There is an example of successful use of driven gimbals as a junction between the main mirror of two-mirror offset antenna of Japanese space radio telescope and SM (Fig. 3a) [8]. However, here the mirror of the antenna has a small mass (200 kg with a diameter 9.26 m) and less stringent requirements for precision, which significantly simplifies the solution of the problem.

To solve the second problem at the present time, there is a tendency to use for these purposes of spatial parallel mechanisms, in the form of tripod, hexapod and other modules SEMS, having both mono and multi-module performance. For example, for the guidance and stabilization of the primary mirror of a space telescope “Kepler” applied spatial precision mechanism in the form of a tripod with three V-shaped supports (Fig. 3b) [6]. However, due to the high rigidity of the main mirror and its small diameter (1.4 m), the use of mirror vibration protection (in contrast to large precision space antenna mirrors with a diameter of 10 m or more) is required.

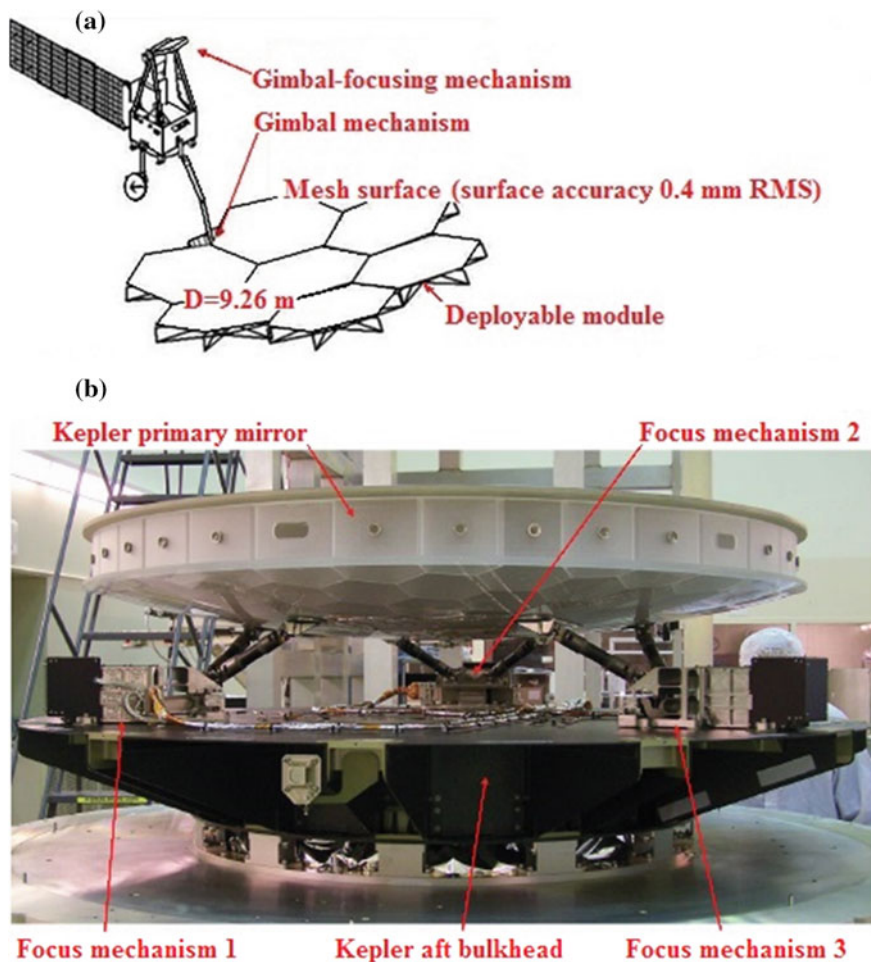


Fig. 3 General view of the space radio telescope “ASTRO-G” (VISOP) with a large deployable reflector (a) and the primary mirror of the telescope “Kepler”, installed on the focus mechanisms (b)

Thus, to solve these problems requires the creation of a system capable of ensuring the vibration isolation of CLST from the external and internal microdynamic disturbances and its ultrahigh-precision pointing on the studied objects in real-time. Taking into account the low frequency of oscillations of the formative elements of the design of CLST, their significant mass and a wide range of microdynamic disturbances, passive vibration isolation is inefficient and requires the use of spatial system low frequency active vibration isolation and precision guidance. Given the huge remove CLST from the Earth, the system must respond appropriately to time-varying the microdynamic disturbances and offline, in real

time, to make the best decisions, ensuring the preservation of the basic ultrahigh-precision characteristics of CLST in the process of operation. Therefore, such structure is in need of an intelligence system for real-time control. We shall examine new concept of design of the intelligence system for active vibration isolation and pointing (ISAVIP) of ultrahigh-precision large space structures, for example, such as CLST.

4 The Description of ISAVIP of Ultrahigh-Precision CLST of SO Millimetron

Currently, almost all known systems of vibration isolation and pointing of any high-precision payload of the spacecraft are used three-level concept of configuration, including the installation of any precision payload on the spacecraft by the series connected following levels (Fig. 4): the intermediate frame (1st level), the system of vibration isolation (2nd level), and the platform of precision pointing (3rd level).

However, this approach inevitably leads to a sharp increase in dimensions and mass characteristics of the system and in some cases unacceptable because of the shortage of useful volume under the fairing of the launch vehicle, especially when precision placement of large payloads, for example, deployed in orbit CLST of SO Millimetron. The system of vibration protection (2nd level) in the high, low and subsonic frequencies is preferable to use active funds over passive are more low-mass characteristics, which is very important when creating a space systems [1, 2, 8, 10–13, 15].

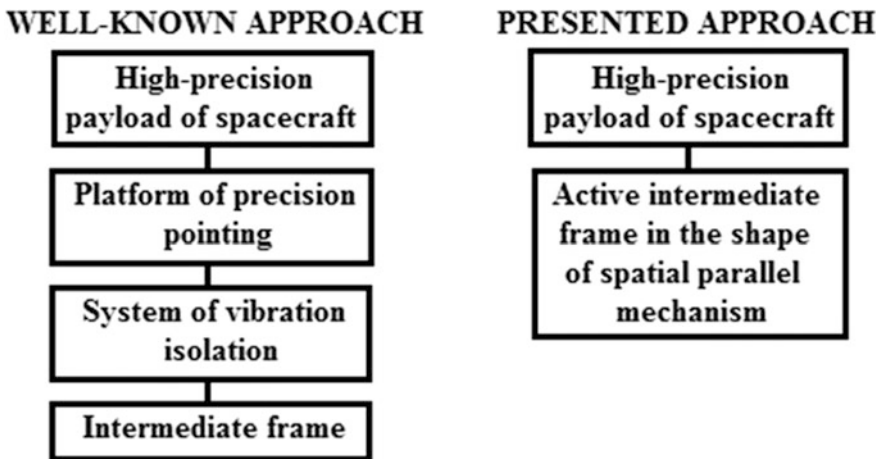


Fig. 4 Well-known and presented approaches of ensuring of vibration isolation and pointing of high-precision payload of spacecraft

In this regard, the authors propose a new concept of creating functionally-sibling ISAVIP of ultrahigh-precision CLST of SO Millimetron project aimed at solving these problems. In single-level spatial concepts ISAVIP of ultrahigh-precision CLST, wherein the global level of innovation [13, 15], was able to increase its efficiency by expanding the functionality of the structural elements SO Millimetron. For example, the implementation of the intermediate frame between CLST and SM is active in the form of a hexapod (executive body of ISAVIP of CLST) [14], allows to synthesize a single-level ISAVIP of CLST practically with the same dimensions and mass characteristics and low power consumption, and also get a new quality for the spacecraft.

The proposed concept of ISAVIP for CLST is able to provide the following regimes:

- the vibration isolation of the solar panels of SM from the low frequency elastic oscillations caused by the disclosure of the radiators, the heat shields, the cryo shield, and the primary mirror (Fig. 4);
- the vibration isolation of the large elements of CLST from the low frequency microdynamic disturbances caused by operation of the SM systems;
- the suppression of the low and high frequency oscillations of the elastic structures of the CLST caused by the external and internal microdynamic disturbances in the orbital flight;
- the periodical ultrahigh-precision angular pointing of the optical axis of the CLST;
- the generation of vibration influences on the elastic structures of the CLST and the SM, and the vibrodiagnostics of the large elements of their designs.

This single-level ISAVIP of ultrahigh-precision CLST, unlike their foreign counterparts [2], is capable of spatial active vibration isolation of any precision object with simultaneously high-precision pointing and stabilization this object [12]. In this regard the ISAVIP of ultrahigh-precision CLST belong to the class of the most promising at the present level of active spatial vibration isolation systems “kinematic type” [12]. While it is believed that the active element, while remaining absolutely rigid (within the accepted assumptions) directionally changing its length and is regarded as the generator of the relative displacement (velocity, acceleration). This kinematic change of the element occurs under the influence of signals from sensors of mechanical quantities (accelerations, forces, displacements, velocities, and other parameters). This takes into account the specificity of the discontinuity of the control from the spacecraft-borne high-performance data-processing and control system (SBHPDPCS). The on-line control of the ISAVIP of the ultrahigh-precision CLST is achieved through the use of a giant-powered computer, implements the methods of neural control [9]. The effective satisfaction of functional requirements for the ISAVIP is possible by the use of the active three-dimensional intermediate frame with the kinematic configuration such as the Stewart platform [2, 11–15]. We note that the use of the Stewart platform as the intermediate three-dimensional frame makes it possible to satisfy not only each regime individually but also their combinations. For example, along with the active vibration isolation of the CLST

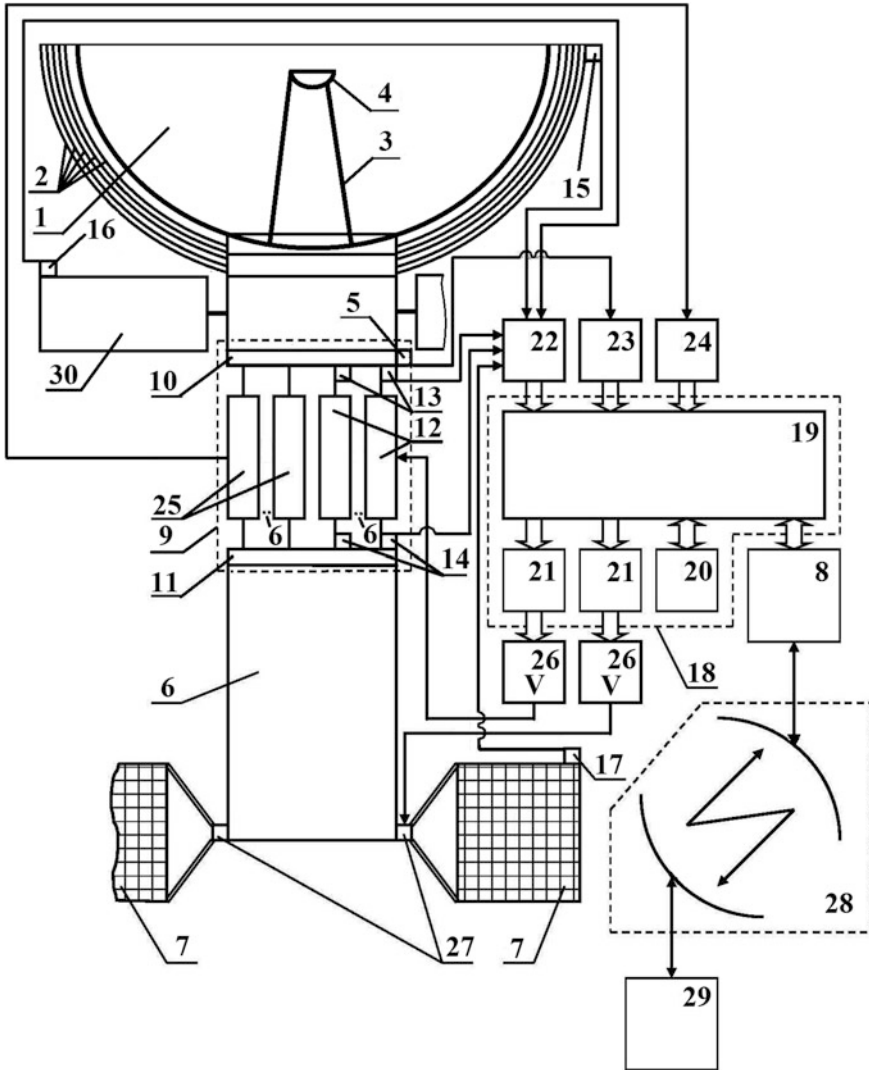


Fig. 5 The schematic diagram of the ISAVIP for the ultrahigh-precision CLST of SO Millimetron

from the low frequency vibrations that are caused by the operation of the SM systems, it is possible to perform the adjusting and ultrahigh-precision pointing of the CLST [11–15].

The proposed concept of the ISAVIP for the ultrahigh-precision CLST of SO Millimetron can be realized as follows. The CLST (Fig. 5), including the deployable primary mirror 1 with the heat shields (including the cryo shield) 2, the support system 3, the secondary mirror, the star trackers 5. The SM 6 with the solar panels 7 and the high-quality radio complex (HQRC) 8 joins with the CLST by the active

three-dimensional intermediate frame 9. The active frame 9 has the kinematic configuration such as the Stewart platform [16] and it includes the platform 10 and the base 11 which are rigidly attached to the mating components of the CLST and the SM, respectively (Fig. 5). The platform 10 is pivotally connected with the base 11 by means of suspension with 6° of freedom, in the form of a spatial manipulator including at least six identical unit individual active vibration isolation modules (IAVIM) 12.

The manipulator is constructed on the basis of parallel-connected driving kinematic chains with the possibility of the active three-dimensional intermediate frame 9 with disconnected drives of the IAVIM 12, which, in turn, the rods form 9. Each of the rods is provided with a linear actuator that provides manipulator-frame the six-degree mobility in working condition and geometric resistance in the off state. In places pivotally fastening each of the IAVIM 12 to the platform 10 and the base 11 are mounted the combined sensors of the spatial position and accelerations 13 and 14, respectively, made in the form of the miniature triaxial blocks gyroscopes-accelerometers to determine the relative movement of the IAVIM 12 and measure components of acceleration acting on their longitudinal axis. At the test points of the heat shields 2, the radiators and the solar panels 7 are mounted the combined sensors of the spatial position and accelerations 15-17, respectively. SBHPDPCS 18 includes neurocomputer 19 with the corresponding means of software 20 and digital/analog converters (DAC) 21. SBHPDPCS 18 through the input bus analog/digital converters (ADC) connected respectively to the outputs of the ADC 22 of the combined sensors of the spatial position and accelerations 13-17, ADC 23 of the star trackers 5, and ADC 24 of the relative displacement and velocity sensors 25. The outputs of SBHPDPCS 18 via output buses are connected to respective inputs connected to the DAC 21, the power amplifier 26 and the executive elements (IAVIM 12 and the slewing drives 27 of the solar panels 7), as well as the entrance connected in series HQRC 8, the radio link 28 and ground-based radio system 29. The cryocooling of the CLST is accomplished by the cryocooling system with the folding radiators 30. The control of the ISAVIP for the ultrahigh-precision CLST is realized from the SBHPDPCS 18.

The ISAVIP for the ultrahigh-precision CLST (Fig. 5) makes it possible to select one of the regimes or some combination of the regimes of control of the dynamic of structure of the deployable very large elements of the CLST that are sensitive to the low frequency elastic vibrations. The control is accomplished by the individual active vibration isolation modules 12, which are articulated between the base 11 and the platform 10, by means of coordinated changing of their lengths on the basis of commands from SBHPDPCS 18.

The functioning of the ISAVIP for the ultrahigh-precision CLST is implemented as follows. After the disclosure of the primary mirror 1 with the heat shields (including the cryo shield) 2, the radiators 30, the solar panels 7, the antenna of the HQRC 8 and other long items, and enable the IAVIM 12 in the active regime, the readings are combined the sensors of the spatial position and accelerations are compared with the values obtained in their terrestrial setting. The results of this comparison are judged on the elastic deformations and oscillations of the elongated

structural members of the space telescope and the SM, as well as on the mutual location of the platform 10 and base 11 in operation. If the deviation exceeds the allowable value, perform one of the following regimes (or combinations thereof) dynamics control CLST and SM in real time.

In the first regime active vibration isolation of the SM and its extended elements (the solar panels 7, the antenna of HQRC 8, etc.) is performed during the opening of the deployable CLST (the primary mirror 1 with the heat shields and the cryo shield 2, the radiators 30). Here the SBHPDPCS 18 performs the control using feedback from the accelerometers that the relative displacement and velocity sensors 25 (basic control algorithm), and from the accelerometers 13, 17, there is superposed on this basic control an additional control signal that makes the accelerations that are measured by the accelerometers 14 equal to zero, i.e., the base essentially becomes stationary in inertial space.

In the second regime, when the ultrahigh precision CLST is isolated from the vibrations of the microdynamic actions that are caused by the operation of the SM systems, the control is accomplished similarly to the first regime with the sole difference that accelerometers 13 and 14 exchange roles in the control, i.e., feedback control is performed from the accelerometers 13, 15, 16 and the relative displacement and velocity sensors 25.

In the third regime we suppress of oscillations of elongated structural elements of the CLST due to their disclosure and external influencing factors.

In the fourth regime we suppress of oscillations of elongated structural elements of the SM, for example, the solar panels 7 and the antenna of HQRC 8 caused by the work of SM in the process of operation.

In the fifth regime there is realized high-precision guidance of the CLST and the investigated object and its stabilization in real time.

In the sixth regime vibration diagnostics is performed of disclosure of folding elements of CLST and SM, as well as control the external microdynamic disturbances on the CLST and the SM.

In the seventh regime there is realized recovery of the coordinates of the center of mass of SO Millimetron relative to the base coordinate system in case of changes in operation, for example due to fuel reserves in the SM.

The control algorithms of the first and second regimes are similar to those described in [10].

In all these regimes the commands from the SBHPDPCS 18 (Fig. 5) control the executive elements of the active three-dimensional intermediate frame 9 (IAVIM 12) and the slewing drives 27 of the solar panels 7. Those commands are based on the readings of sensors 5, 13–17, and 25. The signals from these sensors are sent to the inputs of the analog-digital converters and through the data bus to neurocomputer 19 with the corresponding means of software 20 of the SBHPDPCS 18: signals from sensors 5 to ADC 23; from sensors 13–17 to ADC 22; and from sensors 25 to converter ADC 24. After real-time data analysis by means of software 20, control commands are formulated and sent through DAC 21 and power amplifiers 26 to IAVIM 12 and the slewing drives 27. Then the pre-processed and compressed data sent through the output data bus and the HQRC 8 and the radio

link 28 to the ground-based radio system 29. As a result, the three-dimensional intermediate frame 9 and of the solar panels 7 will be the active elements in these regimes. Here the researches/operators perform the further processing and analysis of the obtained result and - if necessary—correct program is transmitted through the radio link 28 and the HQRC 8 to the SBHPDPCS 18 for implementation.

It should be noted that to ensure with sibling the ISAVIP for the ultrahigh-precision CLST of the SO Millimetron we need each of IAVIM 12 to perform two-stage. 1st cascade—bass precision linear actuator, capable of providing precise movements with an amplitude of 10 μm to 200 mm in the frequency range from 0.1 to 15 Hz and 2nd cascade—precision piezodrive able to provide precision motion with an amplitude of 1 μm to 500 μm in the frequency range from 15 to 100 Hz.

The use the ISAVIP in the CLST will help ensure that the high requirements for precision and to preserve performance characteristics SO Millimetron in the long run.

5 Conclusion

Future trends in any orbit SO are expected to lead to a super long distance from the Earth, for example in the vicinity of the Lagrangian point L2 in the Sun-Earth system. Operating time of these SO such as the SO Millimetron will be about 10 years. Therefore, it is in need of an intelligence system such as the ISAVIP for the ultrahigh-precision CLST for real-time control.

References

1. Bronowicki, A.-J.: Vibration isolator for large space telescopes. *J. Spacecraft Rockets* **43**(1) (2006)
2. Baier, H., Reindl, M.: Adaptive structures and mechatronic components for vibration and shape control of satellite payloads, In: *Proceedings of the 10th European Space Mechanisms and Tribology Symposium*, pp. 391–396. San Sebastián, Spain. Compiled by R. A. Harris. ESA SP-524, Noordwijk, Netherlands: ESA Publications Division, 24–26 September 2003
3. Bely, P.Y. (ed.): *The Design and Construction of Large Optical Telescopes*. Springer, Berlin (2003)
4. <http://millimetron.ru/index.php/en/about-mmtron/about-the-observatory>
5. Imbriale, W.A., Gao, S., Boccia, L. (eds.) *Space Antennas Handbook*. Wiley (2012)
6. Koski, K.: Focus Mechanism for Kepler mission. In: *Proceedings of the 39th Aerospace Mechanisms Symposium*, NASA Marshall Space Flight Center, pp. 359–372. 7–9 May 2008
7. Lebedev, A.P., Polezhaev, V.I.: Mechanics of microgravity: microaccelerations and gravitational sensitivity of processes of mass transfer upon receipt of the materials in space. *J. Uspechy Mechaniky* **13**(1), 3–51 (1990). (in Russian)
8. Murata, Y., Saito, H., Tsuboi, M.: The VSOP-2 (ASTRO-G) project. In: To be published in *Proceedings of Science*, proceedings of “The 9th European VLBI Network Symposium” on “The role of VLBI in the Golden Age for Radio Astronomy and EVN Users Meeting”. Bologna, Italy, 23–26 Sept 2008

9. Omatu, S., Khalid, M., Yusof, R.: *Neuro-control and its applications*. Springer, Berlin (1996)
10. Rybaik, L.A., Sinev, A.V., Pashkov, A.I.: *Syntesis of active vibration isolation system for spacecraft*. Izd-vo "Yanus-K" Moscow (1997) (in Russian)
11. Sayapin, S.N.: Prospects and available application of parallel spatial mechanism in space technology. *J. Probl. Eng. Sci. Mach. Reliab.* **1**, 17–26 (2001) (Izd-vo "Nauka", in Russian)
12. Sayapin, S.N.: *Analysis and synthesis of flexible spaceborne precision large mechanisms and designs of space radiotelescopes of the petal type*, Doctor Tech. Sci. Dissertation. M.: IMash RAN, Moscow (2003) (in Russian)
13. Sayapin, S.N., Kokushkin, V.V.: Russian Patent 2323136, *Byull. Izobret.*, no. 12 (2008)
14. Sayapin, S.N., Artemenko, Y.N., Myshonkova N.V., High precision problems of observatory "MILLIMETRON" cryogenic space telescope. *Nat. Sci.* **2**(53), 50–76 (2014) (*Vestnik MGTU*, in Russian)
15. Sayapin, S.N., Sinev, A.V., Trubnikov, A.G.: Russian Patent 2161109, *Byull. Izobret.*, no. 36 (2000)
16. Stewart, D.: A platform with six degrees of freedom. *Proc. Inst. of Mech. Eng.* **180**(15), 371–386 (1965–1966)
17. Titov, B.A., Dmitriev, V.V.: *Determining the dynamic properties of elastic spacecraft*. Mashinostroenie, Moscow (1995) (in Russian)
18. Wild, W., Kardashev, N.S., Babakin, N.G.: Millimetron—a large Russian-European submillimeter space observatory. *Exp. Astron.* **23**(1), 221–244 (2009)

Semi-automatic Mechatronic Drive Control System Using Bioelectric Potentials

V.G. Gradetsky, I.L. Ermolov, M.M. Knyazkov, A.N. Sukhanov
and A.A. Kryukova

Abstract The main goal of this paper is to improve the quality of human-machine system of an exoskeleton control by using information about bioelectric potentials in the control loop of mechatronic drives. The experiment results shown that under the proposed control technique while moving the position error of the end effector of the exoskeleton was less than the position error caused in the same conditions without using control EMG signal in the experiment. Thus, the proposed control algorithm for the exoskeleton, based on a complex processing of sensor information can improve the quality of exoskeleton movement control.

Keywords Exoskeleton · EMG-control · HMI · Force-torque control · Multilink mechatronic system

V.G. Gradetsky (✉) · M.M. Knyazkov · A.N. Sukhanov · A.A. Kryukova
Institute for Problems in Mechanics of the Russian Academy of Sciences,
Moscow, Russia
e-mail: gradet@ipmnet.ru

M.M. Knyazkov
e-mail: ipm_labrobotics@mail.ru

A.N. Sukhanov
e-mail: sukhانov-artyom@yandex.ru

A.A. Kryukova
e-mail: kryukovaanastasiya1990@mail.ru

I.L. Ermolov
Moscow State Technological University STANKIN, Moscow, Russia
e-mail: i.l.ermolov@mail.ru

1 Introduction

Research in the area of multilink mechatronic systems (such as exoskeletons) are emerging in many countries. Space exploration is one of the most perspective applications of exoskeletons. Russian Federal Future Projects Space Program 2016–2025 gives substantial attention to “on-site” activities in the Moon exploration. This also includes space robotic systems, including anthropomorphous robots. Remote control technique is considered as one of the potential variants of using exoskeleton in human-machine “astronaut—robotic manipulator” systems. Such “astronaut—exoskeleton” system could be used as a master unit to control robotic manipulator placed on the hull of the spaceship for the outer space astronauts’ activities [1–6].

There are two most prospective ways to control an exoskeleton system: force-torque control and EMG-control. Both techniques have their advantages and disadvantages. Measuring muscle activity with electric potential was traditionally used for medical research.

The control technique proposed in this paper is based on the force-torque control method but it uses EMG information about bioelectric potentials of an operator [7]. That provides exoskeleton with the ability to sense its operator and the environment. While moving exoskeleton’s end-effector an operator tracks desired trajectory. At the same time an external disturbing force affects exoskeleton (changing its value in a random way). During experimentation the task for an operator was to track the desired trajectory and to estimate the error under the new technique and without it. The scheme of experiment is shown on the Fig. 1.

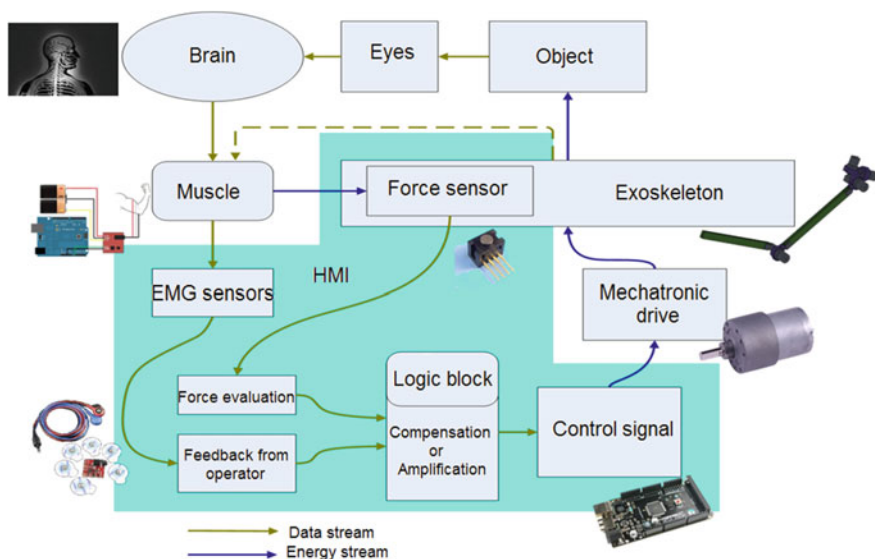


Fig. 1 Semi-automatic mechatronic system used in the experiment

Motion control and orientation system of the exoskeleton is based on various sensors. This allows to get information fusing both human master control and from external forces. The exoskeleton's servo drive system is based on the feedback technique of acquiring information from the actuators and passing it to the control system via the HMI. In this case, the feedback information channel provides different data types. These data show the amount of force-torque feedback, linear and angular metric information to detect errors and automatically reduce them to zero. The "astronaut—exoskeleton" system has direct influence of the actuators on control elements. Thus it is necessary to apply one more feedback information channel which will contain data of the human presence effect. Such data could be provided by noninvasive electromyographic electrodes connected to human skin. This will allow control system to determine the presence of the human control action and adjust actuators' movement in a non-deterministic environment under external force-torque impact. Thus, a handle with a set of piezo-sensors will transmit the force vector from human to control system and exoskeleton will sense its operator and will ignore any other force. Also averaging algorithms applying to EMG sensor readings will solve the problem of arm tremor during control.

2 Methods and Experiments

The EMG requires three electrodes. The reference electrode referred as a ground electrode is essential for providing a common reference to the differential input of the preamplifier in the electrode. Thus, the reference electrode is placed on electrically neutral area of a skin. The two signal electrodes are placed then at two different points on the muscle. One if these is placed in an active area of contraction and the other slightly off center. This gives a point of reference for muscle activity compared to the signal of muscle relaxation.

The amplitude of the EMG signal is stochastic (random) in nature and can be reasonably represented by a Gaussian distribution function [8]. The amplitude of the signal can range from 0 to 10 mV (peak-to-peak). The usable energy spectrum of the signal is limited to the 0–500 Hz frequency range. Usable signals (Fig. 2) are those with energy above the electrical noise level and hence a band pass filter is used to eliminate frequencies below 50 Hz and above 400 Hz in order to abandon power supply's frequency [9].

During the experiment operator attached these three electrodes to his body using the above mentioned approach. EMG electrodes were connected to the preamplifier and band pass filter. Then data from the filter came to the analog input of the microcontroller for processing. The amplified, rectified, and smoothed signal was recorded for integration with measurements systems for analysis. Therefore, there was the necessity for non-permanent memory (real time calculations) and semi-permanent memory (Data Storage). Real-time processing was limited by the sampling speed and the capacity of the data storage.

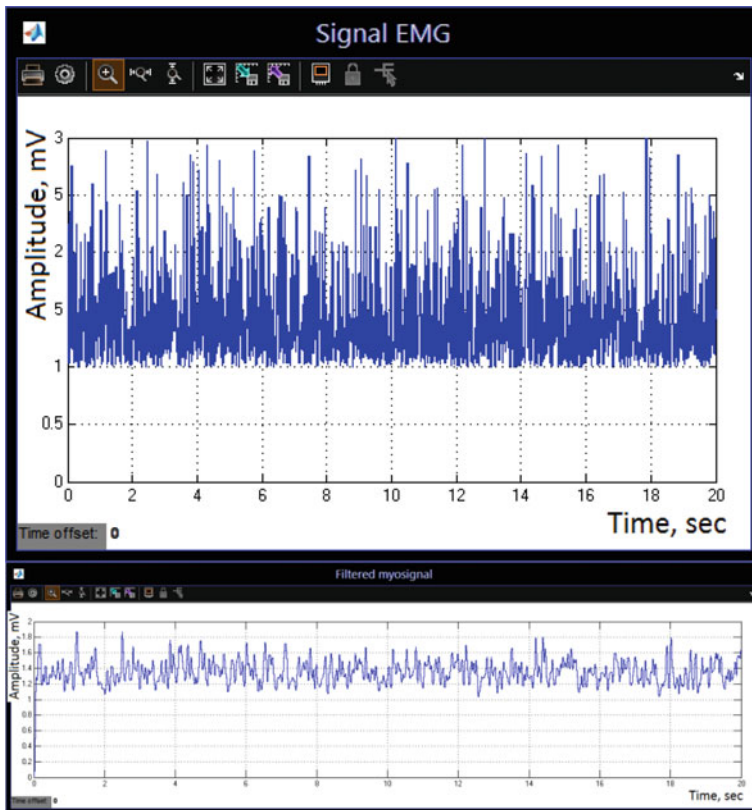


Fig. 2 EMG data with noise (*top*) and EMG data after filtration

The experiment involved a servo drive with three loops—current loop, speed loop and angle loop (Fig. 3).

The discrete transfer function of the close looped servo drive with three feedback loops is presented in (1).

$$\left\{ \begin{array}{l} \overline{\Phi}_n(w) = \frac{(1 + T_{sr}w)(1 + \frac{T_s w}{2})}{1 + A_1 w + A_2 w^2 + A_3 w^3 + A_4 w^4} \\ A_1 = (T_{sr} + \frac{T_s}{2} + \omega_{co}^{-1}) \\ A_2 = T_{sr} \cdot (\frac{T_s}{2} + \omega_{co}^{-1}) \\ A_3 = \frac{T_{sr}}{\omega_{co} \cdot \omega_{sco}} \\ A_4 = \frac{T_{sr} \cdot T_{eq.s}}{\omega_{co} \cdot \omega_{sco}} \end{array} \right. \quad (1)$$

where T_{sr} is time-constant of the speed controller, T_s is sampling time in digital system, ω_{co} is cut-off frequency, ω_{sco} is speed cutoff frequency, $T_{eq.s}$ is equivalent time-constant.

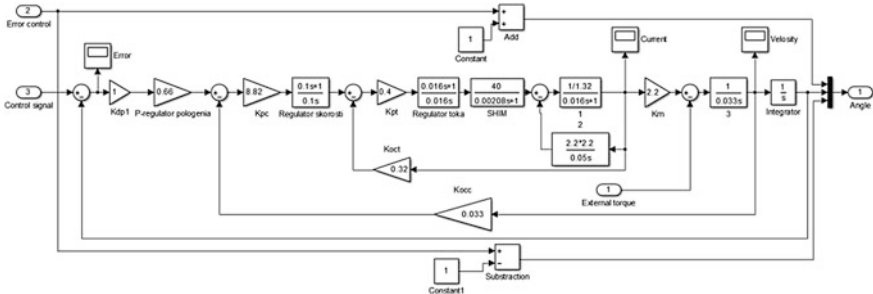
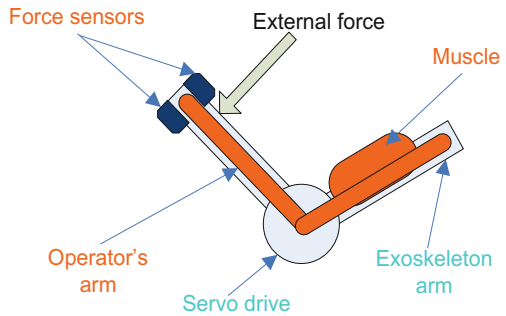


Fig. 3 Servo drive control scheme with three loops

Fig. 4 The scheme of the experiment



The purpose of the experiment was to improve the quality of exoskeleton movement control. The mechanical part of the exoskeleton involved a joint system of two links based on the mentioned servo drive. Both links were connected to the operator’s arm at the forearm and the wrist via clamps. The wrist clamp was equipped with two Force Sensitive Resistors for measuring the interaction force between operator and the exoskeleton’s link. This is done to set the direction of the drive rotation and its speed. The external dynamic force was created by another human who slightly tried to put a crimp in a movement of the exoskeleton arm via a rod with a Force Sensitive Resistor on its end in order to measure stochastic data of external force (Fig. 4).

That was needed to simulate the non-deterministic environment and to evaluate the advantages of the proposed technique. An operator with the exoskeleton had to provide the desired movement in 2 modes:

1. with new control method that involved complex processing of EMG and force sensing,
2. with the old one that involves only force sensors data reading. The control technique that uses only EMG sensors data reading was also tested but due to its instability finally it was not included in consideration. MATLAB software was used for an experimental scheme design (Fig. 5).

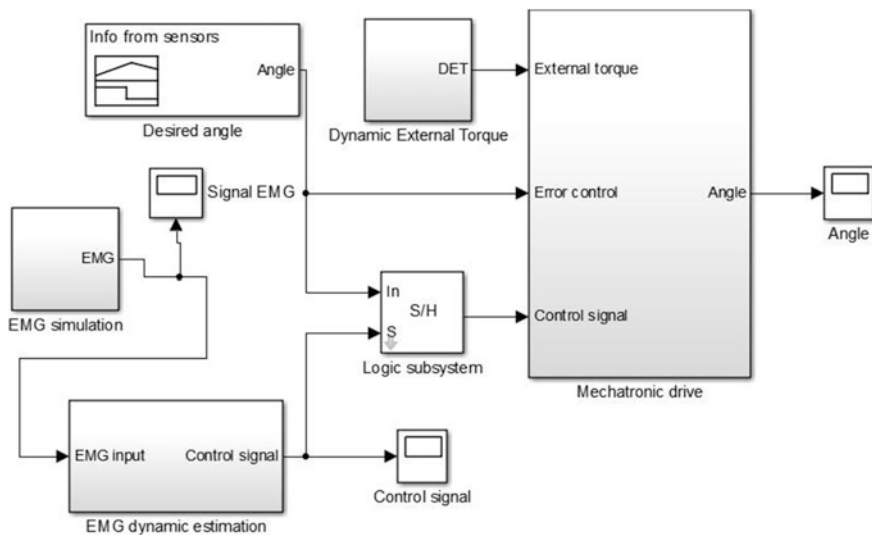


Fig. 5 The dynamic model of the experiment

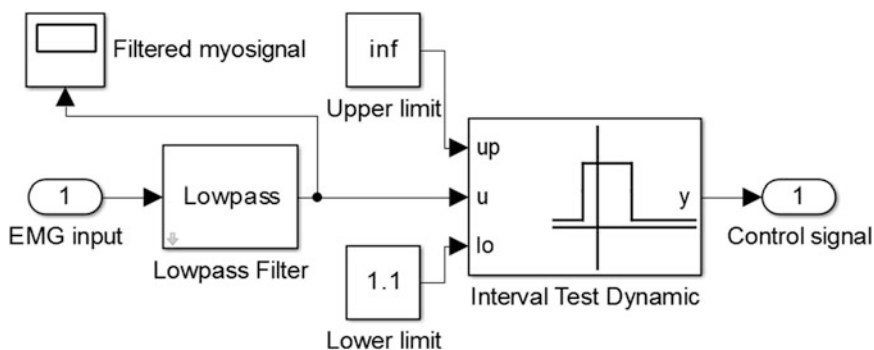


Fig. 6 The scheme of EMG filtration and sorting

Due to instability of the EMG sensors data reading caused by noise and EMG amplitude dependence from arm location in space the useful EMG data has to be detected in a certain amplitude level. Thus there was a certain interval of usable data included in the control scheme. Limits of the interval were set by an operator before the experiment (Fig. 6). In the future these limits should be selected automatically in real-time.

The interference of the external force within movement creates noise in the data from force sensors. Therefore control system should recognize the force generated by an operator and the one caused by unknown obstacles. This provides better control approach. Thus, in our design EMG data is used only as a check signal to realize the desired movement.

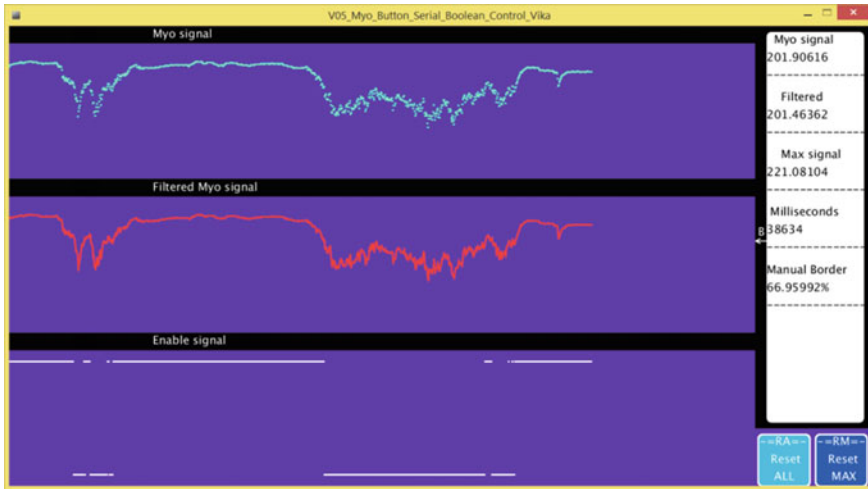


Fig. 7 The human-machine interface (HMI) for signal data real-time testing

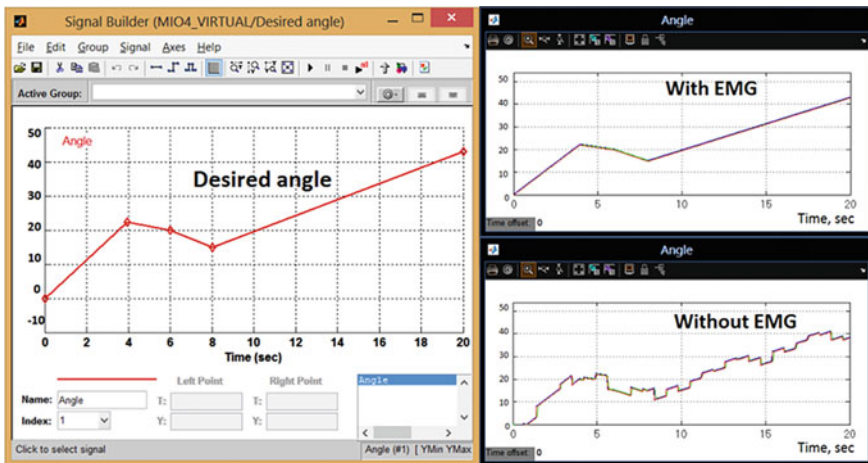


Fig. 8 Results of the experiment

The HMI program was designed to display EMG filtered data and control signal on the screen using Java (Fig. 7). It provides scaled information about amplitude of EMG signal and shows the dynamics of the signal in real-time.

Here the high level of the control signal returns the “enable” command for the servo drive to start rotation according the force sensors data readings.

Experimental results (Fig. 8) show that during motion while using proposed control technique position error of the end effector of the exoskeleton was less than the position error caused in the same conditions without using control EMG signal

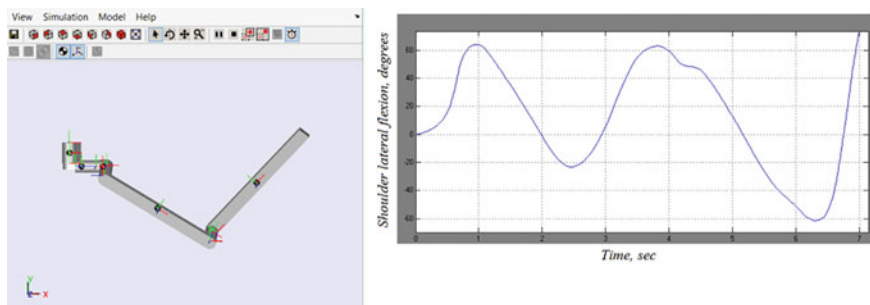


Fig. 9 The virtual model of the exoskeleton made in SimMechanics

in the experiment. Thus, using the designed control algorithm for the exoskeleton, based on a complex processing of sensor information improves the quality of exoskeleton movement control.

Here the left figure presents desired angle and the right figures show the result of the experiments with the suggested control technique (top) and the old technique based on force sensors data use only (bottom).

The virtual mechanical model of the exoskeleton has been examined in the SimMechanics. Angles between links were obtained in dynamics. The obtained data shows the desired flexion in the joints during the control. The model is also provides joint torques and moments of inertia of links (Fig. 9).

3 Conclusion

The main purpose of the authors of this paper was to improve the quality of the human-machine system of an exoskeleton control by using information about human's bioelectric potentials in the control loop of mechatronic drive. The experiment results shown that under the proposed control technique while moving the position error of the end effector of the exoskeleton was less than the position error caused in the same conditions without using control EMG signal in the experiment. Thus, the proposed control algorithm for the exoskeleton, based on a complex processing of sensor information can improve the quality of exoskeleton movement control.

Research supported by RFBR Grant №14-08-00537a.

References

1. Gurfinkel, V.S., Malkin V.B., Cetlin, M.L., Shneider, A.Y.: Bioelectricheskoe upravlenie (Bioelectric control), Nauka, p. 247. Moscow (1972) (in Russian)
2. Gradetsky, V.G., Ermolov, I.L., Knyazkov, M.M., Semyonov, E.A., Sukhanov, A. N.: Experimental investigation of human exoskeleton model. In: Proceedings of ROMANSY 2014 XX CISM-IFTToMM Symposium on Theory and Practice of Robots and Manipulators, no. 22, pp. 275–281. Springer, Moscow, Russia, 29–26 June 2014. ISBN 978-3-319-07057-5
3. Vukobratović, M., Stokič, D.: Scientific Fundamentals of Robotics, Control of Manipulation Robots: Theory and Application, vol. 2. Springer, Berlin (1982)
4. Vukobratović, M., Borovač, B., Surla, D., Stokič, D.: Scientific Fundamentals of Robotics, Biped Locomotion: Dynamics, Stability, Control and Application, vol. 7. Springer, Berlin (1989)
5. Gradetsky, V., Kalinichenko, S., Kravchuk, L., Lopashov, V.: Modular design and mechatronic approaches to the exoskeleton system. Lecture Notes of the ICB Seminars Biomechanics, Biomechanics of the Musculoskeletal System Medical Robotics, pp. 260–269. Polska Akademia Nauk, Warsaw (2000)
6. Word, J., Sugar, T., Standeven, J., Engsberg, J.: Stroke survivor gait adaptation and performance after training on a powered ankle foot arthrosis. In: Proceedings of 2010 IEEE International Conference on Robotics and Automation, pp. 211–216. Anchorage, Alaska, USA, 3–8 May 2010
7. Zuniga, E.N., Simons, G.D.: Nonlinear relations between averaged electromyogram potential and muscle tension in normal subjects. *Arch. Phys. Med. Rehabili.* **50**, 613–620 (1969)
8. De Luca, C.J.: Surface Electromyography: Detection and Recording. DelSys Incorporated (2002)
9. Day, S.: Important Factors in Surface EMG Measurement. Bortec Biomedical Ltd

Part III
Mathematical and Computer Modeling

The Direct Problem of Kinematics SM8 SEMS

A.E. Gorodetskiy, V.G. Kurbanov and I.L. Tarasova

Abstract The kinematic model of the module SM8 SEMS is considered in this article. Such modules have a hexapod-like structure, providing maximum accuracy within minimum execution time on account of process parallelization. As a result of theoretical studies, the direct problem of kinematics has been solved, contributing to the construction of the automatic control system with the required quality of dynamic processes.

Keywords Smart electromechanical systems · Standard module · Structure · Direct kinematic model · Automatic control system

1 Introduction

Research on the development of intelligent robots (IR) designed to operate in conditions of a priori uncertainty dynamically changing environment, actively conducted in all industrialized countries. Applications such robots are vast and varied: automated manufacturing, transportation, household, medical, aerospace, defense, underwater research, rescue and repair work under extreme conditions, etc. Many of these human presence is undesirable or impossible. Therefore, to successfully carry out the necessary IR like the highly sentient beings should possess such important qualities as adaptability to changing formalized working environment [1]. The latter encompasses the control system of a number of IR complex problems.

A.E. Gorodetskiy (✉) · V.G. Kurbanov · I.L. Tarasova
Institute of Problems of Mechanical Engineering,
Russian Academy of Sciences, Saint-Petersburg, Russia
e-mail: g27764@yandex.ru

V.G. Kurbanov
e-mail: vugar_borchali@yahoo.com

I.L. Tarasova
e-mail: g17265@yandex.ru

First of all, it is the problem of adequate perception and recognition of the environment, purposeful planning behavior and effective execution of planned action. The latter problem is successfully solved by the methods of control theory using computers of traditional architecture with consistent principles of information processing. The decision of the first two problems at the same computational tools associated with considerable difficulties. The reason for this is not only the need to handle large amounts of information distributed in space and sensors functioning simultaneously in real time, but also the application of new methods of intelligent processing of information for which they are not oriented computer [2].

In addition the use of IR hexapod similar structures intelligent electromechanical systems (SEMS—smart electromechanical systems) makes it possible to obtain maximum precision actuators with minimal travel time due to the introduction of parallelism in the process of measuring, calculating and movement and the use of high-precision piezomotor able to work in extreme conditions, including open space [3]. A variety associations (serial, parallel, tree, etc.). SEMS structures make it easy to construct new IR with more technological capabilities (lightweight design, combining in a single mechanism of transport and technological operations, design flexibility, etc.). However, such mechanisms have a more complex kinematics, which requires more advanced control algorithms and solving new, complex optimization problems, ensuring the implementation of the optimum path without jamming. In addition to the inclusion of SEMS wireless network interface such as Wi-Fi and intellectual system of strategic planning of cooperative behavior of several SEMS will further expand the scope of IR [4, 5].

The main element is SEMS module SM5, provides, unlike hexapods not only translation and rotation of the upper platform, and compression and expansion of the upper and lower platforms, in conjunction with control systems of measurement and docking it provides versatility.

2 Construction of SEMS

When constructing SEMS for various purposes can be used a wide variety of different standard modules. However, they generally comprise (see Fig. 1) ElectroMechanical System (EMS) (1), of parallel type, a Automatic Control System (ACS) (2), a Measuring System (MS) (3) and a Docking System (DS) (4).

EMS (SM5 SEMS) contains (see Fig. 2) lower platform (LP) (1), the upper platform (UP) (2) and six legs—actuators (LA) (3–8) and the supporting pad (SP) (9 and 10), having at least three control rods (CR) (11–13 and 14–16), attached at one end to the SP, and the other—to the mounting pad (MP) (17–19 and 20–22), in which are mounted, for example screwed, at least three spring-loaded telescopic rods (SLTR) (23–25 and 26–28).

LA contains electric motor (EM) with PID regulator LA, with gearboxes, displacement sensors actuators, such as optoelectronic and sensor power actuators, for

Fig. 1 The block diagram of SM SEMS

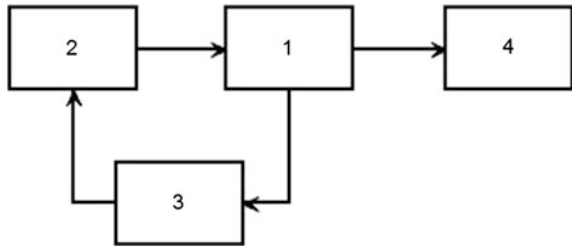
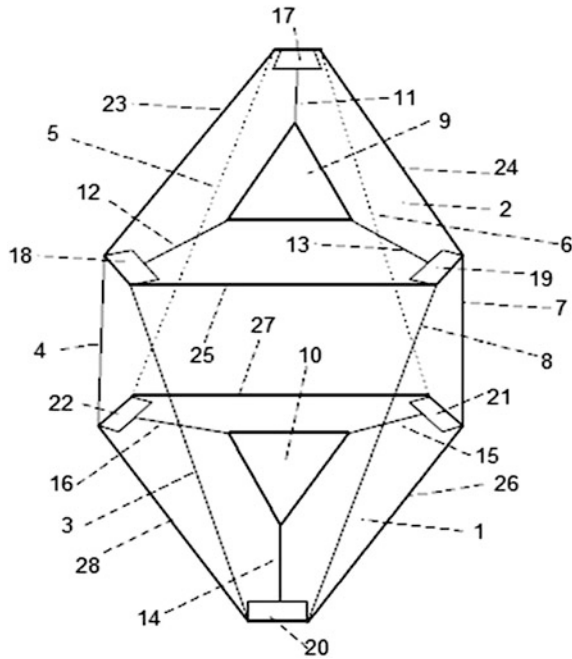


Fig. 2 Sketch module SEMS5



example, piezoelectric, and lower joints, attached to the mounting pads lower the platform and the upper hinge, attached to the mounting pads of the upper platform.

CR contains electric motor (EM) with PID regulator, with gearboxes, displacement sensors, for example, optoelectronic, and force sensors, for example, piezoelectric.

MP contains two slots for attaching threaded SLTR and two slots for threaded joints in other similar modules. Besides MP may contain CCD and LED arrays docking system.

SP lower platform includes grooves for threaded joints in other similar modules and versatile CCD docking system.

SP upper platform includes grooves with thread and an array of LED arrays docking system.

3 The Kinematic Model of the Module SM8 SEMS

Most have full functionality module SM8 SEMS and it can be called a universal module. The other modules are in some of the simplification. It is therefore advisable construct mathematical models, especially the module in order to study the characteristics and properties discussed SEMS standard modules.

Unlike module SM5 SEMS (Fig. 2), this module (see Fig. 3) has rods 29–31 and 32–34, which are mounted on the mounting platforms 17–19 and/or 20–22 platform 1 and/or 2 rotatable in a plane passing through the points of attachment rods and center of the platform 1 and/or 2 perpendicular to the latter by means of a controlled drive 35–37 and 38–40. The rods 29–31 and 32–34 can change their length by means of linear control drives 41–43 and 44–46. Additionally, this module further has rods 47–49 and 50–52, which are mounted on the support plate 9 and/or 10 the platforms 1 and/or 2 to rotate in a plane of the support areas 9 and/or 10 by means of controlled drives 53–55 and 56–58 and inwardly directed platform (Fig. 3). The rods 47–49 and 50–52 can change their length by means of linear control drives 59–61 and 62–64.

SM8 SEMS module has the same advantages and disadvantages as the SM5 SEMS, but has a greater flexibility due to a combination of additional features and modules SM6 SEMS, SM7 SEMS.

Let us calculate the lengths of the LA original (after initialization) position.

The radius vector from the center of the upper platform (O) to the points of projection of the center of the upper hinges LA on the platform (see Fig. 4) will be:

$$\mathbf{r}_{1B} = |r_{1B}^x; r_{1B}^y; r_{1B}^z|^T = |R_B \sin \varphi_B; R_B \cos \varphi_B; 0|^T \quad (1)$$

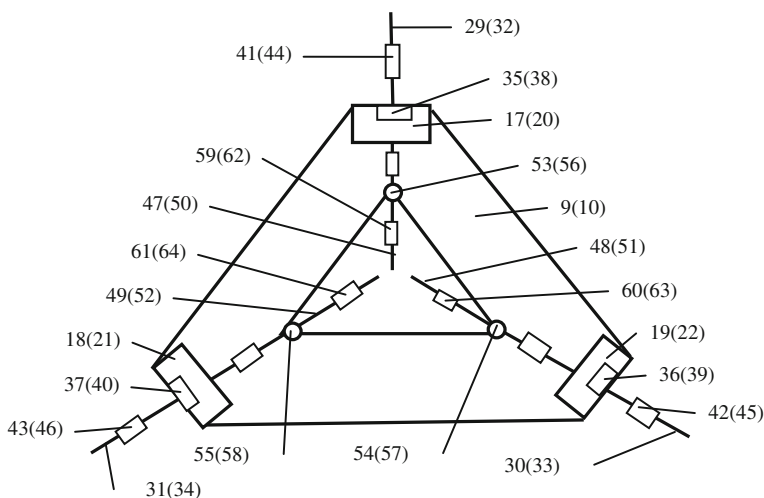


Fig. 3 The design platform module SM8 SEMS

$$\mathbf{r}_{2B} = |r_{2B}^x; r_{2B}^y; r_{2B}^z|^T = |R_B \sin(\varphi_B + \Delta\varphi_B); R_B \cos(\varphi_B + \Delta\varphi_B); 0|^T \quad (2)$$

$$\mathbf{r}_{3B} = |r_{3B}^x; r_{3B}^y; r_{3B}^z|^T = |R_B \sin(\varphi_B + 30^\circ); R_B \cos(\varphi_B + 30^\circ); 0|^T \quad (3)$$

$$\mathbf{r}_{4B} = |r_{4B}^x; r_{4B}^y; r_{4B}^z|^T = |R_B \sin(\varphi_B + \Delta\varphi_B + 30^\circ); R_B \cos(\varphi_B + \Delta\varphi_B + 30^\circ); 0|^T \quad (4)$$

$$\mathbf{r}_{5B} = |r_{5B}^x; r_{5B}^y; r_{5B}^z|^T = |R_B \sin(\varphi_B + 60^\circ); R_B \cos(\varphi_B + 60^\circ); 0|^T \quad (5)$$

$$\mathbf{r}_{6B} = |r_{6B}^x; r_{6B}^y; r_{6B}^z|^T = |R_B \sin(\varphi_B + \Delta\varphi_B + 60^\circ); R_B \cos(\varphi_B + \Delta\varphi_B + 60^\circ); 0|^T \quad (6)$$

Respectively, the radius vector from the center of the lower platform (O_1) to the points of projection of the center of the upper hinges LA on the platform will be:

$$\mathbf{r}_{1H} = |r_{1H}^x; r_{1H}^y; r_{1H}^z|^T = |R_H \sin\varphi_H; R_H \cos\varphi_H; -H|^T \quad (7)$$

$$\mathbf{r}_{2H} = |r_{2H}^x; r_{2H}^y; r_{2H}^z|^T = |R_H \sin(\varphi_H + \Delta\varphi_H); R_H \cos(\varphi_H + \Delta\varphi_H); -H|^T \quad (8)$$

$$\mathbf{r}_{3H} = |r_{3H}^x; r_{3H}^y; r_{3H}^z|^T = |R_B \sin(\varphi_H + 30^\circ); R_B \cos(\varphi_H + 30^\circ); -H|^T \quad (9)$$

$$\mathbf{r}_{4H} = |r_{4H}^x; r_{4H}^y; r_{4H}^z|^T = |R_B \sin(\varphi_H + \Delta\varphi_H + 30^\circ); R_B \cos(\varphi_H + \Delta\varphi_H + 30^\circ); -H|^T \quad (10)$$

$$\mathbf{r}_{5H} = |r_{5H}^x; r_{5H}^y; r_{5H}^z|^T = |R_B \sin(\varphi_H + 60^\circ); R_B \cos(\varphi_H + 60^\circ); -H|^T \quad (11)$$

$$\mathbf{r}_{6H} = |r_{6H}^x; r_{6H}^y; r_{6H}^z|^T = |R_B \sin(\varphi_H + \Delta\varphi_H + 60^\circ); R_B \cos(\varphi_H + \Delta\varphi_H + 60^\circ); -H|^T \quad (12)$$

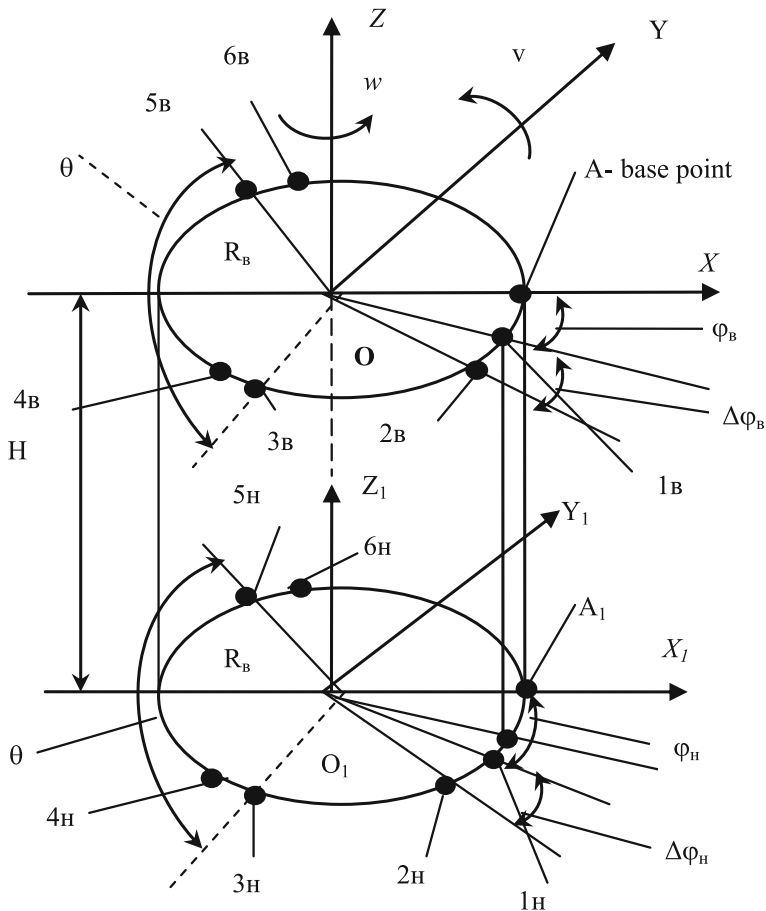
Therefore, the length of the i th LA in the initial position:

$$L_i(0) = \left((r_{iB}^x - r_{iH}^x)^2 + (r_{iB}^y - r_{iH}^y)^2 + (r_{iB}^z - r_{iH}^z)^2 \right)^{1/2} \quad (13)$$

$i = 1, 2, \dots, 6$

When the shifts of the upper platform on the values $x(t)$, $y(t)$ and $z(t)$ the radius vectors r_{iH} not changed ($r_{iH}(x(t), y(t), z(t)) = r_{iH}(0)$) and the radius vector r_{iB} change as follows:

$$\mathbf{r}_{iB}(x(t), y(t), z(t)) = |r_{iB}^x + x(t); r_{iB}^y + y(t); r_{iB}^z + z(t)|^T \quad (14)$$



Introducing the notation $\mathbf{A} = [x(t); y(t); z(t)]^T$, the expression (14) can be rewritten as follows:

$$\mathbf{r}_{iB}(x(t), y(t), z(t)) = \mathbf{r}_{iB}(0) + \mathbf{A} \tag{15}$$

This leads to a corresponding change in the lengths of the LA:

$$L_i(x(t), y(t), z(t)) = ((r_{iB}^x + x(t) - r_{iH}^x)^2 + (r_{iB}^y + y(t) - r_{iH}^y)^2 + (r_{iB}^z + z(t) - r_{iH}^z)^2)^{1/2}, \tag{16}$$

i.e. their relative change:

$$\Delta L_i(x(t), y(t), z(t)) = L_i(x(t), y(t), z(t)) - L_i(0)$$

◀ **Fig. 4** The scheme SM5 SEMS. O_1 —center of the bottom of the platform; Ox, Oy, Oz —the axis of the base coordinate system with the origin at the point O ; Ox —directed horizontally and passes through the base point A ; Oy —directed horizontally and perpendicular to the x -axis; Oz —directed vertically upwards; $1_B, 2_B, 3_B, 4_B, 5_B$ and 6_B —point projection of the center of the upper hinge 1–6 LA on the upper platform; $1_H, 2_H, 3_H, 4_H, 5_H$ and 6_H —point of projection of the center of the bottom hinges LA 1–6 on the lower platform, $\theta = 120$ —the angle between adjacent pairs of hinges LA at lower and upper platform; H —height EMS measured as the distance between the points O and O_1 ; R_B —the radius of the upper platform; R_H —the radius of the lower platforms; φ_B —turning point 1_B angle relative to the point A in the XY plane in an initial position; $\Delta\varphi_B$ —angle of rotation relative to the point 2_B point 1_B in the XY plane in an initial position; A_1 —the projection of the reference point A on the lower platform in the rest position; φ_H —the angle of rotation with 1_H point relative to the point A_1 in the plane X_1Y_1 ; $\Delta\varphi_H$ —angle of rotation relative to the point 2_H point 1_H in the plane X_1Y_1 ; Ψ —the angle of rotation points with 1_H point relative to the projection 1_B on the lower platform in the plane X_1Y_1 ; $X_1Y_1Z_1$ —coordinate system with the origin at the point O_1 ; $x(t)$ —the movement of the upper platform along the x -axis; $y(t)$ —the movement of the upper platform along the axis Oy ; $z(t)$ —the movement of the upper platform along the axis Oz ; $u(t)$ —the angle of counterclockwise rotation of the upper platform relative to the axis X ; $v(t)$ —the angle of counterclockwise rotation of the upper platform relative to the axis Y (the firm PI this angle is clockwise); $w(t)$ —the angle of counterclockwise rotation of the upper platform relative to the axis Z ; $\Delta R_B(t)$ —compression or stretching of the upper platform; $\Delta R_H(t)$ —compression or stretching of the lower platform; i —number of LA; B —the upper platform; H —the lower platform; r_{iB} —vector from point O to point iB ; r_{iH} —vector from point O_1 to point iH ; $x(0) = 0, y(0) = 0, z(0) = 0, u(0) = 0, v(0) = 0, w(0) = 0$ —initial position EMS (after initialization)

Now consider how the length LA when turning angles on the upper platform $u(t), v(t)$ and $w(t)$. We introduce the rotation matrix:

$$C_u = \begin{vmatrix} 1 & 0 & 0 \\ 0 & \cos(u(t)) & -\sin(u(t)) \\ 0 & \sin(u(t)) & \cos(u(t)) \end{vmatrix} \tag{17}$$

$$C_v = \begin{vmatrix} \cos(v(t)) & 0 & \sin(v(t)) \\ 0 & 1 & 0 \\ -\sin(v(t)) & 0 & \cos(v(t)) \end{vmatrix} \tag{18}$$

$$C_w = \begin{vmatrix} \cos(w(t)) & -\sin(w(t)) & 0 \\ \sin(w(t)) & \cos(w(t)) & 0 \\ 0 & 0 & 1 \end{vmatrix} \tag{19}$$

Then while turning angles of $u(t), v(t)$ and $w(t)$ the radius vector r_{iB} will change as follows:

$$\mathbf{r}_{iB}(u(t), v(t), w(t)) = \mathbf{C}_u \mathbf{C}_v \mathbf{C}_w \mathbf{r}_{iB}(0) = |r_{iB}^x(u, v, w); r_{iB}^y(u, v, w); r_{iB}^z(u, v, w)|^T \tag{20}$$

This leads to a corresponding change in the lengths of the LA:

$$L_i(u, v, w) = ((r_{iB}^x(u, v, w) - r_{iH}^x)^2 + (r_{iB}^y(u, v, w) - r_{iH}^y)^2 + (r_{iB}^z(u, v, w) - r_{iH}^z)^2)^{1/2} \quad (21)$$

i.e. their relative change:

$$\Delta L_i(u(t), v(t), w(t)) = L_i(u(t), v(t), w(t)) - L_i(0) \quad (22)$$

In synchronous operation of the actuator control rod upper platform changes the radius of the upper platform:

$$R_B(t) = R_B + \Delta R_B(t) \quad (23)$$

and when the synchronous operation of the actuator control rod bottom platform changes the radius of the lower platform:

$$R_H(t) = R_H + \Delta R_H(t) \quad (24)$$

This leads to a change in the radius vector:

$$\mathbf{r}_{iB}(\Delta R_B(t)) = |r_{iB}^x; r_{iB}^y; r_{iB}^z|^T + \mathbf{B}_{iB}(t) = |r_{iB}^x(\Delta R_B); r_{iB}^y(\Delta R_B); r_{iB}^z(\Delta R_B)|^T \quad (25)$$

$$\mathbf{r}_{iH}(\Delta R_H(t)) = |r_{iH}^x; r_{iH}^y; r_{iH}^z|^T + \mathbf{B}_{iH}(t) = |r_{iH}^x(\Delta R_H); r_{iH}^y(\Delta R_H); r_{iH}^z(\Delta R_H)|^T, \quad (26)$$

where:

$$\mathbf{B}_{1B}(t) = |\Delta R_B(t) \sin \varphi_B; \Delta R_B(t) \cos \varphi_B; 0|^T \quad (27)$$

$$\mathbf{B}_{2B}(t) = |\Delta R_B(t) \sin(\varphi_B + \Delta \varphi_B); \Delta R_B(t) \cos(\varphi_B + \Delta \varphi_B); 0|^T \quad (28)$$

$$\mathbf{B}_{3B}(t) = |\Delta R_B(t) \sin(\varphi_B + 30^\circ); \Delta R_B(t) \cos(\varphi_B + 30^\circ); 0|^T \quad (29)$$

$$\mathbf{B}_{4B}(t) = |\Delta R_B(t) \sin(\varphi_B + \Delta \varphi_B + 30^\circ); \Delta R_B(t) \cos(\varphi_B + \Delta \varphi_B + 30^\circ); 0|^T \quad (30)$$

$$\mathbf{B}_{5B}(t) = |\Delta R_B(t) \sin(\varphi_B + 60^\circ); \Delta R_B(t) \cos(\varphi_B + 60^\circ); 0|^T \quad (31)$$

$$\mathbf{B}_{6B}(t) = |\Delta R_B(t) \sin(\varphi_B + \Delta \varphi_B + 30^\circ); \Delta R_B(t) \cos(\varphi_B + \Delta \varphi_B + 30^\circ); 0|^T \quad (32)$$

$$\mathbf{B}_{1H}(t) = |\Delta R_H(t) \sin \varphi_H; \Delta R_H(t) \cos \varphi_H; 0|^T \quad (33)$$

$$\mathbf{B}_{2H}(t) = |\Delta R_H(t) \sin(\varphi_H + \Delta \varphi_H); \Delta R_H(t) \cos(\varphi_H + \Delta \varphi_H); 0|^T \quad (34)$$

$$\mathbf{B}_{3H}(t) = |\Delta\mathbf{R}_H(t)\sin(\varphi_H + 30^\circ); \Delta\mathbf{R}_H(t)\cos(\varphi_H + 30^\circ); 0|^T \quad (35)$$

$$\mathbf{B}_{4H}(t) = |\Delta\mathbf{R}_H(t)\sin(\varphi_H + \Delta\varphi_H + 30^\circ); \Delta\mathbf{R}_H(t)\cos(\varphi_H + \Delta\varphi_H + 30^\circ); 0|^T \quad (36)$$

$$\mathbf{B}_{5H}(t) = |\Delta\mathbf{R}_H(t)\sin(\varphi_H + 60^\circ); \Delta\mathbf{R}_H(t)\cos(\varphi_H + 60^\circ); 0|^T \quad (37)$$

$$\mathbf{B}_{6H}(t) = |\Delta\mathbf{R}_H(t)\sin(\varphi_H + \Delta\varphi_H + 30^\circ); \Delta\mathbf{R}_H(t)\cos(\varphi_H + \Delta\varphi_H + 30^\circ); 0|^T \quad (38)$$

This will change in the lengths of the legs:

$$L_i(\Delta\mathbf{R}_B, \Delta\mathbf{R}_H) = ((r_{iB}^x(\Delta\mathbf{R}_B) - r_{iH}^x(\Delta\mathbf{R}_H))^2 + (r_{iB}^y(\Delta\mathbf{R}_B) - r_{iH}^y(\Delta\mathbf{R}_H))^2 + (r_{iB}^z(\Delta\mathbf{R}_B) - r_{iH}^z(\Delta\mathbf{R}_H))^2)^{1/2} \quad (39)$$

i.e. their relative change:

$$\Delta L_i(\Delta\mathbf{R}_B(t), \Delta\mathbf{R}_H(t)) = L_i((\Delta\mathbf{R}_B, \Delta\mathbf{R}_H) - L_i(0)) \quad (40)$$

If there is a simultaneous displacement ($x(t)$, $y(t)$ and $z(t)$) and turning through angles ($u(t)$, $v(t)$ and $w(t)$) of the upper platform, as well as compression or stretching of the upper ($\Delta\mathbf{R}_B(t)$) and the lower ($\Delta\mathbf{R}_H(t)$) EMS platforms, then the radius vector will change as follows:

$$\begin{aligned} \mathbf{r}_{iB}(x, y, z, u, v, w, \Delta\mathbf{R}_B(t)) &= \mathbf{C}_u \mathbf{C}_v \mathbf{C}_w (\mathbf{r}_{iB}(0) + \mathbf{A} + \mathbf{B}_{iB}(t)) \\ &= |r_{iB}^x(x, y, z, u, v, w, \Delta\mathbf{R}_B); r_{iB}^y(x, y, z, u, v, w, \Delta\mathbf{R}_B); \\ &\quad r_{iB}^z(x, y, z, u, v, w, \Delta\mathbf{R}_B)|^T \end{aligned} \quad (41)$$

$$\mathbf{r}_{iH}(\Delta\mathbf{R}_B(t)) = (\mathbf{r}_{iH}(0) + \mathbf{B}_{iH}(t)) = |r_{iH}^x(\Delta\mathbf{R}_H); r_{iH}^y(\Delta\mathbf{R}_H); r_{iH}^z(\Delta\mathbf{R}_H)|^T \quad (42)$$

Then:

$$\begin{aligned} L_i(x, y, z, u, v, w, \Delta\mathbf{R}_B, \Delta\mathbf{R}_B) &= (r_{iB}^x(x, y, z, u, v, w, \Delta\mathbf{R}_B) - r_{iH}^x(\Delta\mathbf{R}_B))^2 \\ &\quad + (r_{iB}^y(x, y, z, u, v, w, \Delta\mathbf{R}_B) - r_{iH}^y(\Delta\mathbf{R}_H))^2 \\ &\quad + (r_{iB}^z(x, y, z, u, v, w, \Delta\mathbf{R}_B) - r_{iH}^z(\Delta\mathbf{R}_H))^2)^{1/2} \end{aligned} \quad (43)$$

and

$$\Delta L_i(x, y, z, u, v, w, \Delta\mathbf{R}_B, \Delta\mathbf{R}_H) = L_i(x, y, z, u, v, w, \Delta\mathbf{R}_B, \Delta\mathbf{R}_H) - L_i(0) \quad (44)$$

Taking the first derivative of the expression (16), (21) and (39) can be linear and angular speed hexapod platform.

At small angles $u(t)$, $v(t)$ and $w(t)$ of expression (17)–(19) can be simplified:

$$C_z = \begin{vmatrix} 1 & 0 & 0 \\ 0 & 1 & -(u(t)) \\ 0 & u(t) & 1 \end{vmatrix} \quad (45)$$

$$C_v = \begin{vmatrix} 1 & 0 & v(t) \\ 0 & 1 & 0 \\ -(v(t)) & 0 & 1 \end{vmatrix} \quad (46)$$

$$C_w = \begin{vmatrix} 1 & -(w(t)) & 0 \\ w(t) & 1 & 0 \\ 0 & 0 & 1 \end{vmatrix} \quad (47)$$

Accordingly simplified expressions (20)–(22), (41), (43) and (44), as well as the expression for the velocity EMS platforms.

Unlike module SM5 SEMS (Fig. 2), this module (see Fig. 3) has the movement rods 29–31 and 32–34, which are mounted on the mounting platforms 17–19 and/or 20–22 platform 1 and/or 2 rotatable in a plane passing through the points of attachment rods and center of the platform 1 and/or 2 perpendicular to the latter by means of a controlled drive 35–37 and 38–40. The rods 29–31 and 32–34 can change their length by means of linear control actuators 41–43 and 44–46. Additionally, this module further has gripping rods 47–49 and 50–52, which are mounted on the support plate 9 and/or 10 the platforms 1 and/or 2 to rotate in a plane of the support areas 9 and/or 10 via controlled drive 53–56–58 and 55 and inwardly directed platform (Fig. 3). The rods 47–49 and 50–52 can change their length by means of linear control actuators 59–61 and 62–64.

Suppose that the coordinates of “vector capture” S_0^B (for rods 47–49), and S_0^H (for the rods 50–52) in the fixed coordinate system:

– for the upper platform

$$S_0^B(x_{i0}^{BK} - x_{i0}^{BH}, y_{i0}^{BK} - y_{i0}^{BH}, z_{i0}^{BK} - z_{i0}^{BH}), \quad i = 1, 2, 3. \quad (48)$$

– for the lower platform

$$S_0^H(x_{j0}^{HK} - x_{j0}^{HH}, y_{j0}^{HK} - y_{j0}^{HH}, z_{j0}^{HK} - z_{j0}^{HH}), \quad j = 1, 2, 3. \quad (49)$$

It should be noted that the value of these coordinates depends on the design of the model.

Given that the simultaneous displacement and swing, as their compression or stretching of the coordinates vector “gripping rods” the new coordinate system changes, i.e.

$$\begin{aligned}
 S_T^B \begin{pmatrix} x_{iT}^B \\ y_{iT}^B \\ z_{iT}^B \end{pmatrix} &= S_T^B(x, y, z, u, v, w, \Delta R_B) \\
 &= C_u^B \cdot C_v^B \cdot C_w^B \cdot A_c^B \cdot B_p^B \cdot S_0^B, \quad i = 1, 2, 3.
 \end{aligned} \tag{50}$$

$$\begin{aligned}
 S_T^H \begin{pmatrix} x_{jT}^H \\ y_{jT}^H \\ z_{jT}^H \end{pmatrix} &= S_T^H(x, y, z, u, v, w, \Delta R_H) \\
 &= C_u^H \cdot C_v^H \cdot C_w^H \cdot A_c^H \cdot B_p^H \cdot S_0^H, \quad j = 1, 2, 3.
 \end{aligned} \tag{51}$$

Here, $C_u^B, C_v^B, C_w^B (C_u^H, C_v^H, C_w^H)$ —rotation matrices upper (lower) platform, respectively,

A_c^B, A_c^H —displacement of the upper matrix (lower) platform,

B_p^B, B_p^H —matrix of stretching-contraction the upper (lower) platform.

Suppose we are given relative to the upper (lower) platform shift length and angle of the rods 47–49 (50–52) $L_{i3}^B, \alpha_{i3}^B (L_{j3}^H, \alpha_{j3}^H)$. Then, from (50), (51) the current length of the rods $L_{iT}^B (L_{jT}^H)$ and the current angle $\alpha_{iT}^B (\alpha_{jT}^H)$ of rotation for the upper (lower) platform as follows:

$$L_{iT}^B = [(x_{iT}^B)^2 + (y_{iT}^B)^2 + (z_{iT}^B)^2]^{1/2}, \quad i = 1, 2, 3. \tag{52}$$

$$L_{jT}^H = [(x_{jT}^H)^2 + (y_{jT}^H)^2 + (z_{jT}^H)^2]^{1/2}, \quad j = 1, 2, 3. \tag{53}$$

$$\alpha_{iT}^B = \arcsin \frac{z_{iT}^B}{L_{iT}^B}, \quad i = 1, 2, 3. \tag{54}$$

$$\alpha_{jT}^H = \arcsin \frac{z_{jT}^H}{L_{jT}^H}, \quad j = 1, 2, 3. \tag{55}$$

Taking into account (52)–(55), the following changes in the relative lengths and angles of rotation of the rods to the upper (lower) platforms:

$$\Delta\alpha_i^B = |\alpha_{i3}^B - \alpha_{iT}^B|, i = 1, 2, 3, \Delta\alpha_j^H = |\alpha_{j3}^H - \alpha_{jT}^H|, j = 1, 2, 3. \quad (56)$$

$$\Delta L_i^B(t) = |L_{i3}^B - L_{iT}^B|, i = 1, 2, 3, \Delta L_j^H(t) = |L_{j3}^H - L_{jT}^H|, j = 1, 2, 3. \quad (57)$$

The value of the parameters (56), (57) is used in the design of control systems EMS.

Similar formulas with a few changes you can get to the movements of rods 29–31 and 32–34.

Suppose that the coordinates of “motion vector” M_0^B (for the rods 29–31), and M_0^H (for the rods 32–34) in the fixed coordinate system:

– for the upper platform

$$M_0^B(x_{i0}^{BK} - x_{i0}^{BH}, y_{i0}^{BK} - y_{i0}^{BH}, z_{i0}^{BK} - z_{i0}^{BH}), \quad i = 1, 2, 3. \quad (58)$$

– for the lower platform

$$M_0^H(x_{j0}^{HK} - x_{j0}^{HH}, y_{j0}^{HK} - y_{j0}^{HH}, z_{j0}^{HK} - z_{j0}^{HH}), \quad j = 1, 2, 3. \quad (59)$$

It should be noted that the value of these coordinates depends on the design of the model.

Given that the simultaneous displacement and swing, as their compression or stretching of the coordinates “motion vector” the new coordinate system changes, i.e.

$$\begin{aligned} M_T^B \begin{pmatrix} x_{iT}^B \\ y_{iT}^B \\ z_{iT}^B \end{pmatrix} &= M_T^B(x, y, z, u, v, w, \Delta R_B) \\ &= C_u^B \cdot C_v^B \cdot C_w^B \cdot A_c^B \cdot B_p^B \cdot M_0^B, \quad i = 1, 2, 3. \end{aligned} \quad (60)$$

$$\begin{aligned} M_T^H \begin{pmatrix} x_{jT}^H \\ y_{jT}^H \\ z_{jT}^H \end{pmatrix} &= M_T^H(x, y, z, u, v, w, \Delta R_H) \\ &= C_u^H \cdot C_v^H \cdot C_w^H \cdot A_c^H \cdot B_p^H \cdot M_0^H, \quad j = 1, 2, 3. \end{aligned} \quad (61)$$

Here, $C_u^B, C_v^B, C_w^B (C_u^H, C_v^H, C_w^H)$ —rotation matrices upper (lower) platform, respectively,

A_c^B, A_c^H —displacement of the upper matrix (lower) platform,

B_p^B, B_p^H —matrix of stretching-contraction the upper (lower) platform.

Suppose we are given relative to the upper (lower) platform shift length and angle of the rods 29–31 (32–34) $L_{i3}^B, \alpha_{i3}^B (L_{j3}^H, \alpha_{j3}^H)$. Then, from (60), (61) the current length of the rods $L_{iT}^B (L_{jT}^H)$ and the current angle $\alpha_{iT}^B (\alpha_{jT}^H)$ of rotation for the upper (lower) platform as follows:

$$L_{iT}^B = [(x_{iT}^B)^2 + (y_{iT}^B)^2 + (z_{iT}^B)^2]^{1/2}, \quad i = 1, 2, 3. \quad (62)$$

$$L_{jT}^H = [(x_{jT}^H)^2 + (y_{jT}^H)^2 + (z_{jT}^H)^2]^{1/2}, \quad j = 1, 2, 3. \quad (63)$$

$$\alpha_{iT}^B = \arccos \frac{x_{iT}^B}{L_{iT}^B}, \quad i = 1, 2, 3. \quad (64)$$

$$\alpha_{jT}^H = \arccos \frac{x_{jT}^H}{L_{jT}^H}, \quad j = 1, 2, 3. \quad (65)$$

Taking into account (62)–(65), the following changes in the relative lengths and angles of rotation of the rods to the upper (lower) platforms:

$$\bar{\Delta}L_i^B(t) = |L_{i3}^B - L_{iT}^B|, i = 1, 2, 3, \quad \bar{\Delta}L_j^H(t) = |L_{j3}^H - L_{jT}^H|, j = 1, 2, 3. \quad (66)$$

$$\bar{\Delta}\alpha_i^B = |\alpha_{i3}^B - \alpha_{iT}^B|, i = 1, 2, 3, \quad \bar{\Delta}\alpha_j^H = |\alpha_{j3}^H - \alpha_{jT}^H|, j = 1, 2, 3. \quad (67)$$

The value of the parameters (66), (67) $\bar{\Delta}L_i^B(t), \bar{\Delta}L_j^H(t), \bar{\Delta}\alpha_i^B, \bar{\Delta}\alpha_j^H$ is used in the design of control systems EMS.

4 Conclusion

Received the solution of the direct problem of kinematics module SEMS. This solution can be used in the synthesis of the automatic control system the desired quality of dynamic processes.

References

1. Popov, E.P., Writing, G.V.: Fundamentals of Robotics, Moscow (1990)
2. Chernukhin, Y.V., Pisarenko, S.N.: Extrapolation Structures in Neural Network-Based Control Systems for Intelligent Mobile Robots. Opt. Mem. Neural Netw. **11**(2), 105–115 (2002)

3. Gorodetskiy, A.E., Tarasova, I.L., Agapov, V.A., Kuchmin, A.Y.: Medical microrobot. Patent No. 2469752
4. Gorodetskiy, A.E.: Fundamentals of the theory of intelligent control systems. LAP LAMBERT Academic Publishing GmbH & Co. KG (2011)
5. Merlet, J.P.: Parallel Robots, 2nd edn, 383 p. Springer, INRIA, Sophia-Antipolis, France (2006)

The Inverse Problem of Kinematics SM8 SEMS

V.G. Kurbanov, A.E. Gorodetskiy and I.L. Tarasova

Abstract To solve a problem of control, there is a large interest in solving direct and inverse problems of kinematics for module SM8 SEMS, since it has the most complete functionality, and other modules are its simplifications. The developed algorithm allows the calculation of a real-time and correction of the parameters of the SU SM8.

Keywords Smart electromechanical systems · Standard module · Structure · Inverse kinematic model · Automatic control system

1 Introduction

From the previous paper [1] that if there is a simultaneous displacement ($x(t)$, $y(t)$ and $z(t)$) and turning through angles ($u(t)$, $v(t)$ and $w(t)$) the upper platform, as well as compression or stretching of the upper ($\Delta R_u(t)$) and the lower ($\Delta R_h(t)$) EMS platforms, then the radius vector will change as follows:

$$\mathbf{r}_{iB}(x, y, z, u, v, w, \Delta R_B(t)) = \mathbf{C}_u \mathbf{C}_v \mathbf{C}_w (\mathbf{r}_{iB}(0) + \mathbf{A} + \mathbf{B}_{iB}(t)) \quad (1)$$

$$\mathbf{r}_{iH}(\Delta R_B(t)) = (\mathbf{r}_{iH}(0) + \mathbf{B}_{iH}(t)) \quad (2)$$

V.G. Kurbanov (✉) · A.E. Gorodetskiy · I.L. Tarasova
Institute of Problems of Mechanical Engineering, Russian Academy of Sciences,
Saint Petersburg, Russia
e-mail: vugar_borchali@yahoo.com

A.E. Gorodetskiy
e-mail: g27764@yandex.ru

I.L. Tarasova
e-mail: g17265@yandex.ru

2 Solution of the Inverse Kinematic Problem

Consequently, the length of the legs actuators (LA) has the following form:

$$L_i(x, y, z, u, v, w, \Delta R_B, \Delta R_H) = [(r_{iB}^x(x, y, z, u, v, w, \Delta R_B) - r_{iH}^x(\Delta R_B))^2 + (r_{iB}^y(x, y, z, u, v, w, \Delta R_B) - r_{iH}^y(\Delta R_H))^2 + (r_{iB}^z(x, y, z, u, v, w, \Delta R_B) - r_{iH}^z(\Delta R_H))^2]^{1/2} \quad (3)$$

$$C = C_u \cdot C_v \cdot C_w = \begin{vmatrix} 1 & -w & v \\ uv + w & -uvw + 1 & -u \\ -v + uw & vw + u & 1 \end{vmatrix} \quad (4)$$

Then, (1), (2) can be rewritten in the following form:

$$\mathbf{r}_{iB} = \begin{vmatrix} r_{iB}^x + x + B_{iB}^x - w(r_{iB}^y + y + B_{iB}^y) + v(r_{iB}^z + z + B_{iB}^z) \\ (uv + w)(r_{iB}^x + x + B_{iB}^x) + (1 - uvw)(r_{iB}^y + y + B_{iB}^y) - u(r_{iB}^z + z + B_{iB}^z) \\ (uw - v)(r_{iB}^x + x + B_{iB}^x) + (vw + u)(r_{iB}^y + y + B_{iB}^y) + r_{iB}^z + z + B_{iB}^z \end{vmatrix} \quad (5)$$

$$\mathbf{r}_{iH} = \begin{vmatrix} r_{iH}^x + B_{iH}^x \\ r_{iH}^y + B_{iH}^y \\ r_{iH}^z + B_{iH}^z \end{vmatrix} \quad (6)$$

Considering that given $L_i (i = 1, 2, \dots, 6)$, R_B , R_H , (3), (5) and (6) we obtain the following system of nonlinear equations:

$$\begin{aligned} & [((r_{iB}^x + x + B_{iB}^x) - w(r_{iB}^y + y + B_{iB}^y) + v(r_{iB}^z + z + B_{iB}^z)) - (r_{iH}^x + B_{iH}^x)]^2 \\ & + [((uv + w)(r_{iB}^x + x + B_{iB}^x) + (1 - uvw)(r_{iB}^y + y + B_{iB}^y) - u(r_{iB}^z + z + B_{iB}^z)) - (r_{iH}^y + B_{iH}^y)]^2 \\ & + [((uw - v)(r_{iB}^x + x + B_{iB}^x) + (vw + u)(r_{iB}^y + y + B_{iB}^y) + (r_{iB}^z + z + B_{iB}^z)) - (r_{iH}^z + B_{iH}^z)]^2 = L_i^2, \end{aligned} \quad (7)$$

where, $i = 1, 2, \dots, 6$.

The result:

$$\left\{ \begin{array}{l} f_1(x, y, z, u, v, w) = 0 \\ \vdots \\ f_6(x, y, z, u, v, w) = 0 \end{array} \right\} \quad (8)$$

where, $f_i(x, y, z, u, v, w)$, ($i = 1, \dots, 6$) non-linear functions defined and continuous in predetermined areas. Or in vector form:

$$\begin{aligned}
 \xi &= (x, y, z, u, v, w)^T, F(\xi) = [f_1(\xi), \dots, f_6(\xi)]^T, \\
 0 &\leq x \leq \bar{x}, 0 \leq y \leq \bar{y}, 0 \leq z \leq \bar{z}, \\
 0 &< u \leq \bar{u}, 0 < v \leq \bar{v}, 0 < w \leq \bar{w} \\
 F(\xi) &= 0
 \end{aligned} \tag{9}$$

To find the solution (8) and (9) using Newton’s method, i.e.,

$$\xi^{(k+1)} = \xi^{(k)} - J^{-1}(\xi^{(k)}) \cdot F(\xi^{(k)}), \quad k = 0, 1, 2, \dots \tag{10}$$

where J —Jacobi matrix

$$J = \begin{vmatrix} \frac{\partial f_1(\xi)}{\partial x} & \cdot & \cdot & \cdot & \frac{\partial f_1(\xi)}{\partial w} \\ \cdot & \cdot & \cdot & \cdot & \cdot \\ \cdot & \cdot & \cdot & \cdot & \cdot \\ \frac{\partial f_6(\xi)}{\partial x} & \cdot & \cdot & \cdot & \frac{\partial f_6(\xi)}{\partial w} \end{vmatrix} \tag{11}$$

$$\begin{aligned}
 \frac{\partial f_i(\xi)}{\partial x} &= 2[(r_{iB}^x + x + B_{iB}^x) - w(r_{iB}^y + y + B_{iB}^y) + v(r_{iB}^z + z + B_{iB}^z) - (r_{iH}^x + B_{iH}^x)] \\
 &+ 2(uv + w)[(uv + w)(r_{iB}^x + x + B_{iB}^x) + (1 - uvw)(r_{iB}^y + y + B_{iB}^y) \\
 &- u(r_{iB}^z + z + B_{iB}^z) - (r_{iH}^y + B_{iH}^y)] + 2(uw - v) \cdot \\
 &[[(uw - v)(r_{iB}^x + x + B_{iB}^x) + (vw + u)(r_{iB}^y + y + B_{iB}^y) + r_{iB}^z + z + B_{iB}^z - (r_{iH}^z + B_{iH}^z)],
 \end{aligned} \tag{12}$$

$$\begin{aligned}
 \frac{\partial f_i(\xi)}{\partial y} &= -2w[(r_{iB}^x + x + B_{iB}^x) - w(r_{iB}^y + y + B_{iB}^y) + v(r_{iB}^z + z + B_{iB}^z) - (r_{iH}^x + B_{iH}^x)] \\
 &+ 2(1 - uvw)[(uv + w)(r_{iB}^x + x + B_{iB}^x) + (1 - uvw)(r_{iB}^y + y + B_{iB}^y) \\
 &- u(r_{iB}^z + z + B_{iB}^z) - (r_{iH}^y + B_{iH}^y)] + 2(vw + u) \cdot \\
 &[[(uw - v)(r_{iB}^x + x + B_{iB}^x) + (vw + u)(r_{iB}^y + y + B_{iB}^y) + r_{iB}^z + z + B_{iB}^z - (r_{iH}^z + B_{iH}^z)],
 \end{aligned} \tag{13}$$

$$\begin{aligned}
 \frac{\partial f_i(\xi)}{\partial z} &= 2v[(r_{iB}^x + x + B_{iB}^x) - w(r_{iB}^y + y + B_{iB}^y) + v(r_{iB}^z + z + B_{iB}^z) - (r_{iH}^x + B_{iH}^x)] \\
 &- 2u[(uv + w)(r_{iB}^x + x + B_{iB}^x) + (1 - uvw)(r_{iB}^y + y + B_{iB}^y) - u(r_{iB}^z + z + B_{iB}^z) - (r_{iH}^y + B_{iH}^y)] \\
 &+ 2[((uw - v)(r_{iB}^x + x + B_{iB}^x) + (vw + u)(r_{iB}^y + y + B_{iB}^y) + r_{iB}^z + z + B_{iB}^z - (r_{iH}^z + B_{iH}^z)],
 \end{aligned} \tag{14}$$

$$\begin{aligned}
\frac{\partial f_i(\xi)}{\partial v} &= 2(r_{iB}^x + x + B_{iB}^x)[(r_{iB}^x + x + B_{iB}^x) - w(r_{iB}^y + y + B_{iB}^y) + v(r_{iB}^z + z + B_{iB}^z) - (r_{iH}^x + B_{iH}^x)] \\
&\quad + 2[u(r_{iB}^x + x + B_{iB}^x) - uw(r_{iB}^y + y + B_{iB}^y)][(uv + w)(r_{iB}^x + x + B_{iB}^x) \\
&\quad + (1 - uvw)(r_{iB}^y + y + B_{iB}^y - u(r_{iB}^z + z + B_{iB}^z)) - (r_{iH}^y + B_{iH}^y)] \\
&\quad + 2[-v(r_{iB}^x + x + B_{iB}^x) + w(r_{iB}^y + y + B_{iB}^y)][((uw - v)(r_{iB}^x + x + B_{iB}^x) \\
&\quad + (vw + u)(r_{iB}^y + y + B_{iB}^y) + r_{iB}^z + z + B_{iB}^z) - (r_{iH}^z + B_{iH}^z)]
\end{aligned} \tag{15}$$

$$\begin{aligned}
\frac{\partial f_i(\xi)}{\partial u} &= 2[v(r_{iB}^x + x + B_{iB}^x) - vw(r_{iB}^y + y + B_{iB}^y) - (r_{iB}^z + z + B_{iB}^z)][(uv + w)(r_{iB}^x + x + B_{iB}^x) \\
&\quad + (1 - uvw)(r_{iB}^y + y + B_{iB}^y) - u(r_{iB}^z + z + B_{iB}^z) - (r_{iH}^y + B_{iH}^y)] \\
&\quad + 2[w(r_{iB}^x + x + B_{iB}^x) + r_{iB}^y + y + B_{iB}^y][(uw - v)(r_{iB}^x + x + B_{iB}^x) + (vw + u)(r_{iB}^y + y + B_{iB}^y) \\
&\quad + (r_{iB}^z + z + B_{iB}^z) - (r_{iH}^z + B_{iH}^z)]
\end{aligned} \tag{16}$$

$$\begin{aligned}
\frac{\partial f_i(\xi)}{\partial w} &= -2(r_{iB}^y + y + B_{iB}^y)[(r_{iB}^x + x + B_{iB}^x - w(r_{iB}^y + y + B_{iB}^y) + v(r_{iB}^z + z + B_{iB}^z) - (r_{iH}^x + B_{iH}^x)] \\
&\quad + 2[(r_{iB}^x + x + B_{iB}^x) - uv(r_{iB}^y + y + B_{iB}^y)][(uv + w)(r_{iB}^x + x + B_{iB}^x) + (1 - uvw)(r_{iB}^y + y + B_{iB}^y) \\
&\quad - u(r_{iB}^z + z + B_{iB}^z) - (r_{iH}^y + B_{iH}^y)] \\
&\quad + 2[u(r_{iB}^x + x + B_{iB}^x) + v(r_{iB}^y + y + B_{iB}^y)][((uw - v)(r_{iB}^x + x + B_{iB}^x) + (vw + u)(r_{iB}^y + y + B_{iB}^y) \\
&\quad + r_{iB}^z + z + B_{iB}^z) - (r_{iH}^z + B_{iH}^z)]
\end{aligned} \tag{17}$$

Since inverse matrix calculation is arduous transform (10) as follows:

$$J(\xi^{(k)}) \cdot \Delta \xi^{(k)} = -F(\xi^{(k)}), \quad k = 0, 1, 2, \dots \tag{18}$$

where, $\Delta \xi^{(k)} = \xi^{(k+1)} - \xi^{(k)}$.

We obtain a system of linear algebraic equations with respect to the amendment $\Delta \xi^{(k)}$. After determining it calculated the following approximation:

$$\xi^{(k+1)} = \xi^{(k)} + \Delta \xi^{(k)} \tag{19}$$

3 Algorithm

1. Set the initial approximation $\xi^{(0)}$ and small positive number ε (accuracy). Let $k = 0$.
2. Calculate the Jacobi matrix and solve a system of linear algebraic equations with respect to the amendment $\Delta \xi^{(k)}$.

$$J(\xi^{(k)}) \cdot \Delta \xi^{(k)} = -F(\xi^{(k)}), \quad k = 0, 1, 2, \dots$$

3. Calculate the following approximation:

$$\xi^{(k+1)} = \xi^{(k)} + \Delta \xi^{(k)}$$

4. If $\Delta^{(k+1)} = \max_i \left| \xi^{(k+1)} - \xi^{(k)} \right| \leq \varepsilon$, the process is complete, and $\xi^* \approx \xi^{(k+1)}$. If $\Delta^{(k+1)} > \varepsilon$, put $\xi^* \approx \xi^{(k+1)}$., it is $k = k + 1$ and go to step 2.

For the convergence of Newton's method only if the function is continuous differentiable nondegenerate Jacobi matrix. With good initial approximation is a quadratic convergence of the method. You can use other methods (simplified Newton method, Proyden method, secant method, etc.), but the restrictions on non-linear functions and Jacobi matrix for this task is time-consuming [2, 3].

4 Conclusion

Received the algorithmic solution of inverse kinematics. This solution can be used in the synthesis of the automatic control system the desired quality of dynamic processes.

References

1. Gorodetskiy, A., Tarasova, I., Kurbanov, V.: The direct problem of kinematics SM8 SEMS (in this collection)
2. Bazara, M., Shetty, K.: Nonlinear programming. In: Theory and Algorithms. M., Mir (1982)
3. Kurbanov, V.G.. Mathematical Methods in Control Theory: Textbook. SPb., Publishing House GUAP (2008)

Mathematical Models of the Automatic Control Systems SEMS Modules

I.L. Tarasova, A.E. Gorodetskiy and V.G. Kurbanov

Abstract Here, we describe the structure of the synthesized mathematical model of the automatic control module SM8 SEMS with parallel channel control, measurement and movement, as well as simple mathematical models of blocks of the system, without taking into account possible jamming of control rods and legs of reconfiguration of platforms of electromechanical system related to the possible nonsync drives operation. The possibility of using it for computer modeling and studying the characteristics and properties of standard modules SEMS is shown in the article. It is noted that for the record of jamming, the considered mathematical model must be complemented by a block of logical analysis of displacements and block of choosing the optimum path. In this case, the control system itself has to be provided with additional software for computer blocks or supplemented by a force sensor in the legs and the control rods to prevent jamming situations. At the same time, the structure becomes more complicated,; however, the quality and reliability increase.

Keywords Smart electromechanical systems · Standard module · Mathematical and computer model · Automatic control system · Characteristics and properties

I.L. Tarasova (✉) · A.E. Gorodetskiy · V.G. Kurbanov
Institute of Problems of Mechanical Engineering, Russian Academy of Sciences,
Saint-Petersburg, Russia
e-mail: g17265@yandex.ru

A.E. Gorodetskiy
e-mail: g27764@yandex.ru

V.G. Kurbanov
e-mail: vugar_borchali@yahoo.com

1 Introduction

Research on the development of mathematical models of intelligent robots (IR) are actively conducted in all industrialized countries of the world [1]. These robots are designed to function in conditions of a priori uncertainty dynamically changing environment. At the same time the use of IR hexapod like structures SEMS provides an opportunity to get maximum accuracy of actuating mechanisms with minimal moving time by introducing parallelism in measuring, calculating, movement and use of precision piezoengine capable of operating extreme conditions, including outer space [2, 3]. However, such structures have a complex kinematical scheme, which requires the improvement of their management algorithms and corresponding mathematical models of the Automatic Control Systems (ACS). These models provide solutions to new, complex of optimization tasks find the optimum path without locking of.

The main elements of the SEMS is Standard modules (SM). These modules provide shifts and turns platforms, compression and expansion of the platform and a longer stem the twists and turns of the movement of the elongate shaft and capture which in combination with control systems provides a universal structure SEMS [4, 5]. The most complete functionality of the reviewed in [4], has the module SM8 SEMS through a combination possibilities and modules SM6 SEMS SM7 SEMS and it can be called a universal module. The other modules are in some of the simplification. It is therefore advisable construct mathematical models, especially the module in order to study the characteristics and properties of standard modules SEMS.

2 The Mathematical Model of the Automatic Control System SM5 SEMS

The structure of the mathematical model of the Automatic Control System SM5 SEMS considered in [6] and includes (see Fig. 1), the following units: Calculate Elongation (CE), the Control Rods of the Upper Platform (CRUP) and Lower Platform (CRLP), Control Actuators Feet (CAF), motor rods upper platform (MSUP) and Lower Platform (MSLP), Motor Actuators Feet (MAF), Reducers of Rods of the Upper Platform (RRUP) and Lower Platform (RRLP), Reducers Actuators Feet (RAF), the Definition of Moments and Resistance Forces (DMRF) and Calculate the Coordinates of the Platforms (CCP).

There is a detailed description of the blocks of the mathematical model of ACS SM5 SEMS

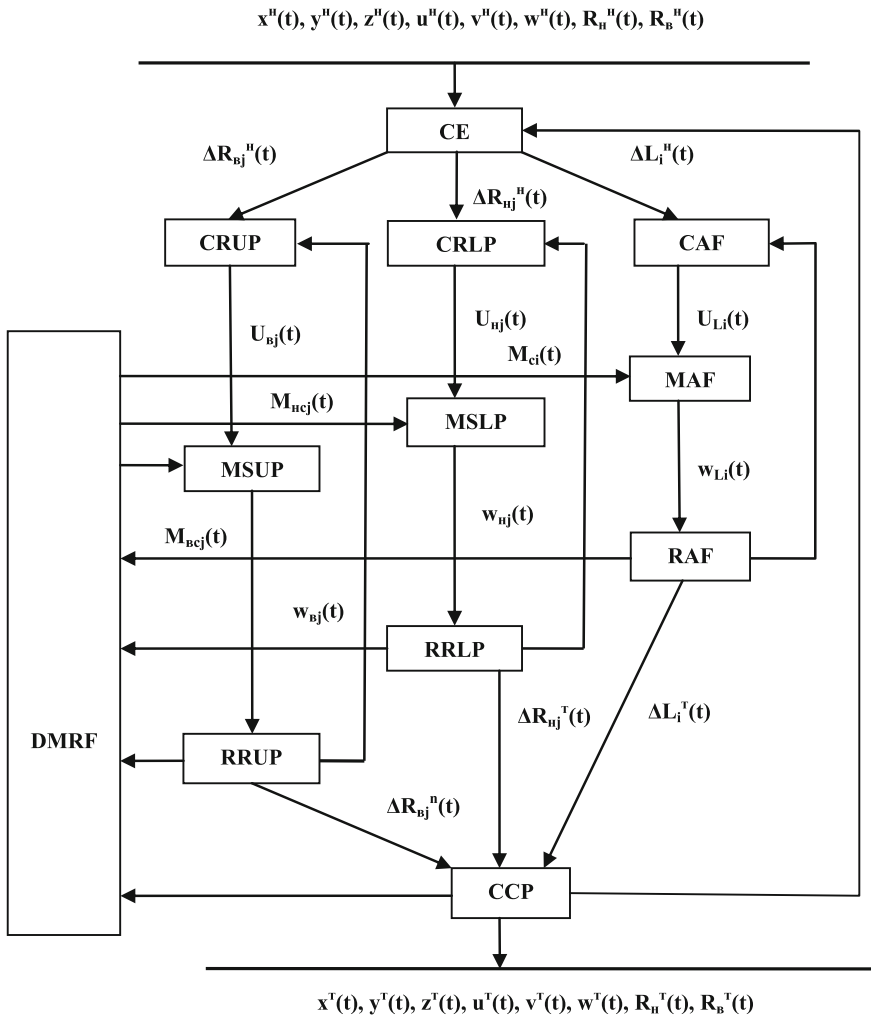


Fig. 1 The structure of the mathematical model of ACS SM5 SEMS

The block calculates the CE:

- The task the two elongation ($j = 3$) of rods of the upper platform by the formula:

$$\Delta R_{ej}^T(t) = R_e^H(t) - R_e^T(t) \tag{1}$$

where: $R_e^H(t)$ and $R_e^T(t)$ —a predetermined and the current radius of the upper platform;

- The task the two elongation ($j = 3$) of rods of the lower platform by the formula:

$$\Delta R_{ij}^T(t) = R_u^H(t) - R_u^T(t) \quad (2)$$

where: $R_u^H(t)$ and $R_u^T(t)$ —a predetermined and the current radius of the lower platform;

Elongation six task for ($i = 6$) feet from the formula:

$$\Delta L_i^T(t) = L_i^H(t) - L_i^T(t) \quad (3)$$

where: $L_i^H(t) = L_i(x^u(t), y^u(t), z^u(t), u^u(t), v^u(t), w^u(t), R_e^u(t), R_u^u(t))$ —calculated according to the given coordinates leg length;

$L_i^T(t) = L_i(x^T(t), y^T(t), z^T(t), u^T(t), v^T(t), w^T(t), R_e^T(t), R_u^T(t))$ —taken from the current magnitude the CCP long legs;

$x^u(t), y^u(t), z^u(t)$ и $x^T(t), y^T(t), z^T(t)$ —given and the current values of the linear coordinates of the upper platform;

$u^u(t), v^u(t), w^u(t)$ и $u^T(t), v^T(t), w^T(t)$ —given and the current values of the angular coordinates of the upper platform;

$R_e^u(t), R_u^u(t)$ и $R_e^T(t), R_u^T(t)$ —given and the current values of the radii of the upper and lower platforms.

The lengths of the legs of the components of Li calculated radius vectors \mathbf{r}_{ib} and \mathbf{r}_{in} upper and lower platforms (see Fig. 2) using the formula:

$$L_i(x, y, z, u, v, w, \Delta R_e, \Delta R_u) = (r_{ie}^x(x, y, z, u, v, w, \Delta R_e) - r_{in}^x(\Delta R_u))^2 + (r_{ie}^y(x, y, z, u, v, w, \Delta R_e) - r_{in}^y(\Delta R_u))^2 + (r_{ie}^z(x, y, z, u, v, w, \Delta R_e) - r_{in}^z(\Delta R_u))^2)^{1/2} \quad (4)$$

The radius vectors of the upper and lower platforms are determined by the following formulas:

$$\mathbf{r}_{ib}(x, y, z, u, v, w, \Delta R_e) = \mathbf{C}_u \mathbf{C}_v \mathbf{C}_w (\mathbf{r}_{ib}(0) + \mathbf{A} + \mathbf{B}_{ib}(t)) \quad (5)$$

$$\mathbf{r}_{in}(\Delta R_u) = (\mathbf{r}_{in}(0) + \mathbf{B}_{in}(t)) \quad (6)$$

where: \mathbf{r}_{ib} —vector directed from the point O to the point ib (Fig. 2);

\mathbf{r}_{in} —vector directed from the point O_1 to the point in (Fig. 2);

$\mathbf{A} = /x(t); y(t); z(t)/^T$ —матрица смещений;

$\mathbf{B}_{ib}(t)$ —matrix compressions of the upper platform;

$\mathbf{C}_u, \mathbf{C}_v$ и \mathbf{C}_w —rotation matrices.

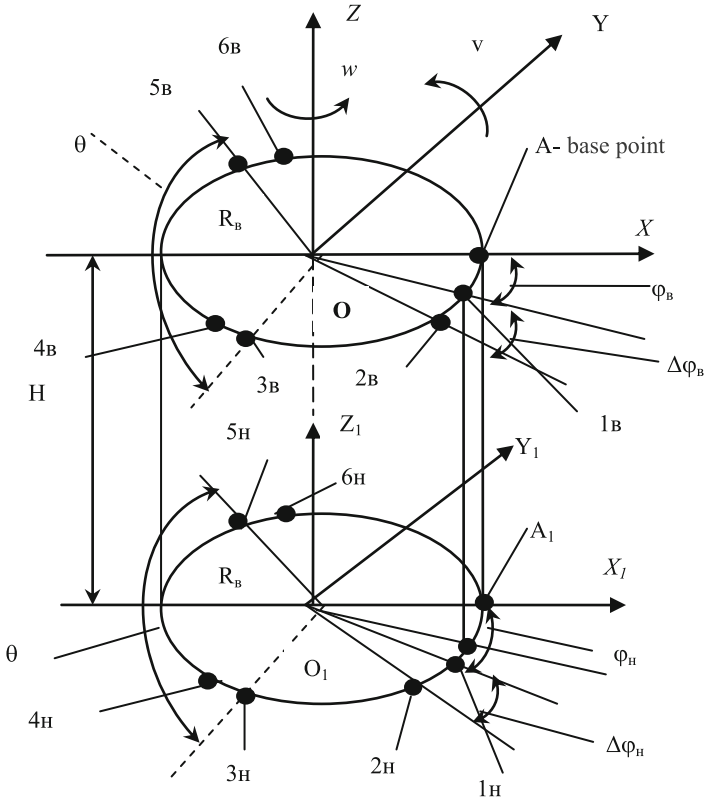


Fig. 2 Scheme of electromechanical system SM5 SEMS

The block CRUP match to the incoming assignment $\Delta R_{ef}^u(t)$ calculates the control action $U_{ef}(t)$, to the motor control rods reconfiguration of the upper platform control law:

$$U_{ef}(t) = k_{1e} e_{ef}(t) + k_{2e} \int e_{ef}(t) dt + k_{3e} \frac{de_{ef}(t)}{dt} \tag{7}$$

where: $e_{ef}(t) = (\Delta R_{ef}^3(t) - \Delta R_{ef}^T(t))$ —deviations from the task;

k_{1e} , k_{2e} и k_{3e} —coefficients that determine nature of the transition process in the system, the values of which are set in the process of setting up the system or the computer model.

Block CAF match to the incoming task $\Delta Li_3(t)$ calculates the control actions $ULi(t)$, supplied to the motor actuators feet on the type of control law (7).

Each of the blocks MSUP and MSLP contains three rods motor and block MAF contains six actuators motors. Each motor is described by [6] the following equations:

$$L_{\mathcal{A}} di(t)/dt + R_{\mathcal{A}} i(t) = U(t) - C_e \omega(t) \quad (8)$$

$$J d\omega(t)/dt = C_M i(t) - M_c(t) \quad (9)$$

where: $L_{\mathcal{A}}$ and $R_{\mathcal{A}}$ —inductance and active resistance of anchor chain, J —reduced moment of inertia of the rotor, C_e and C_M —constant depending on the design parameters of the motor and the quantity of flow of excitation, $i(t)$ —amperage in the anchor winding, $\omega(t)$ —rotational speed of the rotor ($\omega_{\mathcal{A}}(t)$, $\omega_{ij}(t)$ or $\omega_{Li}(t)$, $U(t)$ —input action ($U_{\mathcal{A}}(t)$, $U_{ij}(t)$ or $U_{Li}(t)$), $M_c(t)$ —the reduced moment of loads on the motor shaft ($M_{\mathcal{A}}(t)$, $M_{ij}(t)$ or $M_{ci}(t)$).

Each of the blocks RRUP and RRLP contains three reducer, and the block RAF—six. They are described by the following differential by the equation

$$k_p dl(t)/dt = \omega(t) \quad (10)$$

where: k_p —the reduction coefficient ($k_{p\mathcal{A}}$, k_{pH} or k_{pA}), $l(t)$ —the elongate shaft of the upper platform ($\Delta R_{\mathcal{A}}^T(t)$), lower platform ($\Delta R_{ij}^T(t)$) or legs ($\Delta L_i^T(t)$).

Block CCP describes the movement Δl_k of the places mount the whip rods and hinges of leg on platforms ($\Delta l_{\mathcal{A}j}$, Δl_{ij} or $\Delta l_{\mathcal{A}i}$, $\Delta l_{\mathcal{A}i}$) depending on the elongation rods Δl_c upper platform ($\Delta R_{\mathcal{A}}^T(t)$), the lower platform ($\Delta R_{ij}^T(t)$) or legs ($\Delta L_i^T(t)$) on the following differential by the equation [6]:

$$T_i^2 \frac{d^2 \Delta l_{ki}}{dt^2} + 2T_i \zeta_i \frac{d \Delta l_{ki}}{dt} + 1 = k_i \Delta l_{ci} \quad (11)$$

where: T_i —the time constant, ζ_i —the oscillatory, k_i —amplification.

The quantities T_i , ζ_i and k_i are dependent on constructive of parameters of electromechanical system and can be determined by the results of experiments. If $\zeta_i \geq 1$ oscillating unit (11) is replaced by two aperiodic.

To determine the line (x , y , z) and angle (u , v , w) coordinate platforms known displacements Δl_k necessary, using equations of the form (1)–(6), to solve the inverse problem. This can be done algorithmically using Newton's method.

In the memory block DMRF stored experimentally filmed depending shown torque for motors M_c ($M_{\mathcal{A}}(t)$, $M_{ij}(t)$ or $M_{ci}(t)$) on the deviation $\varepsilon = \Delta l_k - \Delta l_c$. For each locations fastening of rods and of hinges of legs in the block DMRF calculated deviations $\varepsilon_j(t)$ or $\varepsilon_i(t)$. According to them from memory of DMRF selected values $M_{\mathcal{A}}(t)$, $M_{ij}(t)$ or $M_{ci}(t)$, which is fed in a blocks MSUP, MSLP or MAF.

3 Addition of a Mathematical Model of the Automatic Control Module SM8 SEMS

SM8 SEMS contains electromechanical system (EMS), which has a sliding lower and upper platform. These platforms are connected to each other by six legs with motors elongation, reducers and hinges. Each equipped with three control rods each reconfiguration of platforms with motors elongation, reducers and hinges, three control rod movement with motors elongation gear units and motors turning gear units and three control rods capture with motors elongation gear units and motors turning gear units [4]. In addition SM8 SEMS comprises a Control Computer Complex (CCC) based on neuroprocessors, for example NM 6403, the Program Complex (PC) and Measuring System (MS) [7]

Consequently, ACS SM8 SEMS compared with ACS SM5 SEMS has an additional of Automatic Control System Rods Movement (ACSRM) and a Automatic Control System Rods Capture (ACSRC) [7]. These systems, unlike the control systems of control rods and legs a reconfiguration is run as an elongated shaft and capture movements, and their rotation.

The structures are similar to mathematical models ACSRM and ACSRC. Figure 3 shows the structure of a mathematical model ACSRM. The model contains the following blocks:

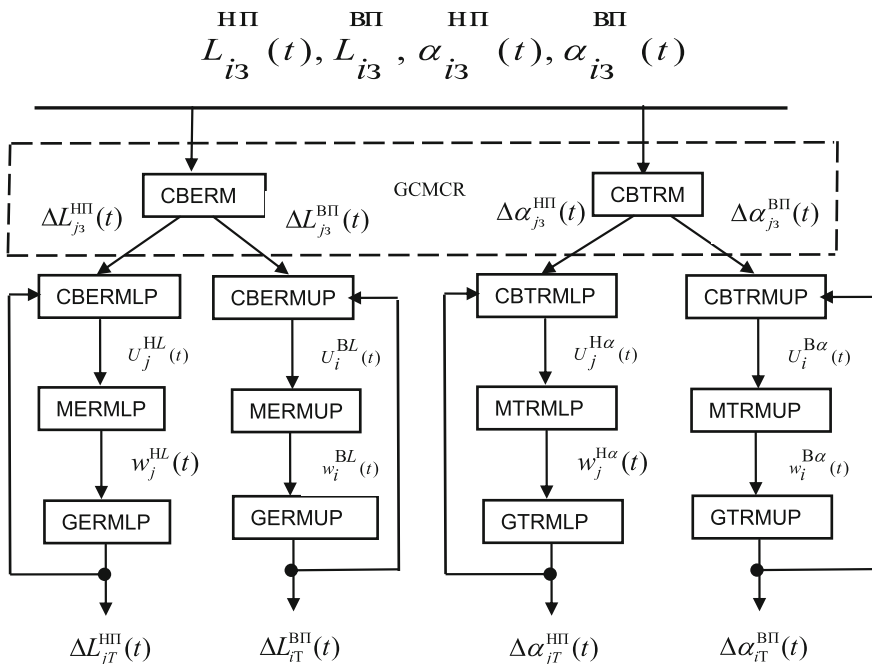


Fig. 3 The structure of the mathematical model ACSRM

- Group Control of the Control Rod Movement (GCCRM), containing Calculating Block Elongated Rod Movement (CBERM) and Calculating Block Turns Rod Movement (CBTRM);
- three Control Block Elongated Rod Movement of the Lower Platform (CBERMLP);
- three Control Block Elongated Rod Movement of the Upper Platform (CBERMUP);
- three Control Block Turns Rod Movement of the Lower Platform (CBTRMLP);
- three Control Block Turns Rod Movement of the Upper Platform (CBTRMUP);
- three Motors Elongated Rod Movement of the Lower Platform (MERMLP);
- three Motors Elongated Rod Movement of the Upper Platform (MERMUP);
- three Motors Turns Rod Movement of the Lower Platform (MTRMLP);
- three Motors Turns Rod Movement of the Upper Platform (MTRMUP);
- three Gear Elongation Rods Movement of the Lower Platform (GERMLP);
- three Gear Elongation Rods Movement of the Upper Platform (GERMUP);
- three Gear Turns Rods Movement of the Lower Platform (GTRMLP);
- three Gear Turns Rods Movement of the Upper Platform (GTRMUP).

CBERM calculates:

- task to elongation of three ($i = 3$) rods movement of the upper platform formulule [8]:

$$\bar{\Delta}L_i^B(t) = |L_{i3}^B - L_{iT}^B|, i = 1, 2, 3. \quad (12)$$

where: L_{i3}^B —given relative upper platform length of shift rods movement of the upper platform,

L_{iT}^B —the current length of the shift rods movement of the upper platform

- task to elongation of three ($i = 3$) rods movement of the lower platform formulule [8]:

$$\bar{\Delta}L_j^H(t) = |L_{j3}^H - L_{jT}^H|, j = 1, 2, 3. \quad (13)$$

where: L_{j3}^H —given relative lower platform length of shift rod movement of the lower platform, L_{jT}^H —the current length of the shift rods movement of the lower platform

CBTRM calculates:

- task to turn of three ($i = 3$) rods movement of the upper platform formulule [8]:

$$\bar{\Delta}\alpha_i^B = |\alpha_{i3}^B - \alpha_{iT}^B|, i = 1, 2, 3. \quad (14)$$

where: α_{i3}^B —given relative upper platform rotation angles rods movement of the upper platform, α_{iT}^B —the current rotation angles rods movement of the upper platform

- task to turn of three ($i = 3$) rods movement of the lower platform formulule [8]:

$$\bar{\Delta}\alpha_j^H = |\alpha_{j3}^H - \alpha_{jT}^H|, j = 1,2,3. \tag{15}$$

where: α_{j3}^H —given relative lower platform rotation angles rods movement of the lower platform, α_{jT}^H —the current rotation angles rods movement of the lower platform

Changes of linear and angular coordinates of the rods by shifts and swing the module described in [8]. They should be taken into account when calculating the elongation and turns of the formulas (12)–(15).

CBERMLP, CBERMUP, CBTRMLP and CBTRULP in accordance with the entering tasks from CBERM and CBTRM ($\Delta L_{j3}^{HII}(t)$, $\Delta L_{i3}^{BII}(t)$ и $\Delta\alpha_{j3}^{HII}(t)$, $\Delta\alpha_{i3}^{BII}(t)$) and obatnoy communication signals ($\Delta L_{jT}^{HII}(t)$, $\Delta L_{iT}^{BII}(t)$ и $\Delta\alpha_{jT}^{HII}(t)$, $\Delta\alpha_{iT}^{BII}(t)$), calculated by formude form (7) the relevant control actions $U_i(t)$ and $U_j(t)$, which are applied to the control rod motors. Each motor MERMLP, MERMUP, MTRMLP and MTRMUP described [6] equations of the form (8), (9) and each gear GERMLP, GERMUP, GTRMLP and GTRMUP—equations of the form (10).

These moments $Mc(t)$ on the shafts of motors depending on the purpose of the simulation can be set in the form of stepped effects, harmonics or random perturbations with given distribution.

4 Conclusion

In order to study the characteristics and properties of standard modules SMS expedient construction of mathematical models primarily module SM8 SEMS. This can be proved by the fact that this module combines the features of other standard modules and it can be called a universal module. Mathematical models of the other modules can be easily obtained from consideration because they are in some of the simplification.

In synthesized mathematical model of the automatic control system of module SM8 SEMS with parallel channel control, measurement and movement not taken into account the possible jamming legs and control rods. But, nevertheless, such mathematical models can be used for computer modeling and studying the characteristics and properties of standard modules SEMS. The same applies to the simple mathematical model blocks of ACS of modules SEMS.

To account for jamming considered a mathematical model must be complemented by a block of logical analysis movements and block of choosing the optimum path. In this case, the control system under consideration to prevent jamming situations should be provided with additional software for computer units or complemented a force sensor in the legs and the control rods. The structure of the control system complicated, but its quality and reliability increase.

References

1. Merlet, J.P.: *Parallel Robots*, 2nd edn. Inria, Springer, Sophia-Antipolis (2006). (383 p)
2. Agapov, V.A. (RU), Gorodetskiy, A.E. (RU), Kuchmin, A.J. (RU), Selivanova, E.N. (RU): Medical microrobot. Patent RU 2469752 (2011)
3. Artemenko, Y.N. (RU), Gorodetskiy, A.E. (RU), Dubarenko, V.V. (RU), Kuchmin, A.J. (RU), Agapov, V.A. (RU): Analysis of the dynamics of actuators automatic control systems of space radio telescope subdish. *Informatsionno-upravliayushchie sistemy* **6**, 2–5 (2011) (In Russian)
4. Gorodetskiy, A.E.: Smart electromechanical systems modules (In this volume)
5. Gorodetskiy, A.E., Tarasova, I.L., Kurbanov, V.G., Agapov, V.A.: Mathematical model of the automatic control module SEMS. *Информационно—управляющие системы*. **3**, 40–45 (2015)
6. Kurbanov, V.G., Gorodetskiy, A.E., Tarasova, I.L.: Automatic control systems of SEMS (In this volume)
7. Gorodetskiy, A.E., Tarasova, I.L., Kurbanov, V.G.: The direct problem of kinematics SM8 SEMS (In this volume)
8. Kurbanov, V.G., Gorodetskiy, A.E., Tarasova, I.L.: The inverse problem of kinematics SM8 SEMS (In this volume)

Definition of a Rigidity of a Hexapod

A.Yu. Kuchmin and V.V. Dubarenko

Abstract One of the directions of increase of accuracy and reliability of electromechanical systems of parallel architecture, for example adaptive platforms (n-pods), application in a contour of control of the models of dynamics allowing to predict special positions (jammings) and to count optimum laws of control is. Rigidity characteristics of similar systems are a basic element of the predicting models. A research objective is development of a technique of creation of a matrix of equivalent rigidity of the adaptive platforms on the mobile basis moved with packages of actuators taking into account change of the line of operation of these actuators.

Keywords Smart electro mechanical systems · Hexapod · Control · Rigidity of a design

1 Introduction

Creation of method of calculation of matrixes of equivalent rigidity of system is an actual task which plays an important role when determining a range of own frequencies of electromechanical systems as objects of management.

Recently there was an interest in use of electromechanical systems of parallel architecture, for example n-pods, in high-precision instrument making, a robotics, adaptive antennas [1–3], etc.

A.Yu. Kuchmin (✉) · V.V. Dubarenko
Russian Academy of Sciences, Institute of Problems of Mechanical Engineering,
Moscow, Russia
e-mail: radiotelescope@yandex.ru

V.V. Dubarenko
e-mail: vladimir.dubarenko@gmail.com

In the existing Smart Electromechanical Systems (SEMS) systems on the basis of a hexapod two main configurations are used: on each platform only three points of fastening or six points are used.

Fastening of six-dot system provides the greatest accuracy of targeting as the mode of the operated jamming (statically indefinable system) is used.

The main lack of six-dot system is that the existing analogs work only in the positioning mode. Therefore it is necessary to predict special positions of system when transfer it from the positioning mode in the tracking mode that is one of problems of this work.

Rather basic point we determine coordinates of an arrangement of platforms of a hexapod, we measure the speed of the movement of a hexapod, length and speed of promotion of rods of actuators. According to these data, proceeding from mathematical model of a hexapod, necessary lengthenings and speeds of lengthening of rods of actuators and equivalent rigidity of a hexapod pay off. This information is used for forecasting of special positions of a hexapod. The design has static uncertainty, at the movement of actuators in system there can be a jamming. For its prevention the rigidity matrix is also calculated. For a hexapod there is a threshold rigidity which is specified in its technical parameters. If the calculated matrix of rigidity of system comes nearer to threshold rigidity, in system there can be a jamming for which prevention it is necessary to change the position of one of actuators.

In case of small angular movements of a platform the formula of calculation of a matrix of equivalent rigidity of system after simplification is similar to a formula for calculation of a matrix of equivalent rigidity for a package of springs [4].

When moving a platform on long distances, unlike a formula for a package of springs in a formula for adaptive platforms it is necessary to consider change of length and the line of operation of actuators.

2 Algorithm of Calculation of an Equivalent Matrix of Rigidity

The algorithm of calculation of an equivalent matrix of rigidity of similar platforms is in detail described in [4] therefore we will give only the simplified formula for calculation of a matrix of equivalent rigidity of a platform with any number of actuators:

$$\mathbf{C} = \sum_{i=1}^n \mathbf{T}_{i*} \mathbf{C}_{pi*} \mathbf{T}_{i*}^T,$$

$$\mathbf{T}_{i*} = \begin{bmatrix} \mathbf{I} & \mathbf{0} \\ \boldsymbol{\varepsilon}_1^T \langle \mathbf{r}_i \rangle \mathbf{c}_1^T & \mathbf{I} \end{bmatrix}, \quad \mathbf{C}_{pi*} = \begin{bmatrix} \bar{\mathbf{C}}_i & \mathbf{0} \\ \mathbf{0} & \mathbf{0} \end{bmatrix},$$

where \mathbf{C}_{pi^*} —symmetric matrix of coefficients of rigidity of i -th actuator of dimension 6×6 , \mathbf{I} —unity matrix with size 3×3 , \mathbf{C} —an equivalent matrix of rigidity, $\mathbf{0}$ —zero matrix with size 3×3 , $\mathbf{\varepsilon}_1$ —Euler’s matrix, \mathbf{c}_1 —a rotation matrix from the angles defining the position of a mobile platform (platform); \mathbf{r}_i —coordinates of hinges of actuators on a platform in coordinate system of (CS) of a mobile platform.

In case of small angular movements of AP expression will assume an form:

$$\mathbf{C} \approx \sum_{i=1}^n \mathbf{T}_{i^{**}} \mathbf{C}_{pi^*} \mathbf{T}_{i^{**}}^T, \quad \mathbf{T}_{i^{**}} = \begin{bmatrix} \mathbf{I} & \mathbf{0} \\ \langle \mathbf{r}_i \rangle & \mathbf{I} \end{bmatrix},$$

where the matrix \mathbf{C}_{pi^*} is as follows:

$$\mathbf{C}_{pi^*} \approx \mathbf{C}_{pi} = \begin{bmatrix} C_i \frac{\mathbf{c}_b^T \mathbf{r}_{bi} \mathbf{r}_{bi}^T \mathbf{c}_b}{l_i^2} & \mathbf{0} \\ \mathbf{0} & \mathbf{0} \end{bmatrix},$$

where C_i —rigidity of the actuator, \mathbf{r}_{bi} —coordinates of hinges of actuators on a motionless platform (basis) in system of coordinates of a motionless platform, \mathbf{c}_b —rotation matrix from the angles defining the position of a mobile platform in the initialization mode, l_i —an actuator length.

3 Algorithm of Experimental Determination of Rigidity of the Actuator

For calculation of a matrix of rigidity we use the following algorithm of finding of rigidity of the actuator of a hexapod at known equivalent rigidity C_z .

Equivalent rigidity of a hexapod in the initial position is calculated on a formula:

$$C_z = C_z^{\xi T} \sum_{i=1}^6 \mathbf{T}_i \tau_i \mathbf{T}_i^T \xi,$$

where

$$\xi = [0 \quad 0 \quad 1 \quad 0 \quad 0 \quad 0]^T, \quad \tau_i = \begin{bmatrix} \frac{\mathbf{r}_i \mathbf{r}_i^T}{l_i^2} & \mathbf{0} \\ \mathbf{0} & \mathbf{0} \end{bmatrix}_{6 \times 6}, \quad \mathbf{r}_i = \mathbf{r}_{pi} - \mathbf{r}_{oi},$$

$$\mathbf{T}_i = \begin{bmatrix} \mathbf{I} & \mathbf{0} \\ \langle \mathbf{r}_i \rangle & \mathbf{I} \end{bmatrix},$$

and C —rigidity of each actuator, $\mathbf{r}_{pi} = [x_{pi} \quad y_{pi} \quad z_{pi}]^T$ —coordinates of a point of fastening of the hinge of the actuator on a platform in CS of basis,

$\mathbf{r}_{bi} = [x_{bi} \ y_{bi} \ z_{bi}]^T$ —coordinates of a point of fastening of the hinge of the actuator on the basis in CS of basis, $\langle \mathbf{r}_i \rangle$ —matrix of a form:

$$\langle \mathbf{r}_i \rangle = \begin{bmatrix} 0 & -z_i & y_i \\ z_i & 0 & -x_i \\ -y_i & x_i & 0 \end{bmatrix}.$$

Then required rigidity is calculated on a formula:

$$C = \frac{C_z}{\xi^T \sum_{i=1}^6 \mathbf{T}_i \tau_i \mathbf{T}_i^T \xi}. \quad (1)$$

Steps of calculation:

1. To measure C_z
2. To find coordinates of points of fastening of hinges on the basis and platform
3. To calculate τ_i for each actuator
4. To calculate \mathbf{r}_{pi}^p for each actuator
5. To calculate \mathbf{T}_i for each actuator
6. To calculate rigidity according to the formula (1)

For performance of objectives methods of mathematical modeling in a Matlab Simulink package, further realization of these methods in the environment of development of Visual Studio in a programming language C are used.

4 Conclusion

Simple formulas of calculation of a matrix of equivalent rigidity of the adaptive platforms moved with packages with any number of actuators are given. It is shown that unlike a formula for a package of springs in a formula for adaptive platforms it is necessary to consider change of length and the line of operation of actuators. The algorithm is developed for calculation of partial rigidity of the actuator at a known equivalent matrix of rigidity of a hexapod.

Practical importance: the offered simple algorithms of calculation of a matrix of equivalent rigidity of an adaptive platform are effective at realization of the predicting model allowing to predict emergence of special provisions and to develop algorithms of their prevention in real time that will lead to increase in reliability of system and its resource.

References

1. Artemenko, Y.N., Gorodetskiy, A.E., Dubarenko, V.V., Kuchmin, A.Y., Tarasova, I.L.: Problems of development of space radio-telescope adaptation systems. *Informatsionno upravliaiushchie sistemy* **46**(3), 2–8 (2010). In Russian
2. Artemenko, Y.N., Agapov, V.A., Dubarenko, V.V., Kuchmin, A.Y.: Co-operative control of subdish actuators of radio-telescope. *Informatsionno-upravliaiushchie sistemy* **59**(4), 2–9 (2012). In Russian
3. Artemenko, Y.N., Gorodetskiy, A.E., Dubarenko, V.V., Doroshenko, M.C., Kuchmin, A.Y.: Data processing and data transfer problems in the local area network of a radio telescope control system. *Informatsionno upravliaiushchie sistemy* **41**(4), 2–8 (2009). In Russian
4. Yu, Kuchmin A.: Modeling of equivalent stiffness of adaptive platforms with the parallel structure executive mechanism. *Informatsionno-upravliaiushchie sistemy* **70**(3), 30–39 (2014). In Russian

Computer Modeling ACS of SEMS Actuator of Space Radio Telescope Subdish

I.L. Tarasova, A.E. Gorodetskiy and V.G. Kurbanov

Abstract In this article, we consider the layout of the subdish in the space radiotelescope Millimetron where the SEMS modules are used. The natural frequency of subdish in this construction is calculated. The results of simulation of vibration of the subdish at sudden perturbations are given. In addition, we suggest the calculation of the parameters of the Automatic Control System of the SubDish (ACS SD) with piezo-motors in use. Then, we analyze the dynamics of the ACS SD with the help of computer modeling in linear and nonlinear mathematical description of the model.

Keywords Module SEMS · Automatic control · Actuator · Subdish · Space radio telescope · Computer model · Mathematical model · Dynamics · The natural frequency

1 Introduction

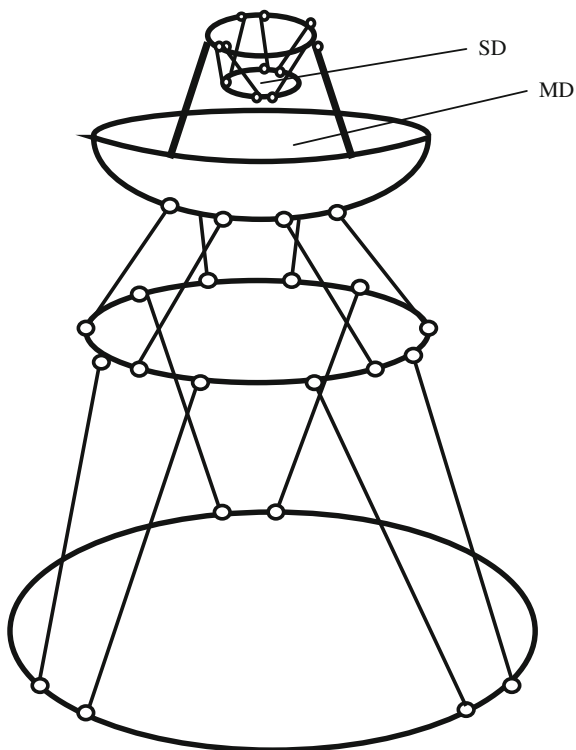
SEMS of space telescope subdish must move it along three linear (x , y and z) and two angular (β and θ) coordinates, where β —rotation about the x -axis, and θ —rotation about the y axis. Subdish designed to track changes in the direction of the received electromagnetic radiation caused by the pointing error and a secondary focus position caused by errors in the profiles of the reflective surfaces of the lobes of the main radio telescope dish. For this subdish sets on mobile platforms of the

I.L. Tarasova (✉) · A.E. Gorodetskiy · V.G. Kurbanov
Institute of Problems of Mechanical Engineering, Russian Academy of Sciences,
Saint-Petersburg, Russia
e-mail: g17265@yandex.ru

A.E. Gorodetskiy
e-mail: g27764@yandex.ru

V.G. Kurbanov
e-mail: vugar_borchali@yahoo.com

Fig. 1 The scheme of installation of the telescope dish



hexapod, that is moved by six actuators (see Fig. 1). Each actuator consists of a rod with a piezoelectric motor that allows to change the length of the rod. The rod is connected to a mobile platform and a fixed platform base with two two-stage joints or springs that allow pushers rotate freely on two corners. The base via respective fixed rod fastened to the structure of the main dish [1].

2 Simulation of Subdish Natural Oscillations

Calculation of subdish natural frequency hold for the approximate subdish model of the telescope “Millimetron” [2]. Subdish parameters of the space radio telescope “Millimetron” as follows:

- The surface shape: a hyperboloid = $(-1.14995818/-1.1472777)$
- Material subdish: silicon carbide
- Coated aluminum,
- Support material: carbon fiber

- Diameter subdish $D_k = 0.5/0.6$ m,
- Height subdish $H_k = 0.1213/0.1544$ m
- Corner Radius subdish $R_k = 0.364$ m,
- Density of the material subdish $\rho_k = (3.2-3.27) 103$ kg/m³,
- Young's modulus $E_k = (400-500)$ Gpa
- Density of the material supports $\rho_o = (1.55-1.62) 103$ kg/m³,
- Young's modulus supports $E_o = 280$ GPa,
- The accuracy of the surface subdish $\Delta = 3$ mm,
- Temperature coefficient subdish $\alpha_k = 0.04 \times 10^{-6}$ 1/K
- Temperature coefficient supports $\alpha_o = 0.1 \times 10^{-6}$ 1/K,
- Thickness subdish $h_k = 4$ mm with ribs 8 mm
- Weight subdish $m_k = 6.4$ kg,
- Weight hexapod $m_g = 12$ kg,
- Weight of the upper platform hexapod $m_p = 4$ kg,
- Hexapod leg radius $R_g = 0.01$ m,
- The length of the leg hexapod $l_g = 0.27$ m,
- The diameter of the base hexapod $D_{go} = 0.348$ m
- The diameter of the upper platform hexapod $D_{gp} = 0.25$ m

The simplest estimate the frequency of natural oscillations subdish can be defined as:

$$f_0 = \frac{1}{2\pi} \sqrt{\frac{C}{M}}, \tag{1}$$

where: $M = m_k + m_p$, $C = 6 C_g$, $C_g = (E_o \pi R_g^2)/R_p$

Suppose that:

$$R_p = 0.7 D_{gp} = 0.7 * 0.25 = 0.175 \text{ m}; C_g = (2.8 \times 10^{11} * 3.14 \times 10^{-4})/0.175 = 5 \times 10^8 \text{ N/m};$$

$$C = 6 * 5 \times 10^8 = 3 \times 10^9 \text{ N/m}.$$

Then

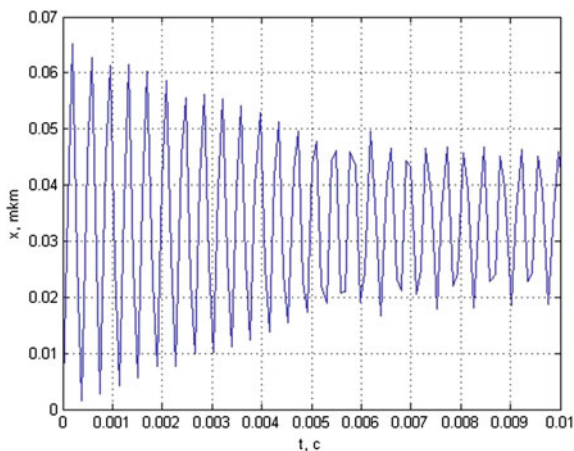
$$f_0 = \frac{1}{6.28} \sqrt{\frac{3 * 10^9}{6.4 + 4}} = 2700 \text{ Gz} \quad \text{and} \quad T = 1/2\pi f_0 = 1/6.28 * 2.7 \times 10^3$$

$$= 6 \times 10^{-5} \text{ s}$$

Modeling vibrations subdish hold after a sudden exposure to a force $F = 100$ N. This vibrations will be simplistically described by the equation:

$$M \ddot{x} = -Cx - r \dot{x} + F \tag{2}$$

Fig. 2 Type of oscillation model subdish at $\lambda = 0.01$



The latter equation using the Laplace transform can be written as follows:

$$x = kF/(T^2p^2 + 2\lambda Tp + 1), \quad (3)$$

where: $k = 1/C = 1/3 * 10^9 = 3.3 * 10^{-10} \text{ m/N} = 3.3 * 10^{-4} \text{ }\mu\text{m/N}$, $\lambda = (0.01-0.05)$

Consider two models:

(1) $\lambda = 0.01$, $2\lambda T = 0.02 * 6 * 10^{-5} = 1.2 * 10^{-6}$, $T^2 = 6 * 6 * 10^{-10} = 3.6 * 10^{-9}$

Then:

$$\begin{aligned} x &= (3.3 * 10^{-4} * 100) / (3.6 * 10^{-9}p^2 + 1.2 * 10^{-6}p + 1) \\ &= 3.3 * 10^{-2} / (3.6 * 10^{-9}p^2 + 1.2 * 10^{-6}p + 1) \end{aligned}$$

At the same time the vibrations are eliminated as shown in Fig. 2

(2) $\lambda = 0.05$, $2\lambda T = 0.1 * 6 * 10^{-5} = 6 * 10^{-6}$,

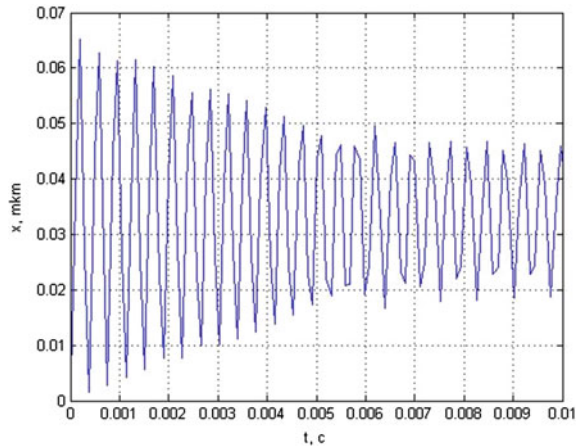
Then:

$$\begin{aligned} x &= (3.3 * 10^{-4} * 100) / (3.6 * 10^{-9}p^2 + 6 * 10^{-6}p + 1) \\ &= 3.3 * 10^{-2} / (3.6 * 10^{-9}p^2 + 6 * 10^{-6}p + 1) \end{aligned}$$

At the same time the vibrations are eliminated as shown in Fig. 3

These transients suggests that the force $F = 100 \text{ N}$ applied by the hexapod actuator is hardly damped oscillations subdish with an amplitude in hundredths of a micron.

Fig. 3 Type of oscillation model subdish at $\lambda = 0.05$



3 Calculation of the ACS

Obviously, the force F acting on the subdish creates a motor actuators. Such motors are usually controlled by PID. Moreover, for precise positioning subdish expedient to use piezomotors [3]. In this case, the transition process should be built within the parameters of the motor and controller.

Piezomotor linear mathematical model is:

$$dF_3/dt = (K_0/C_0R_{BT})e_y - (1/C_0R_{BT})F_3 - (K_0K_{\Pi}/C_0)v \quad (4)$$

$$dv/dt = (1/m_{\Sigma})F_3 - ((K_y + K_{\kappa})/im_{\Sigma})x - (K_{\Delta}/m_{\Sigma})v \quad (5)$$

$$dx/dt = iv \quad (6)$$

where: F_3 —force developed piezomotor, e_y —EMF control, v —speed, x —moving, m_{Σ} —mass to be moved, i —reduction coefficient, R_{BT} —the internal resistance of the source of EMF, C_0 —the capacity of the piezoelectric element, K_{Π} —coefficient of direct piezoelectric effect, K_0 —coefficient the inverse piezoelectric effect, K_y —piezo coefficient of elasticity, K_{κ} —coefficient structural rigidity, K_{Δ} —damping coefficient.

Applying Eqs. (4)–(6) the Laplace transform, it is possible to receive a block diagram shown in Fig. 4

Let hexapod actuator used piezomotor, educational force $F_3 = 25$ N, under control EMF $e_y = 100$ V, with maximum movement $x = \pm 25$ mm and speed $v = 50$ mm/s. Weight rod actuator $m_a = 0.6$ kg

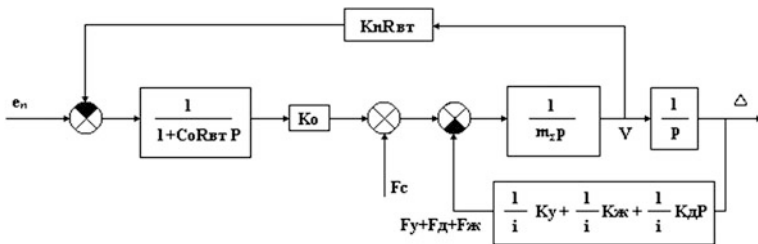


Fig. 4 Structure piezomotor

Then:

$$K_0 = K_{\Pi} = F_y / e_y = 25 / 100 = 0.25 \text{ N/V}$$

$$K_{\Pi} R_{BT} = e_y / v = 100 / 50 = 2 \text{ V s/mm}$$

$$R_{BT} = 2 / 0.25 = 8 \text{ } \Omega$$

The capacity of the piezoelectric element $C_0 = (\epsilon_0 \chi S_0 - S_0 d_p^2 Y) / l_0$, where: $\epsilon_0 = 8.85 \times 10^{-12} \text{ F/m}$ —electric constant, $Y = 5.5 \times 10^{10} \text{ Pa}$ —Young’s modulus of piezo, $d_p = 470 \times 10^{-12} \text{ C/N}$, $d_p = 470 \times 10^{-12} \text{ C/N}$ —piezomodulus, $\chi = 3200$ —dynamic susceptibility piezo, $l_0 = 0.1 \text{ m}$ —the length of the piezoelectric element, $S_0 = \pi r_0^2 = 10^{-4} \text{ m}^2$ —sectional area of the piezoelectric element.

Then:

$$C_0 = 10 * 8.85 * 10^{-12} * 3.2 * 10^3 * 10^{-4} - \dots * 10 * 10^{-4} * 4.7 * 10^{-10} * 4.7 * 10^{-10} * 5.5 * 10^{10} = 10^{-11} \text{ F}$$

$$T_3 = R_{BT} C_0 = 8 * 10^{-11} \text{ s}$$

The equivalent rigidity $K_c = K_y / i + K_{ж} / i = F_y / x = 25 / 50 = 0.5 \text{ N/mm}$

$$K_{д} / i = r = 2 \lambda C / 2 \pi f_0 = (0.02 * 3 * 10^6) / (6.28 * 2.7 * 10^3) = 3.5 \text{ N s/mm}$$

Mass to be moved $m_{\Sigma} = M + m_a = 10.4 + 0.6 = 11 \text{ kg}$

Let $F_c = 0$ or taken into account in the coefficient K_c . Then, a block diagram of the automatic control system (ACS) movement of the actuator rod using piezomotor in the linear approximation can be represented as shown in Fig. 5.

PID controller used in such ACS has a transfer function of the form:

$$W_p = (k_3 p^2 + k_1 p + k_2) / p. \tag{7}$$

The coefficient k_2 selected according to the required accuracy SAU δ_{ω} at a predetermined input frequency ω , and the coefficients k_1 and k_3 —based on the dynamic properties of the control object.

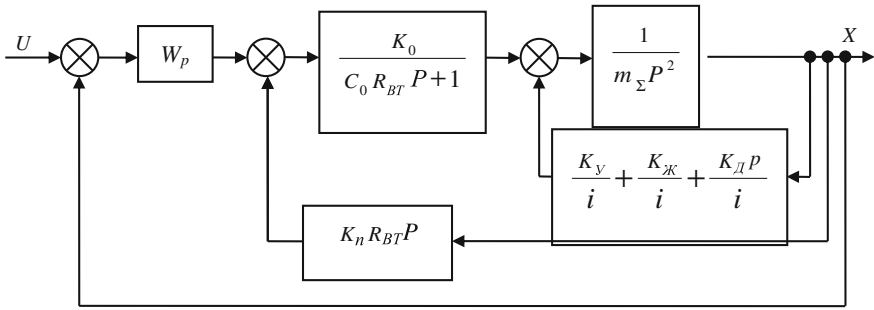


Fig. 5 Block diagram of ACS

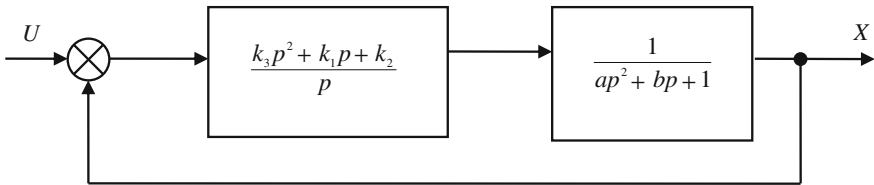


Fig. 6 Transformed block diagram of ACS

Making the internal circuits in the circuit block diagram in Fig. 5, we obtain the block diagram shown in Fig. 6

The transfer function of the control object W_{oy} obtained as follows:

$$W_1 = 1/m_\Sigma p^2 \quad (6), \quad W_2 = K_y/i + K_{\text{ж}}/i + K_{\text{д}} p/i, \quad (8)$$

$$W_3 = K_0/(C_0 R_{BT} P + 1), \quad (9)$$

$$W_4 = K_{\text{И}} R_{BT} P, \quad (10)$$

$$W_5 = W_1/(1 + W_1 W_2), \quad (11)$$

$$W_6 = W_3 * W_5, \quad (12)$$

$$W_{oy} = W_6/(1 + W_4 W_6) \quad (13)$$

Substituting the above parameters into the control object in Eqs. (8)–(13) and neglecting the magnitude

$C_0 R_{BT} P = 8 \times 10^{-11} p$ in Eq. (9), we obtain:

$$W_1 = 1/11p^2, W_2 = 0.5 + 3.5 p, W_3 = 0.25, W_4 = 2p,$$

$$W_5 = 2/(22p^2 + 7p + 1), W_6 = 0.5/(22p^2 + 7p + 1),$$

Hence the transfer function will piezomotor:

$$W_{oy} = 1/(ap^2 + bp + 1) = 1/(22p^2 + 9p + 1) \tag{14}$$

To calculate the parameters of the PID controller is necessary to find the coefficients k_1, k_2, k_3 in the transfer function of the PID controller (7)

First, let's ask a positioning accuracy of the actuator rod $\delta_\omega = 2 \mu\text{m}$. It corresponds to the desired positioning accuracy subdish a frequency change of the input signal $\omega = 0.1 \text{ s}^{-1}$. Then we obtain the required gain at this frequency $K_\omega = x/\delta_\omega = 50/2 \times 10^{-3} = 2.5 \times 10^4$. Now, if we assume that $k_3/k_2 = 22$ and $k_1/k_2 = 9$, we obtain the transfer function of the open-ACS $W = W_p * W_{oy} = k_2/p$. Therefore, when $\omega = 1/p = 0.1 \text{ s}^{-1}$, we obtain: $0.1 k_2 = 2.5 \times 10^4$ and correspondingly $k_2 = 2.5 \times 10^3$. Now we can calculate the other parameters of the PID controller: $k_3 = 22 * 2.5 \times 10^3 = 5.5 \times 10^4, k_1 = 9 * 2.5 \times 10^3 = 2.25 \times 10^4$.

4 Analysis of the Dynamics of the Automatic Control System

The analysis will be carried out using computer modeling of ACS with a block diagram shown in Fig. 7.

First, we assume that the parameters of the PID controller exactly correspond to the parameters control object: $k_1 = 2.25 \times 10^4, k_2 = 2.5 \times 10^3$ и $k_3 = 5.5 \times 10^4$.

In this case, when applied to the input of ACS exposure step transition process will have the form shown in Fig. 8

To test the robustness of ACS were simulated transients setting up controller with an error of +20 % (see Fig. 9) and an error -20 % (see Fig. 10)

As can be seen from Figs. 9 and 10 required a smooth transition process, in both cases remains, indicating that the high robustness of the simulated control system subdish actuator.

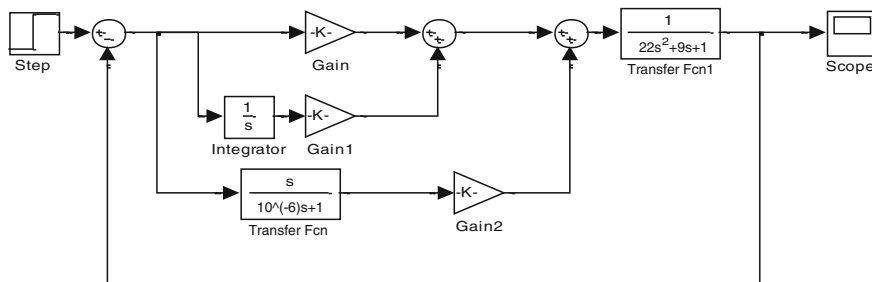


Fig. 7 Model ACS

Fig. 8 The transition process control system at the ideal setting PID controller

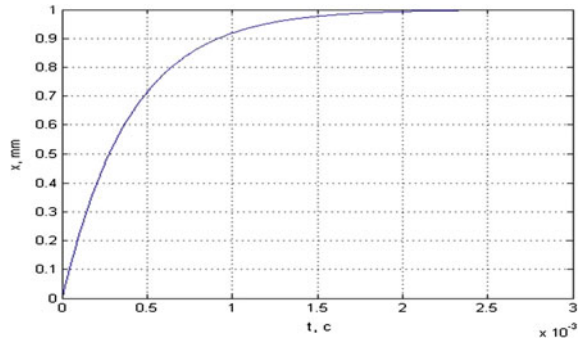


Fig. 9 The transition process in the ACS is not accurate (error + 20 %) setting PID controller

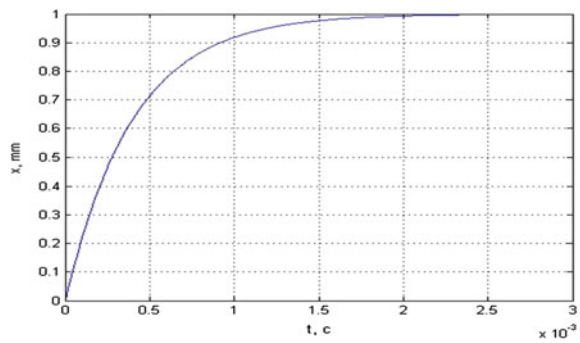
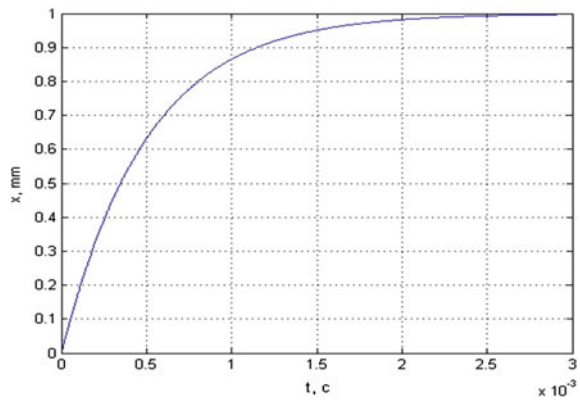


Fig. 10 The transition process in the ACS is not accurate (error -20 %) setting PID controller



5 Accounting for Non-linearities in the Automatic Control System of Actuator

Assume that the actuator hinge has a clearance of 20 μm . For the transition process in the control system with the backlash it is necessary to introduce the model to the output of the respective unit (see Fig. 11).

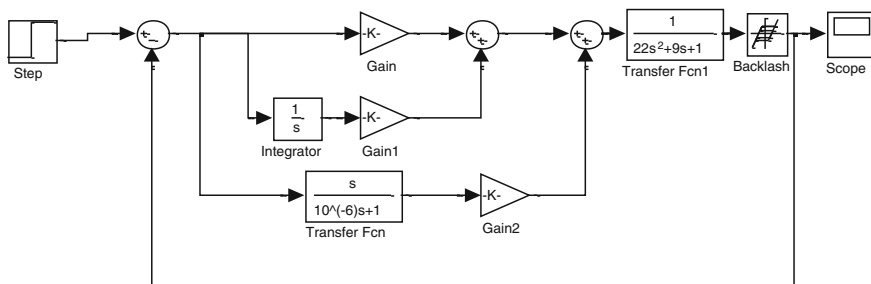
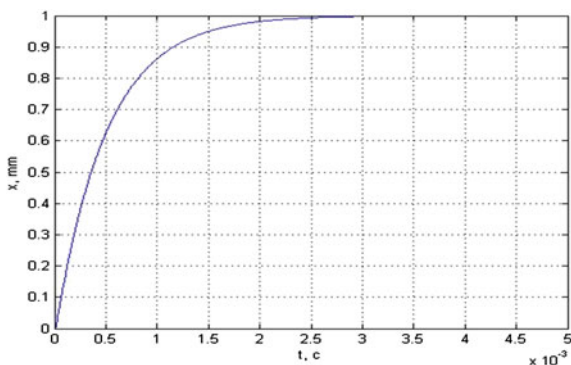


Fig. 11 Nonlinear model of ACS with backlash

Fig. 12 The transition process in the ACS with backlash



The resulting transition process in such a model is shown in Fig. 12. As the figure shows the process is aperiodic, but a little longer for the transition process. This indicates a decrease in the gain in the control loop, which corresponds to the theory of nonlinear control systems.

Now, further take into account the dead zone in the feedback sensor value of 10 microns. For the transition process in the control system with a dead zone and backlash it is necessary to enter the previous model in the feedback corresponding to the unit (see Fig. 13).

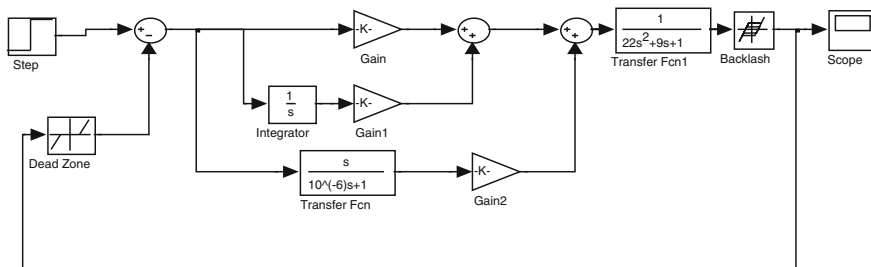


Fig. 13 Nonlinear model of ACS with backlash and dead zone

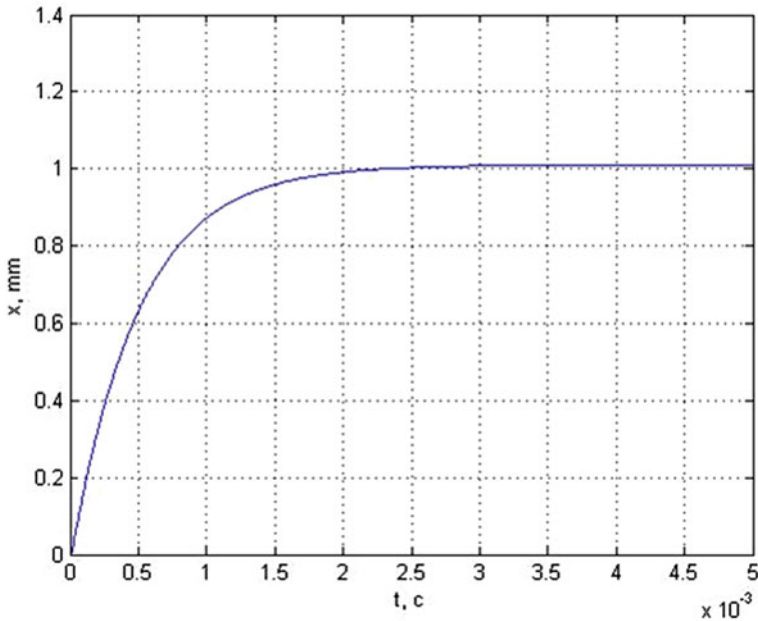


Fig. 14 The transition process in the ACS with backlash and dead zone

The resulting transition process in such a model is shown in Fig. 14.

As can be seen from Fig. 14 is an aperiodic process, but with the static error, equal to the dead zone, which corresponds to the theory of nonlinear control systems.

6 Conclusion

On impact on uncontrollable Space radiotelescope subdish may arise weakly damped oscillations with a small amplitude. However, the automatic control system SEMS subdish after a sudden change in the control voltage transients will be smooth and without overshoot. In this transient time will be in the range 1.5–3 ms. Therefore, when analyzing the behavior of controlled subdish of space radio telescope with SEMS in most cases can be ignored the inertia of the legs and platforms of SEMS.

References

1. Artemenko, Y.N.(RU), Gorodetsky, A.E.(RU), Dubarenko, V.V.(RU), Kuchmin, A.J.(RU), Agapov, V.A.(RU): Analysis of the dynamics of actuators automatic control systems of space radio telescope subdish. *Informatsionno-upravliaiushchie sistemy* **6**, 2–5 (2011) (In Russian)
2. http://www.strf.ru/material.aspx?CatalogId=222&d_no=43273#.VaUKxL9O7cs
3. Gorodetskiy, A.E.(RU), Artemenko, J.N.(RU), Dubarenko, V.V.(RU), Tarasova, I.L.(RU), Kuchmin, A.J.(RU): Problems of creation of systems of adaptation of space radio telescopes. *Informatsionno-upravliaiushchie sistemy* **3**(46), 2–8 (2010) (In Russian)

Features of Manipulator Dynamics Modeling into Account a Movable Platform

Yu.N. Artemenko, A.P. Karpenko and P.P. Belonozhko

Abstract The short review of a current state and the analysis of tendencies of development of objects of perspective space infrastructure are given in this article. The conclusion about the potential constructive variety of perspective robotic systems of space purpose determined by complexity and heterogeneity of the tasks demanding automation is drawn. Relevance of modeling of dynamics of the systems equipped with manipulators is shown and feature of dynamics of systems as “mobile basis—handling mechanism—payload” is emphasized. The approach to modeling of such systems based on a combination of traditional methods of analytical mechanics and opportunities of modern computer tools is substantiated. It can be used to explore qualitative features of dynamics when designing systems of the considered class.

Keywords Manipulator dynamics modeling · Movable platform · Model task · Independent equation of relative motion dynamics

1 Introduction

Among the future tasks to be automated by robotic means, we must first identify the problem of space objects orbital assembly. Which includes a mounted construction parts transportation to the place of assembly and assembly operations automation.

Yu.N. Artemenko (✉)

Lebedev Physical Institute of Russian Academy of Sciences,
Astro Space Center, Moscow, Russia
e-mail: artemenko.akc@yandex.ru

A.P. Karpenko · P.P. Belonozhko

Bauman Moscow State Technical University, Moscow, Russia
e-mail: apkarpenko@mail.ru

P.P. Belonozhko

e-mail: byelonozhko@mail.ru

We will also point out the problem of orbital service that combines the tasks of inspection of technical condition serviced space objects, robotic support for human activities in outer space, the replacement of functional blocks spacecraft refueling satellites in orbit, the spacecraft moving within the orbit and between the orbits and space debris cleaning. The heterogeneity of these tasks implies an applying of different SEMS designs of robotic devices. In this case the space manipulator is the most important component of many robotic systems for space purposes, and the mobility of the platform are the important feature for natural space environment which requires accounting for dynamics modeling for the wide class systems [1].

It's expedient to define a class of mutual positioning of space vehicle and paying load systems. The reason is an existence of characteristic features of controlled movement dynamics of such systems [2–5]. Existing transport system of payload transference over the orbital spacecraft using an anthropomorphic manipulator or promising systems of payload high-accuracy positioning using parallel structured manipulation mechanism controlled by it's degrees of freedom.

These systems' research is notable for follow feature. It's necessary to analyze properly space conditions-specific movement modes using the results of modeling without any possibility to confirm them by a above ground experiment. Model tasks play a large part in such kinds of research. Only elements, which are more essential for analysis of the study processes, are defined in these problems [3–5].

In particular, in the context of the synthesis of the load position (motion) relative to a mobile platform, an independent subsystem of differential equations regarding the generalized coordinates corresponding to controllable degrees of mobility of a manipulator is suitable. For distinct modes of motion it is possible to appoint such a subsystem by the elimination of coordinates of the platform position in an inertia space, connected with one of the system bodies (for example, with a mobile platform)—the six generalized coordinates in a general case.

The paper considers characteristic features of controlled motion of space system “movable platform—manipulator—payload”, which moves in inertial space under the action of the hinged control in conditions free of external forces.

2 Model Task

Let us consider the abovementioned special features for deriving independent dynamical equations relative motion using a plane two-link mechanism on a movable platform as an example, a mechanical design model of which is shown in Fig. 1.

System of two bodies of masses m_1 and m_2 connected via a massless two-link mechanism C_1AC_2 can move freely in the plane XOY (Fig. 1). Links C_1A and AC_2 are connected at the point A . It is suggested that the motion of bodies relative to adjacent links (immovable fixing) is not carried out. The joint A is an ideal one-degree revolute pair. The joint axis is perpendicular to the motion plane

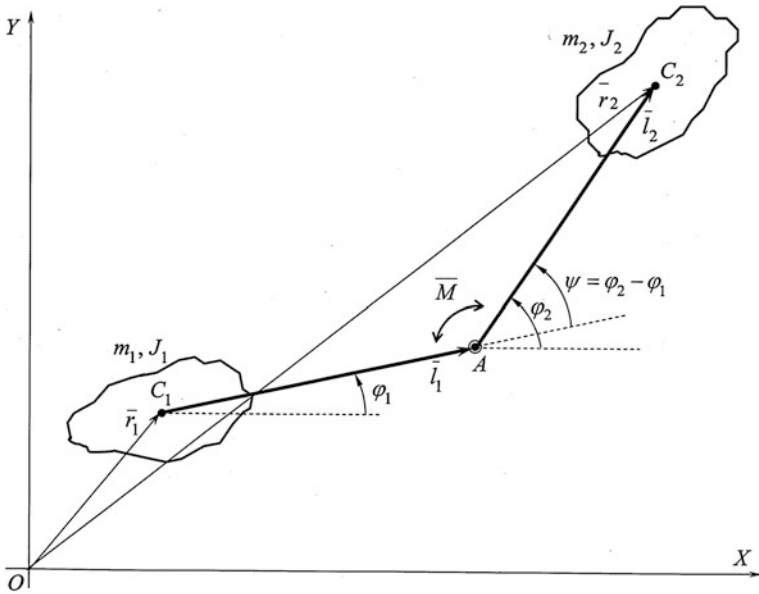


Fig. 1 Design model of a plane two-link mechanism on a movable platform

(pattern plane). C_1 and C_2 are centers of mass of the bodies moving in the pattern plane.

Angular positions of links C_1A and AC_2 in the frame of axis XOY are characterized by the angles ϕ_1 and ϕ_2 , respectively, measured from the horizontal axis in a positive direction counter-clockwise (Fig. 1). Figure 1 illustrates:

J_1, J_2 —bodies mass moments of inertia defined with respect to axes passing through centers of mass C_1 and C_2 perpendicular to the motion plane, respectively;

\bar{M} —control torques in the joint;

\bar{r}_1 and \bar{r}_2 —bodies radii-vectors of centers of mass;

\bar{l}_1, \bar{l}_2 —vectors directed from the center of mass of the first body to the joint and from the joint to the center of mass of the second body, respectively.

Also designate:

x_1, y_1 —coordinates of the vector \bar{r}_1 ;

x_2, y_2 —coordinates of the vector \bar{r}_2 ;

$l_1 = |\bar{l}_1|, l_2 = |\bar{l}_2|$ —lengths of links;

M —projection of the vector \bar{M} on the axis OZ completing system XOY to right-hand coordinate. The system of reference XYZ is presumed to be inertial. The moment \bar{M} increasing the angle $\psi = \phi_2 - \phi_1$, i.e., an increase in the angle ϕ_2 and a decrease in the angle ϕ_1 , will be considered to be positive.

3 Selection of Independent Equation of Relative Motion Dynamics by the Virgin System of Differential Equation Rearrangement

The x_1 , y_1 , ϕ_1 and ϕ_2 are considered as independent generalized coordinates. A kinetic energy as a function of independent generalized velocities \dot{x}_1 , \dot{y}_1 , $\dot{\phi}_1$, $\dot{\phi}_2$ and coordinates ϕ_1 , ϕ_2 are then expressed as:

$$\begin{aligned}
 T = & \frac{1}{2}m_1\dot{x}_1^2 + \frac{1}{2}m_1\dot{y}_1^2 + \frac{1}{2}J_1\dot{\phi}_1^2 + \frac{1}{2}m_2\dot{x}_1^2 - m_2\dot{x}_1\dot{\phi}_1l_1\sin\phi_1 \\
 & - m_2\dot{x}_1\dot{\phi}_2l_2\sin\phi_2 + \frac{1}{2}m_2\dot{\phi}_1^2l_1^2 + m_2\dot{\phi}_1\dot{\phi}_2l_1l_2\sin\phi_1\sin\phi_2 \\
 & + \frac{1}{2}m_2\dot{\phi}_2^2l_2^2 + \frac{1}{2}m_2\dot{y}_1^2 + m_2\dot{y}_1\dot{\phi}_1l_1\cos\phi_1 \\
 & + m_2\dot{y}_1\dot{\phi}_2l_2\cos\phi_2 + m_2\dot{\phi}_1\dot{\phi}_2l_1l_2\cos\phi_1\cos\phi_2 + \frac{1}{2}J_2\dot{\phi}_2^2,
 \end{aligned} \tag{1}$$

and the Lagrange's equations

$$\begin{aligned}
 \frac{d}{dt}\left(\frac{\partial T}{\partial \dot{x}_1}\right) - \frac{\partial T}{\partial x_1} &= Q_{x_1}, \\
 \frac{d}{dt}\left(\frac{\partial T}{\partial \dot{y}_1}\right) - \frac{\partial T}{\partial y_1} &= Q_{y_1}, \\
 \frac{d}{dt}\left(\frac{\partial T}{\partial \dot{\phi}_1}\right) - \frac{\partial T}{\partial \phi_1} &= Q_{\phi_1}, \\
 \frac{d}{dt}\left(\frac{\partial T}{\partial \dot{\phi}_2}\right) - \frac{\partial T}{\partial \phi_2} &= Q_{\phi_2},
 \end{aligned} \tag{2}$$

after substitution of (1) into (2) are expressed as:

$$\begin{aligned}
 m_1\ddot{x}_1 + m_2\ddot{x}_1 - m_2\ddot{\phi}_1l_1\sin\phi_1 - m_2\dot{\phi}_1^2l_1\cos\phi_1 \\
 - m_2\ddot{\phi}_2l_2\sin\phi_2 - m_2\dot{\phi}_2^2l_2\cos\phi_2 = Q_{x_1},
 \end{aligned} \tag{3}$$

$$\begin{aligned}
 m_1\ddot{y}_1 + m_2\ddot{y}_1 + m_2\ddot{\phi}_1l_1\cos\phi_1 - m_2\dot{\phi}_1^2l_1\sin\phi_1 \\
 + m_2\ddot{\phi}_2l_2\cos\phi_2 - m_2\dot{\phi}_2^2l_2\sin\phi_2 = Q_{y_1},
 \end{aligned} \tag{4}$$

$$\begin{aligned}
 - m_2\ddot{x}_1l_1\sin\phi_1 + m_2\ddot{y}_1l_1\cos\phi_1 \\
 + J_1\ddot{\phi}_1 + m_2\dot{\phi}_1^2l_1^2 + m_2\ddot{\phi}_2l_1l_2\sin\phi_1\sin\phi_2 + m_2\dot{\phi}_2^2l_1l_2\sin\phi_1\cos\phi_2 \\
 + m_2\ddot{\phi}_2l_1l_2\cos\phi_1\cos\phi_2 - m_2\dot{\phi}_2^2l_1l_2\cos\phi_1\sin\phi_2 = Q_{\phi_1},
 \end{aligned} \tag{5}$$

$$\begin{aligned}
& -m_2\ddot{x}_1 l_2 \sin \phi_2 + m_2\ddot{y}_1 l_2 \cos \phi_2 \\
& + J_2\ddot{\phi}_2 + m_2\dot{\phi}_2^2 l_2^2 + m_2\ddot{\phi}_1 l_1 l_2 \sin \phi_1 \sin \phi_2 + m_2\dot{\phi}_1^2 l_1 l_2 \cos \phi_1 \sin \phi_2 \\
& + m_2\ddot{\phi}_1 l_1 l_2 \cos \phi_1 \cos \phi_2 - m_2\dot{\phi}_1^2 l_1 l_2 \sin \phi_1 \cos \phi_2 = Q_{\phi_2}.
\end{aligned} \tag{6}$$

where Q_{x_1} , Q_{y_1} , Q_{ϕ_1} и Q_{ϕ_2} —are generalized forces. We point out that Q_{x_1} and Q_{y_1} by definition of generalized forces, accomplish work based on translational displacement of “harden” system along abscissa axis ($\delta x_1 \neq 0$, $\delta y_1 = 0$, $\delta \phi_1 = 0$, $\delta \phi_2 = 0$) and ordinate axis ($\delta x_1 = 0$, $\delta y_1 \neq 0$, $\delta \phi_1 = 0$, $\delta \phi_2 = 0$) accordingly, i.e. they are projections of outside forces applied to system resultant on a co-ordinates axis XOY . Equations (3) и (4) are equations of considering system center of mass C motion with coordinates x_C , y_C in XOY , determined by relationships:

$$\begin{aligned}
(m_1 + m_2)x_C &= m_1 x_1 + m_2 x_2, \\
(m_1 + m_2)y_C &= m_1 y_1 + m_2 y_2.
\end{aligned} \tag{7}$$

After re-arrangement of system (3)–(6) we may easy separate an independent subsystem of differential equations describing rotational body motion for arbitrary set of applied forces

$$\begin{aligned}
& \ddot{\phi}_1 (J_1 + \tilde{m}l_1^2) + \ddot{\phi}_2 \tilde{m}l_1 l_2 (\sin \phi_1 \sin \phi_2 + \cos \phi_1 \cos \phi_2) \\
& + \dot{\phi}_2^2 \tilde{m}l_1 l_2 (\sin \phi_1 \cos \phi_2 - \cos \phi_1 \sin \phi_2) \\
& = Q_{\phi_1} + l_1 \frac{m_2}{m_1 + m_2} (Q_{x_1} \sin \phi_1 - Q_{y_1} \cos \phi_1),
\end{aligned} \tag{8}$$

$$\begin{aligned}
& \ddot{\phi}_1 \tilde{m}l_1 l_2 (\sin \phi_1 \sin \phi_2 + \cos \phi_1 \cos \phi_2) \\
& + \ddot{\phi}_2 (J_2 + \tilde{m}l_2^2) + \dot{\phi}_1^2 \tilde{m}l_1 l_2 (\cos \phi_1 \sin \phi_2 - \sin \phi_1 \cos \phi_2) \\
& = Q_{\phi_2} + l_2 \frac{m_2}{m_1 + m_2} (Q_{x_1} \sin \phi_2 - Q_{y_1} \cos \phi_2),
\end{aligned} \tag{9}$$

where $\tilde{m} = \frac{m_1 m_2}{m_1 + m_2}$.

For conditions under consideration we have:

$$Q_{x_1} = 0, \tag{10}$$

$$Q_{y_1} = 0, \tag{11}$$

$$Q_{\phi_1} = -M, \tag{12}$$

$$Q_{\phi_2} = M. \tag{13}$$

Subject to (10)–(13) the system of Eq. (2) should become:

$$\begin{aligned} m_1\ddot{x}_1 + m_2\ddot{x}_1 - m_2\ddot{\phi}_1 l_1 \sin \phi_1 - m_2\dot{\phi}_1^2 l_1 \cos \phi_1 \\ - m_2\ddot{\phi}_2 l_2 \sin \phi_2 - m_2\dot{\phi}_2^2 l_2 \cos \phi_2 = 0, \end{aligned} \quad (14)$$

$$\begin{aligned} m_1\ddot{y}_1 + m_2\ddot{y}_1 + m_2\ddot{\phi}_1 l_1 \cos \phi_1 - m_2\dot{\phi}_1^2 l_1 \sin \phi_1 \\ + m_2\ddot{\phi}_2 l_2 \cos \phi_2 - m_2\dot{\phi}_2^2 l_2 \sin \phi_2 = 0, \end{aligned} \quad (15)$$

$$\begin{aligned} - m_2\ddot{x}_1 l_1 \sin \phi_1 + m_2\ddot{y}_1 l_1 \cos \phi_1 \\ + J_1\ddot{\phi}_1 + m_2\dot{\phi}_1 l_1^2 + m_2\ddot{\phi}_2 l_1 l_2 \sin \phi_1 \sin \phi_2 + m_2\dot{\phi}_2^2 l_1 l_2 \sin \phi_1 \cos \phi_2 \\ + m_2\ddot{\phi}_2 l_1 l_2 \cos \phi_1 \cos \phi_2 - m_2\dot{\phi}_2^2 l_1 l_2 \cos \phi_1 \sin \phi_2 = -M, \end{aligned} \quad (16)$$

$$\begin{aligned} - m_2\ddot{x}_1 l_2 \sin \phi_2 + m_2\ddot{y}_1 l_2 \cos \phi_2 \\ + J_2\ddot{\phi}_2 + m_2\dot{\phi}_2 l_2^2 + m_2\ddot{\phi}_1 l_1 l_2 \sin \phi_1 \sin \phi_2 + m_2\dot{\phi}_1^2 l_1 l_2 \cos \phi_1 \sin \phi_2 \\ + m_2\ddot{\phi}_1 l_1 l_2 \cos \phi_1 \cos \phi_2 - m_2\dot{\phi}_1^2 l_1 l_2 \sin \phi_1 \cos \phi_2 = M. \end{aligned} \quad (17)$$

The following first integrals of the system (14)–(17) may be write down:

$$m_1\dot{x}_1 + m_2\dot{x}_1 - m_2 l_1 \dot{\phi}_1 \sin \phi_1 - m_2 l_2 \dot{\phi}_2 \sin \phi_2 = 0, \quad (18)$$

$$m_1\dot{y}_1 + m_2\dot{y}_1 + m_2 l_1 \dot{\phi}_1 \cos \phi_1 + m_2 l_2 \dot{\phi}_2 \cos \phi_2 = 0. \quad (19)$$

The expressions (18) and (19) can be easily received using immediate integration of the (14) and (15). Nulling of integration constants corresponds with a case of location of the inertial coordinate system origin in the center of mass of the system ($x_C = 0$, $y_C = 0$).

Substituting (10)–(13) in (8) and (9) and going from generalized coordinates ϕ_1 and ϕ_2 to generalized coordinates ϕ_1 и $\psi = \phi_2 - \phi_1$, we receive:

$$\begin{aligned} \ddot{\phi}_1 (J_1 + l_1^2 \tilde{m} + l_1 l_2 \tilde{m} \cos \psi) + \ddot{\psi} l_1 l_2 \tilde{m} \cos \psi - \dot{\phi}_1^2 l_1 l_2 \tilde{m} \sin \psi \\ - 2\dot{\phi}_1 \dot{\psi} l_1 l_2 \tilde{m} \sin \psi - \dot{\psi}^2 l_1 l_2 \tilde{m} \sin \psi = -M, \end{aligned} \quad (20)$$

$$\ddot{\phi}_1 (J_2 + l_2^2 \tilde{m} + l_1 l_2 \tilde{m} \cos \psi) + \ddot{\psi} (J_2 + l_2^2 \tilde{m}) + \dot{\phi}_1^2 l_1 l_2 \tilde{m} \sin \psi = M. \quad (21)$$

The expression

$$\begin{aligned} \dot{\phi}_1 (J_1 + J_2 + \tilde{m} l_1^2 + \tilde{m} l_2^2 + 2\tilde{m} l_1 l_2 \cos \psi) \\ + \dot{\psi} (J_2 + \tilde{m} l_2^2 + \tilde{m} l_1 l_2 \cos \psi) = L \end{aligned} \quad (22)$$

is the first integral of the system (20)–(21), and therefore of the system (14)–(17) in going from generalized coordinates ϕ_1 and ϕ_2 to generalized coordinates ϕ_1 and ψ

(we may certain of it using immediate substitution). L —is a constant of integration determined by initial conditions $\dot{\phi}_1^{(0)}$, $\dot{\psi}^{(0)}$ и $\psi^{(0)}$:

$$\begin{aligned} &\dot{\phi}_1^{(0)} \left(J_1 + J_2 + \tilde{m}l_1^2 + \tilde{m}l_2^2 + 2\tilde{m}l_1l_2 \cos \psi^{(0)} \right) \\ &+ \dot{\psi}^{(0)} \left(J_2 + \tilde{m}l_2^2 + \tilde{m}l_1l_2 \cos \psi^{(0)} \right) = L \end{aligned} \tag{23}$$

Using of the first integrals (18), (19) and (22) permits to decrease the order of the system of Eqs. (14)–(17) selecting an independent equation of a relative motion (motion of payload about movable platform):

$$\begin{aligned} &\ddot{\psi} \frac{\alpha_1 \alpha_2 - \beta^2 \cos^2 \psi}{\alpha_1 + \alpha_2 + 2\beta \cos \psi} + \dot{\psi}^2 \frac{\beta \sin \psi (\alpha_1 + \beta \cos \psi) (\alpha_2 + \beta \cos \psi)}{(\alpha_1 + \alpha_2 + 2\beta \cos \psi)^2} \\ &+ \frac{L^2 \beta \sin \psi}{(\alpha_1 + \alpha_2 + 2\beta \cos \psi)^2} = M, \end{aligned} \tag{24}$$

where $\alpha_1 = J_1 + \tilde{m}l_1^2$, $\alpha_2 = J_2 + \tilde{m}l_2^2$, $\beta = \tilde{m}l_1l_2$.

If relative motion $\psi(t)$ is known, absolute motion $\phi_1(t)$ of platform should be found using integration of Eq. (23). Thus, for the case $L = 0$, we have

$$\begin{aligned} \phi_1(t) &= -\frac{1}{2}\psi(t) - \frac{b}{a} \operatorname{arctg} \left(\frac{\operatorname{tg} \frac{\psi(t)}{2}}{a} \right) + C_{\phi_1\psi}, \\ a &= \sqrt{\frac{\alpha_1 + \alpha_2 + 2\beta}{\alpha_1 + \alpha_2 - 2\beta}} = \sqrt{\frac{J_1 + J_2 + \tilde{m}(l_1 + l_2)^2}{J_1 + J_2 + \tilde{m}(l_1 - l_2)^2}}, \\ b &= \frac{\alpha_2 - \alpha_1}{\alpha_1 + \alpha_2 - 2\beta} = \frac{J_2 + \tilde{m}l_2^2 - J_1 - \tilde{m}l_1^2}{J_1 + J_2 + \tilde{m}(l_1 - l_2)^2}. \end{aligned} \tag{25}$$

where constant of integration is determined by initial position and system configuration:

$$C_{\phi_1\psi} = \phi_1^{(0)} + \frac{1}{2}\psi^{(0)} + \frac{b}{a} \operatorname{arctg} \left(\frac{\operatorname{tg} \frac{\psi^{(0)}}{2}}{a} \right). \tag{26}$$

If the laws of absolute angular motion of lifting body $\phi_1(t)$ and angular motion of oriented body over lifting body $\psi(t)$ are known, the following expressions define a mass center motion of platform.

$$x_1(t) = -\frac{m_2}{m_1 + m_2} (l_1 \cos \phi_1(t) + l_2 \cos(\phi_1(t) + \psi(t))), \tag{27}$$

$$y_1(t) = -\frac{m_2}{m_1 + m_2} (l_1 \sin \phi_1(t) + l_2 \sin(\phi_1(t) + \psi(t))). \tag{28}$$

4 Derivation of an Independent Dynamic Equation of Relative Motion Using a Transform for Kinetic Energy

Relations (18), (19) и (22) can be derived by formal transformations of the system of differential Eqs. (14)–(17) as the first integrals but can be also written on the base of general theorems of dynamics since, when internal forces and torques are not present, the system momentum and a system angular momentum are constant. A kinetic energy is then expressed as:

$$\begin{aligned}
 T &= T(\dot{\psi}, \psi) \\
 &= \dot{\psi}^2 \left(a_{\dot{\phi}_1^2}(\psi) B^2(\psi) + a_{\dot{\phi}_1 \dot{\psi}}(\psi) B(\psi) + a_{\dot{\psi}^2}(\psi) \right) \\
 &\quad + \dot{\psi} \left(2a_{\dot{\phi}_1^2}(\psi) L B(\psi) D(\psi) + a_{\dot{\phi}_1 \dot{\psi}}(\psi) L D(\psi) \right) \\
 &\quad + a_{\dot{\phi}_1^2}(\psi) L^2 D^2(\psi),
 \end{aligned} \tag{29}$$

where auxiliary notations are used:

$$\begin{aligned}
 a_{\dot{\phi}_1^2}(\psi) &= \frac{1}{2} (J_1 + J_2 + \tilde{m}l_1^2 + \tilde{m}l_2^2 + 2\tilde{m}l_1l_2 \cos \psi), \\
 a_{\dot{\psi}^2}(\psi) &= \frac{1}{2} (J_2 + \tilde{m}l_2^2), \\
 a_{\dot{\phi}_1 \dot{\psi}}(\psi) &= J_2 + \tilde{m}l_2^2 + \tilde{m}l_1l_2 \cos \psi.
 \end{aligned} \tag{30}$$

$$\begin{aligned}
 B(\psi) &= -\frac{J_2 + \tilde{m}l_2^2 + \tilde{m}l_1l_2 \cos \psi}{J_1 + J_2 + \tilde{m}l_1^2 + \tilde{m}l_2^2 + 2\tilde{m}l_1l_2 \cos \psi}, \\
 D(\psi) &= \frac{L}{J_1 + J_2 + \tilde{m}l_1^2 + \tilde{m}l_2^2 + 2\tilde{m}l_1l_2 \cos \psi}.
 \end{aligned} \tag{31}$$

Then, the Lagrange equation can be written for the system under consideration as having one degree of freedom, interpreting Eqs. (18), (19) и (22) as equations of holonomic constraints.

$$\frac{d}{dt} \left(\frac{\partial T}{\partial \dot{\psi}} \right) - \frac{\partial T}{\partial \psi} = Q_\psi. \tag{32}$$

Having regard to $Q_\psi = M$ and substituting Eq. (29) into Eq. (32) due to Eqs. (30) and (31), we derive the same Eq. (24).

Thus, two techniques for deriving Eq. (24) are realized.

In the first case information about restrictions imposed on the modes of the motion under consideration (the main vector and the resultant moment of external forces are equal to zero) causing a specific form of the second members of

Eqs. (14)–(17) allowed to write the first integrals (18), (19) и (22) and to derive the Eq. (24) as a result of transformation of the system (14)–(17) in decreasing its order.

In the second case constraints of the motion modes by immobility of the center of mass of the system relative to inertia reference XOY and by a constant system angular momentum resulted in the validity of the written relations (18), (19) и (22) using the general theorems of dynamics, a formal interpretation of which as equations of holonomic constraints allowed an expression for a kinetic energy to be transformed to Eq. (29), and to derive an Eq. (24) by substituting the expression obtained into Eq. (32).

Both of these cases can result in an independent differential equation to study a guided relative motion for problems of a relative motion of a movable platform and a payload and problems of relative positioning a movable platform and a payload.

5 Analysis of Controlled Relative Motion Dynamics Features Produced by Basis Mobility

The system has four degrees of freedom in general. Initial conditions for generalized coordinates x_1 , y_1 , ϕ_1 , ψ should satisfy the following relations for providing system with viewed (23) and motion regimes

$$x_1^{(0)} = -\frac{m_2}{m_1 + m_2} \left(l_1 \cos \phi_1^{(0)} + l_2 \cos \left(\phi_1^{(0)} + \psi^{(0)} \right) \right), \quad (33)$$

$$y_1^{(0)} = -\frac{m_2}{m_1 + m_2} \left(l_1 \sin \phi_1^{(0)} + l_2 \sin \left(\phi_1^{(0)} + \psi^{(0)} \right) \right) \quad (34)$$

$$\begin{aligned} \dot{x}_1^{(0)} &= \frac{m_2}{m_1 + m_2} \\ &\times \left(\dot{\phi}_1^{(0)} \left(l_1 \sin \phi_1^{(0)} + l_2 \left(\sin \phi_1^{(0)} \cos \psi^{(0)} + \cos \phi_1^{(0)} \sin \psi^{(0)} \right) \right) \right. \\ &\left. + \dot{\psi}^{(0)} l_2 \left(\sin \phi_1^{(0)} \cos \psi^{(0)} + \cos \phi_1^{(0)} \sin \psi^{(0)} \right) \right), \quad (35) \end{aligned}$$

$$\begin{aligned} \dot{y}_1^{(0)} &= -\frac{m_2}{m_1 + m_2} \\ &\times \left(\dot{\phi}_1^{(0)} \left(l_1 \cos \phi_1^{(0)} + l_2 \left(\cos \phi_1^{(0)} \cos \psi^{(0)} - \sin \phi_1^{(0)} \sin \psi^{(0)} \right) \right) \right. \\ &\left. + \dot{\psi}^{(0)} l_2 \left(\cos \phi_1^{(0)} \cos \psi^{(0)} - \sin \phi_1^{(0)} \sin \psi^{(0)} \right) \right). \quad (36) \end{aligned}$$

Equation (24), which is linearized in position neighborhood $\psi = 0$, could be defined as

$$\ddot{\psi} \frac{\alpha_1 \alpha_2 - \beta^2}{\alpha_1 + \alpha_2 + 2\beta} + \psi \frac{L^2 \beta}{(\alpha_1 + \alpha_2 + 2\beta)^2} = M. \quad (37)$$

In case $L = 0$ ($M \neq 0$) Eq. (37) transforms in

$$\ddot{\psi} \frac{\alpha_1 \alpha_2 - \beta^2}{\alpha_1 + \alpha_2 + 2\beta} = M, \quad (38)$$

where quantity $\frac{\alpha_1 \alpha_2 - \beta^2}{\alpha_1 + \alpha_2 + 2\beta} = \frac{J_1 J_2 + \bar{m}(J_1 l_2^2 + J_2 l_1^2)}{J_1 + J_2 + \bar{m}(l_1 + l_2)^2}$ has a meaning of reduced moment of inertia of systems' parts.

In case $M = 0$ ($L \neq 0$) Eq. (37) transforms in

$$\ddot{\psi} + \omega^2 \psi = 0 \quad (39)$$

and describes linear harmonic oscillations of system. Eigenfrequency ω is defined by the expression

$$\omega^2 = \frac{\beta}{(\alpha_1 \alpha_2 - \beta^2)(\alpha_1 + \alpha_2 + 2\beta)} L^2. \quad (40)$$

The Eq. (39) is an illustration of the following fact. If the initial angular moment of system is not equal to zero and control action in the link doesn't exist, the oscillatory movements of system by internal freedom degree are possible.

We should use a special program package for validation of received relations and conclusions, which were made on the basis of these relations. A direct integration of dynamics equations of planar two-link mechanism is made using a program package «Universal mechanism».

Since creation of a model using program packages of this category consists in description of mechanical analytical model, and proper synthesis of dynamic equations and its numerical integration are automatized for defined starting condition, then in the context of the model task given approach may be consider as checking accuracy of analytical analysis results by means of «virtual experiment».

Assume that the following geometric and mass-inertia characteristics of mechanism are known:

$$\begin{aligned} m_1 = 10[\text{kg}], \quad m_2 = 10[\text{kg}], \quad J_1 = 1[\text{kg} \cdot \text{m}^2], \\ J_2 = 1[\text{kg} \cdot \text{m}^2], \quad l_1 = 1[\text{m}], \quad l_2 = 1[\text{m}] \end{aligned} \quad (41)$$

Accept that the initial conditions of relative motion are

$$\dot{\psi}^{(0)} = 0 \left[\frac{\text{rad}}{\text{s}} \right], \quad \psi^{(0)} = -\frac{\pi}{128} = -0.024544 [\text{rad}], \quad (42)$$

the initial angular position of movable platform

$$\phi^{(0)} = \frac{\pi}{128} = 0.024544 \text{ [rad]}, \quad (43)$$

and the angular moment are

$$L = 20 \left[\frac{\text{kg} \cdot \text{m}^2}{\text{s}} \right]. \quad (44)$$

Then according the relations (23) and (33)–(36) we have:

$$\begin{aligned} \dot{\phi}^{(0)} &= 0.90922 \left[\frac{\text{rad}}{\text{s}} \right], \\ \dot{x}^{(0)} &= 0.011157 \left[\frac{\text{m}}{\text{s}} \right], \quad \dot{y}^{(0)} = -0.90908 \left[\frac{\text{m}}{\text{s}} \right], \\ x^{(0)} &= -0.99985 \text{ [m]}, \quad y^{(0)} = -0.012271 \text{ [m]} \end{aligned} \quad (45)$$

The corresponding variable quantities are assigned values of mass-inertia characteristics (41) and initial conditions (42), (43) and (45) we obtain expected harmonic oscillation by internal degree of freedom based from (39). At that the period of oscillation (Fig. 2) coincides with the value calculated by means of relation (40)

$$\begin{aligned} \omega &= \sqrt{\frac{\beta}{(\alpha_1 \alpha_2 - \beta^2)(\alpha_1 + \alpha_2 + 2\beta)}} L = 2.8748 \left[\frac{\text{rad}}{\text{s}} \right], \\ T &= \frac{2\pi}{\omega} = 2\pi \left[\sqrt{\frac{\beta}{(\alpha_1 \alpha_2 - \beta^2)(\alpha_1 + \alpha_2 + 2\beta)}} L \right]^{-1} = 2.1856 \text{ [s]} \end{aligned} \quad (46)$$

The Eq. (37) leads to following fact. If the angular moment is not equal to zero, the resonant effects are possible in the system. The viewed case describes a situation, when the mechanism with mentioned mass-inertia characteristics rotates around the mass center without natural oscillations by internal degree of freedom, $L = 20 \left[\frac{\text{kg} \cdot \text{m}^2}{\text{s}} \right]$. In that case the initial conditions are equal to

$$\dot{\psi}^{(0)} = 0, \quad \psi^{(0)} = 0, \quad (47)$$

$$\begin{aligned} \dot{\phi}^{(0)} &= 0.90909 \left[\frac{\text{rad}}{\text{s}} \right], \quad \dot{x}^{(0)} = 0, \quad \dot{y}^{(0)} = -0.90909 \left[\frac{\text{m}}{\text{s}} \right], \\ x^{(0)} &= -1 \text{ [m]}, \quad y^{(0)} = 0 \end{aligned} \quad (48)$$

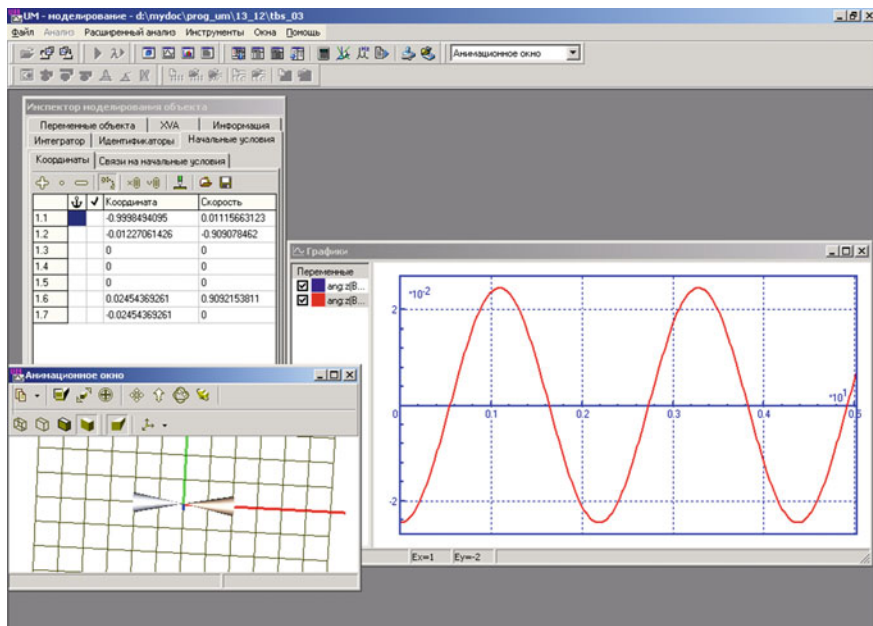


Fig. 2 Natural oscillations by internal degree of freedom given nonzero angular momentum of the system

As far as the movement by internal degree of freedom is viewed, the initial angular position of lifting body could be assigned accidentally. Assume that $\phi^{(0)} = 0$ and the program law of control is

$$M = A_M \sin(\omega \cdot t), \quad (49)$$

where ω is determined by the expression (46), i.e. it is a resonance frequency.

Graphics of changing the angle $\psi(t)$ for different amplitude values of harmonic control action A_M are presented on Fig. 3. If the values of $\psi(t)$ are small, the oscillating process are described by linearized Eq. (37) quite accurately. In this case linear increasing of amplitude takes place (Fig. 3a). If the oscillatory amplitude increases as a result of non-linearity of original Eq. (24), the effect of beating appears (Fig. 3b–d).

Now assume that a system doesn't move at initial point of time and is exerted by control action (49). Transient processes of system are described by linearized Eq. (38) in this case and the resonant effects don't appear.

Thus, if the angular moment of system «movable platform-manipulator-payload» is not equal to zero, it could be possible to mention the existence of restoring forces (a restoring moment in viewed modeling example), which have a character of inertia forces.

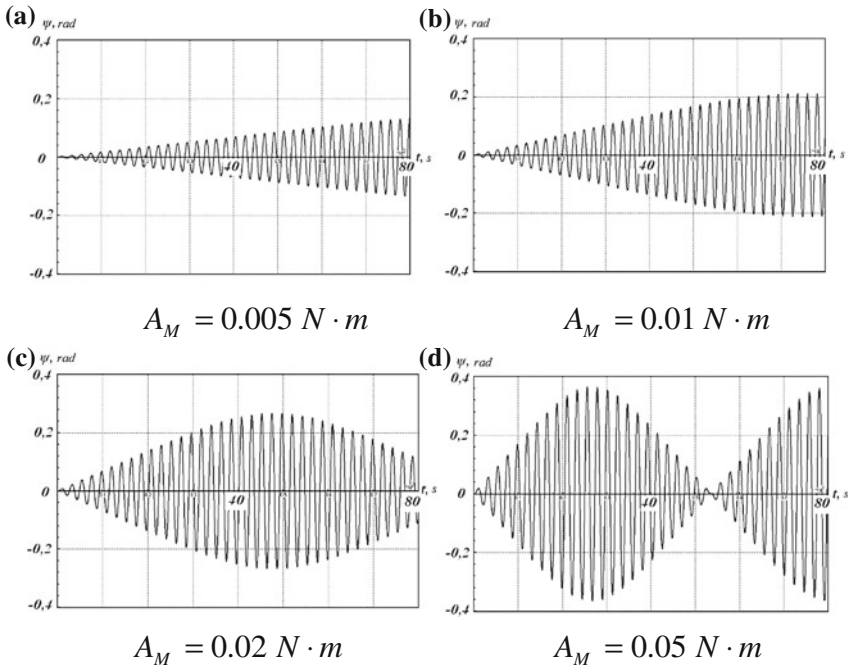


Fig. 3 Mechanism movement by internal degree of freedom given harmonic control action **a** $A_M = 0.005 \text{ N} \cdot \text{m}$ **b** $A_M = 0.01 \text{ N} \cdot \text{m}$ **c** $A_M = 0.02 \text{ N} \cdot \text{m}$ **d** $A_M = 0.05 \text{ N} \cdot \text{m}$

6 Conclusion

Based on the review of the status and development trends analysis of objects of space infrastructure perspective [2–5] it may be concluded about the potential diversity of constructive perspective of robotic systems for space purposes, determined by the complexity and heterogeneity of tasks that require automation. In this case, the appearance of new modes of operation and the tightening of functional requirements increase the relevance of an effective simulation of the dynamics of systems equipped with manipulators.

The dynamics of system “movable base-manipulator-payload” has some important features. Study of specially formed model tasks is reasonable for research of these features. The main advantage of this approach should be a possibility of receiving analytic relations using certain transformations. These relations admit a visual physics interpretation.

The method of attack is founded on combination of traditional methods of analytic mechanics and possibilities of modern computer environment and may be used to study dynamics qualitative features when engineering systems of category under consideration.

References

1. Alpatov, A.P., Belonozhko, P.A., Belonozhko, P.P., Grigor'ev, S.V., Tarasov, S.V., Fokov, A. A.: Modeling the dynamics of space manipulators on mobile base. *Robototekhnika i tekhnicheskaya kibernetika = Robot. Tech. Cybern.* **1**, 59–65 (2013) (in Russian)
2. Artemenko, Y.N., Belonozhko, P.P., Karpenko, A.P., Fokov, A.A.: Research of massive payload targeting features using a space manipulator taking into account a movable platform in conditions free of outside forces. *Sci. Educ. Bauman MSTU. Electron. J.* **12**, 669–691 (2014). doi:[10.7463/0815.9328000](https://doi.org/10.7463/0815.9328000)
3. Alpatov, A.P., Belonozhko, P.A., Gorbunsov, V.V., Ivlev, O.G., Cherniavskaya, S.S., Shichanin, V.N.: *Dynamics of Spatially Extended Mechanical Systems of Variable Configuration—K*, 256 p. Naukova Dumka (1990)
4. Alpatov, A.P., Byelonozhko, P.A., Byelonozhko, P.P., Tarasov, S.V., Fokov, A.A.: Synthesis features of the space manipulator control system. *Actual Probl. Aviat. Aerosp. Syst.* **2**(31), 38–57 (2010) (T. 15)
5. Belonozhko, P.P., Karpenko, A.P., Fokov, A.A.: Some features of dynamics of space system «mobile base—manipulator—payload». In: *Mezhdunarodnaya nauchno-tekhnicheskaya konferentsiya «Ekstremal'naya robototekhnika»: tr.* (Proceedings of the International Scientific and Engineering Conference “Extreme Robotics”), pp. 172–181. Politehnika-servis Publishing, St. Petersburg (2014) (in Russian)

Part IV
Vitality Control and Reliability Analysis

Control of Vitality and Reliability Analysis

V.Y. Ziniakov, A.E. Gorodetskiy and I.L. Tarasova

Abstract We examine the complex system durability control method with the usage of the modelled change of the failure probability, with the passing of time and the degrading of the system. We propose an approach to the problem of the accounting of the relations between the complex system blocks. We describe a modelling algorithm that combines the logical linguistic and logical probabilistic prognosis of the processes of the parameter values' change with the passing of time. The modelling allows getting a time reserve to run the needed maintenance operations, increasing the reliability of the system.

Keywords Complex logical function · Logical probabilistic modelling · Logical linguistic modelling · Prognosis · Complex system maintenance

1 Introduction

The main principles that are used for the complex systems durability control are adaptation, dynamic natural selection (or hot reservation), stress, compensation and borrowing, stupor or enabling of the emergency mode [1]. For the inner system state deviations due to various failures, to achieve the needed durability we traditionally use the hot reservation principle, which is similar to the natural dynamic selection in the living organisms. A signal to enable the mechanism of the dynamic

V.Y. Ziniakov (✉)
Saint-Petersburg Polytechnic University, St. Petersburg, Russia
e-mail: vziniakov@gmail.com

A.E. Gorodetskiy · I.L. Tarasova
Institute of Problems of Mechanical Engineering, Russian Academy of Sciences,
St. Petersburg, Russia
e-mail: g27764@yandex.ru

I.L. Tarasova
e-mail: g17265@yandex.ru

natural selection, that is the switching the channels and the blocks to the spare ones, is the observed overlaps of the blocks' inner state, that can be measured by its expected value of the block's parameters, or by its failure probability [2].

The problem of the system's durability or its reliable functioning provisioning, when the system's inner state deviation exceeds its allowed thresholds, is stated quite a long time ago and is mostly examined [3]. However, while estimating the change with the passing of time of a complex logical function, which describes the system's failure probability with the accounting of the relations between the blocks (excluding only the simplest schemes), there appear certain complexities and ambiguities [4]. The problem of the accounting of the parameters of the system's blocks' influence on the parameters of the blocks they are related to, while calculating the failure probability with the passing of time of the complex system still doesn't have a practically acceptable solution [5], since the analytical account of that issue in a complex system invariably leads to very complex computations. Let us examine one of the possible approaches to the problem of the relations' accounting between the blocks of a complex system.

2 A Simplified Accounting of the Relations Between the Blocks of a Complex System

It is clear that with the passing of usage time T of a complex system the probabilities of correct functioning of its blocks $P_{ic}(T)$ are decreasing by an exponential law [6]:

$$P_{ic0}(t_i) = \exp(-\alpha_{i0}t_i) \quad (1)$$

where t_i is the usage time of the i th block of the system, α_{i0} is the decrease coefficient, which we find out of the Eq. (1), since the mean time between failures t_{i0} and the initial correct functioning probability $P_{ic}(T)$ are usually given for the system blocks.

That decrease of the probabilities may be described by the following change of their parameter values' expected values [6]:

$$P_{i0}(T) = 1 - \Phi((b_i - m_i)/\sigma_i) + \Phi((-b_i - m_i)/\sigma_i) = 1 - P_{ic0}(t_i) \quad (2)$$

where: b_i is the maximum allowed value of the i th parameter.

m_i is the expected value of the i th parameter

σ_i is the root mean square of the i th parameter

$\Phi(x)$ is the probability integral that cannot be expressed through elementary functions, but there are tables of its calculated values [6], or its approximate value can be found as a sum of a decreasing row.

Since the initial values for P_{ic0} , b_i and m_{i0} are usually known for each block, the root mean square value σ_i for each block may be found from the following equations:

$$P_i(-\infty < x_i < -b_i) = \Phi_i((b_i - m_{i0})/\sigma_i) - \Phi_i(-\infty) = (1 - P_{ic0}(t_i))/2 \quad (3)$$

$$\Phi(-\infty) = 0, \quad (4)$$

It is also clear that the approaching of the expected values of the *i*th block’s parameters to the dangerous (critical) threshold *c_i* and, furthermore, to the maximal allowed threshold *b_i* also affect the parameters of the related blocks. For instance, the change in the power supply block’s output voltage also affects the amplification coefficient of the related amplification block. However, the problem of the estimation of the change with the passing of time of a complex logical function, which describes the system’s failure probability with the accounting of the relations between the blocks still doesn’t have a practically acceptable solution [3], since the analytical accounting of that fact in a complex system leads to very complex computations. Thus, we propose the following simplified approach to that problem:

When the expected value *m_i(t_i)* of the block’s parameters in some time moment *t_{ik}* fall into a dangerous zone *c_i ≤ |m_i| < b_i*, we set the coefficients *w(i) = 2, u(i) = 3* for this block. Here,

w(i) is a state characteristic of the *i*th block (*w(i) = 3* is broken, *w(i) = 2* is dangerous, *w(i) = 1* is normal).

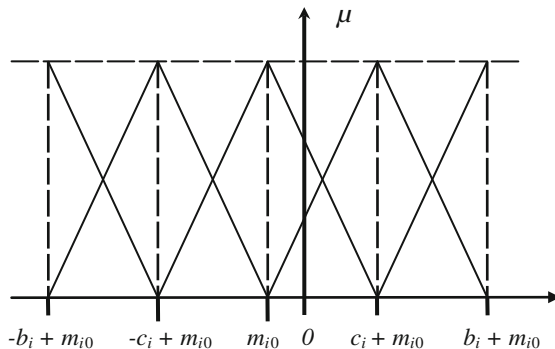
u(i) is the characteristic of the *i*th block proximity to the nearest broken or dangerous block (*u(i) = 0* is far, *u(i) = 1* is connected via a single block, *u(i) = 2* is directly connected, *u(i) = 3* is self).

After, we perform an expected value shift:

$$m_i = m_i + \sigma_i w(i) u(i) m_i \mu(m_i), \quad (5)$$

where $\mu(m_i)$ is the current expected value membership function of a certain interval, which we calculate as following (Fig. 1):

Fig. 1 Fuzzification



1. If $-\infty < m_i < b_i + m_{i0}$, then $\mu(m_i) = 1$
2. If $-b_i + m_{i0} \leq m_i \leq -c_i + m_{i0}$, then $\mu(m_i) = \max\{((m_i - m_{i0} + c_i)/(c_i - b_i)); ((m_i - m_{i0} + b_i)/(b_i - c_i))\}$
3. If $-c_i + m_{i0} \leq m_i \leq m_{i0}$, then $\mu(m_i) = \max\{(-m_i + m_{i0})/c_i; (m_i - m_{i0} + c_i)/c_i\}$
4. If $m_{i0} \leq m_i < c_i + m_{i0}$, then $\mu(m_i) = \max\{(-m_i + m_{i0} + c_i)/c_i; (m_i - m_{i0})/c_i\}$
5. If $c_i + m_{i0} \leq m_i \leq b_i + m_{i0}$, then $\mu(m_i) = \max\{(m_i - m_{i0} - b_i)/(c_i - b_i); ((m_i - m_{i0} - c_i)/(b_i - c_i))\}$
6. If $b_i + m_{i0} \leq m_i < \infty$, then $\mu(m_i) = 1$

Then we set the block numbers j of the blocks that are directly related to the “dangerous” block. For them, we set the values of the relation coefficients $u(j) = 1$, $u(j) = 2$ and perform the expected value shift:

$$m_j = m_j + \sigma_j w(j) u(j) m_j \mu(m_j) \quad (6)$$

where we calculate $\mu(m_j)$ by the same rules (1)–(6).

After, we define the block numbers q , that are connected to the block i via a single block. For them, we set $w(q) = 1$, $u(q) = 1$ and perform the expected value shift:

$$m_q = m_q + \sigma_q w(q) u(q) m_q \mu(m_q) \quad (7)$$

If now, after recounting of the expected values, we find that some block has its absolute value over the allowed threshold ($|m_i| > b_i$), such block is accounted to be broken, its failure probability is set to one ($P_{i0} = 1$), and the whole system’s failure probability is set to one ($P_0 = 1$). Otherwise, we need to calculate the new values of failure probability of all blocks from the new expected values, according to the formula (2), and then to calculate the failure probability of the whole system, by using, for instance, a polynomial formula [3]:

$$P_0 = (-1)^0 \sum_i (P_{i0}(T)) + (-1)^1 \sum_{ij} (P_{i0}(T) P_{j0}(T)) + (-1)^2 \sum_{ijk} (P_{i0}(T) P_{j0}(T) P_{k0}(T)) + \dots + \prod_i (P_{i0}(T)) \quad (8)$$

Thus in the proposed solution to the relations’ accounting problem, when a dangerous situation arouses, we instantly change the expected parameter values of the given block and its related blocks, which allows in a first approximation to account the mutual impacts of the blocks’ parameters to the change of the failure probabilities with the passing of time.

3 The Modelling of Changes with the Passing of Time of the Complex System Failure Probability with the Reservation of the Blocks

While modelling the change with the passing of time of the complex system failure probability with the reservation of the blocks we assume that the system contains N_b basic and N_r reserve blocks. We must determine the change with the passing of time t of the failure probability $P_s\{y = 1\}$ of the system, if we know:

1. The structure of the system, by which we can draw the block relations table
2. The mean time between failures for each i th block of the system t_{i0} .
3. The initial probability of the correct functioning of each i th block of the system $P_i(t_{i0})$.
4. The maximal (critical) deviation threshold of the i th block parameters b_i . When this threshold is surpassed, we assume that the block is broken ($z_i = 1$ — i th block failure).
5. The dangerous deviation of the parameters of the i th block c_i . When surpassed, this leads to the increase of the parameters' deviation of related blocks.
6. The deviation threshold d_i , surpassing of which leads to the substitution of the block with the reserve one.

In a system with reservation the system failure means that:

$$y = (z_{i0} \wedge z_{1p}) \wedge (z_{i0} \wedge z_{2p}) \wedge (z_{i0} \wedge z_{3p}) \wedge \dots \wedge (z_{i0} \wedge z_{Np}) = 1, \quad (9)$$

where z_{ib} is the failure of i th basic block and z_{ir} is the failure of the i th reserve block of the system.

Thus to compute the system's failure probability that characterizes its reliability, in a time moment T we must first compute the probabilities of the conjunctive elements in the Eq. (9):

$$\begin{aligned} P_i\{z_{i0} \wedge z_{ip} = 1\} &= P_{i0}\{z_{i0} = 1\} * P_{ip}\{z_{ip} = 1\} = \dots \\ &= P_{i0}(T_{i0}) * P_{ip}(T_{ip}) = P_i(T), \end{aligned} \quad (10)$$

where T_{ib} , T_{ir} are the corresponding working time of the i th basic and reserve blocks.

Furthermore:

1. Since we are interested in the situations when the blocks' parameters are nearing the dangerous values, when $c_i < |m_i| < b_i$, where c_i is the dangerous parameter threshold and b_i is the critical threshold of the parameter, or the critical values, when $|m_i| \geq b_i$, we may ignore the value $\Phi((-b_i - m_i)/\sigma_i)$ in the equation $P_0(T) = 1 - \Phi((b - m)/\sigma) + \Phi((-b - m)/\sigma_i)$, since $\Phi((-b_i - m_i)/\sigma_i) < \Phi((b_i - m_i)/\sigma_i)$. Thus we may assume that $P_{i0}(T_{i0}) = \Phi((b_i - m_{i0}(T_{i0})/\sigma_{i0})$ and

$P_{ip}(T_{ip}) = \Phi((b_i - m_{ip}(T_{ip}))/\sigma_{ip})$. If the i th reserve block is not connected, $T_{ir} = 0$ and $P_{ir}(T_{ir}) = 0$.

2. If we don't have the i th reserve block, then $P_{ir}(T_{ir}) = 1$
3. If some i th basic block doesn't have a reserve one and for that block $P_{io}(T_{ib}) = 1$ block failure, then $P_c\{y = 1\} = 1$
4. If we don't have any i th block, for which $P_{ib}(T_{io}) = 1$ and $P_{ir}(T_{ir}) = 1$ then:

$$P_c\{y = 1\} = P_c(T) = (-1)^0 \sum_i (P_i(T)) + (-1)^1 \sum_{ij} (P_i(T)P_j(T)) + (-1)^2 \sum_{ijk} (P_i(T)P_j(T)P_k(T)) + \dots + \prod_i (P_i(T)), \quad (11)$$

5. If for some i th block in some ij th moment of time T_{ij} the parameter deviations exceed the threshold d_i , then, providing that we have a reserve block, we change it by that block, for him we set the value $P_{io}(T_{ib}) = 1$ and for the reserve block we set $T_{ir} = T - T_{ij}$. Then, $P_i(T) = P_{ir}(T_{ir})$, и $P_c\{y = 1\}$ we also compute by the formula (11).
6. If after replacing the basic block to the reserve one we have $P_{ir}(T_{ir}) = 1$, then $P_c\{y = 1\} = 1$.
7. The correct functioning probability of each i th block decreases with the passing of its working time t_i according to the exponential law $P_{ib}(T_{ib}) = \exp(-a_{i0} T_{ib})$, (10), and the probability or correct work of each i th reserve block $P_{ir}(T_{ir})$ remain constant until the time moment of their enabling T_{ij} , and then decrease with the time passing $T_{ir} = T - T_{ij}$ also by the exponential law of the type (1).

4 The Algorithm of the Modelling of the Failure Probability with the Passing of Time of the Complex System with the Reservation of the Blocks

Taking into account the facts described above, we compose the following algorithm:

1. *Initializing*

- N the quantity of blocks of the system
- $\Phi(x)$ the normal distribution function, given as a linearly interpolated table values [6]
- V system time; $V: = 0$
- T final modelling time
- Δ modelling time step
- C square binary matrix of rank N , which describes the pointed graph of the system's blocks relations
- $m_i(V)$ expected value of the i th block condition before accounting the relations in a time moment V

- M_i addition to the expected value of the i th block condition after accounting the relations in the time moment V
- σ_i root mean square of the i th block condition
- $P_i(V)$ i th block failure probability in a time moment V , $P_i(V) = P_i(0) = 0.004$ (according to standards, or the block's documentation)
- t_i mean time between failures of the i th block (according to standards or the block's documentation)
- V_i a time moment of the i th block's replacing with a spare one (0 if the change didn't occur), $V_i = 0$
- a_i an exponential coefficient of the i th block failure probability
- b the critical threshold for a block's parameter values, $b = 0.15$
- c_i the dangerous threshold for the i th block's parameter values
- d_i the threshold for the i th block's parameter values when the block is replaced by a spare one
- $\mu_i(V)$ the membership function of the i th block in the time moment V
- $w_i(V)$ the block condition coefficient in the time moment V
- $u_i(V)$ the coefficient of dangerous/critical blocks proximity to the i th block in the time moment V
- k_i reserving coefficient of the i th block ($k_i = 0$ for no reserve block, $k_i = 1$ for 1 reserve block, $k_i = 2$ for 2 reserve blocks etc.)
- $P(V)$ system failure probability in the time moment V

2. Computing the root mean square value σ_i for each i th block

We calculate $x_i = P_i(0)/2$

We calculate the function's $\Phi(x_i)$ value from the table [6].

We calculate $\sigma_i = -b/\Phi(x_i)$

3. Computing the exponential coefficient a_i for each i th block

$$a_i = -1/t_i * \ln(P_i(0))$$

4. Computing the failure probability and the expected value $m_i(V)$ for each i th block in the time moment V

We calculate $P_i(V) = \exp(-a_i * (V - V_i))$

We calculate the value of the function $\Phi(P_i(V))$ from the table [6].

We calculate $m_i(V) = b - \Phi(P_i(V)) * \sigma_i$

5. Computing the membership function for each i th block

If $m_i(V) \leq -3 * \sigma_i$, then $\mu_i(V) = 1$

If $m_i(V) > -3 * \sigma_i$ and $m_i(V) \leq -\sigma_i$, then $\mu_i(V) = \max(\mu_i([-3 * \sigma_i, -\sigma_i]), \mu_i([-2 * \sigma_i, -\sigma_i]))$

If $m_i(V) > -\sigma_i$ and $m_i(V) \leq 0$, then $\mu_i(V) = \max(\mu_i([-\sigma_i, 0]), \mu_i([-\sigma_i, 0]))$

If $m_i(V) > 0$ and $m_i(V) \leq \sigma_i$, then $\mu_i(V) = \max(\mu_i([0, \sigma_i]), \mu_i([0, \sigma_i]))$

If $m_i(V) > \sigma_i$ and $m_i(V) \leq 3 * \sigma_i$, then $\mu_i(V) = \max(\mu_i([\sigma_i, 3 * \sigma_i]), \mu_i([\sigma_i, 2 * \sigma_i]))$

If $m_i(V) \geq 3 * \sigma_i$, then $\mu_i(V) = 1$

If $m_i(V) < -b$ or $m_i(V) > b$, then $w_i(V) = 0$ and $P_i(V) = 1$ (*i*th block is critical)

If $(m_i(V) > -b$ and $m_i(V) < -c_i)$ or $(m_i(V) > c_i$ and $m_i(V) < b)$, then $w_i(V) = 2$ (*i*th block is dangerous)

If $m_i(V) \geq -c_i$ or $m_i(V) \leq c_i$ then $w_i(V) = 1$ (the block is functional)

6. *Computing the proximity coefficient $u_i(V)$ for each dangerous/critical *i*th block in the time moment V*

If $w_i(V) = 0$ (*i*th block is critical), then $u_i(V) = 0$

Furthermore:

If a dangerous and/or critical block is related to the *i*th, then $u_i(V) = 3$

If a dangerous and/or critical block is related to the *i*th through a single block, then $u_i(V) = 2$

In all other cases $u_i(V) = 0$

If $w_i(V) = 2$ (*i*th block is dangerous), then $u_i(V) = 3$

Furthermore:

If a dangerous and/or critical block is related to the *i*th, then $u_i(V) = 2$

If a dangerous and/or critical block is related to the *i*th through a single block, then $u_i(V) = 1$

In all other cases $u_i(V) = 0$

We define the related blocks from the matrix \mathbf{C} .

7. *Computing the addition to the expected value*

$$M_i(V) = \bar{\sigma}_i * w_i(V) * u_i(V) * m_i(V) * \mu_i(V)$$

8. *Computing the expected value $m_i(V)$ after accounting the relations in the time moment V*

If $m_i(V) < -d_i$ or $m_i(V) > d_i$, then $m_i(V) = m_i(0)$, else $m_i(V) = m_i(V) + M_i(V)$

9. *Computing the failure probability $P_i(V)$ for each *i*th block*

If $w_i(V) = 0$ and $k_i = 0$, then $P_i(V) = 1$

If $w_i(V) = 0$ and $k_i = 1$, then $P_i(V) = p_i(V) = 0.004$ and $V_i = V$

If $w_i(V) \neq 0$ and $k_i = 1$ and $m_i(V) < -d_i$ or $m_i(V) > d_i$, then

$V_i = V$, $P_i(V) = p_i(V) = 0.004$, else:

$$P_i(V) = \Phi((-b - m_i(V))/\bar{\sigma}_i) - \Phi((b - m_i(V))/\bar{\sigma}_i)$$

We calculate the value of the function Φ according to the table [6].

10. *Computing the system's failure probability*

$$P(V) = (-1)^0 \sum_i (p_i(T)) + (-1)^1 \sum_{ij} (p_i(T)p_j(T)) \\ + (-1)^2 \sum_{ijk} (p_i(T)p_j(T)p_k(T)) + \dots + \prod_i (p_i(T))$$

From these values, we draw the graph $P(V)$

11. If $P(V) = 1$, stop, else:
12. If $V \geq T$, stop, else $V = V + \Delta$ and go to step 4

5 Example

Let us examine a following example system, displayed in the Fig. 2. That is a schematic representation of a standard module for a smart electromechanical system (SM SEMS).

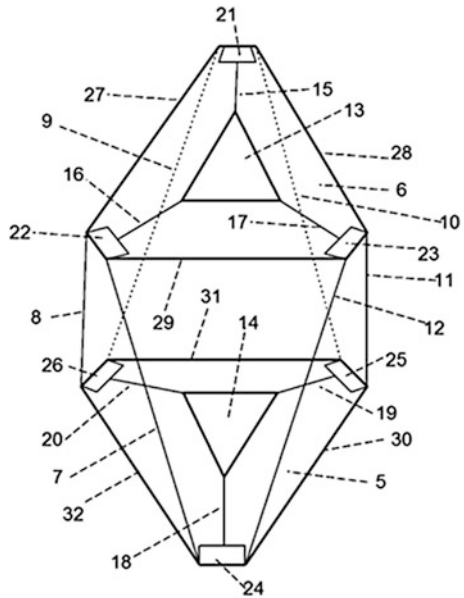
For it, let us assume that, $P_{c0} = 0.996$, $m_{i0} = 0$, $b_i = 0.15$, $t_{0i} = 27,000$ h, $c_i = \sigma_i$, $\Delta = 10,000$ h.

When displayed as a directed graph on a scheme, the system looks as shown in the Fig. 3.

Here:

- MC is Main Controller
- LP is Lower Platform
- UP is Upper Platform
- C1–C6 are Controllers

Fig. 2 SM SEMS



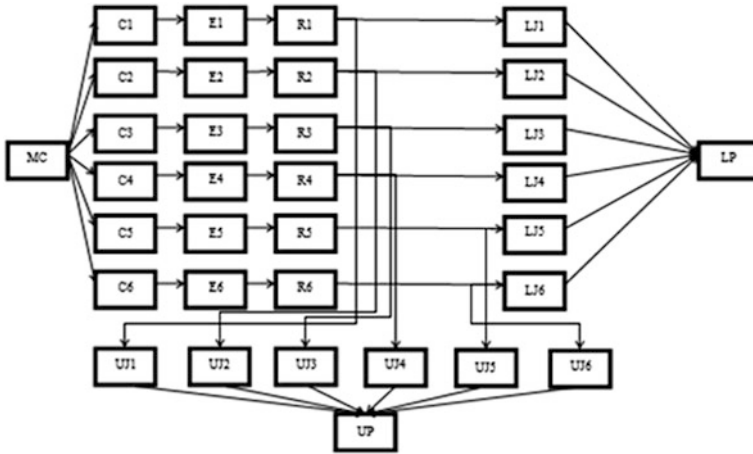


Fig. 3 SM SEMS scheme

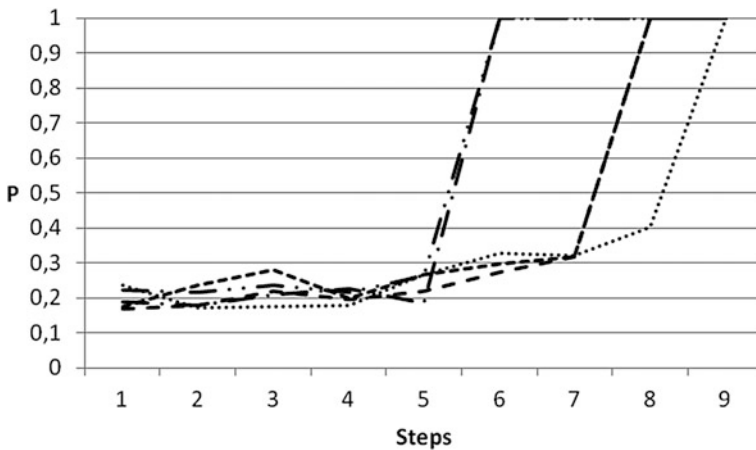


Fig. 4 System failure probability graph, without spare blocks

- E1–E6 are Engines
- R1–R6 are Reducers
- LJ1–LJ6 are Lower Joints
- UJ1–UJ6 are Upper Joints

In the first example case, let us assume that we don't have spare blocks for any of the system's blocks. Then, after running series of test simulations, we gain the following system probability from step # dependency, which is shown in Fig. 4.

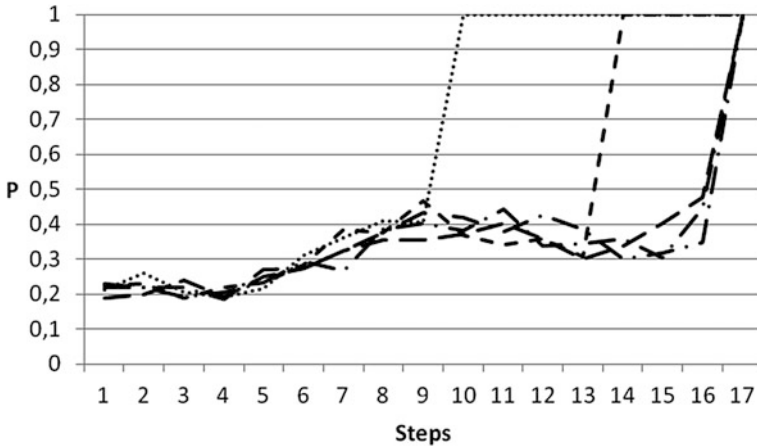


Fig. 5 System failure probability graph, with spare blocks

When running series of test simulations assuming that we do have a single spare block for each of the system's blocks, we gain the following dependency, shown in Fig. 5.

6 Decision Making Methods for Durability Control

Let us examine the pros and cons of the possible decision making methods while controlling the durability of a system with hot reserving.

1. Let us control the block parameters x_i and switch to a reserve block when $x_i \geq b_i$
Pros: simplicity. Cons: system hiatus while switching the block and the high probability of false alerts on random short-timed parameter value peaks.
2. Let us control the block parameters x_i while computing the expected values m_i , and switch to a reserve block when $m_i \geq b_i$ Pros: lower false alert probability. Cons: system hiatus while switching the block, and the system complexity is higher.
3. Let us control the block parameters x_i while computing the current expected value m_i , modelling the expected value $m_i(t)$ with the passing of time t **with or without** accounting the relations between the system's blocks, defining by the modelling results the probable time moment T_a of a situation when $m_i \geq b_i$, and in a time moment $T_p = k_p T_a$ ($k_p < 1$) we switch the block to a reserve one and perform the fixing of partial failures. Pros: low probability of false alerts, low probability of system hiatus while switching the block. Cons: low prognosis precision of the time moment T_p , high system complexity.

7 Conclusion

The proposed modelling method allows to increase the probability of the prognosis of the critical situation occurring time for each block of the system, thus increasing the system durability via timely activation of reserving mechanism. By doing so, we may receive a time reserve to perform the needed technical measures for reserve block switching and for the partial failures fixing.

References

1. Wenzl, E.S.: Theory of Probabilities. Nauka (1969)
2. Ryabinin, I.A.: Reliability and Safety of Structural Complex Systems. Polytechnic, St. Petersburg (2000)
3. Gorodetskiy, A.E.: Basics of Intellectual Control Systems Theory. LAP LAMBERT Academic Publishing GmbH@Co. KG (2011)
4. Gorodetskiy, A.E., Tarasova, I.L.: Control and Neural Networks. SPbSTU Publishing, St. Petersburg (2005)
5. Gorodetskiy, A.E., Tarasova, I.L.: Fuzzy Mathematical Modelling of Poorly Formalized Processes and Systems. SPbSTU Publishing, St. Petersburg (2010)
6. Chervony, A.A., Lukyaschenko, V.I., Kotin, L.V.: Complex System Reliability. Mashinostroyenie (1976)

System Failure Probability Modelling

V.Y. Ziniakov, A.E. Gorodetskiy and I.L. Tarasova

Abstract We examine the logical probabilistic modelling of a complex system's blocks failures with the considerations of the connections between the blocks, based on the logical linguistic approach. We describe the modelling procedure, implementing the logical probabilistic and logical linguistic modelling approaches. We developed a model describing a simplified solution of accounting the blocks' connections.

Keywords Complex logical function · Logical probabilistic modelling · Logical linguistic modelling · Prognosis · Complex system maintenance

1 Introduction

While any block of the system is used, it experiences the impact of various factors, which leads to altering (worsening) of its technical condition with the passing of time. That leads to failure probability of that block as well as that of the entire system. The peculiarity of those factors is their values' stochastic vibration with the passing of time. The most considerable factors are technological strains, durability characteristics of the unit's material, its geometrical parameters. In addition, it is vital to distinguish the fulfillment of the technological process conditions, the quality of maintenance, repairs, etc. [1]. The mentioned factors are stochastic, and,

V.Y. Ziniakov (✉)

Saint-Petersburg Polytechnic University, Saint Petersburg, Russia
e-mail: vziniakov@gmail.com

A.E. Gorodetskiy · I.L. Tarasova

Institute of Problems of Mechanical Engineering, Russian Academy of Sciences,
199178 Saint Petersburg, Russia
e-mail: g27764@yandex.ru

I.L. Tarasova

e-mail: g17265@yandex.ru

as such, the time of the failure is also random. Thus, it is suitable to perform the analysis of the complex system failure probability altering with the passing of time and the prediction of its failure via the mathematical and computer modelling.

While modelling, it is common to set the four types of the initial information: the repair statistics, the technological stress data, the resource estimation, and the diagnostic statistics [2]. That allows to divide the existing models to four types, namely resource model, based on the repair dates' data; the force model, based on the durability and the geometrical parameters of the block and the statistics of the technological stresses; diagnostic model, based on the diagnostic data; and expert model, based on the expert estimations of the system blocks' resources. While using any of the mentioned models we have first to define the predicted parameters, and then perform the prediction procedure.

The expert model is the most simple of all the parametrized models. We define its parameters are defined based on the expert estimations of the system blocks' resources. The set of the initial data for this model is given as the expert estimations. Usage of this model is suitable for the early stage of the running of the equipment, when no sufficient statistical information on repairs and technical maintenance is available.

One of the most promising approaches for creating of the expert models is the development of the logical probabilistic methods, which use the functions of algebra of logic (FAL) for analytical views of the system's working conditions and the strict ways of converting FAL to probabilistic functions, which objectively express the reliability of this system [3]. The benefit of the logical probabilistic approach for the engineers is mainly in their high strictness and the vast possibilities for the analysis of every element's impact to the whole system's reliability. However, there are also complexities for the active usage of such methods. Namely, for the complex tasks and structures, which are described by a FAL of any form, it is quite complex to transform the system's description into the probabilistic form.

While transforming the FAL into a Zhegalkin polynomial it is easy to formalize the computation of the probability of the resulting complex logical function (CLF) [4]. However, a CLF describing the failure of a complex system contains a high number of summands. Thus, even more summands will be present in the formula, which computes its probability, since the number of the summands in the expression of the CLF probability is an exponent function of the logical summands' count. It is unlikely that an algorithm for drastic simplifying of exponential computations will be found. In the case of transforming the CLF to orthogonal format (of a perfect disjunctive normal form), the quantity of its summands is also an exponential function of the initial count. Thus, the computing of the probability of the logical function directly, without any initial approximations of the significant summands count leads to very high expends of the processing time or memory [5].

However, we can decrease the amount of computations if we estimate the errors of the summands that are remote from the start of the polynomial, which have a small impact on the computed probability. That lets us to decrease the computations' amounts if we do not take into account the small members of the polynomial of the CLF [5].

For instance, while computing the probability of a CLF polynomial, which contains 45 summands, it is enough to account the first 10–15 ones, and then the computation time will be more than 3 times less [6]. In addition, the lexical graphic ordering of the fundamental vector of the CLF ensures the independent computing of the summands in the polynomial expression for its probability, which allows to control the computation process and to make decisions about its terminating while approaching the needed precision [6]. The drawback of such approach is that we need to ensure the independence of the logical variables that we use in the CLF.

We can also make the computing of the complex system failure based on the orthogonal transformations in the algebra of tuples [7]. This is quite a consuming operation; however, there were developed methods of its simplifying [8], which in many cases allow to drastically decrease the computing time for formulae with a high number of variables. For instance, if we use the computation result in numerous subsequent usages with the altering probability values, then the time consumption is justified.

We can considerably reduce the number of computation operations in those cases, when the initial logic formula changes itself due to the changes in the examined system [8]. Furthermore, in the algebra of the tuples we can get the computation formula for precise probability computation even in those cases when the sub formulae in the disjunction are not mutually independent [9]. Yet while estimating the changes in CLF describing system's failure with the passing of time and with the accounting the connections between the blocks (excluding the cases with the simplest schemes), there appear certain complexities and ambiguities [3]. In the current chapter, we examine the possible solutions to the problem of the complex system failure probability modelling with the passing of time with the accounting of connections between the system's blocks.

2 Computing the Failure Probabilities of a Complex System

While using the method of FAL algebraic transformation, described in [1, 3], we can write down the following CLF which describes the failure probability of an n blocks system.

$$\mathbf{Y} = \mathbf{A}\mathbf{F} \quad (1)$$

where \mathbf{A} is a rectangular binary matrix containing the identification failure rows \mathbf{C}_{ij} , which have the length of $N = 2n - 1$ and consist of ones and zeroes; \mathbf{F} is a fundamental vector of the logical failure system φ_i ($\varphi_i = 1$ means that the i th block is broken) which is also of the length $N = 2n - 1$.

The fundamental vector \mathbf{F} is the ordered set of the elements of the Cartesian multiplication of the basis vector of the system's blocks failures:

$$\Phi^T = \langle \varphi_1, \varphi_2, \dots, \varphi_n \rangle \quad (2)$$

Thus

$$\mathbf{F}^T = \langle \varphi_1, \varphi_2, \dots, \varphi_n, \varphi_1\varphi_2, \varphi_1\varphi_3, \dots, \varphi_{n-1}\varphi_n, \dots, \varphi_1\varphi_2\varphi_3, \dots, \varphi_{n-1}\varphi_n \rangle \quad (3)$$

The distribution of zeroes and ones in the identification failure rows \mathbf{C}_{ij} has to represent the physically feasible system failures. So, if $n = 4$ and if we account the failures of only the first and the second system blocks the row should be as follows:

$$\mathbf{C}_j = \langle 1, 1, 0, 1, 0, 0, 0, 0, 0, 0, 0, 0, 0, 0, 0, 0 \rangle \quad (4)$$

That means that either $(\varphi_1 = 1 \wedge \varphi_2 = 1)$ or $(\varphi_1 = 1 \vee \varphi_2 = 1)$ and all the other members equal to zero. That means that depending on the failure type \mathbf{Y}_j there will be different combinations in the rows \mathbf{C}_j . Then we define the failure type by the following formula:

$$\mathbf{Y}_j = \mathbf{C}_j \mathbf{F} \quad (5)$$

If we know the failure probabilities for the i th system blocks $P_{fi}\{x_i = 1\}$, then if their failures are independent the probability of the j th failure type of the system $P_{ff}\{\mathbf{Y}_j = 1\}$ can be computed approximately, using the following polynomial formula [2]:

$$P_{ff} = (-1)^0 \sum_{\gamma-1}^r P_\gamma + (-1)^1 \sum_{\gamma\eta} P_\gamma P_\eta + \dots + (-1)^{r-1} \prod_{\gamma-1}^r P_\gamma \quad (6)$$

where r is the length of \mathbf{Y}_j or the number of ones in the row \mathbf{C}_j , $j \neq \eta$ are the numbers of the members of the polynomial (5), P_i are the computed or given probability values of the i th member of the polynomial (5). However, we should define the required computation precision ΔP_{fi} and continue the computation process, started from the first member of the polynomial (6), until the delta is lesser than ΔP_{fi} . As the result of the computation, we shall receive the vector of the system failure probabilities

$$P_c^T = \langle P_{c1}, P_{c2}, \dots, P_{cj}, \dots, P_{cM} \rangle \quad (7)$$

where M is the number of j -identified system rows.

It is obvious that we must define the system reliability as the maximal probability of all P_{ff} , which corresponds to the identification row \mathbf{C}_j , which contains only ones. With the passing of time T of the complex system working (usually $T = \max\{t_{ik}\}$) the probabilities of correct working of its blocks $P_{ci}(t_{ik})$, where t_{ik} is the k th moment of time of the i th block running, decrease with different velocity, also, different blocks may have different t_{ik} . The latter requires the periodical re-computing of all the P_{cj}

and re-considering of the current system reliability, while running the system. However, different situations are also possible. For instance, some i th system blocks may have the reserve blocks, which are initiated only by failure signal v_i of the failed block. There may be some j th blocks in the system, which have the fixed running time intervals Δt_{jk} . There may also be s th blocks in the system, which switch on and off by the external signals θ_s , that may be initiated by a human operator. Also, there may be q th blocks, which reliability may be defined not by their medium time before failures and their correct working probability, but rather by their switching on and off number g_{qk} , as, for instance, various switches. For the latter blocks, we must watch such blocks' switching during the system's running time T and, depending on that number, decrease its modelled correct working probability according to a given rule.

Let us assume that the decreasing of the correct working probability $P_{ci}(t_{ik})$ happens, as usual, by the exponential law [4]:

$$P_{ci}(t_{ik}) = \exp(-\alpha_{ik}t_{ik}) \quad (8)$$

where α_i is the coefficient of the correct work probability, corresponding to the k th moment of the i th block working [for the q th blocks we must substitute t_{ik} with g_{qk} in the equation of the type (8)]. We may find the initial coefficient α_i from the Eq. (8), if we have the medium time before failure t_i for the i th blocks and the probability of the correct work $P_{ci}(t_i)$ in that moment of time. Usually such parameters are given in the blocks' technical documentation. Similarly, we may compute the values q_0 for the q th blocks. Thus the estimation of the current block reliability as well as the whole system's if the blocks' failures are independent, is not complex, since we may assume that the coefficients α_i are not time-dependent.

If we do not know some probability P_i or we are not sure if the system's blocks failures are independent, the given approach may result in considerable errors [7]. In some cases, we may perform the computing of the complex system's failure probability based on the orthogonal transforming and the algebra of the tuples. However, in that case the process of finding the system's FAL is much more complex, as are the computations. We may solve the given problem approximately using the proposed simplified blocks' connections' accounting method.

3 A Simplified Approach to the Blocks' Connections' Accounting Problem

If we know only the fact of the connections' existence or absence, that is, we know only the topology, but the connections' characteristics are unknown, we may increase the precision of the system's failure probability changing with the passing of time by the proposed procedure of simplified mutual interconnected blocks' impact and of the values of the failure probabilities of such blocks. That means that we will use the probabilities that are approximately equal to the conditional probabilities in the Eq. (6).

The increase of the blocks' failure probabilities with the passing of time is primarily caused by the changes in their parameters. For instance, with the passing of time the sizes of the details alter due to friction. That causes the increase in the vibrations' amplitude. Thus, the failure probability of such block increases. Therefore, the failure probability depends on the expected value (EV) of the block's parameter. With the normal distribution, we may describe the mentioned dependency by the following well-known expression (9):

$$P_{fi}(t_{ik}) = 1 - \Phi((b_i - m_i(t_{ik}))/\sigma_i) + \Phi((-b_i - m_i(t_{ik}))/\sigma_i) = 1 - P_{ci}(t_{ik}) \quad (9)$$

where b_i is the maximal allowed values of the i th block parameter, $m_i(t_{ik})$ and σ_i are respectively its expected value and root mean square, $\Phi(x)$ is the Gaussian probability interval, which cannot be expressed via the elementary functions, but there are tables of its values [5] or its approximate expressions in the form of a row with the decreasing members, such as (10):

$$\Phi(x) = \frac{1}{\sqrt{\pi}} \left(x - \frac{x^3}{1!3} + \dots + \frac{(-1)^l}{l!(2l+1)} x^{2l+1} + \dots \right) \quad (10)$$

Since we usually know the initial expected parameter values $m_i(t_0)$ for each block and the values t_i , $P_{ci}(t_0)$, b_i , then we can calculate the value σ_i from the expression of type (9) with the usage of either the table of values $\Phi(x)$ [5], or the simplified value of $\Phi(x)$ in the form of the row (10).

The value of σ_i of each parameter of the each block depends on the physical processes in that block, which are only slightly altered, which the block is running correctly. Then let us assume that the root mean square σ_i does not depend on the block's running time, although it slightly decreases the modelling precision. Furthermore, for each i th block we can calculate the initial values of their decrease coefficients α_{i0} from the expression of the type (8).

Due to this, before me start modelling the complex system's of n interconnected blocks failure probability changing with the passing of time, we need to create the table of system blocks interconnections, based on the system's topology, and set the dependency of each block's running time t_{ik} from the system's working time. After, for each block, based on its known values of the medium time before failure and its correct working probability from the equation of type (8), we must calculate the initial values of their decrease coefficients α_i , and, by setting their maximal allowed values b_i and the initial expected values m_i , we must calculate their root mean square σ_i from the Eq. (9) with the usage of the table of values $\Phi(x)$ or the row (10).

In the system, there may be blocks that:

During the system's working time T work all the time t_{ik} (Table 1).

During the system's working time T work episodically (Table 2).

Have reserve blocks. In that case the main block during the system's work time T works while its failure probability $P_{fi}(t_{ik})$ is lower than the allowed probability P_{afi} , after which we plug in the reserve block and its failure probability $P_{rfi}(t_{rik})$ increases by the exponential law (Table 3), where t_{rik} is the reserve block running time.

Table 1 During the system’s working time T work all the time t_{ik}

k	1	2	3	4	5	6	...	K
t_{ik}, h	10^4	2×10^4	3×10^4	4×10^4	5×10^4	6×10^4	...	T

Table 2 During the system’s working time T work episodically

k	1	2	3	4	5	6	...	K
t_{2k}, h	10^4	10^4	2×10^4	2×10^4	3×10^4	3×10^4	...	T
t_{3k}, h	0	10^4	10^4	2×10^4	2×10^4	3×10^4	...	$T - 10^4$

Table 3 The main block during the system’s work time T works while its failure probability $P_{f4}(t_{ik})$ is lower than allowed

k	1	2	3	4	5	6	...	K
P_{f4}	$<P_{mf4}$	$<P_{mf4}$	$<P_{mf4}$	$\geq P_{mf4}$	$\geq P_{mf4}$	$\geq P_{mf4}$...	$\geq P_{mf4}$
t_{i4}, h	10^4	2×10^4	3×10^4	4×10^4	5×10^4	0	...	0
P_{si4}	$<P_{mf4}$	$<P_{mf4}$	$<P_{mf4}$	$<P_{mf4}$	$<P_{mf4}$	$<P_{mf4}$...	$<P_{mf4}$
t_{si4}, h	0	0	0	0	0	10^4	...	$(K - 5)\Delta T$

During the system’s working time T are switched on and off depending on the external signal θ_i (Table 4).

Also, during the modelling process the expected values of the blocks’ parameters $m_i(t_{ik})$, while changing, will be approaching the dangerous (critical) d_i , that has to be set before the modelling process, and to the maximal allowed value b_i . It is obvious that such situation influences the failure probabilities of those and connected blocks. For instance, the change in the output voltage of the power block leads to the change of the enhancing coefficient of the connected enhancement block. However, the problem of accounting of the blocks’ connections influences while computing the failure probabilities still does not have a practically suitable solution [6]. Thus, there are no simple solution to accounting of the connected blocks’ failure probabilities, which leads to major errors while computing the complex system’s failure probability changing with the passing of time. An

Table 4 During the system’s working time T are switched on and off depending on the external signal θ_i

k	1	2	3	4	5	6	...	K
θ_i	0	0	1	1	0	0	...	1
t_{ik}, h	0	0	10^4	2×10^4	2×10^4	2×10^4	...	$\Delta T(K - 1)/2$

analytical accounting of that fact in a complex system, even if we know the required (usually stochastic) dependencies, inevitably leads to complex computations. Thus, we propose a simplified approach to that problem.

We can perform the modelling discretely with some time step ΔT , which is set before the modelling. Thus the system's working time $T = k\Delta T$, where $k = 0, 1, \dots, K$, and K is the number of modelling steps, that we set a priori.

During the first modelling step ($k = 0$) the expected values of the blocks' parameters are known, and during the subsequent step in the time moments $k\Delta T$ we define the working time t_{ik} for each block, and by the Eq. (8) we compute the probabilities of correct work $P_{ci}(t_{ik})$ and their corresponding failure probabilities $P_{fi}(t_{ik}) = 1 - P_{ci}(t_{ik})$. Then, by the Eq. (9) with the usage of the table [5] or the approximate value of $\Phi(x)$ we calculate the expected values of the blocks' parameters $m_i(t_{ik})$.

During the modelling, on each step k for each i th block we calculate H values of random parameters ξ_{nih} with the normal distribution and the known expected value $m_i(t_{ik})$ and the root mean square σ_i . For this, we may calculate each parameter ξ_{nih} by the formula (11):

$$\xi_{ih}^n = m_i(t_{ik}) + \sigma_i \left(\sum_{j=1}^{12} \xi_j - 6 \right) \quad (11)$$

where ξ_j is a random number, equally distributed in the interval $[0; 1]$, which we may get using a standard random number generator.

Then we calculate the medium values of those parameters by the formula (12)

$$M_i(t_{ik}) = \left(\sum_{n=1}^H (\xi_{ih}^n) \right) / H \quad (12)$$

If the medium value $M_i(t_{ik})$ of some block's parameters in some time moment t_{ik} falls into a dangerous zone $d_i < |M_i(t_{ik})| < b_i$, we set the connections' coefficients $w(i)$ for this block, that signify the condition of the i th block, and $u(i)$, which signify the i th blocks' proximity to the failed and dangerous block. These parameters may be set as follows:

$w(i) = 0$ —failed, $w(i) = 2$ —dangerous, $w(i) = 1$ —normal

$u(i) = 0$ —dangerous is farther than over one, $u(i) = 1$ —dangerous is over one block,

$u(i) = 2$ —dangerous is connected, $u(i) = 3$ —dangerous is self.

Then we perform the expected value shift according to formula (13):

$$m_i^*(t_{ik}) = m_i(t_{ik}) + \sigma_i w(i) u(i) M_i(t_{ik}) \mu(M_i(t_{ik})) \quad (13)$$

where $m_i^*(t_{ik})$ is the shifted expected value of the i th block, $\mu(M_i(t_{ik}))$ is the membership function of the computed expected value to a certain interval, that is defined via the following rules:

$$\text{if } -\infty < M_i(t_{ik}) < -b_i + m_i(t_{i0}), \text{ then } \mu(M_i(t_{ik})) = 1$$

$$\text{if } -b_i + m_i(t_{i0}) \leq M_i(t_{ik}) < -d_i + m_i(t_{i0}),$$

$$\text{then } \mu(M_i(t_{ik})) = \max\{(M_i(t_{ik}) - m_i(t_{i0}) + d_i)/(d_i - b_i); (M_i(t_{ik}) - m_i(t_{i0}) + b_i)/(b_i - d_i)\}$$

$$\text{if } -d_i + m_i(t_{i0}) \leq M_i(t_{ik}) < m_i(t_{i0}),$$

$$\text{then } \mu(M_i(t_{ik})) = \max\{(M_i(t_{ik}) + m_i(t_{i0}))/d_i; (M_i(t_{ik}) - m_i(t_{i0}) + d_i)/d_i\}$$

$$\text{if } m_i(t_{i0}) \leq M_i(t_{ik}) < d_i + m_i(t_{i0}),$$

$$\text{then } \mu(M_i(t_{ik})) = \max\{(-M_i(t_{ik}) + m_i(t_{i0}) + d_i)/d_i; (M_i(t_{ik}) - m_i(t_{i0}))/d_i\}$$

$$\text{if } d_i + m_i(t_{i0}) \leq M_i(t_{ik}) < b_i + m_i(t_{i0}),$$

$$\text{then } \mu(M_i(t_{ik})) = \max\{(M_i(t_{ik}) - m_i(t_{i0}) - b_i)/(d_i - b_i); (M_i(t_{ik}) - m_i(t_{i0}) - d_i)/(b_i - d_i)\}$$

$$\text{if } b_i + m_i(t_{i0}) \leq M_i(t_{ik}) < \infty, \text{ then } \mu(M_i(t_{ik})) = 1$$

Then we set the j th block numbers, that are directly connected to the dangerous block, and for them set the coefficient values $w(j) = 1$, $u(j) = 2$, and also make the expected value shift, as in the formula (13), and calculate $\mu(M_j(t_{jk}))$ via the rules (1)–(6).

Then we define the numbers of q th blocks, that are connected to the found i th block over a single block, and for them we set $w(q) = 1$, $u(q) = 1$, and also make the expected value shift, as if in the formula (13), and calculate $\mu(M_q(t_{qk}))$ via the rules (1)–(6).

Now, if on the first modelling step ($k = 0$) after the expected value shift we'll have a block, which has its parameter absolute value more than the maximal allowed ($|m_i(t_{ik})| > b_i$), we consider such block failed, its failure probability is set to 1 ($P_{fi} = 1$), and the whole system's failure probability equals 1 ($P_f = 1$). Otherwise, we must calculate, based on the shifted expected values, the failure values on all the blocks by the formula (9), which is a simplified equivalent of the conditional probabilities computation. Afterwards we may calculate the failure probability of the whole system, using, for instance, the polynomial formula (6). We may increase the computation precision for each system by tuning the connections' coefficients w and u according to the experimental results.

During the next modelling steps ($k > 0$) by the computed failure probabilities values and their working time moments from the equations of type (8) we compute the new values of the decrease coefficients α_{ik} . Then, during the next time moment from the Eq. (8) we compute their failure probabilities, from the Eq. (9) we compute their expected values $m_i(t_{ik})$, compute new random values, etc.

Thus, in the proposed modelling method we reach the accounting of the connections with the dangerous situation by the discrete changing of the expected value of the current and the connected blocks, which allows accounting the blocks'

interconnections impact to the change in their failure probability. We may simplify the procedure even more, if we discretely alter the values of the decrease coefficients α_i .

4 Example of Modelling the System’s Failure Probability Modeling

Let us examine a system of four blocks, which scheme is depicted in the Fig. 1.

Let us assume, that all blocks work continuously, and that each block’s medium time before failure is 27,000 h, and the initial failure probability is 0.004. The time step value is 10,000 h.

After making five test modellings, we depicted the resulting data in the graph seen in the Fig. 2.

As you can see in the graph, the failure probability prediction in the simplest case is very stochastic, since a single random peak may cause the whole system’s instability. In the following chapters, we will show how to control the system’s vitality by applying various methods.

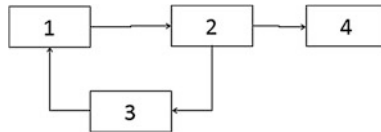


Fig. 1 Example system scheme

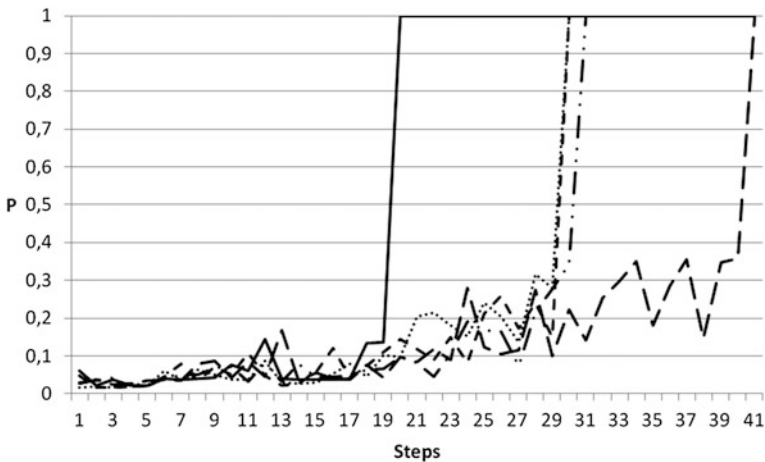


Fig. 2 System failure probability modelling

5 Conclusion

The proposed approach to the connections accounting method between the blocks of a complex system while modelling its failure probability with the passing of time allows accounting the impact of the connected blocks, thus increasing the failure probability prognosis.

We implemented the described algorithm as a C# computer program. We may increase the reliability and precision of the modelling by tuning the connection coefficients and the sampling intervals according to the running results and the prediction of the failure of existing systems.

References

1. Wenzl, E.S.: Theory of Probabilities. Nauka, Russian (1969)
2. Ryabinin, I.A.: Reliability and Safety of Structural Complex Systems. St.Petersburg, Polytechnic (2000)
3. Kulik, B.A.: Probabilistic logic bases on the algebra of the tuples. RAS (2007)
4. Gorodetsky, A.E.: Basics of Theory of Intelligent Control Systems. LAP Lambert Academic Publishing, Berlin (2011)
5. Beitman, G., Erdeii, A.: Higher Transcendental Functions. Nauka, Russian (1974)
6. Gorodetsky, A.E., Dubarenko, V.V.: Combinatory method of calculating the probability of complex logical functions JVM and MF (1999)
7. Gorodetsky, A.E., Kulik, B.A.: Calculating of the Probabilities of Logical Functions with the Logical Probabilistic Modelling of Complex Systems. SPbSTU Publishing, St.Petersburg (2010)
8. Kulik, B.A., Zuenko, A.A., Fridman, A.Y: Algebraic Approach to Intelligent Processing of Data and Knowledge. SPbSTU Publishing, St.Petersburg (2010)
9. Gorodetskiy, A.E., Tarasova, I.L.: Fuzzy Mathematical Modelling of Poorly Formalized Processes and Systems. SPbSTU Publishing, St.Petersburg (2010)

Methods of Dealing with Jamming in Automatic Control Systems of the Modules SEMS

A.E. Gorodetskiy, I.L. Tarasova and V.G. Kurbanov

Abstract The article discusses the following methods of dealing with seizure: using force sensors and logic block, using pickoffs and logic block, using calculation block of optimal trajectories. Describes circuit solutions that implement these methods. Analyzes the advantages and disadvantages of each method. The expediency of sharing each of the above methods to improve the survivability of ACS SEMS.

Keywords Architecture · Smart electromechanical systems · Intelligent robots

1 Introduction

In recent years, it is considered a very promising use of intelligent robots (IR) hexapod structure of the smart electromechanical systems (SEMS). Such structures allow to obtain maximum precision actuators with minimal travel time due to the introduction of parallelism in the process of measuring, calculating and movement [1]. In addition to the use of these systems, high-precision drives piezomotor capable of operating in extreme environments, significantly expands the scope of IR to use in outer space [2, 3].

However, in the standard modules (SM SEMS) such structures may occur a state where one or more legs actuators or of the control rods of the platform reconfig-

A.E. Gorodetskiy (✉) · I.L. Tarasova · V.G. Kurbanov
Institute of Problems of Mechanical Engineering, Russian Academy of Sciences,
Saint-Petersburg, Russia
e-mail: g27764@yandex.ru

I.L. Tarasova
e-mail: g17265@yandex.ru

V.G. Kurbanov
e-mail: vugar_borchali@yahoo.com

uration enter in jamming zone [4]. This may reduce the accuracy of control and damage the drives or gearboxes actuators.

The existing system of automatic control SM SEMS [5], as a rule, do not contain blocks ensure the prevention of possible jamming of the legs and the control rods of the electromechanical system, related primarily to the operation of electric desync. To solve this problem required a logical analysis of movements or efforts, or to solve the problem of choosing the optimal path of movement without jamming. In this case, the controller must be equipped with additional software and computing units complemented force sensors in the legs and the control rods. Then control system structure complicate, but the quality and reliability increase.

Usually, to fight jamming using low stringency, for example through the installation of springs in his legs and rods, as in hexapod company PI [6]. However, the reduced dynamic accuracy and performance of the ACS SM SEMS. However such a solution is not acceptable in many practical cases. Consider the other, free from this drawback, the possible options for preventing wedge ACS SM SEMS.

2 The Use of Force Sensors

Automatic control systems SM SEMS, usually contain: elongation calculating block (ECB), upper platform rods control block (UPRCB), lower platform rods control block (LPRCB), actuators legs control block (ALCB), upper platform rods motors block (UPRMB), lower platform rods motors block (LPRMB), actuators legs motors block (ALMB), upper platform rods reducers block (UPRRB), lower platform rods reducers block (LPRRB), actuators legs reducers block (ALRB), legs (L) of the SM SEMS, upper platform rods (UPR), lower platform rods (LPR), upper platform (UP), lower platform (LP), legs lengthening sensors block (LLSB), upper platform rods lengthening sensors block (UPRLSB), lower platform rods lengthening sensors block (LPRLSB), upper platform coordinates calculating block (UPCCB), lower platform force sensors block (LPFSB), upper platform force sensors block (UPFSB), legs force sensors block (LFSB) and Logic Block (LB) (Fig. 1).

System works as follows.

The ECB receives setpoints koodinat of the upper platform $x^3(t)$, $y^3(t)$, $z^3(t)$, $u^3(t)$, $V^3(t)$, $w^3(t)$ and setpoints radii of the upper and lower platforms $R_B^3(t)$, $R_H^3(t)$. Simultaneously, the ECB receives measured in the UPRLSB radius $R_B^T(t)$, measured in the LPRLSB radius $R_H^T(t)$ and calculated in the UPCCB current coordinates $x^T(t)$, $y^T(t)$, $z^T(t)$, $u^T(t)$, $v^T(t)$, $w^T(t)$ based on measurements extensions of legs measured in LLSB. From this information, ECB computes the required lengthening legs $\Delta L_i^3(t)$ and rods $\Delta R_{Bj}^3(t)$ and $\Delta R_{Hj}^3(t)$ and transmits them to the ALCB, UPRCB and LPRCB. At the same time, these blocks receive information on current values of lengthening $\Delta L_i^T(t)$, $\Delta R_{Bj}^T(t)$, $\Delta R_{Hj}^T(t)$.

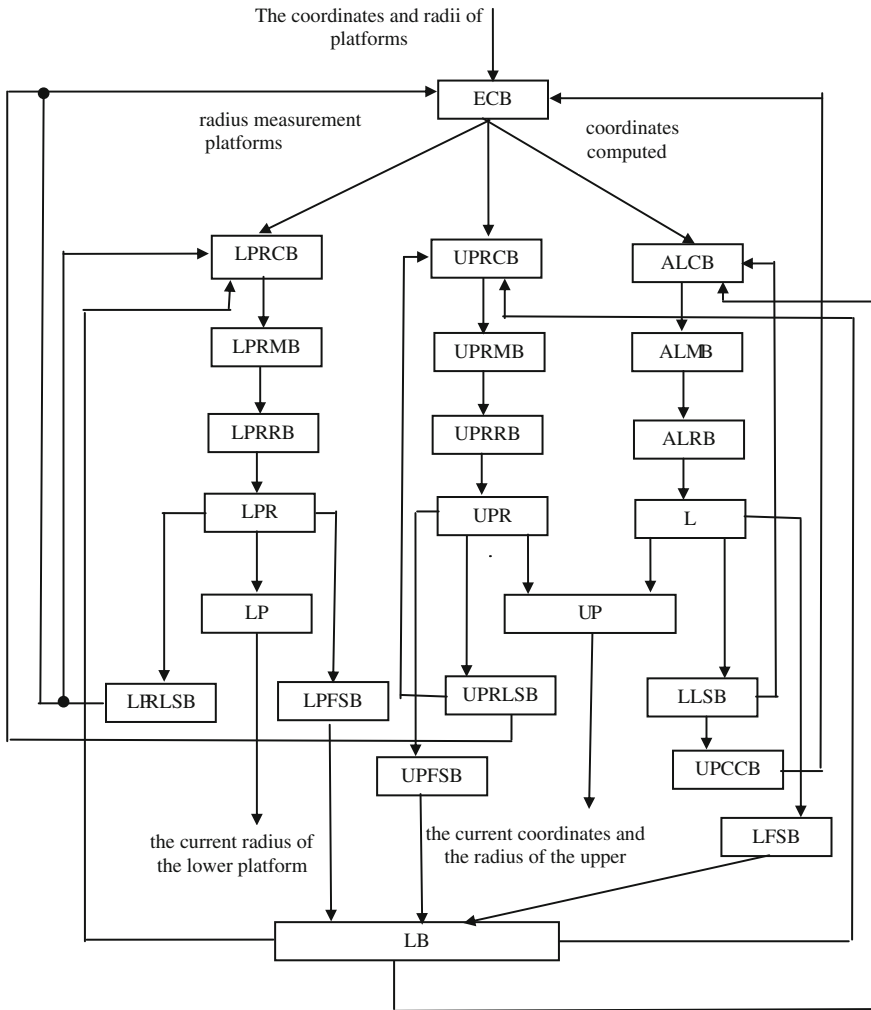


Fig. 1 Blok-scheme ACS to the logic block and force sensors

ALCB calculates an error: $e_i(t) = (\Delta L_i^3(t) - \Delta L_i^T(t))$ and control action:

$$U_i(t) = k_{1i}e_i(t) + k_{2i} \int e_i(t)dt + k_{3i} \frac{de_i(t)}{dt}$$

They are served in ALDB that performs through ALRB elongation of legs (L) and a corresponding change in the coordinates of the upper platform (UP).

UPRCB calculates an error: $e_{ej}(t) = (\Delta R_{Bj}^3(t) - \Delta R_{Bj}^T(t))$ and control action:

$$U_{ej}(t) = k_{1e} e_{ej}(t) + k_{2e} \int e_{ej}(t) dt + k_{3e} \frac{de_{ej}(t)}{dt}$$

They served in UPRDB, which performs through UPRRB elongation of rods upper platform (UP) and the corresponding change in the radius UP.

LPRCB calculates an error: $e_{ej}(t) = (\Delta R_{Bj}^3(t) - \Delta R_{Bj}^T(t))$ and control action:

$$U_{ej}(t) = k_{1e} e_{ej}(t) + k_{2e} \int e_{ej}(t) dt + k_{3e} \frac{de_{ej}(t)}{dt}$$

They served in LPRDB, which performs through LPRRB elongation of rods lower platform (LP) and the corresponding change in the radius LP.

To prevent jams in this case, the actuator rods and legs of the upper and lower platforms are set corresponding force sensors. They are combined in force legs sensors block (FLSB), force upper platform sensors block (FUPSB) and force lower platform sensors block (FLPSB) (see Fig. 1). The signals from these blocks served in the logic block (LB). It is designed to calculate the variables ξ_i , ξ_{Uj} and ξ_{Lj} equal to either 0 or 1. These signals allow the exclusion of dangerous tension in the legs and rods by zero error, calculated in ALCB, UPRCB and LPRCB:

$$\begin{aligned} e_i(t) &= (\Delta L_i^3(t) - \Delta L_i^T(t)) \xi_i, \\ e_{ej}(t) &= (\Delta R_{Bj}^3(t) - \Delta R_{Bj}^T(t)) \xi_{Bj} \\ e_{ej}(t) &= (\Delta R_{Hj}^3(t) - \Delta R_{Hj}^T(t)) \xi_{Hj} \end{aligned}$$

Work LB is reduced to verify the type of logical rules:

- (1) If $F_i > F_{di}$, the $\xi_i = 0$, otherwise $\xi_i = 1$,
where: F_i —measured LFSB of force in the i th leg, F_{di} —permissible force
- (2) If $F_{Bj} > F_{dj}$, the $\xi_{Bj} = 0$, otherwise $\xi_{Bj} = 1$,
where: F_{Bj} —measured UPPFSB of force in the j th rod of the upper platform, F_{dj} —permissible force
- (3) If $F_{Hj} > F_{dj}$, the $\xi_{Hj} = 0$, otherwise $\xi_{Hj} = 1$,
where: F_{Hj} —measured LPPFSB of force in the j th rod of the lower platform, F_{dj} —permissible force

This approach makes it easy to avoid jams. However, this complicates the design and ensures smooth movement of the platform along a predetermined path. In some cases, when the requirements for ACS on the dynamics and accuracy is not high, can be used current sensors in electric motors.

3 Use of Pickoffs

In this case, LB uses signals $l_i(t)$, $l_j(t)$ with a displacement sensor located in the legs and signals $R_{vi}(t)$, $R_{vj}(t)$, $R_{ni}(t)$, $R_{nj}(t)$ with a displacement sensor located in rods. These signals are received in LP from LLSB, UPRLSB and LPRLSB (see Fig. 2).

LB checks the following logical rules for the feet:

If the i th leg lengthens ($l_i(t) > l_i(t - 1)$) and j th—lengthens ($l_j(t) > l_j(t - 1)$) and $\Delta > \delta$ and $l_i > l_j$, then $\xi_i = 0$, $\xi_j = 1$

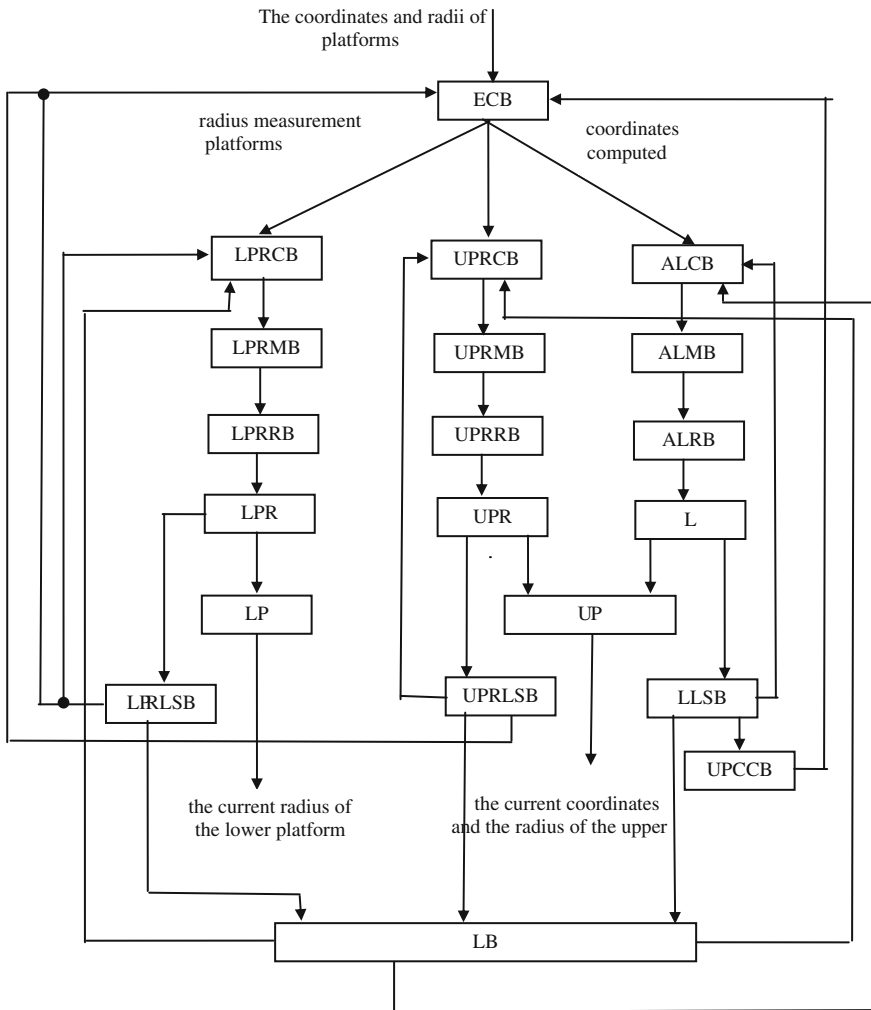


Fig. 2 Blok-scheme ACS to the logic block and displacement sensors

If the i th leg lengthens ($l_i(t) > l_i(t-1)$) and j th lengthens ($l_j(t) > l_j(t-1)$) and $\Delta > \delta$ and $l_i < l_j$, then $\xi_i = 1$, $\xi_j = 0$

If the i th leg lengthens ($l_i(t) > l_i(t-1)$) and j th—shortens ($l_j(t) < l_j(t-1)$) and $\Delta > \delta$ and $l_i(t) - l_i(t-1) > l_j(t-1) - l_j(t)$ then $\xi_i = 0$, $\xi_j = 1$

If the i th leg lengthens ($l_i(t) > l_i(t-1)$) and j th—shortens ($l_j(t) < l_j(t-1)$) and $\Delta > \delta$ and $l_i(t) - l_i(t-1) < l_j(t-1) - l_j(t)$ then $\xi_i = 1$, $\xi_j = 0$

If the i th leg shortens ($l_i(t) < l_i(t-1)$) and j th—lengthens ($l_j(t) > l_j(t-1)$) and $\Delta > \delta$ and $l_i(t-1) - l_i(t) > l_j(t) - l_j(t-1)$ then $\xi_i = 0$, $\xi_j = 1$

If the i th leg shortens ($l_i(t) < l_i(t-1)$) and j th—lengthens ($l_j(t) > l_j(t-1)$) and $\Delta > \delta$ and $l_i(t-1) - l_i(t) < l_j(t) - l_j(t-1)$ then $\xi_i = 1$, $\xi_j = 0$

If the i th leg shortens ($l_i(t) < l_i(t-1)$) and j th—shortens ($l_j(t) < l_j(t-1)$) and $l_i, l_j < 0$ and $\Delta > \delta$ and $l_i > l_j$ then $\xi_i = 0$, $\xi_j = 1$

If the i th leg shortens ($l_i(t) < l_i(t-1)$) and j th—shortens ($l_j(t) < l_j(t-1)$) and $l_i, l_j < 0$ and $\Delta > \delta$ and $l_i < l_j$ then $\xi_i = 1$, $\xi_j = 0$

At the same time, the following designations: Δ —module of length difference of adjacent actuators, l_i, l_j —leg lengthening i and j , δ —admission to the module deformation, $\xi_i = 0$ stop the i th motor, $\xi_i = 1$ —the work of the i th motor.

For rods rules easier:

If $R_{Bj}^T(t) > R_{Bi}^T(t)$, then $\xi_{Bj} = 0$ и $\xi_{Bi} = 1$

If $R_{Bi}^T(t) > R_{Bj}^T(t)$, then $\xi_{Bi} = 0$ и $\xi_{Bj} = 1$

If $R_{Bj}^T(t) = R_{Bi}^T(t)$, then $\xi_{Bj} = 1$ и $\xi_{Bi} = 1$

If $R_{Hj}^T(t) > R_{Hi}^T(t)$, then $\xi_{Hj} = 0$ и $\xi_{Hi} = 1$

If $R_{Hi}^T(t) > R_{Hj}^T(t)$, then $\xi_{Hi} = 0$ и $\xi_{Hj} = 1$

If $R_{Hj}^T(t) = R_{Hi}^T(t)$, then $\xi_{Hj} = 1$ и $\xi_{Hi} = 1$

These values $\xi_i, \xi_j, \xi_{Bi}, \xi_{Bj}, \xi_{Hi}$ and ξ_{Hj} equal to either 0 or 1 as in the previous case, enter the blocks ALCB, UPRCB and LPRCB. This allows the exclusion of dangerous tension in the legs and rods by zero error, calculated in these blocks.

The proposed approach also allows you to avoid jams. However, the accuracy and reliability of LB in this case highly dependent on the tolerance given by δ . To improve the situation may be setting the tolerance δ . To do this, you can apply the following algorithm to select δ with ballroom ratings B_i and preference factor K_j .

Choosing δ for which $J = K_1 * B_1 + K_2 * B_2$ there is max. At the same time let:

If $\delta = 1$, then maximum accuracy and $B_1 = 5$

If $\delta = 2$, then average accuracy and $B_2 = 3$

If $\delta = 3$, then the accuracy of small and $B_3 = 1$

If $\delta = 1$, then low reliability; $B_1 = 1$

If $\delta = 2$, the reliability of the average; $B_2 = 3$

If $\delta = 3$, then the maximum reliability; $B_3 = 5$

Now, we got some prefer the reliability, we believe $K_1 = 1$; $K_2 = 2$. Therefore $J = 1 * 1 + 2 * 5 = 11$ —is max, if $\delta = 3$. This value δ we set in LB.

Illogical if we got some prefer the accuracy, we believe $K_1 = 2$; $K_2 = 1$. Therefore $J = 2 * 5 + 1 * 1 = 11$ —is max, if $\delta = 1$. This value δ we set in LB.

In this method the same can not be guaranteed smooth movement of the platform along a predetermined path.

4 Using a Calculation Block of Optimal Trajectories

In this case ECB does not calculate the required leg lengthening $\Delta L_i^3(t)$ and rods $\Delta R_{B_j}^T(t)$ and $\Delta R_{H_j}^T(t)$, but determines the optimum path (smooth and without jamming) to move from the current location coordinates $x^T(t)$, $y^T(t)$, $z^T(t)$, $u^T(t)$, $v^T(t)$, $w^T(t)$ and radii $R_H^T(t)$, $R_B^T(t)$ at predetermined coordinates $x^3(t)$, $y^3(t)$, $z^3(t)$, $u^3(t)$, $v^3(t)$, $w^3(t)$ and radii $R_H^T(t)$, $R_B^T(t)$. Preparation of these paths is complicated and time-consuming task that may be performed in various ways [7].

In this method, it is advisable to pre-beta stage to create a matrix of jamming, which correspond to the forbidden path. Then we do not need real-time to produce additional complicated calculations, thus increasing the speed of control computation. However, this requires a large number of calculations in the design and debugging. The same issue is complicated by the fact that the first payment made under the theoretical parameters of the device with the load. Unfortunately, the manufacture and assembly inaccuracies allowed, which can not be accounted for in the calculations. This leads to possible cases when not all of the zones described in Table jamming and it is necessary to correct in the debugging process. Also, during use of the device may experience uneven development of the individual actuators in the uneven load. This can adversely affect safety. The latter would require an adjustment of the table jams in the operation of high-precision systems. In addition, this method does not prevent jamming with significant differences in the dynamic characteristics of the automatic control system for the individual legs and rods. Accordingly, this method of dealing with jamming suitable for use in conjunction with 1 or 2 methods.

5 Conclusion

Each of the considered methods of combating jamming has its advantages and disadvantages. If you want high-precision electromechanical system based on parallel kinematics, the most accurate and reliable method is to duplicate the system calculate the optimal trajectory logic block to prevent jamming, analyzing the measured force or pressure sensors, or the measured linear displacement and elongation.

Using neuroprocessors considered in the automatic control system will allow to parallelize the process of calculating the control actions and signaling adaptation

SM SEMS. This improves the speed and accuracy of control. The main computational element of such a system can be neuroprocessor designed to handle 32-bit scalar data and a programmable bit packed in 64-bit words. In neuroprocessor software implements the functions of the main blocks. Using a force sensor to simplify the neural algorithms and improve the accuracy of the calculation. The accuracy of position sensors used in SM SEMS will determine the maximum achievable positioning accuracy, and their time of conversion-performance.

References

1. Merlet, J.-P.: *Parallel Robots*, 2nd edn, p. 383. Springer, INRIA, Sophia-Antipolis, France (2006)
2. Agapov, V.A. (RU), Gorodetskiy, A.E. (RU), Kuchmin, A.J. (RU), Selivanova, E.N. (RU): Medical microrobot. Patent RU, no. 2469752 (2011)
3. Artemenko, J.N., Agapov, V.A., Dubarenko, V.V., Kuchmin, A.J.: Group control of radiotelescope subdish actuators. *Informatsionno-upravliaiushchie sistemy* **4**(59), 2–9 (2012). (In Russian)
4. Yangulov, V.S.: *Designing Programs with Linear Movement of the Output Link: Tutorial*, 169 p. Publishing house of Tomsk Polytechnic University, Tomsk (2011)
5. Gorodetskiy, A.E., Tarasova, I.L., Kurbanov, V.G.: Automatic Control System SEMS. (in this volume)
6. Gorodetskiy, A.E., Artemenko, J.N., Dubarenko, V.V., Tarasova, I.L., Kuchmin, A.J.: Problems of creation of systems of adaptation of space radio telescopes. *Informatsionno-upravliaiushchie sistemy* **3**(46), 2–8 (2010)
7. Glazunov, V.A., Phong, H.X., Nguyen Van, H., Nguyen Van, D.: Multi-criteria optimization of the parameters of the executive system of parallel structures. *J. Eng. Phys.* **2**, 3–6 (2008) (Moscow, MIFI)

Expert System for Condition Estimation of a Faulty SEMS Module

V.Y. Ziniakov

Abstract We propose an automated expert system used to vitality improvement of an SM SEMS (Standard Module of Smart ElectroMechanic System). We describe two working modes: the supervising mode and the prognosis mode.

Keywords Expert system · SEMS module · Failure probability

1 Introduction

By creating an expert system, which issues recommendations about the changes in the working SEMS system to the operator, we can increase the system's vitality, and to perform in-before planning of the needed preventive actions, based on the system's degradation and failure modellings' results. In this article, we propose an expert system, which is suitable for vitality improvement in a vast array of complex systems. The expert system can function in two modes, namely the collecting and analysis of the exploited system's data in real-time mode, and the failures' prognosis while modelling the complex system's behavior.

The research object in this work is SM2 SEMS (hexapod), which is used in numerous scientific and industrial systems, such as the radio telescopes RT-70 (currently being built on the Suffa plateau in Uzbekistan) [1], "Millimetron" which is used in open space [2], the space radio telescope James Webb [3] and many others.

V.Y. Ziniakov (✉)

Saint-Petersburg Polytechnic University, Saint-Petersburg, Russia
e-mail: vziniakov@gmail.com

2 SEMS Module Structure

SM SEMS, Standard Module of Smart ElectroMechanic System, is used for controlled relocation of its upper platform, equipped with six-axis positioning system, and the controlling block. We perform the movement of the platform by six mutually independent precision engines of the SEMS module limbs' actuators. This allows us to perform the positioning by three linear (X, Y, Z) and three angular coordinates (that is, we can rotate the upper module's platform around the Ox, Oy, and Oz axis). In Fig. 1, we can see a scheme of a common SEMS module, known as hexapod. Its main structural parts are [4]:

MC is Main Controller

LP is Lower Platform

UP is Upper Platform

C1–C6 are Controllers

E1–E6 are Engines

R1–R6 are Reducers

LJ1–LJ6 are Lower Joints

UJ1–UJ6 are Upper Joints

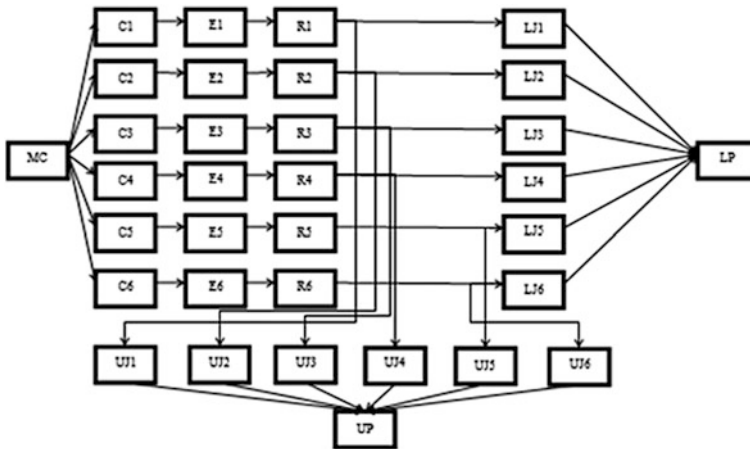


Fig. 1 SEMS hexapod scheme

3 Failure Examples for SEMS Modules Condition Estimation

In this work, we measure the following SM SEMS block parameters:

Main controller: signal level

Controllers: signal level

Engines: voltage, rotation velocity

Reducers: rotation velocity, mechanical stress

Lower and upper joints: mechanical stress, deformation

Lower and upper platforms: linear coordinates, angular coordinates.

4 Expert System Structural Scheme

In this work, we developed and used a problem-oriented expert system. It consists of the following modules, displayed in the Fig. 2: knowledge base (KB), database (DB), recommendation base (RB), logical derivation machine (LDM), controllers used for connection to the controlling hardware (C), imitational model (IM), human-machine interface (HMI), controlled object (CO), and sensorial data measurement system (SDMS).

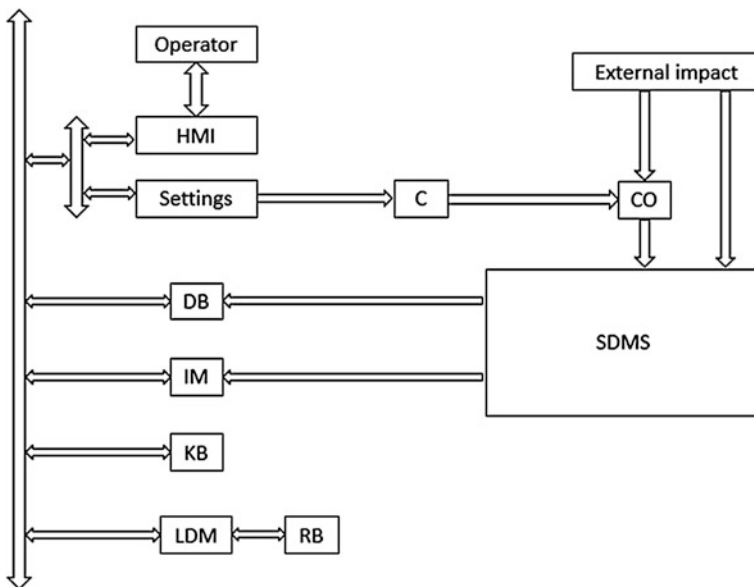


Fig. 2 Expert system scheme

The knowledge base should contain the knowledge about the controlled object's dynamics, the interval of the input and disturbing signals, and the recommendations from the recommendation base. The recommendation base should contain the set of recommendations that the system displays to the operator. The database should contain the data about the control targets, the system's blocks' current states.

The logical derivation machine should allow the selection of a recommendation from the recommendation base in the real-time mode.

In this work, we used the system with hard logic. In it, the knowledge base is read-only, and the task of the expert system is to make the logical derivation machine to function optimally by logically analyzing the data that we acquire from the hardware-connected controllers and the database. In this system, the knowledge base is a set of rules that we create while initializing the expert system. This set is constant while the expert system is functioning. The logical derivation machine analyses these rules using the data from the database (which we update through the hardware-connected controllers), and takes a decision about outputting a recommendation to the operator. If needed, the operator may input a command through the human-machine interface.

While the expert system is functioning in the modelling mode, the logical derivation machine may select a recommendation while comparing the data received from the hardware with the data from the imitational model. In this case, we add an imitational model block to the expert system, and connect it to the other blocks [5].

We developed the software part of this expert system in C# programming language. It contains the altering set of structured interlinked entities, which the program loads into RAM while expert system is working. There are the following types of entities:

Complex system contains the formalized data of the exploited complex system.

Block contains the data of the complex system's block.

Parameter describes the block's technical parameter, which we measure (or model) while the expert system is working.

Rule describes the rule of the expert system. It contains the parameter's threshold value, and the recommendation, which we output to the operator.

5 Expert System Functioning Algorithm

Our expert system can function in two modes: the supervising mode and the prognosis mode.

In **supervising mode**, on each step k the expert system receives the current values of the j th parameters of the i th blocks through the hardware-connected controllers. Then we calculate the expected value $m(i, j, k)$ of the current parameter according to formula $m(i, j, k) = \sum_{l=k-n}^k x(i, j, l) / (n + 1)$, where $n \approx 100$ and is

dependent on the block's technical parameters. If the resulting expected value exceeds the threshold value of some expert system's rule, we output the recommendation of this rule to the operator.

In **prognosis mode**, the expert system receives the value $m(i, j, k)$ from the hexapod's mathematical model. The algorithm that we use is described in the chapters [6] and [7]. As it is in the supervising mode, if the resulting expected value exceeds the threshold value of some expert system's rule, we output the recommendation of this rule to the operator.

Rules of the expert system

For each of the SM SEMS hexapod's measured parameters, we created two expert system's rules.

If the parameter's value falls into the "dangerous" interval, we output the recommendation message "Please check the parameter <parameter_name> of the block <block_name> and take the preventive measures, if needed."

If the parameter's value falls into the "critical" interval, we output the recommendation message "The value of the parameter <parameter_name> of the block <block_name> is critical. Please stop the system immediately!"

6 Expert System Testing Results

Below is the log of the expert system's typical usage, with the computer model of the described hexapod. In the log, k is the step number, while P is the system's failure probability in the beginning of the step k .

The starting block parameters are the following: medium time between failures is 27,000 h, the initial failure probability is 0.004, the modelling step value is 1000 h. We stop the modelling when a block's parameter value falls into the critical interval, providing that the block doesn't have a spare one.

($k = 1; P = 0.19$), ($k = 2; P = 0.20$), ($k = 3; P = 0.21$), ($k = 4; P = 0.24$), ($k = 5; P = 0.21$)

Please check the parameter "mechanical stress" of the block "Upper joint 4" and take the preventive measures, if needed

($k = 6; P = 0.20$), ($k = 7; P = 0.23$), ($k = 8; P = 0.23$), ($k = 9; P = 0.22$), ($k = 10; P = 0.20$), ($k = 11; P = 0.17$), ($k = 12; P = 0.22$), ($k = 13; P = 0.21$), ($k = 14; P = 0.19$)

Please check the parameter "mechanical stress" of the block "Upper joint 5" and take the preventive measures, if needed

Changing the block "Reducer 3"

($k = 15; P = 0.18$)

Changing the block "Controller 2"

Changing the block "Reducer 6"

$(k = 16; P = 0.22)$, $(k = 17; P = 0.22)$, $(k = 18; P = 0.19)$, $(k = 19; P = 0.24)$

Please check the parameter “mechanical stress” of the block “Reducer 4” and take the preventive measures, if needed

Changing the block “Engine 6”

$(k = 20; P = 0.25)$

Please check the parameter “controlling signal” of the block “Controller 2” and take the preventive measures, if needed

$(k = 21; P = 0.27)$, $(k = 22; P = 0.28)$

Please check the parameter “controlling signal” of the block “Controller 3” and take the preventive measures, if needed

Please check the parameter “controlling signal” of the block “Controller 4” and take the preventive measures, if needed

$(k = 23; P = 0.25)$, $(k = 24; P = 0.30)$

Please check the parameter “angular coordinates” of the block “Upper platform” and take the preventive measures, if needed

Please check the parameter “rotation velocity” of the block “Reducer 2” and take the preventive measures, if needed

Please check the parameter “rotation velocity” of the block “Reducer 5” and take the preventive measures, if needed

$(k = 25; P = 0.25)$, $(k = 26; P = 0.30)$, $(k = 27; P = 0.27)$, $(k = 28; P = 0.29)$, $(k = 29; P = 0.29)$, $(k = 30; P = 0.30)$, $(k = 31; P = 0.32)$

Please check the parameter “rotation velocity” of the block “Engine 6” and take the preventive measures, if needed

$(k = 32; P = 0.30)$, $(k = 33; P = 0.31)$, $(k = 34; P = 0.34)$

Please check the parameter “mechanical stress” of the block “Lower joint 6” and take the preventive measures, if needed

$(k = 35; P = 0.34)$, $(k = 36; P = 0.33)$

Please check the parameter “deformation” of the block “Lower joint 4” and take the preventive measures, if needed

$(k = 37; P = 0.34)$

Please check the parameter “voltage” of the block “Engine 1” and take the preventive measures, if needed

Please check the parameter “rotation velocity” of the block “Engine 5” and take the preventive measures, if needed

Changing the block “Controller 5”

($k = 38$; $P = 0.36$)

Please check the parameter “rotation velocity” of the block “Engine 2” and take the preventive measures, if needed

Changing the block “Reducer 2”

Changing the block “Upper joint 5”

($k = 39$; $P = 0.40$)

Please check the parameter “rotation velocity” of the block “Reducer 2” and take the preventive measures, if needed

Please check the parameter “mechanical stress” of the block “Upper joint 1” and take the preventive measures, if needed

Please check the parameter “mechanical stress” of the block “Upper joint 5” and take the preventive measures, if needed

Please check the parameter “deformation” of the block “Upper joint 6” and take the preventive measures, if needed

Changing the block “Reducer 5”

($k = 40$; $P = 0.36$)

Please check the parameter “mechanical stress” of the block “Reducer 5” and take the preventive measures, if needed

($k = 41$; $P = 0.35$)

Please check the parameter “rotation velocity” of the block “Reducer 1” and take the preventive measures, if needed

Please check the parameter “deformation” of the block “Lower joint 3” and take the preventive measures, if needed

The value of the parameter “mechanical stress” of the block “Reducer 6” is critical. Please stop the system immediately!

The value of the parameter “rotation velocity” of the block “Reducer 6” is critical. Please stop the system immediately!

7 Conclusion

We developed an expert system, which works with a SEMS module in two modes: the supervising mode and the prognosis mode. In automated mode, it allows to define and predict the occurrences of critical situations. We performed a testing run of the developed expert system, which showed its functionality and effectiveness.

References

1. Radio telescope RT-70 of the Suffa international radio astronomical observatory. <http://www.radioastron.ru/index.php?dep=16>
2. Artemenko, Y.N., Gorodetskiy, A.E., Doroshenko, M.S., Konovalov, A.S., Kuchmin, A.Y., Tarasova, I.L., Dubarenko, V.V.: System of automatic control of the Millimetron space radio telescope counter-reflector. In: Russian astronomic conference (VAK-2010), 13–18 Sept 2010, Nizhny Arkhyz, SAO RAS
3. James Webb Space Telescope (JWST) NASA. <http://www.jwst.nasa.gov>
4. Gorodetskiy, A.E., Tarasova, I.L., Kurbanov, V.G., Agapov, V.A.: Mathematical model of the automatic control system of a SEMS module. *Inf. Control Syst.* 3 (2015)
5. Tarasova, I.L., Gorodetskiy, A.E.: Control and Neural Networks, pp. 15–18. Polytechnic university publishing, Saint Petersburg (2005)
6. Ziniakov, V.Y., Tarasova, I.L., Gorodetskiy, A.E.: Part 4: Control of Vitality and Reliability Analysis (In this volume)
7. Ziniakov, V.Y., Tarasova, I.L., Gorodetskiy, A.E.: Part 4: System Failure Probability Modeling (In this volume)

Part V
Information-Measuring Soft
and Hardware

SEMS-Use Platform with a Matrix Receiver for Obtaining the Radio Images of Astronomy

A.E. Gorodetskiy, V.G. Kurbanov and I.L. Tarasova

Abstract Proposed to estimate the optimal size of pixels and the algorithm to adapt to different modes of matrix receivers. Describes the control system of adaptive matrix receivers.

Keywords Matrix detector · The optimal pixel size · Adaptation algorithm · The control system

1 Introduction

Recently, the problems of developing the new methods and means of “radio imaging”, i.e. conversion of received radio waves into optical images, have drawn much attention. Such systems are being developed for both applied problems (e.g. navigation) and astronomy [1–3]. However, to receive the radio image of some area by means of the antenna with the point receiver it is necessary to observe consecutively separate sites. Therefore, recently it is offered to use the matrix receiver which will allow seeing all the area entirely and at once. The advantages of such approach are obvious. First, in principle in N times (N -number of pixels), at the same signal/noise relation, we save the time of observation which is always limited. Second, if a source is variable, by consecutive mapping we receive a picture which won't adequately reflect the condition of the object for the given period of time.

A.E. Gorodetskiy (✉) · V.G. Kurbanov · I.L. Tarasova
Institute of Problems of Mechanical Engineering,
Russian Academy of Sciences, Saint-Petersburg, Russia
e-mail: g27764@yandex.ru

V.G. Kurbanov
e-mail: vugar_borchali@yahoo.com

I.L. Tarasova
e-mail: g17265@yandex.ru

It is possible to specify a number of matrix receivers already used in radio astronomy. For example, the 1.3 mm receiver of National radio-astronomical observatory of the USA, representing an array of 2×4 SIS receivers with the general heterodyne and a quasi-optical input [4]. A system with a little higher level of integration where there is a uniform reception module with seven irradiators, the waveguide SIS-mixers and IFA created at Chalmers University of Technology (SISYFOS project [5]). JPL (CalTech) create quasi-optical systems for 230 and 492 GHz on the basis of an array consisting 2×5 SIS-transitions integrated with dipolar antennas and placed on flat surface of a parabolic quartz lens with the metalized parabolic surface [6]. The similar device on the basis of Schottky-barrier diode and hyper hemispherical lens was created about 15 years ago in R&D Salyut and successfully tested in Institute of Applied Physics of the Russian Academy of Sciences [7].

For the successful solution of the problem finding objects of observation necessary to carry out its capture field of view matrix receiver with subsequent focus, i.e. you need to quickly and accurately scan, followed by moving the center of the matrix in the focus of the dish telescope. This is usually done via the subdish. However, for large radio telescopes to achieve the desired accuracy and speed of scanning is very difficult [8]. It is therefore proposed to establish a matrix receiver on the platform SEMS and to scan directly by the receiver. Thus there is a fast and precise scanning with simultaneous focusing.

Thus, the use of matrix receivers for radio imaging is topical and expedient, but at the same time there is a number of problems related to the compromise between the resolution ability of a radio telescope and the time of accumulation of the signal providing the desired sensitivity. These problems are going to be considered here in detail.

2 The Problems of Creation of Radio Wave Matrix Receiver

The problems of creation of radio wave matrix receiver are significantly different for the bolometric receivers, used for measurements in continuous spectrum, and for heterodyne receivers which are used for spectral measurements. It is much simpler to create an array of bolometers with a large number of elements than a matrix heterodyne receiver, as in the latter case we would need one heterodyne for all channels. And as the power of heterodyne is always limited, and the number of channels cannot be increased to some and quite modest value ($\sim 10-15$), unlike arrays of bolometers where the number of elements has already reached ~ 100 and more [1].

Other problem specific to heterodyne arrays is connected with processing of signals at spectral measurements as here a parallel spectrum analyzer has to be attached to each element. And this device is bulky and expensive. This

circumstance also limits possibilities of accumulating higher number of elements in a heterodyne matrix receiver.

The next problem concerns cooling of receivers. Modern highly sensitive receivers work at ultra-low temperatures to decrease their own noise. Heterodyne receivers demand cooling to ~ 4.5 K. Such temperatures are reached when cooling is done by means of liquid helium. But the long-term use of deluge systems for radio telescope is inconvenient and expensive. Therefore, close-cycle cooling systems are implemented here more often. Their cooling capacity doesn't exceed 1–1.5 W that also limits possibilities of accumulating higher number of elements of a receiver. Bolometers work at lower temperatures, ≤ 0.3 K. Such temperatures are carried out in cooling systems based on helium isotope.

The optical scheme of matrix receivers has to provide formation of the necessary directional pattern of each element, their rather dense “packing”, minimum level of cross-polarizing component, and, if possible, long time of accumulation, etc. Calculation of the quasi-optical scheme is usually conducted on the basis of the theory of Gaussian bunches. At that, there is a problem with “packing” of the irradiators placed usually in the focal plane of the antenna. On the one hand, for receiving a full *in the sense of Nyquist* selection, irradiators have to be located at distances:

$$l_0 \leq \lambda F / 2D, \quad (1)$$

where

F effective focal length,

D diameter of the antenna,

and the pixel sizes of a matrix for ensuring the maximum resolution have to correspond to the width of directional pattern in the focal plane H which depends on wavelength and diameter of

$$H \sim \lambda / d_a \quad (2)$$

where

d_a the size of aperture (mouth) of the antenna.

However, for optimum radiation of the antenna the sizes of loud-hailers have to be several times bigger, and for providing sufficient time of accumulation and, accordingly, higher sensitivity of pixels, their sizes have to be several times bigger than width of the directional pattern as well. So, for example, from the amplitude-frequency characteristic received experimentally on RT-70 in Yevpatoria by Postnikov Yu. V., research worker of Saint Petersburg Electrotechnical University “LETI”, (see Fig. 1) it is visible that for ensuring accumulation of a signal on pixel in the course of supervision upon a dot source, i.e. for providing a condition where its image cannot leave the limits of a pixel, the sizes of pixels as $l \approx 10 H$ are required. Besides, in Fig. 1 one can see that amplitude of fluctuations depends on an antenna elevation angle, and also on a design of the antenna and parameters of the

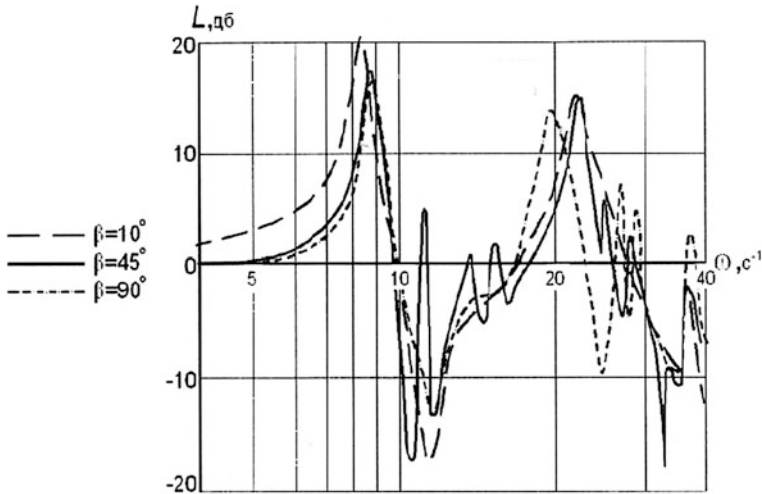


Fig. 1 The amplitude-frequency characteristic of RT-70 in Yevpatoria

system of automatic control over antenna drives, i.e. own frequencies ω . Therefore, for ensuring high efficiency of use of matrix receivers for obtaining radio images in astronomy, first of all it is necessary to solve a problem of an optimum choice of pixels sizes taking into consideration an elevation angle and a wavelength of radiation; and this problem can be solved through a compromise between the specified requirements and adaptations of the matrix receiver to the current values of an elevation angle and a wavelength of the radiation accepted by this antenna.

Let us consider one of the solutions of the specified problem.

3 Assessment of the Optimum Pixel Sizes of Matrix Receivers

One of the reasons why we use the intensity of fluctuation of focus in the focal plane of the radiation receiver as an assessment of the optimum pixel size for receiving the maximum time for accumulation and, accordingly, sensitivity of the receiver can be the fact that the radiation wave activity upon a receiver is defined, as a rule, by its intensity I , i.e. a time-average value of density of energy flux [8]. Therefore, as the maximum pixel size of the matrix receiver it is reasonable to take the following:

$$l_{\max} = \sqrt{2I}, \quad (3)$$

where

$$I = \frac{1}{T} \int_{-\frac{T}{2}}^{\frac{T}{2}} i^2(t) dt, \quad (4)$$

$i(t)$ fluctuation of focus of the antenna in the course of its functioning,

T period of fluctuation of focus of the antenna in the course of its functioning.

It is usually possible to consider that for dual reflector antenna

$$T = \frac{4\pi^2}{\omega_1\omega_2}, \quad (5)$$

where

ω_1 and ω_2 frequencies of the first tones of fluctuations of a main mirror and a counter-reflector respectively

Then, fluctuation of the focus of a dual reflector antenna can be expressed, as a first approximation, through fluctuations of edges of a main dish and a subdish as follows:

$$i(t) = k_z a_1 \sin \omega_1 t + k_r a_2 \sin(\omega_2 t + \varphi), \quad (6)$$

where

a_1 , amplitudes of fluctuations of edges of a main dish and a subdish respectively,

φ phase shift between fluctuations of edges of a main dish and a subdish,

k_z fluctuations of focus-fluctuation of edge of a main dish dependency coefficient, and

k_r fluctuations of focus-fluctuation of edge of a subdish dependency coefficient.

Coefficients k_z and k_r can be expressed

$$k_z = \frac{\sin \psi_1}{\sin \psi_3} \quad (7)$$

$$k_r = \frac{2 \sin \psi_2}{\sin \psi_3}, \quad (8)$$

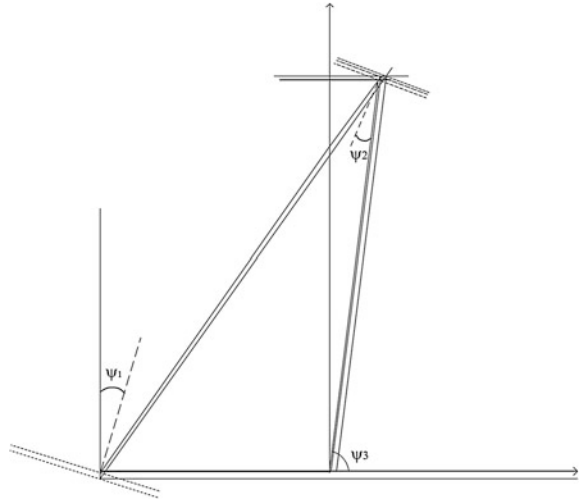
where

ψ_1 a radiation descent angle on edge of a surface of a Main Dish (MD),

ψ_2 a radiation descent angle on edge of a surface of a SubDish (SD),

ψ_3 a radiation descent angle of edge of a SD surface on the focal plane.

Fig. 2 Path of rays



Angles ψ_1, ψ_2, ψ_3 are calculated through antenna parameters as follows (see Fig. 2):

$$\psi_1 = \frac{1}{2} \arctg \left(\frac{D}{2(F_z - h)} \right), \tag{9}$$

where

- F_z focal length of a main dish,
- h depth of a main dish,
- D diameter of a main dish of the antenna.

$$\psi_2 = \psi_1 - \frac{1}{2} \arctg \left(\frac{dD}{2(DF + dF_z - dh)} \right), \tag{10}$$

where

- d diameter of SD,
- F inter-focal length.

$$\psi_3 = \arctg \left(\frac{2(DF + dF_z - dh)}{Dd} \right), \tag{11}$$

Now, taking into account expressions (3), (4) and (6), the maximum sizes of a pixel of a matrix receiver can be determined by the following expression:

$$I_{\max} = \sqrt{\frac{2}{T} \int_{-\frac{T}{2}}^{\frac{T}{2}} (k_z^2 a_1^2 \sin^2(\omega_1 t) + 2k_z a_1 k_r a_2 \sin(\omega_1 t) \sin(\omega_2 t + \varphi) + k_r^2 a_2^2 \sin^2(\omega_2 t + \varphi)) dt} \quad (12)$$

The last expression can be simplified having calculated its maximum value. Let us input the following designations:

$$i_1 = \int_{-\frac{T}{2}}^{\frac{T}{2}} \sin^2 \omega_1 t dt \quad (13)$$

$$i_2 = \int_{-\frac{T}{2}}^{\frac{T}{2}} \sin^2(\omega_2 t + \varphi) dt \quad (14)$$

$$i_3 = \int_{-\frac{T}{2}}^{\frac{T}{2}} 2 \sin \omega_1 t \sin(\omega_2 t + \varphi) dt \quad (15)$$

then

$$i_1 = \int_{-\frac{T}{2}}^{\frac{T}{2}} \sin^2 \omega_1 t dt = \int_{-\frac{T}{2}}^{\frac{T}{2}} \frac{1}{2} (1 - \cos 2\omega_1 t) dt = \frac{T}{2} \quad (16)$$

$$i_2 = \int_{-\frac{T}{2}}^{\frac{T}{2}} \sin^2(\omega_2 t + \varphi) dt = \int_{-\frac{T}{2}}^{\frac{T}{2}} \frac{1}{2} (1 - \cos(2\omega_2 t + 2\varphi)) dt = \frac{T}{2} - \cos 2\varphi \int_{-\frac{T}{2}}^{\frac{T}{2}} \cos 2\omega_2 t dt + \sin 2\varphi \int_{-\frac{T}{2}}^{\frac{T}{2}} \sin 2\omega_2 t dt$$

$$i_2 = \frac{T}{2}$$

$$i_3 = \int_{-\frac{T}{2}}^{\frac{T}{2}} 2 \sin \omega_1 t \sin(\omega_2 t + \varphi) dt = \cos \varphi \int_{-\frac{T}{2}}^{\frac{T}{2}} (2 \sin \omega_1 t \sin \omega_2 t) dt + \sin \varphi \int_{-\frac{T}{2}}^{\frac{T}{2}} (2 \sin \omega_1 t \cos \omega_2 t) dt \quad (17)$$

because

$$\begin{aligned} 2 \sin \omega_1 t \sin \omega_2 t &= \cos(\omega_1 - \omega_2)t - \cos(\omega_1 + \omega_2)t \\ 2 \sin \omega_1 t \cos \omega_2 t &= \sin(\omega_1 + \omega_2)t + \sin(\omega_1 - \omega_2)t \\ \int_{-\frac{T}{2}}^{\frac{T}{2}} \sin(\omega_1 + \omega_2)t dt &= 0 \quad \int_{-\frac{T}{2}}^{\frac{T}{2}} \sin(\omega_1 - \omega_2)t dt = 0 \end{aligned}$$

TO

$$i_3 = -\frac{2 \sin\left((\omega_1 - \omega_2)\frac{T}{2}\right) \cos \varphi}{\omega_2 - \omega_1} - \frac{2 \sin\left((\omega_1 + \omega_2)\frac{T}{2}\right) \cos \varphi}{\omega_2 + \omega_1} \quad (18)$$

Substituting values from (16), (17) and (18) in expression (12) we shall receive the following expression (19):

$$l_{\max} = \sqrt{2 \left(\frac{k_z^2 a_1^2 + k_r^2 a_2^2}{2} - \frac{4k_z k_r a_1 a_2 \cos \varphi \left((\omega_2 + \omega_1) \sin\left(\frac{T(\omega_1 - \omega_2)}{2}\right) + (\omega_2 - \omega_1) \sin\left(\frac{T(\omega_1 + \omega_2)}{2}\right) \right)}{T(\omega_2^2 - \omega_1^2)} \right)} \quad (19)$$

Let us enter the following designations:

$$\begin{aligned} I_1 &= k_z^2 a_1^2 + k_r^2 a_2^2, \\ I_2 &= \frac{8k_z k_r a_1 a_2 \cos \varphi \left((\omega_2 + \omega_1) \sin\left(\frac{T(\omega_1 - \omega_2)}{2}\right) + (\omega_2 - \omega_1) \sin\left(\frac{T(\omega_1 + \omega_2)}{2}\right) \right)}{T(\omega_2^2 - \omega_1^2)} \end{aligned}$$

If one considers that $(\omega_1 - \omega_2)$ and $(\omega_1 + \omega_2)$ —whole numbers, then the second summand in the last expression will be 0. Then:

$$l_{\max} = \sqrt{k_z^2 a_1^2 + k_r^2 a_2^2} \quad (20)$$

In most cases, expression (20) can be used with a sufficient accuracy to assess the maximum size of a pixel of a matrix receiver. Thus, for the minimum size of a pixel it is possible to take the following value

$$l_{\min} = H. \quad (21)$$

As an example, to assess the maximum size of a pixel of a matrix receiver we take the following value of parameters of the PT 70 antenna: $F = 24.2$ m, $F_z = 21$ m, $D = 70$ m, $d = 3$ m, $h = 14.58$ m.

Let us suppose that $a_1 = 2$ mm, $a_2 = 2$ mm (a_1 , a_2 —amplitudes of fluctuations of edges of a main dish and a subdish respectively).

In Fig. 1 one can define that $\omega_1 = 8.5$ c⁻¹, $\omega_2 = 23.7$ c⁻¹ (ω_1 and ω_2 —frequencies of the first tones of fluctuations of a main dish and a subdish respectively). From formula (9), (10), (11) we obtain: $\psi_1 = 39.8^\circ$, $\psi_2 = 38.04^\circ$, $\psi_3 = 38.04^\circ$. Further, from formula (5), (7), (8) we obtain $T = 0.195$, $k_z = 0.646$, $k_r = 1.232$. Then, by substituting the obtained values of expression (19) we will obtain: $I_1 = 7.736$ and $I_2 = 0.004 \cos \phi$. Therefore, in expression (19) value I_2 can be neglected. Thus, to assess the maximum size of a pixel of a matrix receiver it is possible to use formula (20). In the reviewed example: $l_{\max} = 2.781$ mm.

4 Algorithms of Adaptation of Matrix Receivers

It was shown above that in millimetre-wave radio telescopes of the pixel size providing the maximum sensitivity of a receiver considerably differs from the size of the pixel providing the maximum spatial resolution of an antenna. Therefore, during radio-astronomical supervision and radio-astronomical location it is reasonable to adapt the sizes of pixels of radiation matrix receivers to the observed sources of radiation to ensure optimum parameters of such radio telescopes. Thus, algorithms of adaptation of matrix receivers will slightly vary depending on operating modes of a radio telescope.

In the **scanning mode**, antenna continuously moves along a set trajectory with a set speed. At the same time, reading of a signal and information on position of the antenna is done with such frequency that during an interval between counting the antenna is displaced only at a small part of the directional pattern (DP). To increase the accuracy of performance of this mode in millimetric range we need a continuous tuning of focusing of the antenna through the control over of the panels of the main dish and subdish. Besides, to meet the requirements of movement accuracy on the set trajectory in millimetric range it is necessary to control the position of an optical axis of the antenna depending on such revolting factors as weight and wind indignations and adjust the trajectory for the respective set displacement account platform SEMS with a matrix receiver.. Increase of accuracy of control over the position of an optical axis is possible due to reduction of the size of pixel of the matrix receiver. However, the time of signal accumulation due to fluctuations of elements of the design of the antenna decreases (see Fig. 1). Therefore, for the purpose of achievement of an optimum compromise between inconsistent requirements of sensitivity and spatial resolution, it is reasonable to use the following algorithm of adaptation of the matrix receiver in this operating mode of the antenna.

1. Basic data is input: λ , H , v , $f_1(\beta)$, $f_2(\beta)$, k_1 , k_2 , k_z , k_r , $n = 1$, l_0 , N , where, H —DN width in focal plane, v —the speed of movement of the antenna, k_1 —the coefficient chosen by the operator in the range from 0,1 to 1, f_1 and f_2 —

pre-calculated or experimentally defined main dish and subdish own frequencies (first tone) respectively, k_2 —the coefficient chosen by the operator in the range from 50 to 200 provided that $\Delta t_1 \ll \Delta t$; λ —wavelength of the accepted radiation, the l_0 —initial size of pixel, N —the size of a matrix of the set receiver.

2. Calculate $\Delta t = k_1 H/v$; $\Delta t_1 = 1/k_2 f_1 f_2$.
3. Move the antenna along a predetermined path to position correction with matrix platform SEMS receiver.
4. While moving the antenna along the set trajectory, from time to time at intervals Δt :

- 4.1. measure the angle of elevation β ,
- 4.2. according to calculated values of β choose from tables $f_1(\beta)$ and $f_2(\beta)$ the values f_1, f_2 and calculate $T = 1/f_1 f_2$,
- 4.3. from time to time (period $\Delta t_1 = T/k_2$) measure amplitudes of oscillation a_1 (the edge of main dish) and a_2 (the edge of subdish),
- 4.4. calculate l_n —the size of pixel of matrix receiver according to formula:

$$l_n = \frac{l_0 \cdot N}{2^n}, \quad (22)$$

- 4.3. unite outputs of pixels of the matrix receiver so that the square matrix consisting of l_n size pixels be developed.
5. If $l_n \leq H$ or $l_n \leq l_{\max}$, then halt, otherwise $n = n + 1$ and move to step 3.

The offered algorithm allows to find the most remote and (or) low-power space sources of radio emission (SSRE) due to the maximum sensitivity of the receiver, but with the low spatial resolution, when the antenna moves along the set trajectory for the first time. Then, during the following passes, spatial resolution due to work of system of adaptation of the receiver will be increased all the time. The last measure will allow to specify parameters (coordinates, speed, etc.) of the found SSRE at each following pass of the antenna.

In the mode of **pointing testing**, regularly in the course of observation of the studied SSRE, usually at interval of about 1 h, the antenna is directed at a basic source to the maximum of the signal accepted from a basic source with the use, for example, of the equisignal-zone method (ESZM). Coordinates of this maximum are calculated, and by comparison with known coordinates of a basic source deflections of the observed position from the expected one are calculated and by that one may receive a targeting error which is input into the antenna control system when tracking the studied SSRE. In this operating mode of the antenna it is reasonable to use the following algorithm of adaptation of the matrix receiver.

1. Basic data is input: $\lambda, H, f_1(\beta), f_2(\beta), k_2, k_z, k_r, \alpha(0), \beta(0), n = 0, i = 0.2$.
2. According to the set angle of elevation $\beta(0)$, choose from the tables $f_1(\beta)$ and $f_2(\beta)$ values f_1, f_2 and calculate $T = 1/f_1 f_2$ and $\Delta t_1 = T/k_2$.
3. Move the antenna according to the set coordinates of a basic source according to the angle of elevation $\beta(0)$ and to the azimuth $\alpha(0)$.

4. Measure amplitudes of fluctuations a_1 (the edge of main dish) and a_2 (the edge of subdish) k_2 once at the interval Δt_1 .
5. Calculate l_{\max} (maximum size of pixel) of the matrix receiver according to the formula (22).
6. Unite outputs of pixels of the matrix receiver so that the square matrix consisting of l_n size pixels be developed.
7. Direct the antenna according to the angle of elevation and azimuth at a basic source to the maximum of the signal accepted from a basic source using the equisignal-zone method.
8. Direct SEMS platform with a matrix receiver according to the angle of elevation and azimuth at a basic source to the maximum of the signal accepted from a basic source using the equisignal-zone method.
9. Take $i = i + 1$, and coordinates of this maximum $\alpha(i)$, $\beta(i)$ are calculated.
10. If $l_{\max} \leq H$, deflections of the observed position from (i) the expected one $\Delta_\alpha = \alpha(i) - \alpha(0)$, $\Delta_\beta = \beta(i) - \beta(0)$ are calculated, and it is input into the antenna control system as the amendment, otherwise $n = n + 1$ and move to step 4.

The offered algorithm allows obtaining the most possible accuracy of calculation of amendments Δ_α and Δ_β for the antenna control system and by that to increase the accuracy of supervision over the studied SSRE; and all is due to the repetitive antenna pointing at the basic source with gradual increase of resolution of the receiver.

In the mode of **aiming** at the studied SSRE, the calculated according to the given above algorithm amendments are used in a control system. Upon positioning according to the coordinates of the studied SSRE, *at initium* consider $n = 0$ and calculate l_{\max} according to the formula (17). Unite outputs of pixels of the matrix receiver so that the square matrix consisting of l_n size pixels be developed. Then, gradually increase n , calculate new l_{\max} and unite outputs of pixels of the matrix receiver so that the square matrix consisting of the pixels of this l_{\max} size be developed and until SSRE can be seen against noise background. At that, the parameters of the observed SSRE can be determined with the most possible resolution.

In the **tracking** mode, the antenna watches a certain point of the heavenly sphere during a set time by its turn according to the angle of elevation and azimuth. To meet the requirements of the accuracy of tracking the weak SSRE in millimeter range, the elevation and azimuthal drives are not enough to measure positions of axes with high precision and accordingly to calculate the control actions, because the position of the optical axis of the antenna (which also depends on such revolting factors as weight and wind indignations) won't be controlled [2]. At small wavelength (millimeter range) of the accepted radiation and at frequency modulation on big radio telescopes in the tracking mode, it is additionally required to constantly agree on positions of panels of the main dish and subdish. Besides, since in the course of tracking SSRE the angle of elevation and azimuth of the antenna change and parameters of fluctuations of the main dish and subdish change respectively, in the course of tracking SSRE it is necessary to periodically change the sizes of pixels

of the matrix receiver determined in the course of aiming at the studied SSRE, using the following algorithm:

1. Basic data is input: λ , H , v , $f_1(\beta)$, $f_2(\beta)$, k_1 , k_2 , k_z , k_r , δ_n , t_k , $k = 0$, $n = 0$, where, δ_n —permissible deflection, t_k —termination time of supervision session over SSRE.
2. Calculate $\Delta t = k_1 H/v$; $\Delta t_1 = T/k_2$.
3. While antenna moving along the trajectory of the studied SSRE from time $t = k\Delta t$.
 - 3.1 Calculate the angle of elevation β .
 - 3.2 According to calculated values β choose from tables $f_1(\beta)$ and $f_2(\beta)$ values f_1 , f_2 and calculate $T = 1/f_1 f_2$.
 - 3.3 Measure amplitudes of fluctuations a_1 (the edge of main dish) and a_2 (the edge of subdish) at the interval Δt_1 .
 - 3.4 Calculate l_{\max} maximum pixel size of the matrix receiver according to the formula (22).
 - 3.5 Unite outputs of pixels of the matrix receiver so that the square matrix consisting of l_n size pixels be developed.
 - 3.6 Define pixel with the maximum signal.
 - 3.7 Calculate a difference δ between signals of this and neighbor pixels.
 - 3.8 If $\delta \leq \delta_n$ or $l_{\max} \leq H$, then $t = k\Delta t$, the values of the matrix receiver are transferred to memory, otherwise $n = n + 1$ and move to step. 3.
4. If $t \leq t_k$, then halt, otherwise $k = k+1$ and move to step 3.

The offered algorithm allows to provide the maximum sensitivity of the receiver and spatial resolution of the antenna due to tuning of the pixel sizes of the matrix receiver to the changing parameters of the studied moving SSRE.

Besides the installation of the matrix receiver on the platform SEMS in some cases may allow significantly reduce the impact of fluctuations the focus of the mirror system antenna due to wind and the weight of perturbations (see Fig. 1) due to their measurements and matched against them, displacement platform with a matrix receiver.

5 Control System Over the Adaptive Matrix Receiver

The flowchart of a control system over the adaptive matrix receiver is shown in Fig. 3.

Let us consider the work of a control system on the example of realization of the given above algorithm in the scanning mode. In this case interaction of blocks of a control system happens as follows.

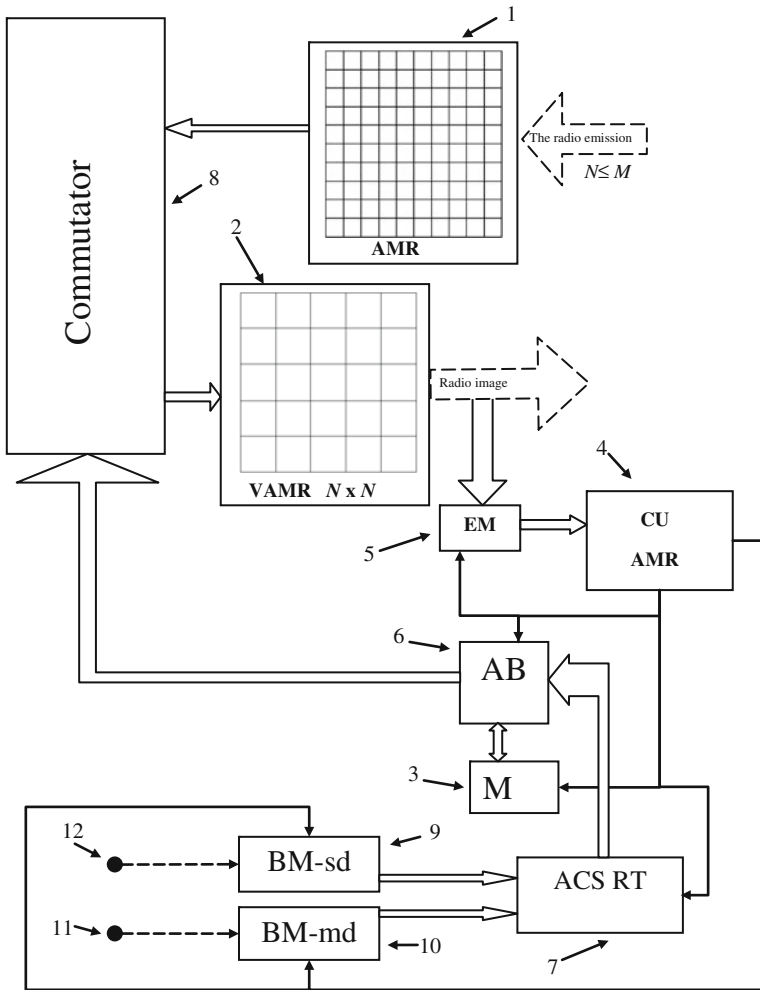


Fig. 3 Control flowchart. 1 Adaptive Matrix Receiver (AMR), 2 Virtual Adaptive Matrix Receiver (VAMR), 3 Memory (M), 4 Control Unit of the Adaptive Matrix Receiver (CU AMR), 5 External Memory (EM), 6 Adaptation Block (AB), 7 Automatic Control System of Radio Telescope (ACS RT), 8 Switchboard, 9 Block of Measuring fluctuations of subdish (BM-sd), 10 Block of Measuring fluctuations of the main dish (BM—md), 11 point of measuring fluctuations on the edge of the counter-reflector, 12 point of measuring fluctuations on the edge of the main reflector. Single lines designate transmission lines of the control actions, double lines data transmission between blocks

1. Upon the command of CU AMR (4) from M (3) in AB (6) the basic data is input: $\lambda, Fz, Fr, F, D, d, H, h, v, f_1(\beta), f_2(\beta), k_1, k_2, k_z, k_r, n = 0$.
2. Upon the command of CU AMR (4), AB (6)—calculates $\Delta t = k_1 H/v$; $\Delta t_1 = 1/k_2 f_1 f_2$; $l_0 = \lambda F/2D$ and transfer to switchboard (8) the desired pixel sizes $l_p = l_0$ for VAMR (2), obtained from AMR (1) by switching the outputs of its pixels.
3. Switchboard (8) switches the outputs of pixels AMR (1), and by doing so gets VAMR (2) of desired scale, and transfers to CU AMR (4) the command about the end of installation of the sizes of a matrix VAMR (2).
4. CU AMR (4) delivers a control action for beginning recording of radio imaging from VAMR (2) into EM (5) and simultaneously instructs the antenna to begin moving along the set trajectory in ACS RT (7).
5. While antenna is moving, the angle of elevation β is measured by means of ACS RT (7).
6. According to measured values β , values f_1, f_2 are selected from tables $f_1(\beta)$ and $f_2(\beta)$ which are stored in M (3), then these values are transferred to AB (6) and it calculates $T = 1/f_1 f_2$.
7. Periodically, amplitudes a_1 and a_2 of fluctuations of edges of main reflector (11) and counter-reflector (12) are measured by means of BM-sd (9) and BM-md (10) at the interval $\Delta t_1 = T/k_2$ and transferred to AB (6).
8. AB (6) uses formula (22) to calculate the desired pixel size $l_p = l_{\max}$ for VAMR (2).
9. ACS RT (7) upon the end of moving along the set trajectory instructs CU AMR (4) to start installing a new size of pixels VAMR (2), which gives the corresponding command to switchboard (8).
10. Switchboard (8) unites the outputs of pixels of matrix receiver AMR (1) the way that in VAMR (2) a square matrix consisting of l_{\max} size pixels is developed.
11. If $l_{\max} \leq H$, then halt, otherwise $n = n + 1$ and move to step 4.

Similarly, it is possible to consider the functioning of a control system of the adaptive matrix receiver during carrying out the other algorithms of operation of the radio telescope. It is necessary to notice that the use of adaptive matrix receivers in radio telescopes allows optimizing tuning of the control system of radio telescope drives to the parameters of the observed space source of radio emission. This task demands more detailed analysis and will be considered in the following publications.

6 Conclusion

The offered device of the adaptive matrix receiver and its control system will allow increasing efficiency of the use of matrix receivers for obtaining radio images in astronomy in millimeter range due to optimum tuning of the sizes of pixels of receivers to the parameters of the observed objects and conditions of supervision.

At the same time, there is a possibility of fast and reliable detection of remote space objects, and then, due to reduction of the sizes of pixels, their more and more detailed studying and specification of their coordinates.

As a result of the carried-out analysis of the dynamics of the reflector system of big antenna at its movements, engineering formulas for calculation of the optimum sizes of pixels of adaptive matrix receivers which can be used in its control system have been obtained. Besides, these ratios can be used for tuning the control system of radio telescope to optimum speed at a set sensitivity.

The offered algorithms of adaptation of matrix receivers and the corresponding control system of matrix receivers demand application of the new offered algorithms of control over operating modes of radio telescopes which considerably increase their efficiency upon supervising weak and (or) considerably remote space sources of radio emission in millimeter range.

The installation of the matrix receiver on the platform SEMS in some cases may allow significantly reduce the impact of fluctuations the focus of the mirror system antenna due to wind and the weight of perturbations due to their measurements and matched against them, displacement platform with a matrix receiver.

References

1. Zinchenko, I.I.: "Radio-wave" in astronomy. In: Proceedings of the 34th International Student Conference. Publishing House of the Ural University, Kourvka, Russia (2005) (in Russian)
2. Vdovin, V.F., Zinchenko, I.I.: Low noise receivers millimeter and submillimeter waves, vol. 41, p. 1424. Proceedings of the Universities, Radiofizika (1998) (in Russian)
3. Zinchenko, I.I.: Modern millimeter and submillimeter astronomy, vol. 46. p. 641. Proceedings of the Universities, Radiofizika (2003) (in Russian)
4. Payne, J.M., Jewell, P.R.: The upgrade of the NRAO 8-beam receiver. In: Emerson, D.T., Payne, J.M. (eds.) Multi-feed systems for radio telescopes. ASP Conferences Series, vol. 75, p. 144 (1955)
5. Johansson, J.F.: SISYFOS—a project presentation and progress report. Ibid. p. 130
6. Stimson, P.A., Dengler, R.J., Leduc, H.G. et al.: Superconducting heterodyne planar array using a dielectric filled parabola: status and measured performance. Ibid. p. 245
7. Zabitov, Y.M., Lebskii, Y.V., Fedoseev, L.I., et al.: Multibeam superheterodyne receiver millimeter wavelengths. Radiotekhnika i elektronika, vol. T.38. p. 2240. (in Russian) (1993)
8. Gorodetsky, A.E., Artyomenko, Y.N., Dubarenko, V.V., Tarasova, I.L., Kuchmin, A.Y.: Problems of creation of systems of adaptation of space telescopes. Inf Control Sys 3 (2010) (in Russian)
9. Gorodetsky, A.E., Tarasova, I.L., Artyomenko, Y.N.: Interference-code converters, p. 472. St. Petersburg, Nauka (2005) (in Russian)

Analysis of Errors at Optic-Electronic Autocollimation Control System with Active Compensation

A.E. Gorodetskiy, I.A. Konyakhin, I.L. Tarasova and Li Renpu

Abstract The structure and metrological parameters of the autocollimation sensor to generate SEMS control signals at rotating subdish of the radiotelescope are analyzed. The series structure of SEMS is used. Autocollimator measures the angular shifts of the mirror on subdish. The method of increase the measuring range of autocollimator by means of the active compensation the mirror rotation is described. The influence of the automatic control system on an error of measurements is analyzed. The using of the galvanometer-based automatic control system in autocollimator for reduction of dynamic errors and time of measurement is reasonable.

Keywords Autocollimator · Vignetting error · Automatic control system · Dynamic error · Angular shifting the subdish

1 Introduction

Operating modern radio telescopes demands exact mutual positioning of the elements of its mirror system. To shift parts of antennas of space radio telescopes in the course of their opening and then in subsequent positioning the elements of the

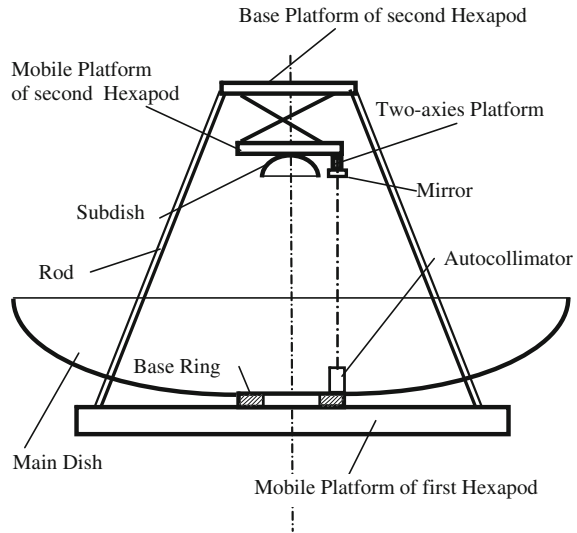
A.E. Gorodetskiy (✉) · I.L. Tarasova
Institute of Problems of Mechanical Engineering, Russian Academy of Sciences,
Saint-Petersburg, Russia
e-mail: g27764@yandex.ru

I.L. Tarasova
e-mail: g17265@yandex.ru

I.A. Konyakhin · L. Renpu
ITMO University, Saint-Petersburg, Russia
e-mail: igor@grv.ifmo.ru

L. Renpu
e-mail: lirenpu@hotmail.com

Fig. 1 Structure of the system for control the angular orientation the counter reflector



mirror system in the process of directing a radio telescope, it is suggested to use hexapod-like structures of smart electromechanical systems (SEMS).

An example of employing such a structure is given by the SEMS-based design of subdish for the “Millimetron” space radio telescope. The series structure of SEMS is used. According to the design, the radiotelescope main dish is positioned on a mobile platform of the first hexapod and the subdish is positioned on a mobile platform of second hexapod. The base platform of second hexapod is fixed with respective stationary rods to the base platform of the first hexapod (Fig. 1).

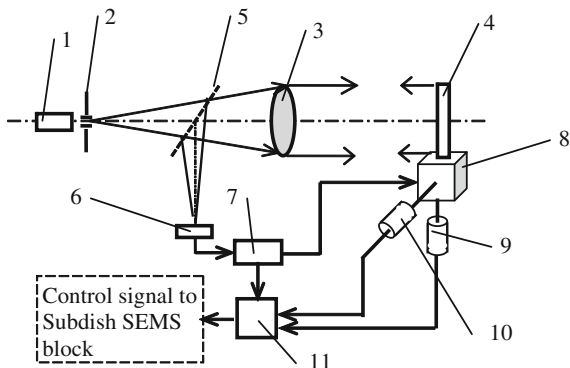
To generate SEMS control signals at angular shifting the subdish, one needs to measure its angle position with respect to the axis of the main dish. For high accuracy measurements of angular orientation of the subdish it is suggested to use an optic-electronic autocollimation system as an optical sensor [1].

Following the autocollimation technique, a glass passive control element (CE), that is an autocollimating mirror, is positioned on a controlled two-axes platform which is fixed on the mobile platform of the second hexapod, along with the subdish. The emitting-receiver autocollimator (AC) is placed on the base ring at the apex of the main dish (Fig. 1).

2 Autocollimator Structure, Principle of Operation

Figure 2 presents the structure of the autocollimating sensor. Radiation from the source 1 passes mark 2 positioned in the focal plane of autocollimator objective 3, and is shaped into a parallel beam that falls onto the flat mirror 4. The reflected beam upon passing objective 3 on its reverse path, forms an image of the mark in

Fig. 2 Autocollimator generalized structural layout



the focal plane of the side channel (formed by beam splitter 5). That image of the mark is formed on the sensitive surface of matrix photosensor 6.

With the flat mirror rotating, the orientation of the axis of reflected beam changes, resulting in the proportional displacement of image on matrix photosensor 6. Upon microprocessor unit 7 processing video frames produced by matrix 6 (that correspond to the initial and the displaced positions of flat mirror 4), a value of the image displacement, x , is retrieved if the focal distance of the lens f is known one may calculate the angle Θ of mirror rotation as:

$$\Theta = \frac{1}{2} \cdot \arctg\left(\frac{x}{f}\right) \tag{1}$$

The principal feature of autocollimating technique is the displacement of the reflected beam off the center of autocollimator objective aperture when the mirror goes through its rotation. As a result the vignetting of the beam that forms the image of the mark causes certain measurement error [2].

It is possible to compensate for the error due to image vignette algorithmically, provided the displacement of the reflected beam caused by the mirror positioned at distance L rotating by angle Θ does not exceed half the aperture D of the autocollimator objective [3, 4]:

$$D/2 \geq L \cdot tg(2 \cdot \Theta) \tag{2}$$

To realize the measurements in the process opening and in the process of directing the main dish and subdish it is necessary to use active compensation for beam displacement while the mirror 4 rotates. The autocollimator then includes automatic control system (ACS) that rotates the flat mirror 4 in the direction opposite to that of the rotation of the controlled subdish. ACS contains the controlled two-axes platform 8 with two transducers “angle-code” 9 and 10.

That compensation is executed in the course of the measurements taken, e.g., using an electric train motors of two-axes platform to keep the reflected beam within the entry aperture of its objective.

The ACS is started by the signals generated by microprocessor unit 7 when the mark image is displaced off its zero-rotation position on the surface of the matrix photosensor. Training flat mirror rotation proceeds prior to the initial position is recovered of the mark image.

At any given moment the value of the measured angle Θ of subdish rotation relatively one axis is equal to the sum of two angles: angle Θ_1 yielded by relationship (1) from microprocessor unit 7 and angle α_1 , generated by one transducer “angle-code”. The special converter 11 processes the measured angles of the subdish rotations and generates the control signals to subdish SEMS block.

Thus using the ACS, makes it possible to overcome the limitation of the measurement range (or operation distance) prescribed by condition (2).

3 Structure of Automatic Control System

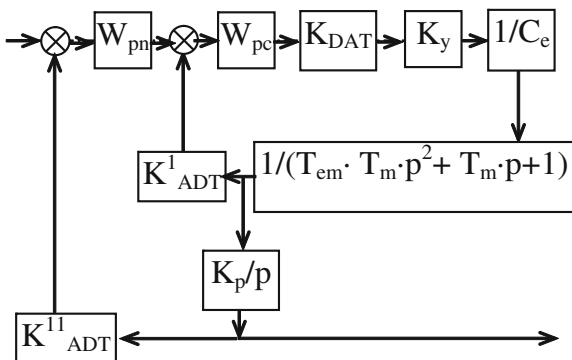
However, such a technique of expanding the measurement range calls for a high accuracy ACS to control the angle of rotation, and that involves a feedback on the position of reflected beam. Also, an important feature of such a system is the dependence of dynamic error in measuring angle α generated by the ACS on measurement time, t_m , understood as the time that the mirror takes to rotate from its initial position to the position corresponding to its extreme angle, as per condition (2). ACS performance should be fast enough to keep reflected beam within the aperture range of the lens while mirror rotation proceeds further (we assume the rate of mirror rotation resulting from the rotation of the controlled target to remain constant).

Consider the dynamic errors occurring, when a typical ACS is used to compensate for mirror rotation. Assume the ACS is built on a DC electric motor with its following parameters: nominal rotation rate $\omega_h = 314$ 1/s; nominal torque $M = 0.3$ Nm; nominal voltage $U_h = 220$ V; inertia moment $J = 2.93 \times 10^{-4}$ kg m²; torque factor $C_M = 0.73$ Nm/A; EMF factor $C_e = 0.7$ Vs; time constants $T_M = 2.6 \times 10^{-3}$ s and $T_{eM} = 1.3 \times 10^{-6}$ s.

The ACS structural layout presented in Fig. 3 uses the following notations: W_{pn} is the transfer function of displacement controller, W_{pc} is the transfer function of rate controller, K_{DAT} is the digital-amplitude transducer (DAT) transformation factor, K_{ADT}^1 is the amplitude-digital-transducer (ADT) transformation factor for motor rate, K_{ADT}^{11} is the displacement transformation factor, K_y is the amplifier amplification factor, $C_e = U_h/\omega_h$, where U_h and ω_h are the nominal voltage and motor rate, K_p is the reduction factor, p is the differentiation operator.

To control the motor rate we choose a proportional integro-differential (PID) controller with its transfer function $W_{pc} = (K_3 p^2 + K_1 p + K_2)/p$, its

Fig. 3 ACS structural layout



parameters tuned as follows: $K_1 = T_M$; $K_2 = 1$; $K_3 = T_M T_{eM}$ to provide for the best control of motor rate. As for the DAT and ADT bit rate, n , we choose them from the condition that transformation error does not exceed 0.01 %, namely: $2^n \geq 100/0.01$. Assuming $n = 14$ we obtain for $x = 2 * 10^{-2}$ m:

$$K_{DAT} = \frac{2U}{2^{14}} = 26.4 \times 10^{-3} ; \quad K_{ADT}^1 = \frac{2^{14}}{2\omega_H} = 26.089; \quad K_{ADT}^{11} = \frac{2^{14}}{2x} = 4.1 \times 10^5$$

Next, if we use a standard 12 V output voltage DAT for our ACS, then $K_y = 220/12 = 18.7$. As for the reduction factor K_p , we choose it starting from the needed rotation rate for the flat mirror: $V_{ak} = 2000$ m/s, $K_p = V_{ak}/\omega_H = 6.4$ m.

4 Computer Simulation Results

To analyze the effect of shift controller tuning we performed a computer simulation of the ACS. Two types of controllers were analyzed: the proportional ($W_{pn} = K_n$) and the proportionally integrating controller ($W_{pn} = K_n + K_i/p$). Simulation results are presented in Fig. 4.

One may see from the analysis of the two graphs that employing a standard motor in its train mode large dynamic error may occur for measurement times shorter than (0.5–0.6 s).

To reduce dynamic error and shorten measurement time one needs to employ a specialized fast electric drive. In particular, a galvanometer may be used as such fast drive; its linear mathematical model is presented by the expression:

$$\left. \begin{aligned} I &= \frac{U - C_e p \alpha}{R(T_e p + 1)} \\ \alpha &= \frac{k_1 I}{(c - k_2)(T_m^2 p^2 + 2\zeta T_m p + 1)} \end{aligned} \right\} \quad (3)$$

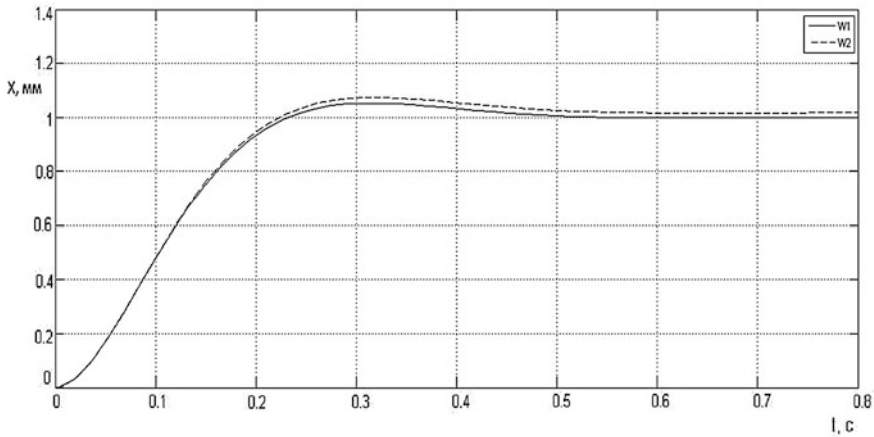


Fig. 4 Computer simulation results for $K_n = 1 * 10^{-4}$ (W_1), $K_i = 2 * 10^{-5}$ (W_2)

where α is the angle of rotation, $p = d/dt$, R and L are active resistance of the instrument electrical circuit with a frame and its inductance, respectively, C_e is its electric constant, $T_e = L/R$ is the electromagnetic time constant, J is the moment of inertia of the instrument frame, η and c are the spring damping factor and rigidity, $k_1 = C_m \alpha_0$, $k_2 = C_m I_0$, α_0 and I_0 are steady state values of frame rotation angle and current, C_m is the torque factor, U is the voltage fed to the frame, $T_m = \sqrt{\frac{J}{c-k_2}}$ is its mechanical time constant, $\zeta = \frac{\eta}{2T_m(c-k_2)}$ is the damping factor.

The value T_e is commonly very low for galvanometers and should be disregarded, the galvanometer damping ζ stays within 0.4–0.6, and its eigen frequency $f = 1/2\pi T_m$ lies within 100–7000 Hz.

Denoting $K = k_1/R(c - k_2)$ and assuming $T_e = 0$ and $C_e = 0$ due to their smallness, we find for model (8): $W_g = \alpha(p)/U(p) = K/(T_m^2 p^2 + 2\zeta T_m p + 1)$. Then the structural scheme of ACS may be presented in the form shown in Fig. 5.

It is also advisable to employ a PID controller in the ACS, its transfer function being:

$$W_p = K_1 + K_2 p + K_3/p, \tag{4}$$

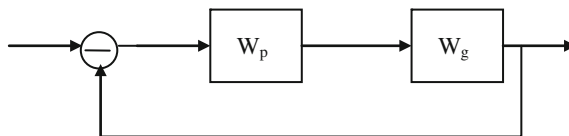
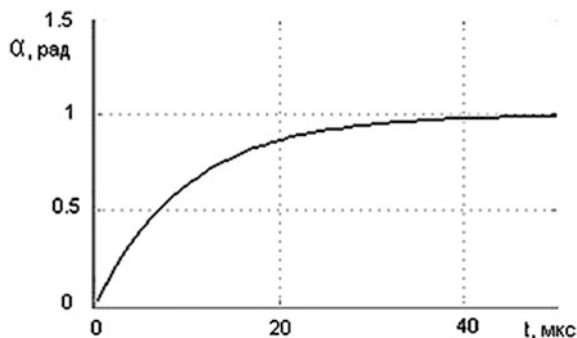


Fig. 5 The galvanometer-based ACS structural scheme

Fig. 6 Computer simulation of a galvanometer-based ACS (α is the angle of rotation the mirror)



where $K_3 = \omega_3/K\delta_n$, δ_n is the admissible error of training a sine input signal of frequency ω_3 ($U = \sin \omega_3 t$, $\omega_3 < 1/T_m$), $K_2/K_3 = T_m^2$, $K_1/K_3 = 2\zeta T_m$.

Figure 6 demonstrates the results of computer simulation of ACS built on the basis of an M004.3.5 galvanometer (Vibroprigor Corp, Moldova) that features the following characteristics: operational frequency band 0–1700 Hz, maximum admissible current $I = 80$ mA, internal resistance $R = 15$ Ohm, sensitivity $S_A = 1.5$ rad/A, eigen frequency $f = 3500$ Hz. Simulation was carried out for the following values of principal parameters of the system: $T_m = 1/2\pi f_0 = 1/6.283500 = 4 \times 10^{-5}$ s; $K = k_1/R(c - k_2) = S_A/R = 1.5/15 = 0.1$; $\zeta = 0.4$; $\delta_n = 0.001$; $\omega_3 = 100$ 1/s.

It follows from simulation results that the dynamic error becomes negligibly small for measurement times in excess of 40 μs . Such a fast reaction of an angle measuring system is quite sufficient for retrieving angular deformations of large scale structures.

5 Conclusion

Objective of the research was the automatic control system for the optic-electronic autocollimation sensor which generates SEMS control signals. The autocollimator performs the measuring of the angular position of the mirror on subdish of the radiotelescope.

The computer simulation of the automatic control system shows that the using in automatic control system the standard electromagnetic motors for compensation of the mirror rotation is possible only for slow-changing rotation angles of measurement targets. In case the target rotation angles change fast it is feasible to use galvanometer-based automatic control system to expand the measurement range of the autocollimation sensor.

This work was financially supported by the Government of the Russian Federation, Grant 074-U01.

References

1. Konyakhin, I.A., Timofeev, A.N., Usik, A.A., Zhukov, D.V.: Optic-electronic systems for measuring the angle deformations and line shifts of the reflecting elements at the rotateable radio-telescope. Proc. SPIE **8082**, 80823R (2011). doi:[10.1117/12.89005](https://doi.org/10.1117/12.89005)
2. Konyakhin, I., Smekhov, A.: Survey of illuminance distribution of vignetted image at autocollimation systems by computer simulation. Proc. SPIE **8759**, 87593F (2013). doi:[10.1117/12.2014609](https://doi.org/10.1117/12.2014609)
3. Konyakhin, I.A., Timofeev, A.N., Konyakhin, A.: Three-axis optic-electronic autocollimation system for the inspection of large-scale objects. Proc. SPIE **8788**, 87882C (2013). doi:[10.1117/12.2020343](https://doi.org/10.1117/12.2020343)
4. Kleshchenok, M.A., Anisimov, A.G., Lashmanov, O.U., Timofeev, A.N., Korotaev, V.V.: Alignment control optical-electronic system with duplex retroreflectors. Proc. SPIE **9131**, 91311X (2014)

Optic-Electronic Autocollimation Sensor for Measuring Angular Shifts of the Radiotelescope Subdish

I.A. Konyakhin, A.E. Gorodetskiy, Hoang Van Phong
and A.I. Konyakhin

Abstract The structure and metrological parameters of the autocollimation sensor to generate SEMS control signals at rotating subdish of the full rotatable radiotelescope are analyzed. Autocollimation sensor measures the pitch and yaw angular shifts of the special reflector on subdish. The method of increase the work distance of the autocollimation sensor is described. The metrological properties of the tetrahedral reflector with flat reflecting sides and invariant axis is researched. Technical characteristics of the experimental setups of new reflector are presented. Features of the tetrahedral reflector as the control element for autocollimation measurements are discussed.

Keywords Autocollimator · Pitch and yaw measurements · Tetrahedral reflector · Matrix photo receiver · Radiotelescope · Invariant axis · Angular shifts of the subdish

I.A. Konyakhin (✉) · H. Van Phong · A.I. Konyakhin
ITMO University, Saint-Petersburg, Russia
e-mail: igor@grv.ifmo.ru

H. Van Phong
e-mail: vanphongkqh@yahoo.com

A.I. Konyakhin
e-mail: igalkon@yandex.ru

A.E. Gorodetskiy
Institute of Problems of Mechanical Engineering, Russian Academy of Sciences,
Saint-Petersburg, Russia
e-mail: g27764@yandex.ru

1 Introduction

There is a necessity to construct the new large size aperture radio telescopes for the millimeter wave range researches. These instruments are designed in many countries: USA (NRAO Green Bank with 100 m main dish), Italy (SRT with 64 m diameter main dish), Mexico (LMT with 50 m main dish).

Russia designed the radiotelescope RT70 Suffa with 70 m diameter parabolic main dish and the 3 m elliptical subdish. Subdish is placed on the distance closely 20 m relatively top of main dish [1].

The research in the millimeter wave range requires the few (no more 2 arc.seconds) deviation the direction of the subdish axis relatively the axis of main dish.

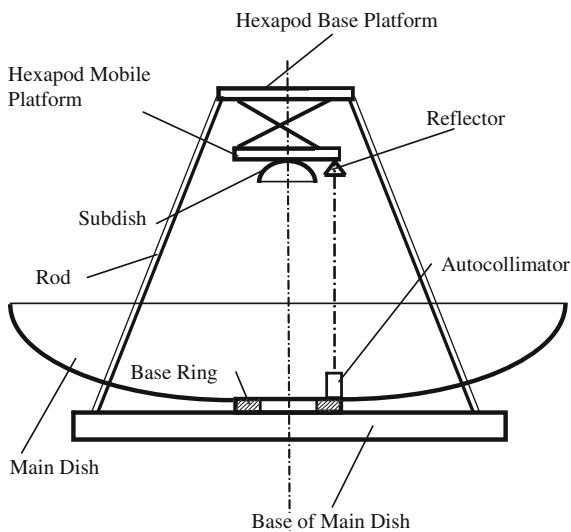
The deformation of the radio telescope construction components creates the change of the direction subdish axis relatively the axis of main dish. Therefore it is necessary to use active compensation for subdish angular shifts.

For correction the angular shifts of subdish it is suggested to use hexapod-like structures of smart electromechanical systems (SEMS). According to the design the subdish is positioned on a mobile platform of the hexapod. The base platform of hexapod is fixed with stationary rods to the base of radiotelescope main dish (Fig. 1).

To generate SEMS control signals at angular shifting the subdish, one needs to measure its angle position with respect to the axis of the main dish. For high accuracy measurements of angular orientation of the subdish it is suggested to use an optic-electronic autocollimation sensor [2, 3].

In this sensor a special reflector is positioned on the mobile platform of the hexapod along with the subdish. The emitting-receiver autocollimator is placed on the base ring at the apex of the main dish (Fig. 1).

Fig. 1 Driving mirror system



2 The Structure of the Optic-Electronic Autocollimation Sensor

The optic-electronic autocollimation sensor concludes the autocollimator and reflector [4]. The fixed XYZ coordinate system is associated with the autocollimator, and the mobile $X_1Y_1Z_1$ coordinate system, whose axes are parallel to the corresponding axes of the fixed coordinate system, is associated with the reflector on control object (Fig. 2). The OZ axis of fixed coordinate is parallel to axis of the main dish and the OZ_1 axis is parallel to axis of the subdish as controlled object.

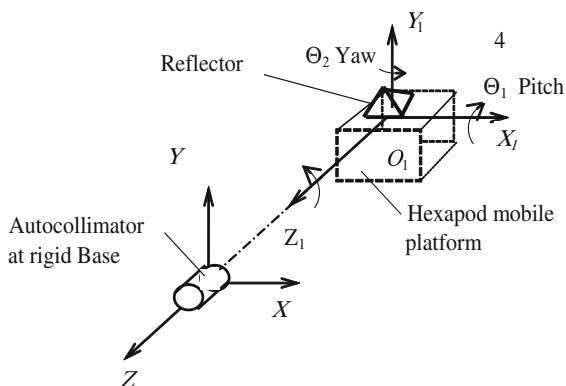
After angular deformation of the stationary rods, the parallelism of the corresponding axes in the two coordinate systems is violated. The angular spatial displacement of the subdish is determined by two angular coordinates Θ_1 , and Θ_2 .

The rotation angle Θ_1 relative to the O_1X_1 axis is the “pitch”, the rotation angle Θ_2 relative to the O_1Y_1 axes is “yaw”.

The radiating system of autocollimator includes the laser diode 3 as the source of radiation and aperture-mark 2, which is placed in the focal plane of objective 1 (Fig. 3). The radiation channel generates the collimation optical beam and directs it on reflector 4. The ort of this beam is **A**. The reflected beam with ort **B** is received by the receiving channel of autocollimator. The receiving channel includes the objective 1, semi-reflecting splitter 6 and the photo-receiving CMOS matrix 5, which is placed in the focal plane of objective 1. The reflected beam forms on the photo-receiving matrix 5 the image of the aperture-mark 2. The video-frame from matrix 5 is calculated by the digital microprocessor 7.

When the reflector 4 rotates on angles Θ_1 and Θ_2 , the reflected beam is deviated from the original direction **B**. As result the image shifts on the matrix photo-receiver. For another variant of the reflector the shape of the image is varying. The microprocessor 7 calculates the video-frames from the matrix photo-receiver and determines the parameters of the image. The angular coordinates Θ_1 , Θ_2 of the reflector 4 are determined as a result of the processing value of the image shift.

Fig. 2 Coordinate axis of the measuring system



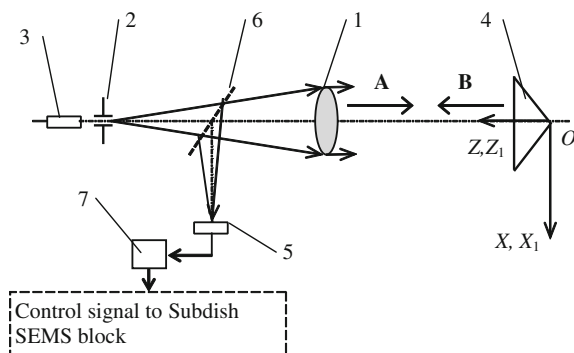


Fig. 3 Structure of the optic-electronic autocollimation sensor: 1 objective, 2 aperture-mark, 3 source of optic radiation, 4 reflector, 5 photo-receiver matrix, 6 beam splitter, 7 microprocessor system

The advantage of the autocollimator is a passive working regime under which a passive glass prism or a mirror system is used instead of active elements on the controlled object.

3 Problem of Measuring the Three-Axis Angular Shift of the Controlled Object

The traditional reflector for autocollimation sensors is a plane mirror. The disadvantage of the autocollimation sensor with plane mirror as reflector is the short work distance L between autocollimator and reflector. The reason is the shift of the reflected beam in the plane of the entrance pupil of the receiver objective after mirror rotation. As result at the some angle of rotation the reflected beam can not return into the objective of autocollimator. For the measurement range Θ and the diameter of the objective pupil d the working distance L is determined by the equation (Fig. 4):

$$d > L \cdot \operatorname{tg}(\xi) = L \cdot \operatorname{tg}(Q \cdot \Theta), \quad (1)$$

where ξ is the angle of the reflected beam deviation, Q is a conversion coefficient as the proportionality factor between the angle Θ of rotation of the reflector and the angle ξ of the deviation of the reflected beam. For the plane mirror the value of conversion coefficient is constant $Q = 2$. For example, for a measured angular displacement up to 20 arc minutes and diameter of the receiving objective of the autocollimator equal to 50 mm, a working distance L is less than 4 m, which is insufficient for measure the angle position of the subdish. One of the methods to increase the work distance is to decrease the value Q of the conversion coefficient of the reflector.

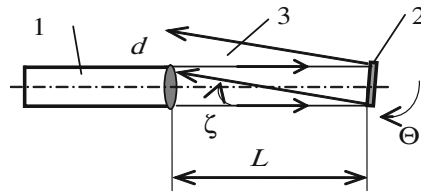


Fig. 4 Deviation the reflected beam: 1 autocollimator, 2 mirror as reflector, 3 reflected beam

For increasing the work distance of the autocollimation sensor it is necessary to synthesize the special reflector with variable value of the conversion coefficient Q .

4 Reflection Matrix of the Tetrahedral Reflector with Variable Value of the Conversion Coefficient

For analyze the properties of reflectors is using the general expression for an ort \mathbf{B} of a reflected beam:

$$\mathbf{B} = M_r \cdot M_d \cdot M_r^{-1} \mathbf{A}, \tag{2}$$

where \mathbf{A} is an ort of the incident beam, M_d is the reflection matrix, M_r and M_r^{-1} are the matrices of the direct and inverse transformation coordinates from axes $O_1X_1Y_1Z_1$ to $OXYZ$, corresponding to angles of rotation (Fig. 2). The matrix M_r^{-1} is the transpose of matrix M_r . The matrix M_r for small rotations is determined by the approximation of the exact formula (14.10–26) after substitute $\nu = \Theta_2$, $\psi = 0$, $\varphi = \Theta_1$:

$$M_r \approx \begin{pmatrix} 1 - \frac{1}{2} \cdot \Theta_2^2 & 0 & \Theta_2 \\ \Theta_1 \cdot \Theta_2 & 1 - \frac{1}{2} \cdot \Theta_1^2 & -\Theta_1 \\ -\Theta_2 & \Theta_1 & 1 - \frac{1}{2} \cdot (\Theta_2^2 + \Theta_1^2) \end{pmatrix}. \tag{3}$$

The error of the formula (3) is in the order 0.1 % for angles Θ_1 , Θ_2 of rotation not more than 1.8°.

Reflection matrix M_d of the reflector for the measuring the pitch Θ_1 and yaw Θ_2 can be written in the form of an improper matrix of the rotation around axis O_1Z_1 [5]:

$$M_d = \begin{pmatrix} \cos(\omega) & -\sin(\omega) & 0 \\ \sin(\omega) & \cos(\omega) & 0 \\ 0 & 0 & -1 \end{pmatrix}, \tag{4}$$

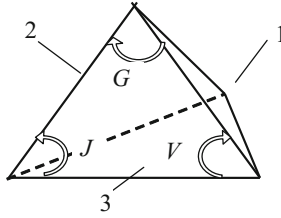


Fig. 5 Configuration of the tetrahedral reflector

where ω is the angle of rotation the ort **A** to position of the ort **B** around axis O_1Z_1 as the invariant axis of the reflector.

The reflector is the tetrahedral composition of three plane mirrors 1, 2, 3 (Fig. 5).

Geometric parameters of the reflector are following: the angle G between sides 1, 2 is $90^\circ - \delta_{12}$, angle J between sides 2, 3 is $90^\circ - \delta_{23}$ and angle V between sides 3, 1 is $90^\circ - \delta_{13}$. The value δ_{12} , δ_{23} , δ_{13} are not more than 1° . There are three pairs sequences of the beam reflection from three sides: 2–1–3 and 3–1–2; 1–2–3 and 3–2–1; 2–3–1 and 1–3–2. The pair beam with sequences 2–1–3 and 3–1–2 are used for measuring the angles pitch Θ_1 and yaw Θ_2 .

The vector **U** of the invariant axis are determined by coordinates U_1 , U_2 , U_3 in system coordinate $X_1Y_1Z_1$ for the sequence 2–1–3 of the beam reflection as:

$$U_1 = \frac{\sqrt{2}}{2} (\sin(\delta_{23}) \cdot \cos(\delta_{12}) \cdot \cos(\delta_{13}) + \sin(\delta_{13})), \quad (5)$$

$$U_2 = \frac{\sqrt{6}}{6} (\sin(\delta_{23}) \cdot \cos(\delta_{12}) \cdot \cos(\delta_{13}) - \sin(\delta_{13}) + 2 \cdot \sin(\delta_{12}) \cdot \cos(\delta_{13})), \quad (6)$$

$$U_3 = \frac{\sqrt{3}}{3} (-\sin(\delta_{23}) \cdot \cos(\delta_{12}) \cdot \cos(\delta_{13}) + \sin(\delta_{13}) + \sin(\delta_{12}) \cdot \cos(\delta_{13})). \quad (7)$$

The coordinates U_1 , U_2 , U_3 for sequence 3–1–2 of the beam reflection are the opposite sign.

For the measuring the pitch Θ_1 and yaw Θ_2 it is necessary to direct the vector **U** on parallel to axis O_1Z_1 as $\mathbf{U} = (0, 0, 1)^T$. The conditions of this position is the equations $U_1 = 0$ and $U_2 = 0$. The relations between values δ_{12} , δ_{23} , δ_{13} are found from Eqs. (5) and (6):

$$\delta_{13} = \arctg(\sin(\delta_{12})) \quad (8)$$

$$\delta_{23} = -\arcsin(\tg(\delta_{12})) \quad (9)$$

The angle ω of the ort rotation is determined by equation:

$$\cos\left(\frac{\omega}{2}\right) = |U| = |U_3| \quad (10)$$

For reflector the value of the angle is $\omega = \pi - \Delta$, where value Δ is not more than several degrees. Value Δ is determined from the Eqs. (7)–(10) as: градусы

$$\Delta = 2 \cdot \arcsin\left(\sqrt{3} \cdot \sin(\delta_{13})\right) \quad (11)$$

The tetrahedral reflector with found configuration is effective for measuring pitch Θ_1 and yaw Θ_2 angles.

5 The Measurement Algorithm of Pitch and Yaw Angles

For reflection matrix M_d the following equation results:

$$M_d = \begin{pmatrix} -\cos(\Delta) & -\sin(\Delta) & 0 \\ \sin(\Delta) & -\cos(\Delta) & 0 \\ 0 & 0 & -1 \end{pmatrix} \approx \begin{pmatrix} -1 + \frac{\Delta^2}{2} & -\Delta & 0 \\ \Delta & -1 + \frac{\Delta^2}{2} & 0 \\ 0 & 0 & -1 \end{pmatrix}, \quad (12)$$

where Δ is small angle. The error of the formula (12) is in the order 0.1 % for angle Δ not more than 1.8° .

The projections ξ_x and ξ_y of ort \mathbf{B} of reflected beam on axis OX and OY for ort $\mathbf{A} = (0; 0; -1)^T$ are determined from Eq. (2):

$$\xi_x = \Delta \cdot \Theta_1 + \frac{1}{2} \cdot \Delta^2 \cdot \Theta_2, \quad \xi_y = \Delta \cdot \Theta_2 - \frac{1}{2} \cdot \Delta^2 \cdot \Theta_1, \quad (13)$$

The reflected beams form six images in the photoreceiver matrix of the autocollimator (Fig. 6).

On this figure f is the focal length of the objective. The image 1 for the sequence 2–1–3 of the beam reflection and image 2 for the sequence 3–1–2 of the reflection are used for measuring pitch Θ_1 and yaw Θ_2 angles.

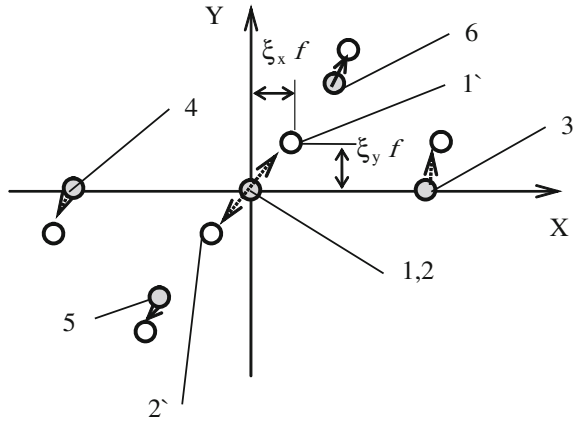
The receiving system of the autocollimator measures the projections ξ_x and ξ_y and the pitch Θ_1 and yaw Θ_2 angles are calculated from Eq. (13) as:

$$\Theta_2 = \frac{2 \cdot (2 \cdot \xi_y + \xi_x \cdot \Delta)}{\Delta \cdot (4 + \Delta^2)}, \quad \Theta_1 = \frac{2 \cdot (2 \cdot \xi_x - \xi_y \cdot \Delta)}{\Delta \cdot (4 + \Delta^2)} \quad (14)$$

From the Eqs. (13) and (14) follows what the conversion coefficient Q is proportional to the value Δ and it has variable and small value.

As result it is increasing the work distance of the autocollimation sensor with tetrahedral reflector relatively ordinary autocollimator.

Fig. 6 Images on the matrix photoreceiver: 1, 2 images for measuring pitch and yaw angles before rotations; 1', 2' images after rotations; 3, 4, 5, 6 unusable images



6 Conclusion

The autocollimator with reflector as special tetrahedron with invariant axis has advantage as the reflector for measuring pitch and yaw deformations. The small value of the conversion coefficient is realizes the measurements on the work distances more than 20 m.

To verify the theoretical results, an autocollimation experimental setup was designed. The value of the conversion coefficient was 0.1. The experimental setup had the following characteristics: infrared emission diode AL107B by power 15 mWt as sources of radiation; the objective by the focal length 450 mm as aperture of receiver part of the autocollimator, the CMOS matrix receiver by type OV05620 Color CMOS QSXGA with 2592 * 1944 pixels and one pixel size (2.2 * 2.2) μm^2 produced OmniVision as image analyzer. The experimentally determined characteristics: work distance is 16 meters, range of measurement is 20 arc minutes and the error of measuring pitch and yaw deformations is 2 arc second.

The experimental researches of the autocollimation sensor have confirmed the correctness of theoretical results.

The researched autocollimation sensors are effective to generate SEMS control signals at angular shifting the subdish of fully rotatable radiotelescopes.

Acknowledgments This work was financially supported by Government of Russian Federation, Grant 074-U01.

References

1. Konyakhin, I., Artemenko, Y., Timofeev, A.: Control of the deformation for the millimeter wave range radiotelescope mirrors. Proc. SPIE **7133**, 71333R (2009)
2. Konyakhin, I., Timofeev, A., Usik, A., Zhukov, D.: Optic-electronic systems for measuring the angle deformations and line shifts of the reflecting elements at the rotateable radio-telescope. Proc. SPIE **8082**, 80823R (2011)
3. Kleshchenok, M., Anisimov, A., Lashmanov, O., Timofeev, A., Korotaev, V.: Alignment control optical-electronic system with duplex retroreflectors. Proc. SPIE **9131**, 91311X (2014)
4. Turgalieva, T., Konyakhin, I.: Research of autocollimating angular deformation measurement system for large-size objects control. Proc. SPIE **8788**, 878832 (2013)
5. Korn, Granino A., Korn, Theresa M.: Mathematical handbook for scientists and engineers: definitions, theorems, and formulas for reference and review, vol. 1152. Dover Publications, New York (2000)

Electrooptic Converter for Measuring Linear Shifts of the Section Boards at the Main Dish of the Radiotelescope

I.A. Konyakhin, A.S. Vasilev and A.V. Petrochenko

Abstract The article analyzes the construction matters and metrological parameters of the electrooptic converter to generate SEMS control signals at shifting the structure elements of adaptive surface. The parallel structure of SEMS is used. Converter measures the shifts of section boards at the adaptive surface of radiotelescope main dish. The converter includes the base module, the processing module and a set of the reference marks. The base module includes the receiving optical system and the CMOS photodetector. The methods of the frame-to-frame difference, adaptive threshold filtration, binarization and objects search by the tied areas to detect the marks against accidental contrast background is the basis of the algorithm. The developed and manufactured converter experimental model was tested in laboratory conditions at the metrological bench at the distance between the base module and the mark 50 ± 0.2 m. The static characteristic was read during the experiment of the reference mark displacement at the pitch of 5 mm in the horizontal and vertical directions for the displacement range 40 mm. The error of the experimental model converter not exceeding 0.2 mm was obtained in the result of the experiment.

Keywords Electrooptic converter · Linear displacements · Reference marks · Adaptive surface of main dish

I.A. Konyakhin (✉) · A.S. Vasilev · A.V. Petrochenko
ITMO University, Saint-Petersburg, Russia
e-mail: igor@grv.ifmo.ru

A.S. Vasilev
e-mail: yoshikawa06@gmail.com

A.V. Petrochenko
e-mail: petroch@inbox.ru

1 Introduction

Nowadays new radio astronomy instruments are designed for researches in the millimeter wave range. For example, the Green Bank radio-telescope (RT) with 100 m diameter dish is realized in USA, Sardinia SRP radiotelescope with 64 m diameter dish is designed by Italy.

The Russian Academy of Sciences realizes the project of radio observatory on a mountain Suffa in Uzbekistan. Full rotatable radiotelescope RT-70 for researches in millimeter wave range will be the main observatory tool. The RT 70 Suffa parameters are the following: the main dish is realized as a 3-D parabola with a 21 m focal length. The full diameter of the main dish is 70 m; the diameter of subdish is 3 m. The surface of the main dish consists the 12,000 metal section boards. It is necessary to realize the small deviation of this section surface relatively a theoretical 3-D parabola [1].

For working at the millimeter wave range it is necessary the high quality of the main dish parabolic surface. The root mean square of the point deviation on a surface from theoretical parabola is not more than 0.1 mm.

However, the construction weight and the temperature influence are the reasons of the radiotelescope component deformations. For example, the linear deformations of the main dish surface have got value close to 30 mm.

The required parameters of reflecting components are realized if the main dish surface adaptation system is used.

To shift section boards of main dish surface in the process of adaptation it is suggested to use hexapod-like structures of smart electromechanical systems (SEMS).

The parallel structure of SEMS is used. According to the design, every section board is positioned on the mobile hexapod platform and the hexapod foundation is fixed to the antenna former (Fig. 1).

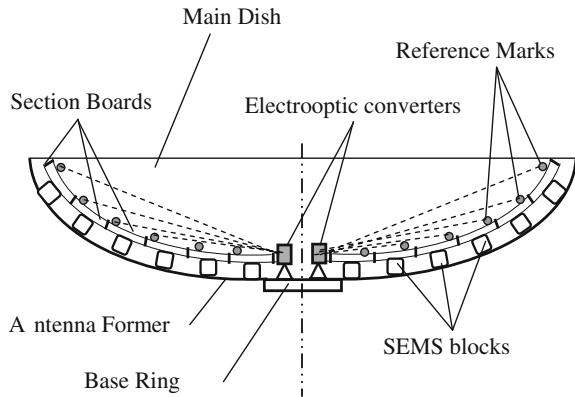
To generate SEMS control signals at shifting the section boards, one needs to measure the position of section boards with respect to the theoretical position of the main dish surface.

For high accuracy measurements the shift of the section board it is suggested to use an optic-electronic sensor [2, 3].

Following the technique, a source of optic radiation as reference mark is positioned on the measurement target, i.e. the section board on the mobile hexapod platform, while electrooptic converter is placed on the base ring at the apex of the main dish (Fig. 1).

The preliminary analysis showed that the multi-point control converters of the spatial attitude of the reference marks directly linked to the structure elements [4–6] are the most promising. Such converters are able to perform parallel and independent measurements with the error not exceeding 0.1 mm at the high frequency (up to 10 Hz), information updates in the case of the long-term displacements control in several points of a facility.

Fig. 1 Structure of the system for control the shifts of the section boards on main dish surface



2 Converter Structure, Principle of Operation and Design

The converter (Fig. 2) includes the base module, the processing module, and a set of the reference marks (up to 250 marks can be connected to one module). The converter is intended for the outdoors operation within the temperature range -60 to $+40$ °C. The base module is the main unit of the system, it includes the receiving optical system, and the CMOS photodetector matrix that realizes the instrument OXYZ coordinate system that controls the traverse mark coordinates in the space.

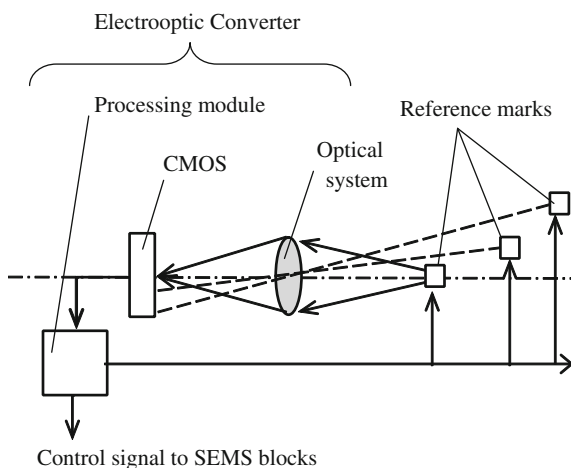
The reference marks are set at the distance 6–50 m from the base module on the section board of the adaptive main dish. Marks are active units and include a set of emitting diodes and their operation is controlled by the processing module. Diodes layout form, the distance between the same implement the test-object that allows determining reliably the mark in the real operational conditions. The reference marks displacements are registered in the instrument coordinates system of the base module followed by recalculation into the main system by the processing module. When several marks are connected the measuring network is formed which can be realized both via the wireless communication channel of the type ZigBee or via wire channel RS-485.

In order to obtain the maximum accuracy of the marks location control, we suggest that the base should be constructed with one optical front end and the field of analysis realized as the matrix CMOS of the photosensitive structure with adaptive split-screen field.

To ensure possible control of the reference mark displacement ± 40 mm at the operational distances 6–50 m the optical system as photographic lens objective with angular field of view 12° and focal length $f = 200$ mm was selected. Accuracy requirement and fast response (measurement time shall not exceed 2 s) determined selection of the radiation receiver in favor of CMOS matrix Aptina MT9P031 (2592×1944 , 2.2×2.2 μm).

The processing module controls the base module, and provides communication via wireless and wire communication channel with the reference marks and has the

Fig. 2 Scheme of electrooptic converter to control linear displacements of the referents marks on section boards



coupling interface with the external control device. The processing module is realized on the basis of the Field-Programmable Gate Array (FPGA) Altera Cyclone IV EP4CE22F17C6N.

The realized procedure for the converter measuring information extraction includes:

- preliminary image processing in order to improve the signal/noise correlation and optimization of other image parameters;
- search and localizing of the reference marks image in the base module field of view;
- determination of the images coordinates of the detected reference marks in the base module field of view in the instrument coordinates system

One of the problems in ensuring the high control accuracy is the marks detection against a random contrasting background followed by determination of the coordinates for the marks slowly displacing in time against the rapidly changing background.

The converter operation cycle supposes coordinates generation of the reference marks current position upon the request from an external control device and actuates two stages of an image acquisition.

At the first stage request is received from the external control device with the unique number of the reference mark, the processing module generates consecutively two control signals—the first is transmitted to the reference mark and sets the maximum emission brightness of its semiconductor-based LEDs [7] the second—is transmitted to the base module as the command for the mark image acquisition. The base module registers and converts the input optic emission into digital electrical signal and transmits, upon the command receipt, the received digital image into the processing module.

At the second stage the converter operation is the same, but the frame is acquired and transmitted with the brightness required for the accurate measurements.

Upon operation cycle completion the processing module performs digital processing of two registered images for the mark image detection in accordance with the developed algorithm of the type “frame-to-frame difference”, followed by its coordinates calculation in the instrument coordinates system of the base module. After the mark detection, the multiple images acquisitions are performed in the adaptive areas of interest limited by the mark dimensions. The averaged value of the reference mark current position is calculated from a series of acquired measurements, using the weighted summing algorithm. Such cycle of the image multiple acquisition allows reducing the random error component of the measurement result caused by the temperature and turbulence gradient fluctuations in the air duct [8, 9].

The processing result is transmitted to the external control device in the form of actual coordinates for the reference mark current position which unique number has been specified in the initial request.

Let's consider the image processing algorithm. The electronic image $A_1(x, y)$ of the first frame from the photodetecting module, in coordinates x, y of the module matrix sensitive pad formed for the reference mark with the maximum emission brightness LED shall be determined as the result of brightness deconvolution $L(x', y')$ of the mark and of the background $L_b(x', y')$, preset in the coordinates x', y' of the facility and the function of the receiving optical system weight $w(x, y)$, taking into account the root mean square of the electronic noises.

$$A_1(x, y) = S \cdot [(L(x', y') + L_b(x', y')) \cdot \tau(\lambda)] * w(x, y) + \eta_1(x, y) \quad (1)$$

where $\tau(\lambda)$ is the atmosphere spectral transmittance, S —is the matrix sensitivity of the photodetecting module, $\eta_1(x, y)$ —is the adaptive noise component of the image.

The second frame formed for the reference mark with the minimum LED emission brightness will be described by a similar function:

$$A_2(x, y) = S \cdot [L_b(x', y') \cdot \tau(\lambda)] * w(x, y) + \eta_2(x, y) \quad (2)$$

In this case the place of the frame-to-frame difference will be the electronic image $A_3(x, y)$ determined as:

$$A_3(x, y) = A_1(x, y) - A_2(x, y) = S \cdot [L(x', y') \cdot \tau(\lambda)] * w(x, y) + \eta_3(x, y) \quad (3)$$

The threshold filtration and binarization is performed on the basis of the frame-to-frame difference:

$$A_4(x, y) = \begin{cases} 1, & A_3(x, y) \geq T \\ 0, & A_3(x, y) < T \end{cases} \quad (4)$$

where $T = 0,75 \cdot \max(A_3(x, y))$ is the threshold filtration level.

Search and segmentation of the reference mark image is performed by the resulting array $A_4(x, y)$ and based on the search algorithm of the related areas. The algorithm analyses the “eight” of the pixel neighbors, at the same time each pixel of the image will be assigned with the facility number to which it belongs [10]. Based on the statistics collected on the detected separate facilities they are filtered in terms of their sizes. The remaining facilities serve for the checks to determine if at least four of the facilities form the regular tetragon—square (Fig. 3). The square as regular tetragon, with some admission, shall be considered the combination of facilities which:

- have equal opposite sides,
- have equal neighboring sides,
- have equal diagonals.

If the conditions are met the decision is made on detection of the reference mark and the area of interest is formed for the multiple image acquisition.

Based on the weighted summing up algorithm the coordinates on the sensitive pad of the photodetecting matrix are calculated in the preset area of interest followed by recalculation to the values of the reference mark displacement:

$$X_{pix} = \frac{\sum_i^{ROI_x} \sum_j^{ROI_y} A_3(i, j) \cdot i}{\sum_i^{ROI_x} \sum_j^{ROI_y} A_3(i, j)}, \quad Y_{pix} = \frac{\sum_i^{ROI_x} \sum_j^{ROI_y} A_3(i, j) \cdot j}{\sum_i^{ROI_x} \sum_j^{ROI_y} A_3(i, j)} \quad (5)$$

Here X_{pix}, Y_{pix} are the coordinates of the reference mark geometric center in pixels; ROI_x, ROI_y —is the area of interest on the reference mark image (Fig. 3).

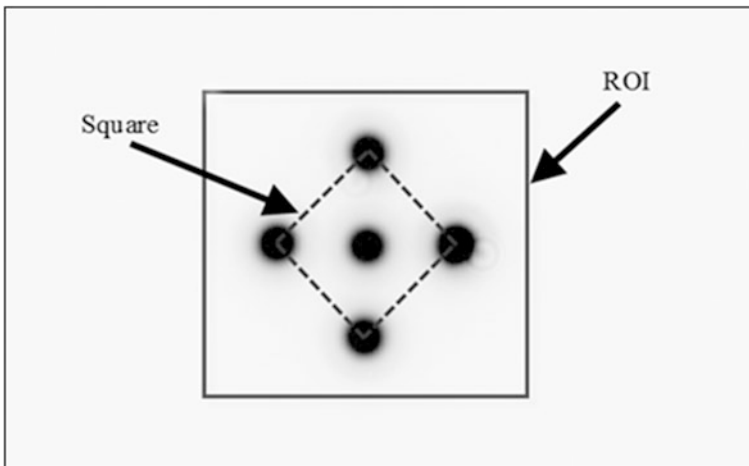


Fig. 3 Reference mark image

The measurements result shall be averaged for several acquired images and recalculated in millimeters.

3 Experimental Research

The converter experimental model was developed and manufactured to check the long-term functioning and to assess the metrological characteristics and was tested in the winter period in the outdoors operation with changing weather conditions (the ambient air temperature was varying from -23 $+10$ °C). The converter was mounted on a bracket attached on the building wall. The reference mark was installed at the opposite wall at the distance 29 ± 0.2 m. The converter ensured the fault-free system operation within the entire test period. The root-mean-square error of the reference mark static position did not exceed 0.2 mm.

The correlation dependence was detected, in the course of the test, of the error systematic component and of the ambient air temperature (Fig. 4). To eliminate the temperature effect on the measurements results the temperature sensor was introduced as the base module component, temperature correction in the result of the measurement was entered in the readings of the sensor.

Metrological characteristics of the converter in laboratory conditions were also studied with the distance between the base module and the mark 50 ± 0.1 m. The static characteristic for the reference mark displacement at the pitch 5 mm in horizontal direction for the range 80 mm was taken in the course of the experiment. The value of the preset displacement was controlled by the laser tracker API Radian 50. The value of the root-mean-square random error component did not exceed 0.2 mm (Fig. 5).

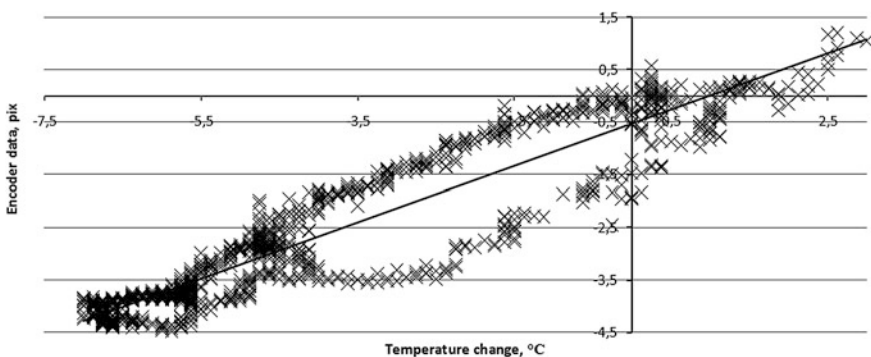


Fig. 4 Temperature and result of the measurement correlation

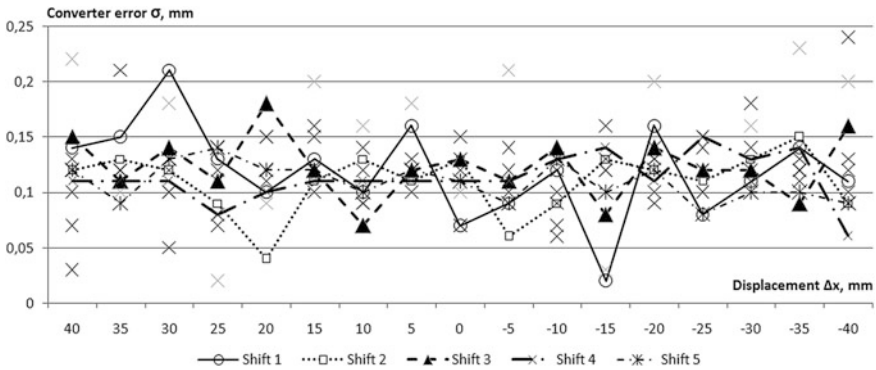


Fig. 5 Error of measuring at 50 m distance

4 Conclusion

This research was the practical realization of the electrooptic converter to generate SEMS control signals at shifting the structure elements of adaptive surface. The converter performs the multi-point control of the spatial position of the reference active marks rigidly tied to the section boards at the adaptive surface of the radiotelescope main dish.

The developed and manufactured converter experimental model was tested in the outdoors operation with changing weather conditions. The correlation dependence was detected, in the course of the experiment, of the converter readings and of the ambient air temperature. To eliminate the temperature effect the temperature sensor was introduced to enter the correction ratio in the result of the measurements.

Analysis of the external factors effect on the operation of the developed converter showed that the main direction for such devices perfection is in weakening of the air tract (temperature gradient, temperature fluctuations and turbulence) effect especially with the significant distances and temperature differentials. The promising way of the problem resolution is in use of new images processing methods, and design upgrades of the converter module.

The converter model error not exceeding 0.2 mm was obtained in the laboratory conditions at the metrological bench at the distance between the base module and the mark 50 ± 0.2 m. Experiments have shown the way of realization the electrooptic system for control the quality of the parabolic radiotelescope dish with diameter 70 m.

Acknowledgments This work was financially supported by Government of Russian Federation, Grant 074-U01.

References

1. Konyakhin, I., Artemenko, Y., Timofeev, A.: Control of the deformation for the millimeter wave range radiotelescope mirrors. Proc. SPIE **7133**, 71333R (2009)
2. Konyakhin, Igor A., Timofeev, Alexandr N., Usik, Alexandr A., Zhukov, Dmitry V.: Optic-electronic systems for measuring the angle deformations and line shifts of the reflecting elements at the rotateable radio-telescope. Proc. SPIE **8082**, 80823R (2011). doi:[10.1117/12.890059](https://doi.org/10.1117/12.890059)
3. Konyakhin, I.A., Turgalieva, T.V., Li, R.: Optic-electronic sensor for measuring the deformations of the axle at the radio-telescope. Proc. SPIE **9141**, 914123-914123 (2014)
4. Anisimov, A.G., Krasnyashchikh, A.V., Timofeev, A.N., Korotaev, V.V.: Accuracy characteristics of the shift control optical-electronic measurement system. Proc. SPIE **7427**, 74270L (2009)
5. Kleshchenok, M.A., Anisimov, A.G., Lashmanov, O.U., Timofeev, A.N., Korotaev, V.V.: Alignment control optical-electronic system with duplex retroreflectors. Proc. SPIE **9131**, 91311X (2014)
6. Pantyushin, A.V., Korotaev, V.V.: Control measurement system for railway track position. Proc. SPIE **8486**, 84861B-1–84861B-7 (2012)
7. Chertov, A.N., Gorbunova, E.V., Korotaev, V.V., Peretiagin, V.: Solution of multi-element LED light sources development automation problem. Proc. SPIE **9190**, 919015 (2014)
8. Maraev, A.A., Vasilev, A.S., Timofeev, A.N.: Study of irradiance distribution in optical equisignal zone. Proc. SPIE **9138**, 91380Q (2014)
9. Anisimov, A.G., Yarishev, S.N., Timofeev, A.N., Lashmanov, O., Korotaev, V.V.: Multispectral method for air tract influence attenuation. OSA Technical Digest, Optical Society of America, paper JWA24 (2011)
10. Klaiber, M., Rockstroh, L., Wang, Z., Baroud, Y., Simon, S.: A memory-efficient parallel single pass architecture for connected component labeling of streamed images. IEEE Field-Programmable Technology (FPT), pp. 159–165 (2012)